AN *IN VITRO* MODEL FOR ASSESSMENT OF SKELETAL MUSCLE ADAPTATION FOLLOWING EXERCISE RELATED PHYSIOLOGICAL CUES

A thesis submitted to the University of Bedfordshire, in partial fulfilment of the requirements for the degree of Doctor of Philosophy

Darren James Player

Muscle Cellular and Molecular Physiology Research Group, Institute for Sport and Physical Activity Research, University of Bedfordshire.

October, 2013.

I. Contents

II. Table of Figures

III. Authors Declaration

I, Darren J Player, declare that the work in this Thesis was carried out in accordance with the regulations of the University of Bedfordshire. The work was completed entirely by myself, with all other contributing individuals being acknowledged.

This Thesis has not been presented to any other University for examination either in the United Kingdom or overseas. No portion of the work referred to in this Research Project has been submitted in support of an application for another degree or qualification of this or any other university or institute of learning.

Signed  **Date** 14th October 2013

Darren J. Player

IV. Acknowledgements

I would like to take this opportunity to thank my Director of Studies, Professor Mark P. Lewis. Mark, I would like to thank you greatly for encouraging me to develop a passion for SkM biology and science in general. Thank you for giving me the opportunity to work with and here's to many more years to come. Thanks must also go to Dr. Vivek Mudera, whose scientific support and guidance has been much appreciated throughout my PhD.

A special thank you must go to Neil Martin, whom I started my PhD journey with. We have developed a great friendship throughout our three years together and I would not have enjoyed my PhD nearly as much if we had not studied together. The hrs of success and distress in the lab has all been brilliant! I would also like to thank Dr. Samantha Passey, Dr. Adam Sharples, Dr. Alec Smith and Dr. Amarjit Saini, whose experience and support in the lab and in the pub has been very much appreciated.

I would also like to thank all of the members of the Muscle Cellular and Molecular Physiology Research Group (MCMPRG) in Bedford and the Musculoskeletal Biology Research Group in Loughborough for their support and encouragement throughout my PhD.

I also wish to thank the University of Bedfordshire for providing a scholarship, which has provided me with the financial support to allow me to complete this Thesis.

Finally I would like to give my thanks to my Wife, Meena, to my Mum and Dad and to my Brother. Thank you for supporting me in everything that I do- you have made the person I am today. This is for you.

V. Abbreviations

3D	3-dimensional
˚C	Degrees Celsius
%	Per cent
βGPA	Beta-guanidinopropionic acid
ADP	Adenosine diphosphate
AICAR	5-aminoimidazole-4-carboxamide-1-β-D-ribonucleoside
AK	Adenylate kinase
ALAS	delta-aminolevulinate synthase
AMP	Adenosine monophosphate
AMPK	Adenosine monophosphate-activated protein kinase
ATP	Adenosine triphosphate
bHLH	Basic helix-loop-helix
BSA	Bovine serum albumin
Ca^{2+}	Calcium ion
CaMK	Calmodulin kinase
cDNA	Complementary DNA
(t)-CFM	(Tensioning)-Culture force monitor
CK	Creatine kinase
CO_2	Carbon dioxide
COX	Cytochrome c oxidase subunit
CRE	Cyclic AMP response element
CSA	Cross-sectional area
C_T	Cycle threshold
dH2O	distilled water
DM	Differentiation medium
DMD	Duchenne muscular dystrophy
DMEM	Dulbecco's modified Eagles medium
DMSO	Dimethyl Sulphoxide
DNA	Deoxyribonucleic acid

dNTP	Deoxynucleoside triphosphate
ε	Strain
ECC	Excitation contraction coupling
ECM	Extra cellular matrix
EDL	Extensor digitorum longus
EDTA	Ethylenediaminetetraacetic acid
EGF	Epidermal growth factor
eIF-2B	Eukaryotic translation initiation factor 2B
EPS	Electrical pulse stimulation
ER	Endoplasmic reticulum
ERK	Extra cellular signal regulated kinase
ETOH	Ethanol
FBS	Foetal bovine serum
FGF	Fibroblast growth factor
(m) g	(Milli)Gram
g	G-force
GDN	Guaifenesin dinitrate
GLUT-4	Glucose transporter-4
β-GPA	Beta guanadinopropionic acid
HDAC	Histone deacetylase
HFS	High frequency stimulation
HGF	Hepatocyte growth factor
hr(s)	Hr(s)
Hz	Hertz
IL-6	Interleukin-6
IGF	Insulin-like growth factor
IGFBP	Insulin-like growth factor binding protein
IMS	Industrial methylated spirit
JNK	c-Jun N-terminal kinase
kDa	Kilo Dalton

LFS	Low frequency stimulation
M	Molar
MAFBx	Muscle atrophy factor BOX
MAPK	Mitogen activated protein kinase
MDC	Muscle-derived cell
MEF-2	Myocyte enhancer factor
MEK	Mitogen activated protein kinase
mg	Milligram
Mg^{2+}	Magnesium ion
MGF	Mechano-growth factor
MHC	Myosin heavy chain
min(s)	Minute(s)
ml	Millilitre
MMP	Matrix metalloproteinases
mRNA	messenger RNA
MHC	Myosin heavy chain
MPC	Muscle precursor cells
MRFs	Myogenic regulatory factors
mtDNA	Mitochondrial DNA
mTOR	Mammalian target of rapamycin
MuRF-1	Muscle RING-finger protein-1
NAD	Nicotinamide adenine dinucleotide
NF-κβ	Nuclear factor-kappa beta
NO	Nitric oxide
NRF	Nuclear respiratory factor
nNOS	Neuronal nitric oxide synthase
µ	micro
OD	Optical density
Pax	Paired box family
PBS	Phosphate buffered saline

PCr	Phospho-creatine
PCR	Polymerase chain reaction
PDGF-BB	Platelet derived growth factor-BB
PFK	Phosphofructokinase
pH	Potential hydrogen
PGC-1α	Peroxisome proliferator-activated receptor γ coactivator-1 alpha
PI3-K	Phosphatidylinositol 3-kinase
PKB	Protein Kinase B
PPAR-γ	Peroxisome proliferator-activated receptor-gamma
qRT-PCR	Quantitative reverse transcriptase polymerase chain reaction
RFD	Rate of force development
RNA	Ribonucleic acid
ROS	Reactive oxygen species
rpm	Revolutions per minute
RT	Room temperature
RT-PCR	Reverse transcription polymerase chain reaction
SAC	Stretch-activated channel
SC	Satellite cell
SDF-1α	Stromal cell-derived factor-1 alpha
SDH	Succinate dehydrogenase
Sec(s)	Second(s)
SEM	Standard error of the mean
siRNA	Small interfering RNA
SkM	Skeletal Muscle
TBS	Tris buffered saline
TGF-β	Transforming-growth factor beta
Triton X-100	t-octyl phenoxypoly-ethoxyethanol

Trizma base or	
Tris base	(Tris (hydroxymethyl)aminomethane)
UPP	Ubiquitin proteasome pathway
UTRs	Untranslated regions
UV	Ultra-violet
VEGF	Vascular endothelial growth factor
Zn^{2+}	Zinc

VI. Thesis Abstract

The aim of this Thesis was to further characterise and utilise an *in vitro* skeletal muscle (SkM) model, to investigate its potential use in further understanding the cellular and molecular adaptations to exercise *in vivo*. Candidate genes and proteins have been identified using *in vivo*, *ex vivo* and targeted *in vitro* experiments, however the complete picture of these molecular mechanisms are far from understood. Furthermore, the extent to which mechanical signals contribute to the intra-cellular mechanisms associated with exercise is also underinvesitgated. To this end, developing an *in vitro* model of SkM that can recapitulate *in vivo* SkM and respond to mechanical stimulation in a similar way to exercise will provide a means to begin to delineate the complex cellular and molecular regulation of SkM.

The initial investigation (Chapter 3) characterised an optimal seeding density and culture period of C2C12 myoblasts within a 3 ml collagen gel. These data provided support for the use of collagen constructs seeded at 4 x 10^6 cells/ml, with no statistical differences observed in peak force, rate of force development and relative force compared to other seeding densities examined (table 3-2, all $p > 0.05$). However the use of 4 x 10^6 cells/ml supports previous data in a larger construct volume model, whilst the highest cell density possible in the system increases cell-cell contact required for fusion. Immunohistochemical and gene expression analyses provided evidence for the fusion of single seeded myoblasts into multinucleate myotubes, demonstrating an *in vivo*-like architecture.

Chapter 4 presented data towards the characterisation and use of two distinct cyclical stretch regimens with respect to the acute biochemical and transcriptional responses. Data revealed increases in peak media lactate and reductions in peak media glucose, following cyclical stetch compared to control ($p = 0.000$ and $p = 0.001$ respectively, Fig. 4-2). Changes in mtDNA (Fig. 4-5) and associated mRNA transcriptional signals (Fig. 4-7) were mode dependent.

Chapter 4 presented a model of *in vitro* mechanical overload to investigate whether such a system could be used to investigate the mechanisms that regulate hypertrophy in SkM. Continuous static and ramp loading induced a transcriptional hypertrophic response (increases in IGF-I, MMP-9, $p < 0.05$, Fig. 5-3 and reduction in IGFBP-5 mRNA's, $p = 0.027$ and $p = 0.059$, Fig. 5-4) with disticint differences in the modes of overload employed, suggesting a mechano-specific response of certain genes.

Efforts towards optimising metods to investigate the intra-cellular signalling mechanisms that may underpin the responses to mechanical stretch were investigated and presented in appendix 1.

The data presented in this Thesis demonstrates the development and novel use of an *in vitro* SkM model to investigate the acute response of SkM to increase loading. The characterisation detailed here will allow for future investigations to further advance our understanding of the complex interactions of mechano-responsive genes and proteins in that regulate SkM plasticity.

1 General Introduction and Review of the Literature

1.1 General Introduction

The experiments described in this Thesis represent work that has been undertaken to further develop, characterise and utilise an *in vitro* skeletal muscle (SkM) model to investigate the effect of mechanical loading upon the biochemical and molecular responses to SkM cells. This novel model characterisation presents a highly controllable and dynamic system, whereby the effects of mechanical signals on muscle cell biology can be investigated.

When seeking to further understand *in vivo* SkM cell biology, it is necessary to appreciate existing knowledge concerning normal SkM development. When developing bio-mimetic tissue *in vitro*, the process of embryonic development is highly recapitulated. To this end, the mechanisms involved in this process will be highlighted to provide background to the processes underpinning the SkM tissue engineering. Furthermore, when seeking to develop a bio-mimetic model *in vitro* it is important to understand the structure and function of the native tissue. The review of literature will describe the structure and function of *in vivo* SkM, drawing on the important features to recreate *in vitro*.

Investigating whether an *in vitro* model can recreate mechanisms which are key to *in vivo* SkM adaptation, it is crucial to highlight the key genes and proteins involved. As such, the review of literature will focus upon the key genes and proeteins that are postulated to regulated SkM adaptation, allowing for the targeted identification of manipulated mechanisms in the experimental model used.

1.2 Embryonic Skeletal Muscle Development

The embryonic development of SkM is a highly sophisticated process, but has been investigated extensively in the hope of understanding the mechanisms that contribute to musculoskeletal abnormalities from birth. Research has also sought to identify the stem cell populations that SkM is derived from in the embryo, to ascertain potential mechanisms that could provide therapy for musculoskeletal diseases.

The formation of SkM in the embryo stems from the paraxial mesoderm which divides into somites on each side of the neural tube and the notochord (Buckingham, et al., 2003). Work in the 1970's identified that the muscles of the limb and body develop from the dermomyotome edge of the somites (Christ, et al., 1974, Christ, et al., 1977). Further evidence suggests the epaxial region of the dermomyotome gives rise to the back musculature whilst the hypaxial region gives rise to the limb muscles (Buckingham, et al., 2003).

Conversely, muscles of the head and neck develop from the preoptic axial and paraxial head mesoderm (Noden, 1983), contributing to a population of muscle precursor cells that are distinct from limb muscle in relation to molecular characterisation (McLoon, et al., 2007). The surface of the epaxial region of the dermomyotome de-epithelises and gives rise to a progeny of cells termed mesenchymal muscle precursor cells (MPC's), which have the ability to migrate to the somatopleural mesoderm of the limb anlagen (Christ and Brand-Saberi, 2002). These cells then proliferate, differentiate and fuse to form the developing muscles. The patterning and migration of cells derived from the dermomytome rely on the presence of key proteins, including c-met and hepatocyte growth factor (HGF, Dietrich, et al., 1999). The presence of the transcription factor Pax3 is essential for the expression of c-met, with Pax3 mutant mice displaying the absence of limb musculature (Tajbakhsh, et al., 1997).

The mechanisms associated with the specification of myogenic cells rely heavily on a group of proteins belonging to the basic helix-loop-helix (bHLH) family of proteins, also termed the myogenic regulatory factors (MRF's, Hawke and Garry, 2001). Commitment of MPC's to the myogenic lineage (cells now termed myoblasts) is characterised by the expression of MyoD and Myf5, with transgenic overexpression of these proteins inducing myogenic cell fate of cells from multiple lineages (Choi, et al., 1990).

The expression of these determination factors is present even before the formation of the myotome and they bind to the promotor regions of genes required for the execution of the myogenic programme (Buckingham, et al., 2003, Fig. 1-1). The expression of MRF's myogenin and MRF-4 mark the differentiation and fusion of myoblasts to differentiated multinucleated myotubes (Buckingham, 2003, Fig. 1-1). The number of these post-mitotic cells is set *in utero* and as a consequence do not have the ability to regenerate following damage and/or trauma. The regenerative process is therefore supported by population of resident stem cells.

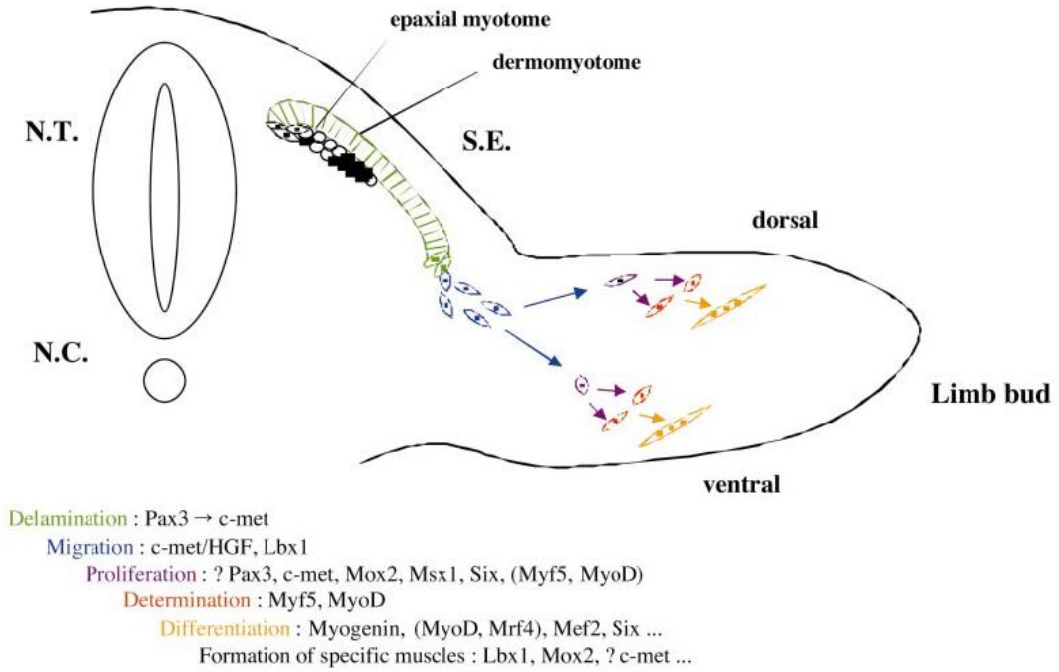

Figure 1-1. The embryonic development of SkM. (From Buckingham et al., 2003).

1.3 Skeletal Muscle Structure and Function

SkM facilitates the controlled voluntary movement of the body through attachments directly or indirectly via tendons, to the skeleton. The macroscopic orientations of SkM fibres are longitudinal in relation to the direction of movement, towards the proximal site of attachment (Smith, et al., 2010). The highly organised structure of SkM, both grossly and ultra-structurally permits the controlled generation of vector force for movement.

1.3.1 Gross Structure and the Extra-Cellular Matrix

SkM comprises of both cellular and extra-cellular components, working synergistically for the transmission of force. SkM consists of bundles of multinucleated cells (fibres), which align parallel to the axis of movement (Sciote and Morris, 2000, Fig. 1-2). The size of each muscle fibre can range in terms of diameter and length, with some fibres stretching the length of the whole muscle itself. The gross contractile protein filaments of the muscle fibre (termed myofibrils), occupy much of the intracellular space, and consequentially the nuclei, mitochondria and other organelles are located peripherally (Sciote and Morris, 2000).

The extra cellular matrix (ECM) of SkM functions not only to support the muscle fibres, but also the supplying blood vessels and the motor nerves. There are three main layers of ECM within SkM, providing a supporting network of anchorage for the tissue. Each individual fibre is surrounded by the endomysium (basal lamina), incorporating a random network of collagen fibres in order to facilitate contraction (Smith, et al., 2010). In turn, fibres are grouped into bundles (fascicles) surrounded by the perimysium. This layer is more organised than the endomysium, with a multi-layered structure lying transverse to the axis of the muscle fibres (Gillies and Lieber, 2011). The complete tissue is surrounded by a double layered structure termed the epimysium.

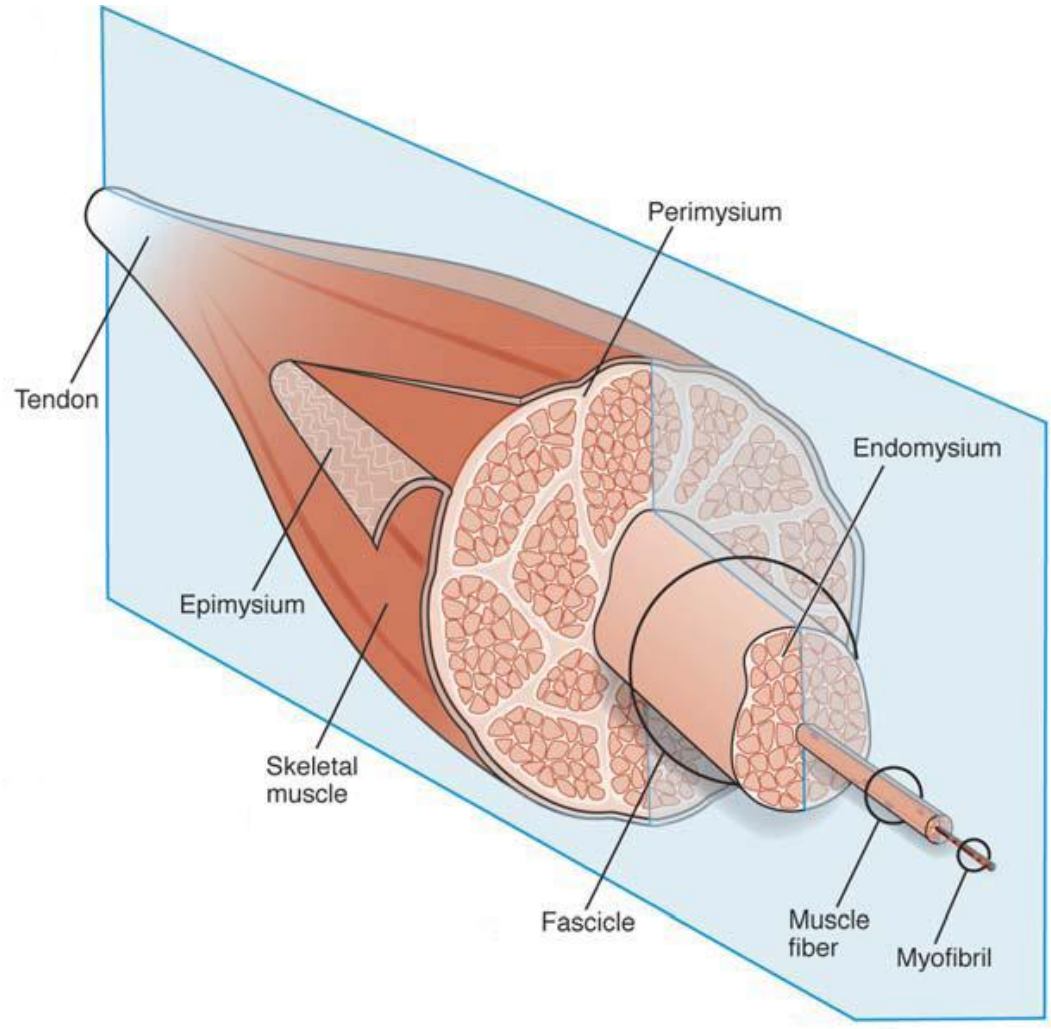

Figure 1-2. The gross structure of SkM. (From, Gillies and Lieber, 2011).

1.3.1.1 Collagen as a Major Structural Protein of Skeletal Muscle Extracellular Matrix

There are four classes of extracellular matrix proteins within SkM; collagenous glycoproteins, non-collagenous glycoproteins, proteoglycans and elastin (Lewis, et al., 2001). Collagenous-glycoproteins and in particular collagens are abundantly found in SkM. Indeed, the connective tissue layers discussed form a reasonable component of SkM mass; up to 10 % of dry weight mass in the adult animal. Approximately 10 collagen protein types are expressed during embryonic SkM development, whereas Type I and III predominate in adult SkM (Kjaer, 2004, Gillies and Lieber, 2011).

The abundance of type I collagen is variable and has been cited to be from 30 % to 97 % of all collagen found in SkM (Bailey, et al., 1979, Bailey, 2001). The distribution of collagen types throughout the ECM hierarchical structure is debated in the literature due to methodological limitations of analysis, however it considered that type I collagen forms a major structural component of the perimysial layer (Gillies and Lieber, 2011).

The organisation of collagen fibrils within the ECM plays a major role in the transmission of force throughout the tissue, with the fibril distribution and orientation a function of tissue activity (Gillies and Lieber, 2011). Despite the ECM having a distinct role in structure and force transmission it appears the influence of the ECM upon the development of passive tension is questionable. Experiments have provided evidence for the muscle fibre intrinsic nature of tension development (Magid and Law, 1985). This finding has steered much attention to the 'molecular spring', titin in providing answers as to the origin of passive tension (Magid and Law, 1985).

1.3.1.2 Alternative ECM Function

However, the ECM is not regarded as purely a structural component of SkM, rather it co-ordinates many cellular processes; including regeneration, neural transmission and myogenesis (Lewis, et al., 2001). The ECM and in particular ECM remodelling, play significant roles in satellite cell (SC) activation and myoblast migration required for regeneration (Lewis, et al., 2000). Moreover, the ECM plays a role in harbouring growth factors and binding proteins required for muscle cell differentiation and hypertrophy (Coppock, et al., 2004).

1.3.1.3 Muscle Fibre Attachment to the ECM

The cytoskeleton of SkM fibres is attached to the ECM via a complex network of proteins, including integrins and the dystrophin-dystroglycan complex (Hoffman, et al., 1987, Lewis, et al., 2001). Coupling the sarcolemma with the ECM, via numerous protein complexes, provides structural stability to SkM tissue.

Congenital defects in the dystrophin gene, leads to muscular dystrophy a disease characterised by pathophysiological regeneration (Hoffman, et al., 1987) .The interaction between the ECM and SkM cells is also vastly important for the transmission of mechanical signals into biochemical signals within the cell (often termed mechano-transduction, (Yamada, et al., 2012). Integrins play an important role in transmitting this signal following ligand binding (Lewis, et al., 2001), with these mechanisms being highly induced following SkM contraction *in vivo* (Boppart, et al., 2011, Lueders, et al., 2011).

1.3.2 The Ultra-Structure of Skeletal Muscle as a basis for contraction

Myofibrils are long cylindrical structures that appear in parallel with repeating contractile subunits termed sarcomeres, aligned in series (Lieber, et al., 2002), which form the units of the complete SkM fibre. A sarcomere contains all the necessary proteins for contraction, organised into a highly complex interwoven network.

The extent of muscle shortening directly relates to the sum of sarcomere shortening within the myofibril, whilst increases in the number of sarcomeres in series forms physiological hypertrophy and contributes to increased force (Lieber, et al., 2002, Jones, et al., 2004).

The sarcomere itself comprises of two contractile filaments termed myofilaments, of which there is one thick and one thin filament related to the composition of the contractile protein within it; either myosin (thick) and actin (thin). The interdigitation of these filaments gives rise to the striated appearance (seen with light and dark banding) of SkM under light microscopes (Jones, et al., 2004). Accordingly, the light refractive properties of the particular regions has allowed for their definition, namely the *anisotropic* band (A-band, containing only myosin filaments) and the *isotropic* band (I-band, containing only actin filaments).

The region of the A-band where there is no actin-myosin interaction is termed the H-zone, whilst the dark narrow banding through the middle of the I-band is named the Z-line (Z standing for *zwitter*, meaning 'between' in German, Jones, et al., 2004). The final definition of structure within the sarcomere is termed the M-line, which is a dense zone in the centre of the A-band (McArdle, et al., 2004, Fig. 1-3).

1.3.3 Actin-Myosin Interaction: The Cross-Bridge Theory

The molecular basis for contraction is based around the complex interaction between the two contractile proteins, actin and myosin. The complex and co-ordinated interaction is mediated by the regulatory proteins, troponin and tropomyosin (McArdle, et al., 2004). In the non-contracted state, tropomyosin is positioned by the troponin complex in order to cover the myosin binding sites and hence preventing any interaction with actin.

Following depolarisation of the cell surface membrane, the wave of depolarisation passes down the T tubules which are positioned within invaginations of the sarcolemma (plasma membrane, Gomes, et al., 2002, Jones, et al., 2004). Calcium (Ca^{2+}) is released from the sarcoplasmic reticulum (SR) following interaction from the T tubules. Ca^{2+} then binds to Troponin C initiating the interaction of Troponin T and Troponin I. This in turn leads to the translocation of the Troponin-Tropomyosin complex from the actin filament, revealing a myosin binding site (Gomes, et al., 2002). This allows for the cyclic action (or contraction) of the actin-myosin interaction to occur.

The process of the excitation of the membrane leading to active contraction myofilaments is termed Excitation-Contraction Coupling (ECC, Dulhunty, 2006). The sliding of the actin filament caused by myosin head movement was evident when under passive stretch conditions under an electron microscope, when the active contraction revealed only movement of the I-band (Huxley and Niedergerke, 1954).

This observation was also independently found in another laboratory at a similar time (Huxley and Hanson, 1954). These observations led to the development of the 'sliding filament' or 'cross-bridge' hypotheses, which aimed to describe the interaction and consequential actions of actin and myosin.

Huxley (1957) postulated that there are two cross-bridge states; attached and detached, processes which are driven by the hydrolysis of ATP (Huxley, 1957). The release of phosphate from the actomyosin complex (bound actin and myosin) initiates the rotation of the S1 head of the myosin protein (Jones, et al., 2004). As the rotation phase comes to an end, ADP is released allowing for the binding of ATP to the actomyosin complex. Upon the binding of ATP to the actomyosin complex, the complex is dissociated with ATP bound to myosin where it is hydrolysed by ATPase, leaving the association of ADP and Pi with myosin. These products of ATP hydrolysis are thought to activate the S1 unit of the myosin head, in order to initiate the further binding of actin, where the cycle begins again.

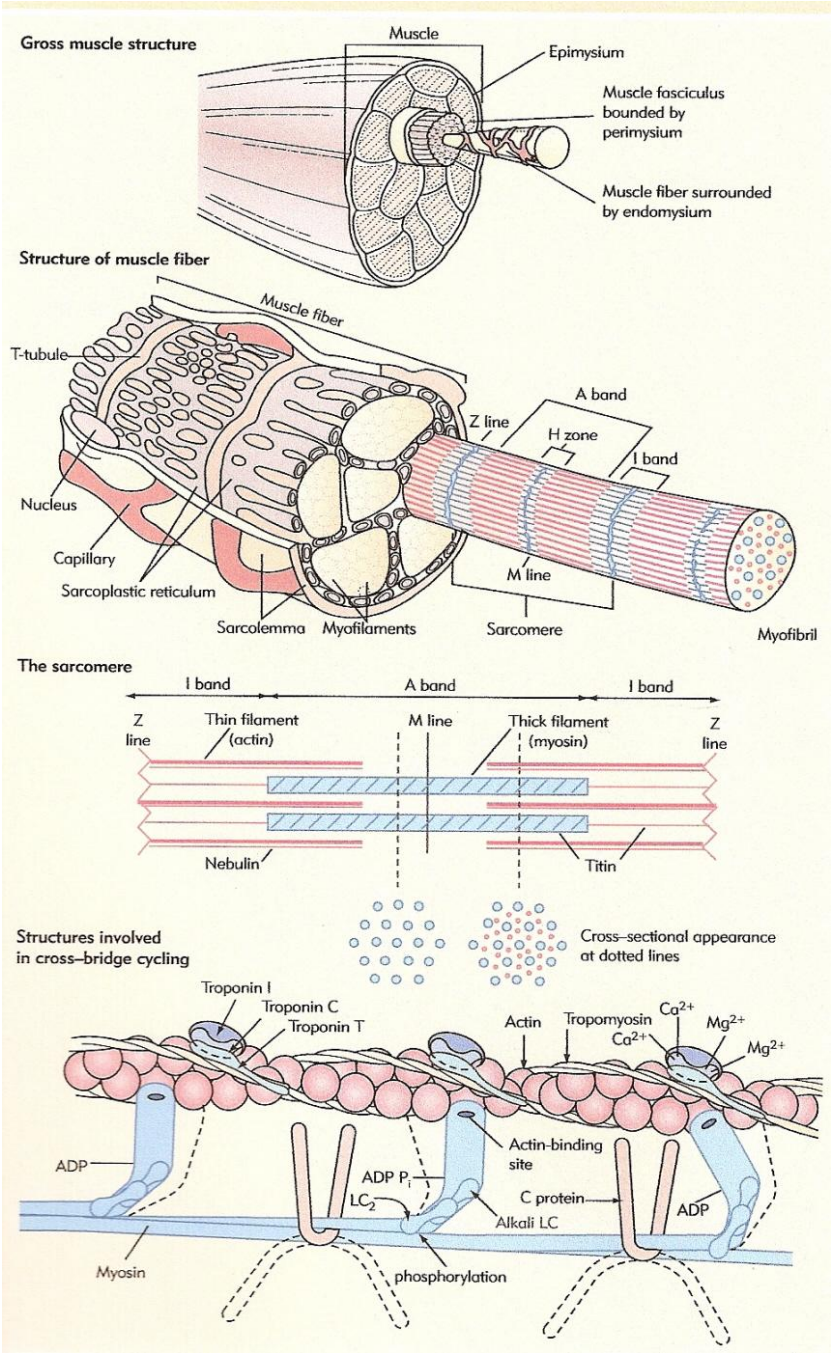

Figure 1-3. The hierarchical structure of SkM: the molecular basis of contraction.

(From, Hopkins, 2005).

1.4 Postnatal Skeletal Muscle Regeneration

1.4.1 Satellite Cells (SC's)

SkM is a post mitotic tissue; therefore the existing differentiated cells do not have the intrinsic capacity to regenerate themselves. In this regard, the growth and regenerative capability of SkM from trauma (physiological or pathophysiological), comes from a resident population of stem cells termed SC's (Sinanan, et al., 2006). These cells were identified and named as such due to their anatomical position between the sarcolemma and the basal lamina of isolated frog SkM tissue (Mauro, 1961). Since this discovery there has been a wide interest in SC biology concerning their activation, capacity for growth and regeneration and their 'stem-like' nature (Zammit, et al., 2006). As such, the SC has been deemed a potential target either intrinsically or extrinsically for the treatment of many SkM pathologies, including muscular dystrophies.

1.4.1.1 Activation, proliferation and the identification of a muscle specific 'stem' cell

One defining feature of a SC is that the basal lamina that surrounds the myofibre and SC is continuous (Hawke and Garry, 2001), positing the SC in an advantageous location for proliferation and chemotaxis to the site of regeneration. SC's are mitotically quiescent in the adult and display limited gene expression in this state; characteristically CD34, Pax7 and Myf5 (Le Grand and Rudnicki, 2007). These markers are commonly used to identify SC's in their niche (*in vivo* studies), along with the characterisation of such cells during *ex vivo* or *in vitro* preparations (Beauchamp, et al., 2000, Zammit, et al., 2006). The quiescent nature of a SC can be confirmed by the high nuclear-to-cytoplasmic ratio indicative of limited cellular activity, coupled with fewer organelles compared to the adjacent myonuclei (Hawke and Garry, 2001). Following trauma, they are activated from their quiescent state and express genes which are associated with commitment or determination to the myogenic lineage (discussed in section 1.3.2, Sinanan et al., 2006).

The activation of these quiescent cells is complex in nature and the exact mechanisms in control are largely unknown. It is beyond the scope of this review to detail all of the proposed mechanisms; however the most well understood researched mechanisms will be detailed.

1.4.1.1.1 Sphingosine-1-phosphate

The intrinsic production of sphingosine-1-phosphate signals the entry of the SC into the cell cycle (i.e. activated from quiescent state in G_0 into G_1 phase of cell cycle, (Le Grand and Rudnicki, 2007). It has been shown that the inhibition of the synthesis of this protein severely reduces muscle regenerative capacity (Nagata, et al., 2006) and thus appears to play a key role in the activation and regenerative capacity of SC's.

1.4.1.1.2 Growth Factors

Another protein that has been demonstrated to activate SC's is the hepatocyte growth factor (HGF). Early experiments identified a protein contained within the extract of crushed muscle tissue, that what capable of stimulating the proliferation of quiescent SC's (Bischoff, 1986), however the exact protein was not identified. Further studies demonstrated fibroblast growth factor-2 (FGF2), transferrin and platelet derived growth factor BB (PDGF-BB) effect SC proliferation from quiescence, without being able to account for all of the mitogenic activity evident within the extract (Chen, et al., 1994). The work of Tatsumi et al (1998) provided insight into the protein responsible for the activation of SC's that has been described in the previous experiments. It was shown that HGF is localised to the ECM surrounding the muscle fibre and following damage, translocation of this protein to SC's leads to the co-localisation of HGF to its receptor c-met (Tatsumi, et al., 1998). Furthermore, injecting exogenous HGF to uninjured SkM activates SC's from the quiescent state, whilst using an antibody against HGF abolishes SC activation following crush injury (Tatsumi, et al., 1998). These data together provide strong evidence for the positive effect of HGF on SC activation following trauma.

Another growth factor, IGF-I, has been shown to influence SC activation in single fibre analyses, where the cell is deemed to remain in a quiescent state (Bischoff, 1986). Experiments utilising cell culture methodologies have suggested IGF-I may influence SC activation, despite the limited evidence of the cells remaining quiescent in this state (Tatsumi, et al., 2009). Indeed, IGF-I and the splice variant MGF, positively stimulate the proliferation of muscle derived cells (MDC's) in culture (Ates, et al., 2007). PDGF-BB, epidermal growth factor (EGF) and transforming growth factor-β (TGFβ) have also been shown to increase SC proliferation, despite minimal evidence for their role in the activation of SC's (Tatsumi, et al., 2009).

These experiments were conducted using *in vitro* activation assays, based upon tissue digestion protocols therefore the activation of SC's during the isolation process may confound results utilising this method. Alternative isolated single fibre-based methods for analysing the activation of SC's, whereby the SC is mainted in its niche may provide a more physiological environment for experimentation (Nagata et al., 2006). The use of an *in situ* experimental design incorporating *in situ* hybridisation of genes of interest with the utilisation of specific activation reporters, would allow for the identification of SC activation related to particular influencing genes (Beauchamp et al., 2000).

Fibroblast growth factors (FGF's) were the first growth factors identified to have an effect on myogeninc cells (Sheehan and Allen, 1999). Early evidence suggested a mitogenic effect of FGF upon myoblasts, with a delayed differentiation capability (Gospodarowicz, et al., 1976). Much work from Ronald Allen's lab has demonstrated the mitogenic effect of FGF's upon SC's and myoblasts, with data to suggest a synergistic role with IGF-I (Allen and Boxhorn, 1989, Allen and Rankin, 1990), with little effect on differentiation.

1.4.1.1.3 Nitric Oxide

Nitric oxide (NO) has also been shown to play a significant role in activating SC's. In SkM neuronal nitric oxide synthase (nNOS) is localised to the sarcolemma by the association of its amino acid sequence to an element of the dystrophin cytoskeleton (Tatsumi, et al., 2009). The synthesis of NO is stimulated by exercise, along with trauma, mechanical stretch and shear force from L-arginine (Centeno-Baez, et al., 2011).

The most compelling evidence for the impact of NO on SC activation has been shown following the oral administration of guaifenesin dinitrate (GDN) to mice (Wang, et al., 2009), which is an NO donor directed to accumulate in SkM. Indices of myogenesis were increased 24 hrs post administration of GDN, including myf-5, myogenin and follistatin (Wang, et al., 2009). Transdermal treatment of GDN, also results in a significant (38 %) increase in DNA synthesis 24 hrs post treatment (Wang, et al., 2009) and coupled with the myogenic data provides a strong evidence base for the role of the NO pathway in stimulating SC activation, proliferation and myogenesis *in vivo*.

1.4.2 Satellite Cell Determination, Migration and Myogenesis

Many of the gene and protein regulatory networks that control post-natal SkM regeneration and growth are the same as those that govern embryonic SkM development. Following the activation of the SC it asymmetrically divides, with one daughter cell returning to quiescence to replenish the stem cell pool (Morgan and Partridge, 2003). Following the correct cellular signals, the activated progeny commit to the myogenic lineage, regulated by the transcription factor MyoD (Buckingham, et al., 2003). The intermediate filament protein Desmin, is one of the earliest markers of commitment to the myogenic lineage and thus serves as key tool in identifying activated and committed SC's.

Following commitment to the myogenic lineage, the migration of the myoblasts to the site of injury for regeneration is regulated by chemokines; these are proteins released by the damaged muscle cells to ensure the efficient migration of the regenerating cell (Griffin, et al., 2010). An extensive network of chemokines has been identified in the migration and fusion of myoblasts, with the stromal cell-derived factor-1α (SDF-1α) clearly displaying an important role following its inhibition (Griffin, et al., 2010).

Other proteins including; matrix metallo-proteinase-9 (MMP-9, Lewis et al., 2000), mitogen-activated protein kinase (MAPK), phosphatidylinositol 3-kinase (PI3 kinase, Al-Shanti, et al., 2011) and angiotensin II (Johnston, et al., 2010), all have a positive effect upon myoblast migration. Following the migration of the myoblasts to the site of injury these cells are capable of exiting the cell cycle, differentiating and fusing into the region requiring regeneration, concomitantly expressing myogenin and myogenic regulatory factor-4 (MRF-4, Hawke and Garry, 2001). The process of myogenesis (myoblast fusion) can be recapitulated *in vitro*, with the fusion of myoblasts into newly formed myotubes. The gene and protein regulation involved in myogenesis have most commonly been identified with *in vitro*-based experiments. The expression of myogenin mRNA has been shown to reflect the commitment of single cells to fuse with other myogencially determined cells (Mudera, et al., 2010). In this respect, the identification of myogenin mRNA allows for the molecular identification of fusion potential of myogenic cells *in vitro*.

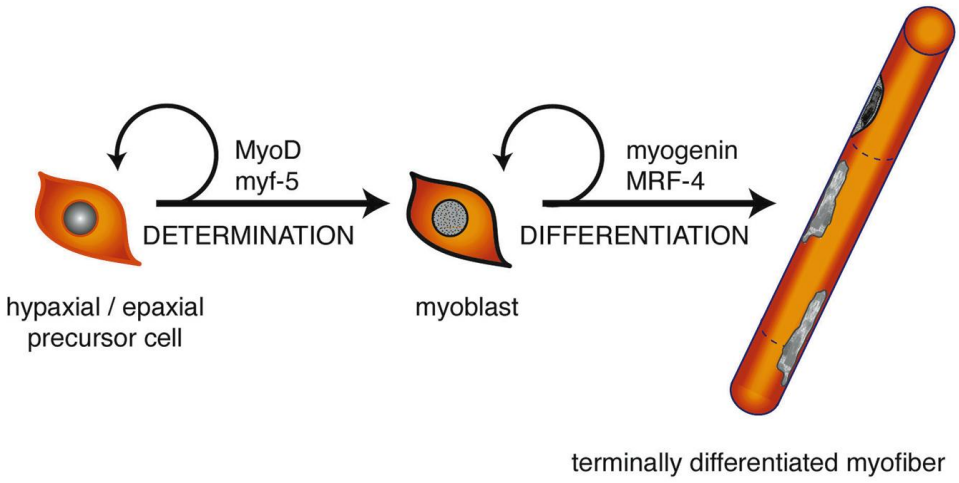

Figure 1-4. Satellite cell (muscle precursor cell) myogenic lineage determination and differentiation to a terminally differentiated myofibre or myotube (From Hawke and Garry, 2001)**.**

1.5 Skeletal Muscle Energy Metabolism: Products and Bi-Products?

1.5.1 ATP Synthesis: The Currency for Skeletal Muscle Contraction

As described previously (1.3.3), ATP is required for the cleavage of the myosin head from the actin filament during muscle contraction. The supply of ATP for this process is essential during continued muscle contraction and must be synthesised at a rapid and sustained rate to meet demands for voluntary movement.

The synthesis of ATP occurs from two main sources; aerobic and anaerobic metabolism (De Feo, et al., 2003). The yield of ATP from aerobic metabolism of stored substrates (carbohydrate, fat and protein) is far greater than anaerobic metabolism; however the rate of synthesis is reduced (Wells, et al., 2008). The initial high rate of ATP synthesis from anaerobic sources and the prolonged high yield of ATP from aerobic sources, makes this system of ATP generation near ideal for SkM and sub-maximal voluntary exercise. The classified mechanisms of ATP production (phosphagen, glycolysis and mitochondrial respiration) work in synergy at the onset of contraction to generate ATP.

It is only the relative contribution of ATP yield from each source that alters throughout contraction duration (Baker, et al., 2010). The phosphagen system is characterised by the production of ATP from two reactions catalysed by Creatine Kinase (CK) and Adenylate Kinase (AK) respectively (Equations 1 and 2).

Equation 1 and 2. The Phosphagen System of ATP Synthesis (Adapted from Baker et al., 2010).

$$CrP + ADP + H^+ \xrightarrow{\text{creatine kinase}} ATP + Cr,$$

$$ADP + ADP \xrightarrow{\text{adenylate kinase}} ATP + AMP,$$

The synthesis of ATP from the CK reaction is extremely fast due to the high abundance of Creatine Phosphate (CrP) found within SkM cells (Baker et al., 2010). The production of AMP from the AK reaction is vastly important for the production of ATP in glycolysis through the allosteric activation of phosphorylase and phosphofructokinase (PFK, Bogdanis, et al., 1996).

The ATP required for sustained muscle contraction is increasingly derived from breakdown of stored substrates. The breakdown of stored glycogen (glycogenolysis) forms a major process in the rapid generation of ATP (Greenhaff, et al., 1994, Pilegaard, et al., 1999), however the yield is still significantly lower compared to mitochondrial respiration. The complex reaction processes that form the glycolytic pathway results in the breakdown of glucose 6-phosphate to pyruvate, rapidly generating ATP (Greenhaff, et al., 1994). The high generating capacity of pyruvate from glycolysis and the inability of the mitochondria to take up pyruvate, results in conversion of pyruvate to lactate (through the pyruvate dehydrogenase reaction) in order to prevent the product inhibition of glycolysis (Baker, et al., 2010).

The production of lactate during intense SkM contraction was once thought to be a negative consequence of the inability of the mitochondria to sustain pyruvate transport, however it now considered that lactate plays a pivotal role in sustaining pyruvate production and regenerating cytosolic NAD^+ (Robergs, et al., 2004). The measurement of lactate that has been transported out of the SkM cells into the circulatory system has provided a key tool in understanding the metabolic responses to exercise (Beneke, et al., 2011). Moreover it has allowed for the characterisation of a subjects work rate and has been an important diagnostic tool of endurance performance in athletes and clinical populations (Faude, et al., 2009).

Additionally the measurement of lactate kinetics in predicting oxidative capacity of SkM during exercise has also been demonstrated to be highly accurate (Roecker, et al., 1998). However to date, much of the experiments investigating lactate production and associated biochemical and functional outcomes, have been limited to *in vivo* situations. Thus, studying the production of lactate from SkM cells can provide evidence for the metabolic dynamics associated with SkM response to contraction. Furthermore, the specific investigation of lactate production following mechanical signals is yet to be fully investigated and could provide evidence for a mechano-metabolic effect of exercise. The investigation of lactate production *in vitro* would also allow for a more controlled approach to assessing the potential for lactate as a signalling molecule to stimulate SkM adaptation (Hashimoto, et al., 2007).

Aerobic metabolism of stored substrates in the form of mitochondrial respiration (also termed electron transport chain and oxidative phospohorylation) produces the greatest yield of ATP (Holloszy and Kohrt, 1996, Baker, et al., 2010), but by definition requires the adequate supply of oxygen. The contribution of stored substrates to energy expenditure during muscular contraction is highly dependent on the intensity and duration of the exercise. An example of the differential substrate utilisation during exercise is depicted in Fig. 1-5.

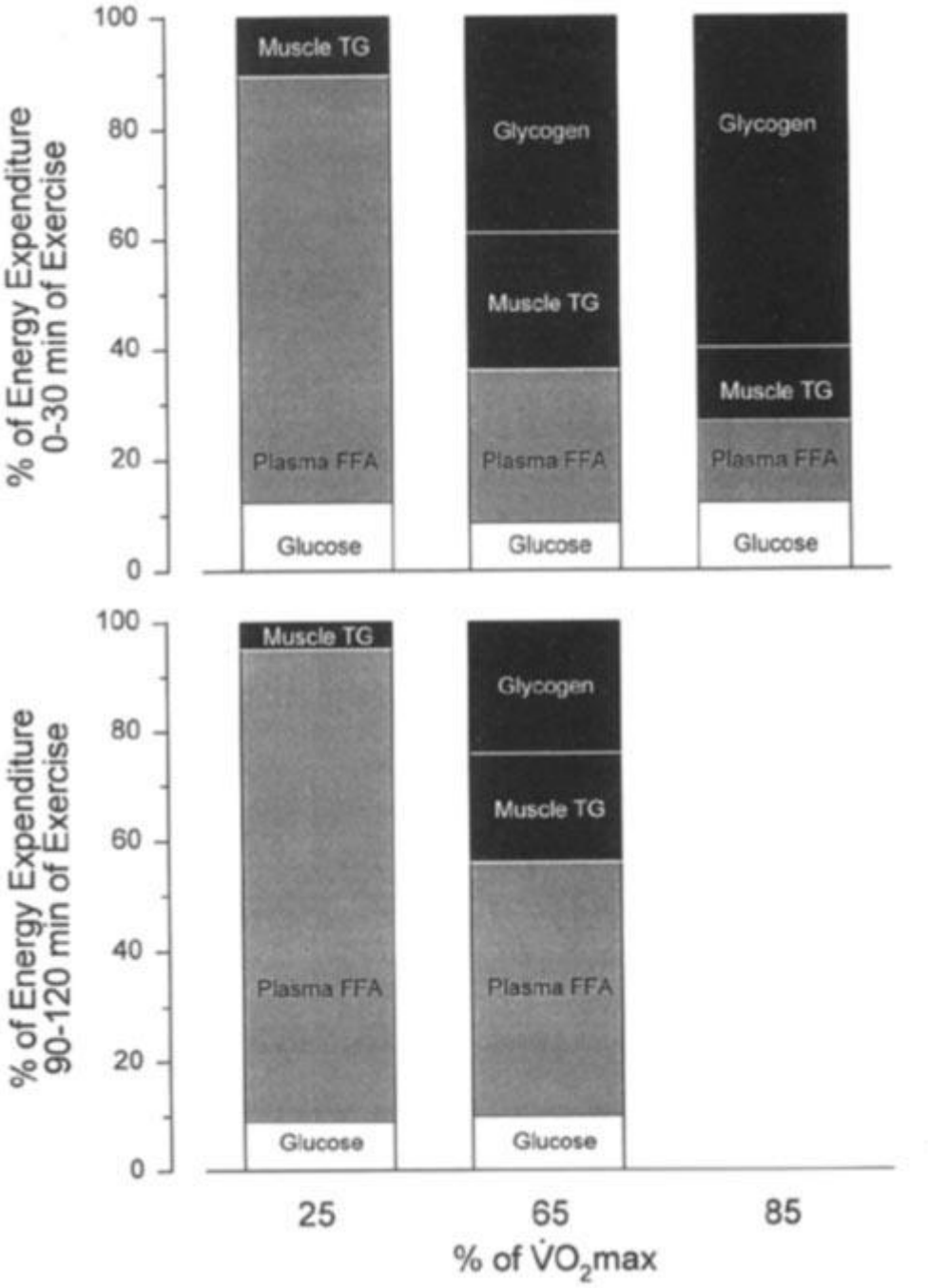

Figure 1-5. The percentage contribution to energy expenditure relating to available substrates and the intensity and duration of muscular contraction. (Taken from Holloszy and Kohrt, 1996).

Following the production of pyruvate from the reactions of glycolysis, it is converted to Acetyl co-ezyme A (Acetyl CoA) for entry into Kreb's cycle (also termed citric acid cycle and tricarboxylic cycle, Fig. 1-6) before the electron transfer process of the electron transport chain. One particular protein complex which is of great interest to SkM physiologists is the succinate dehydrogenase (SDH) complex (also known as complex II, Fig. 1-6). This complex has been shown to participate in both Kreb's cycle and the electron transport chain (Oyedotun and Lemire, 2004). In this regard, the activity of this complex has been shown to increase with exercise and training (Ishihara, et al., 2002, Silva, et al., 2009) and be reduced in pathological conditions such as SkM dysfunction associated with heart failure (Wust, et al., 2012). The measurement of this protein complex has been shown to reflect Kreb's cycle activity and maximal rate of oxygen consumption, when oxygen availability is not rate limiting (Bekedam, et al., 2003) and therefore can reflect SkM ability to produce ATP from aerobic metabolism.

Much of the literature surrounding the biochemical and molecular aspects of aerobhic metabolism in SkM is limited to *in vivo* contexts. If proteins such as SDH are going to be potential targets for the treatment of SkM pathologies, *in vitro* experimentation will be required to screen potential pharmacological agents. Furthermore, *in vitro* experimentation would allow for the investigation of such proteins in an isolated system to determine the exent of extrinsic and intrinsic mechanisms in dystregualting aerobic metabolism.

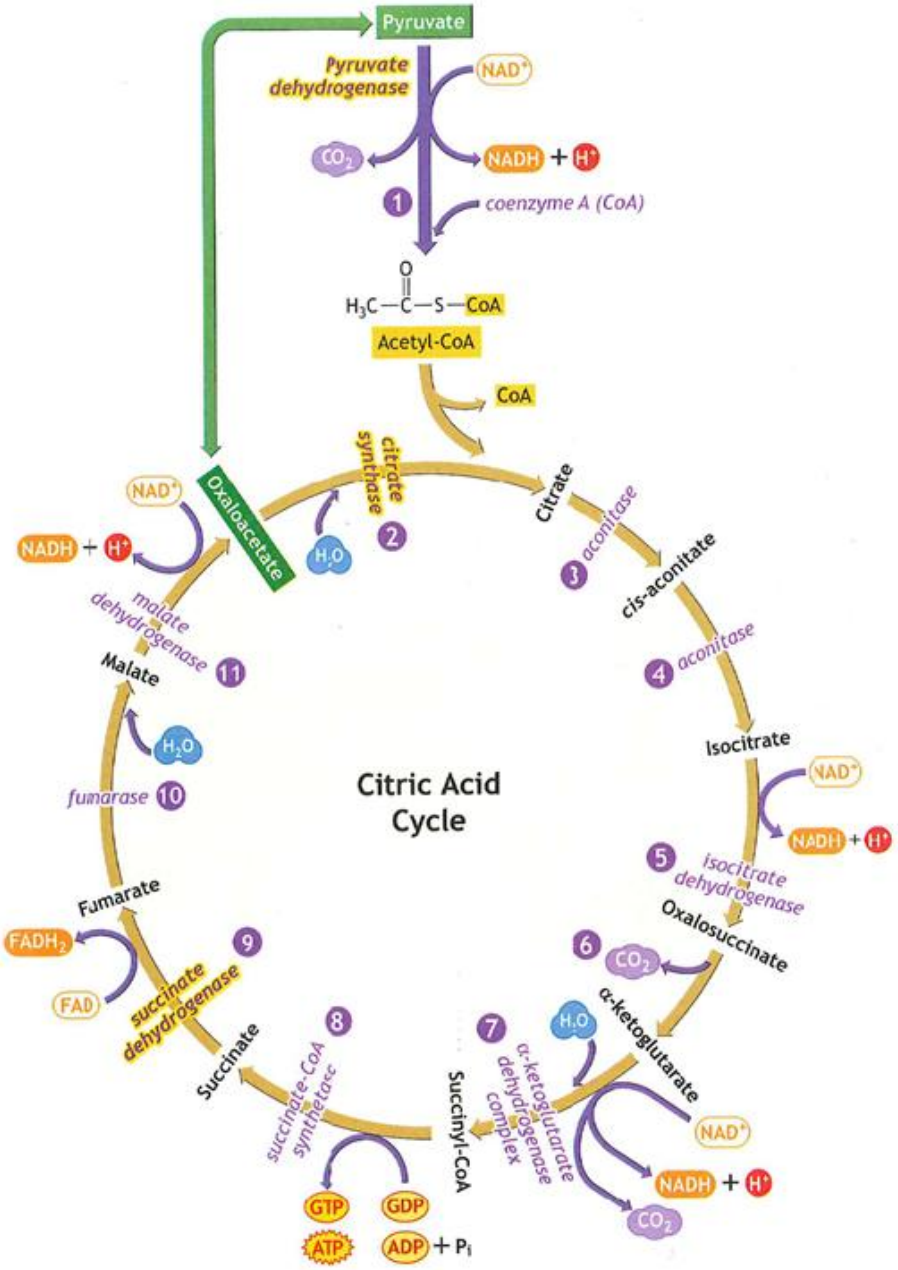

Figure 1-6. The Kreb's (Citric Acid) cycle- the complex nature of ATP generation. (From McArdle, et al., 2004).

1.6 Skeletal Muscle Mitochondrial Biogenesis

1.6.1 Increasing the oxidative potential of SkM following SkM contractile activity: PGC-1α, the master regulator of mitochondrial biogenesis (Adapted from Player and Lewis, 2012)

Increased glucose uptake and an alteration in substrate utilisation towards a greater reliance on fat metabolism, represent some of the fundamental adaptations in SkM metabolism in response to endurance exercise (Holloszy, 1967, Mole, et al., 1971, Oscai and Holloszy, 1971, Baldwin, et al., 1972). As such, endurance exercise has the ability to play a key role in the fight against epidemic metabolic disorders including; obesity, diabetes and hypertension. Further understanding the mechanisms that regulate this response will provide evidence for the development of exercise, but also pharmacological and potential genetic therapies for use in the clinic.

Despite the potential for physical activity in targeting these diseases, the exact cellular and molecular mechanisms that govern the adaptations have only recently begun to be understood (Coffey, et al., 2006). The pioneering work of John Holloszy demonstrated an increase in mitochondrial content and enzymes following exercise, providing the basic mechanism behind an increase in aerobic capacity with exercise training (Holloszy, 1967). The complex nature of the mechanisms along with many experimental limitations has hindered progress with regards to the co-ordinated nature of the genes and proteins involved in regulating this response. In the post genomic era it is now possible to investigate the role of every candidate gene with regards to its effect in SkM adaptation. In light of this, a surge in research investigating the molecular adaptations to exercise has provided us with a broad spectrum of potential mechanisms.

1.6.2 Signalling Mechanisms to activate PGC-1α protein: Primary and Secondary Messengers

The peroxisome proliferator-activated receptor co-activator-1α (PGC-1α) has been identified as a tissue specific transcriptional co-activator capable of regulating the response of metabolic pathways to external stimuli (nutritional, physical and environmental, Puigserver, et al., 1998). The activity of this protein has therefore been proposed to play a primary role in the adaptive response to exercise. The mechanisms activating this co-activator are varied and complex and therefore it is beyond the scope of this review to detail every proposed mechanism.

1.6.2.1 Ca^{2+}, Calmodulin Kinases and p38 MAPK

Despite the well characterised role for Ca^{2+} in excitation contraction coupling (ECC), a further role for this ion in regulating contraction induced-gene expression and muscle fibre phenotypes has been proposed (Berchtold, et al., 2000). This hypothesis stemmed from the seminal work of Buller et al., (1960) who demonstrated the change in phenotype of SkMs upon the transplantation of an opposing motor neuron in the cat (i.e. fast to slow and *vice versa*, Buller, et al., 1960). Force output and longevity is in part controlled and driven by motor nerve stimulation, which relates to the amplitude and duration of Ca^{2+} transients (Chin, 2005). The particular expression and level of expression of genes directly relates to the Ca^{2+} transient, a term that has been described as excitation-transcription coupling (Chin, 2005, Gundersen, 2011). A large number of genes have been suggested to be activated upon increases in Ca^{2+} transients including; Myosin Heavy Chain (MHC) isoforms (Allen, et al., 2002), Glucose Transporter 4 (GLUT4, (Olson and Williams, 2000, Ojuka, et al., 2002a, Ojuka, et al., 2002b, Ojuka, et al., 2003) and genes related to mitochondrial biogenesis (Ojuka, et al., 2002b).

Investigations into the acute effects of Ca^{2+} transients upon the SkM related to exercise have specifically taken the form of *in vitro* based models, using Ca^{2+} stimulants including Caffeine and Ca^{2+} ionophores.

Raising intra-cellular Ca^{2+} in L6 rat SkM myotubes increases the expression of proteins involved in mitochondrial biogenesis, an effect that was blocked by dantrolene, which prevents the release of Ca^{2+} from the sarcoplasmic reticulum (SR, Ojuka, et al., 2003). Furthermore, ionophore A23187 increases the gene expression of Cytochrome *c* in L6 myotubes, suggesting a role for Ca^{2+} in regulating this gene transcript associated with oxidative phosphorylation (Freyssenet, et al., 1999).

Ex vivo SkM preparations have further provided a mechanism of action for increases in genes and proteins associated with mitochondrial biogenesis. Increasing cytosolic Ca^{2+} using 3.5mM caffeine in rat epitrochlearis, does not elicit contraction, despite significant increases in the gene and protein expression of PGC-1α, COX-1 (cytochrome *c* oxidase I) and ALAS (δ-aminolevulinate synthase, (Wright, 2007). This increase is coupled with an increase in p38 MAPK, a response which is negated upon incubation with KN93, a Calmodulin Kinase (CaMK) inhibitor (Wright, 2007).

The increase in the mitochondrial enzymes was completely diminished by the addition of a p38 MAPK inhibitor SB202190, suggesting a p38 MAPK-dependent mechanism of action (Wright, 2007). Recently, isoform specific data has revealed a significant role for p38γ MAPK in the adaptive response of mitochondrial biogenesis and vascular angiogenesis. Using a muscle specific gene deletion in mice, a dominant negative allele for p38γ MAPK but not p38α MAPK and p38β MAPK, blocked the phenotypic and underpinning transcriptional mechanisms (PGC-1α and vascular endothelial growth factor, VEGF) to motor nerve stimulated contraction (Pogozelski, et al., 2009).

Together, these *in vitro, ex vivo* and *in vivo* data provide substantiation for the role of Ca^{2+} in activating a signalling cascade through CaMK and p38γ MAPK to induce mitochondrial biogenesis and metabolic adaptation.

1.6.2.2 AMPK: A critical energy sensing protein required to stimulate mitochondrial biogenesis

Muscle contraction is sustained by the production of ATP, generated from oxidation of stored and non-stored fuels sources alike; principally plasma glucose, stored muscle glycogen, plasma lipids and intramuscular triglycerides.

The 5' AMP-activated protein kinase (AMPK) is activated in response to a reduction in high energy phosphates (increase in the ATP:ADP and ADP:AMP ratios, (Xiao, et al., 2011) and hence acute energy deprivation (Reznick and Shulman, 2006) and as such has received attention as a putative energy sensor. The main function for AMPK is to increase the potential for ATP synthesis, whilst inhibiting energy consuming anabolic processes, along with acting as a signalling protein for gene transcription during and following rapid energy depletion (Jorgensen, et al., 2006).

Given this function of AMPK, it is not surprising that it has received widespread attention with respect to responses to exercise, a potent energy depleting stimulus. Various forms of experimental design have been used to investigate the role for AMPK as a signalling protein to activate PGC-1α.

Pharmacological agents have provided a central understanding for the influence of activation of AMPK in regulating increases in mitochondrial enzymes, increasing the potential for oxidative phosphorylation production of ATP. Bergeron et al., (2001) used *β*-guanadinopropionic acid (*β*-GPA) to chronically activate AMPK in rats for eight weeks (wk). Data demonstrated the increased binding of nuclear respiratory factor-1 (NRF-1), along with an increase in cytochrome *c* protein expression and total mitochondrial content (Bergeron, et al., 2001). Moreover, a dominant negative form of AMPK in mice ablates the *β*-GPA stimulated an increase in mitochondrial content as evidenced by electron microscopy in wild type (WT) littermates (Zong, et al., 2002) illustrating the necessity for AMPK in stimulating mitochondrial biogenesis.

These data provide key mechanistic evidence for the role of AMPK activation and subsequent signalling in inducing mitochondrial biogenesis through the activation of NRF-1 DNA binding activity (a downstream target of PGC-1α). The use of 5-aminoimidazole-4-carboxamide-1-β-D-ribonucleoside (AICAR) has also demonstrated a clear association between AMPK activation of PGC-1α and consequential increases in mitochondrial proteins (Leick, et al., 2010). Repeated injection of AICAR resulted in increases in cytochrome *c* oxidase I and cytochrome *c* protein expression (relative to a saline vehicle control) in white gastrocnemius of wild type animals, but not in whole body PGC-1α knock-out mice (Leick, et al., 2010). This data offers a clear pathway of AMPK-PGC-1α activation for increases in the mitochondrial proteins measured.

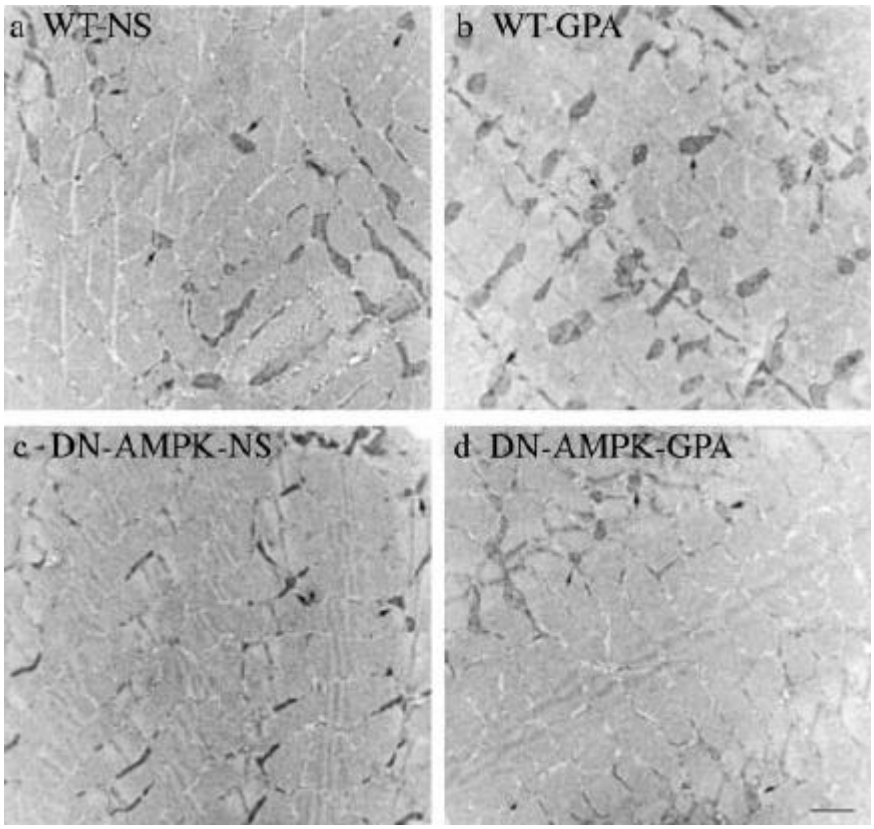

Figure 1-7. The necessity for AMPK in stimulating mitochondrial biogenesis. Electron micrograph demonstrating the requirement of AMPK in mitochondrial biogenesis. Dark staining represents the presence of mitochondria. (a) WT mouse (saline treated), (b) WT mouse (GPA treated to stimulate AMPK), (c) Dominant negative (DN)-AMPK transgenic mouse (saline treated), and (d) DN-AMPK transgenic mouse (GPA treated). Scale (bar = 1 μm). Note the reduced amount of dark staining in the AMPK-DN micrographs (c and d) in basal and AMPK stimulated conditions, illustrating the importance of AMPK in stimulating and maintaining mitochondrial content in SkM. Taken from Zhong et al. (2002).

Evidence for the exercise/contraction specific activation of AMPK-PGC-1α has been established using *ex vivo* and *in vivo* models. Atherton et al., (2005) used low frequency stimulation (LFS) of isolated rat extensor digitorum longus (EDL) to mimic endurance exercise and high frequency stimulation (HFS) to mimic resistance exercise. AMPK was activated at three hours (hr) post LFS, whilst HFS failed to increase AMPK activity (Atherton, et al., 2005).

In vivo data has provided contrasting findings with regards to the role of endurance and resistance exercise activation of AMPK, with particular emphasis on training status.

Some indication for the training specific nature of AMPK activation was shown by Coffey et al., (2006), who demonstrated an increase in AMPK activation following endurance exercise in non-endurance trained weight lifters, whilst no AMPK activation was evident in endurance trained athletes (Coffey, et al., 2006).

Conversely, AMPK was activated in endurance trained athletes that undertook strength training, whilst no activation was observed in strength trained athletes (Coffey, et al., 2006). This data suggests the activation of AMPK is dependent on a novel stimulus to induce the metabolic milieu required. Contrary to this data, it has been shown that ten wk of training is not sufficient to suppress the activation of AMPK in either strength or endurance trained athletes, data that is coupled with increases in mitochondrial protein fractional synthetic rate (Wilkinson, et al., 2008). Together these data demonstrate the necessity for AMPK activation during and following exercise for the resulting increases in mitochondrial protein, leading to enhanced oxidative potential for future periods of metabolic challenge.

The up-stream intra-cellular mechanisms that regulate the activation of these primary and secondary messengers for PGC-1α stimulation are yet to be elucidated. The degree to which such proteins are mechano-senistive has not been explored, with much focus on the metabolic determinants. As such, this provides a rationale for the use of a mechanically regulated controlled model to investigate whether mechanical signals have a part to play in this important cellular response. Furthermore, the ability to analyse intra-muscular metabolites alongside the activation and localisation of particular proteins, presents problems with regards to tissue abundance in human exercise studies. Moreover, the influence of single genes and proteins required for the activation of PGC-1α can only be achieved through the development of animal mutant models.

It is also difficult to isolate the intrinsic mechanisms that regulate PGC-1α activation *in vivo* due to the integrated nature of SkM. Thus, it is problematic to identify the key primary and secondary messengers intrinsic an extrinsic to SkM in realtion to PGC-1α and related transcriptnioal mechanisms. Targetted *in vitro* experiments delineating the primary and secondary activators of PGC-1α are warranted, in order to fully elucidate its role in response in mitxchondrial biogenesis.

1.6.3 PGC-1α: Post activation Transcriptional Regulating Mechanisms

Mitochondrial biogenesis occurs through the co-ordinated expression of both nuclear and mitochondrial genomes. Upon the activation of PGC-1α following exercise through the many mechanisms discussed here, it co-activates transcription factors required to induce mitochondrial biogenesis. PGC-1α activates many genes indirectly associated with increasing mitochondrial respiratory chain content, including NRF-1 and NRF-2 (Scarpulla, 2011). PGC-1α has been shown to activate the estrogen-related receptor-α (ERRα) and in conjunction with NRF-2α increases the expression of respiratory chain genes (Scarpulla, 2006, Zhang, et al., 2006).

Cytochrome *c* has been used in a multitude of experiments as a marker of mitochondrial density. Therefore, understanding the transcriptional regulation of this gene is key to determining what regulates mitochondrial density.

Evans and Scarpulla (1988) identified key elements on the promoter region of the cytochrome *c* gene, one of which binds NRF-1 protein, along with a cAMP response element (CRE) site (Evans and Scarpulla, 1989). If the NRF-1 or CRE sites are mutated, any effect in cytochrome c gene transcription to electrical stimulation of SkM is attenuated, suggesting an NRF-1 and CRE dependent mechanism for the increased transcription of cytochome *c* (Xia, et al., 1998). The co-ordinated expression of NRF-1 and NRF-2 also activates Tfam, which co-ordinates the transcription of mitochondrial DNA (mtDNA, Scarpulla, 2008).

Tfam has also been shown to play a significant role in mtDNA replication, providing a RNA primer required for initial mtDNA synthesis (Hood, 2001).

The myocyte enhancer factor-2 (MEF-2) is a transcription factor required for the expression of many muscle specific genes, including the regulation of the glucose transporter-4 (GLUT-4) promoter (Ojuka, et al., 2002a) and subunits of the respiratory chain COXVIaH and COXVIII (Lenka, et al., 1996). The transcriptional activity of MEF-2 is controlled as a balance between suppression by histone deacetylases (HDAC's) and activation by PGC-1α and p38 MAPK (McGee and Hargreaves, 2004). Following cycling exercise HDAC-5 is exported from the nucleus, allowing for the association between PGC-1α and MEF-2 (McGee and Hargreaves, 2004). Moreover, at rest the majority of PGC-1α is found in cytosolic fractions, translocating to the nucleus 3 hr following an acute bout of high intensity exercise (Little, et al., 2010), an association that is related with increased levels of mitochondrial protein content 24 hr following exercise (Safdar, et al., 2011). These data together provide evidence for the role of PGC-1α in the activation of MEF-2 and nuclear encoding genes associated with increasing mitochondrial content and glucose transportation.

Exercise is a potent stimulator of mitochondrial biogenesis, a compensatory mechanism to increase the oxidative potential of SkM. In doing so, SkM has the greater potential to oxidise fat and as such exercise forms a key preventative and treatment modality for metabolic diseases. To this end, the use of exercise and other therapies which have the potential to activate PGC-1α will be useful in the clinic for metabolic diseases. The molecular mechanisms that govern this response have begun to be elucidated; however the co-ordination of *in vivo* and targeted *in vitro* based experiments will provide further evidence into this complex cellular adaptation. Moreover, the specific use of tissue engineered SkM constructs will provide a highly controlled experimental design to delineate the molecular regulation of this vastly complex.

Particulaly, the use of models that are amenable to electrical and mechanical stimulation will be fundamental in identifying the basic mechanisms that are activated in response to these key stimuli for SkM contraction. Additionally, the ability to exogenously add proteins, pharmacological agents and potential neutraceuticals to an isolated system demonstrates the plausibility of tissue engineered SkM in understanding PGC-1α and mitochondrial mechanisms.

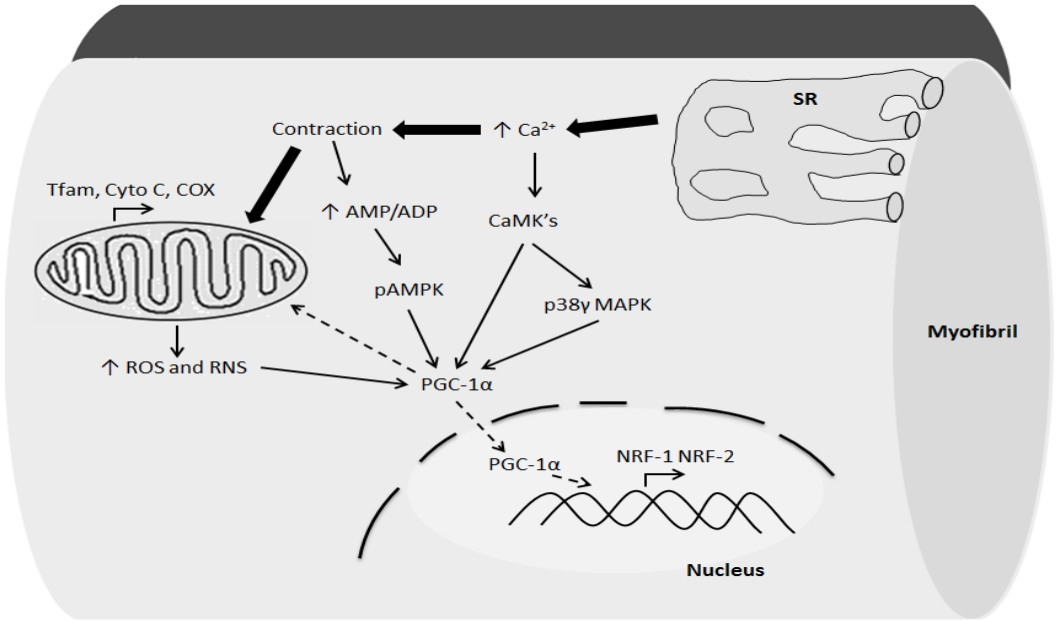

Figure 1-8. Intra-cellular signalling mechanisms regulating PGC-1α activation and post-activation transcriptional mechanisms.

Abbreviations; SR (sarcoplasmic reticulum), Ca^{2+} (Calcium ion), CaMK's (calmodulin kinases), p38γ MAPK (p38 gamma mitogen activated protein kinase), PGC-1α (peroxisome proliferator-activated receptor co-activator-1 alpha), NRF-1 and NRF-2 (nuclear respiratory factors 1 and 2), AMP (adenosine mono-phosphate), ATP (adenosine tri-phosphate), pAMPK (phosphorylated 5' AMP-activated protein kinase), Tfam (mitochondrial transcription factor A, mTFA), Cyto C (cytochrome *c*), COX (cytochrome *c* oxidase subunits), ROS (reactive oxygen species), RNS (reactive nitrogen species).

1.7 The Molecular Regulation of Skeletal Muscle Mass

SkM mass contributes to overall health and wellbeing and it is clear that the loss of SkM mass with age (sarcopenia) or disease (cachexia) contributes to morbidity and mortality (Carmeli, et al., 2002, Rantanen, et al., 2003). SkM not only functions to provide movement and stability of the skeleton, but also contributes to the greatest metabolic pool within the human body (Bouzakri, et al., 2005). In this regard SkM mass loss contributes to increased risk of developing metabolic diseases such as type II diabetes (Srikanthan and Karlamangla, 2011). These health implications make the maintenance of SkM mass of significant clinical importance.

SkM mass is maintained when a balance between protein synthesis and protein loss is achieved, with muscle mass loss presenting when there is a shift to net protein loss (Wust and Degens, 2007). Situations of tissue protein loss can be observed in the systemic system and has been characterised in urine, whereby nitrogen balance can be estimated (Wagenmakers, 1998). Muscle mass gain is achieved with a net increase in protein synthesis, which is a common consequence of resistance exercise (Dreyer, et al., 2006, Holm, et al., 2008) and nutritional stimulus (Phillips, 2012). The molecular regulation of muscle mass is vastly complex, with integration between systemic and intrinsic factors that stimulate transcriptional and post-translational mechanisms. The control of anabolic and catabolic signals will be explored in the following sections.

1.7.1 Insulin-like Growth Factor-I (IGF-I)

The unique characteristic of insulin-like growth factors is that the receptor (IGF-I receptor) is expressed in all tissues and cell types (Clemmons, 1998), indicating the high degree of importance this protein family plays in whole organism physiology. With regards to SkM physiology, IGF-I is of particular interest as it functions in embryonic SkM development (Liu, et al., 2012), myo-nuclear accretion (Vandenburgh, et al., 1991), protein synthesis (Adams and McCue, 1998) and *in vitro* myogenesis (Hill, et al., 1985).

IGF-I acts at all levels of the endocrine system (endocrine, paracrine and autocrine), with 75 % of systemic IGF-I being produced by the liver (Schwander, et al., 1983). Remarkably, abolishment of IGF-I produced from hepatocytes in mice leads a 75 % reduction in systemic IGF-I without impairing growth (Sjogren, et al., 1999). This demonstrates the importance of IGF-I production from sources other than the liver in regulating growth and tissue maintenance. Increasing IGF-I through exogenous means, does not lead to increase protein synthesis in skeletal of humans (Yarasheski, et al., 1993, Musaro, et al., 2001), however genetic manipulation in mice using global or muscle specific overexpression leads to hypertrophy (Musaro, et al., 2001). Moreover, IGF-I mutant mice (IGF-I -/-) display underdevelopment of SkM (Powell-Braxton, et al., 1993). These data together provide evidence that IGF-I derived from muscle sources is of particular importance in stimulating myogenesis, hypertrophy and maintaining muscle mass.

The action of IGF-I occurs through the IGF-I receptor, which is a heterotetramer that undergoes a conformational change following ligand binding with IGF-I (Clemmons, 2009, Fig. 1-7). This conformational change leads to the activation of the intrinsic tyrosine kinase which allows the docking of IRS-I (Clemmons, 2009). IRS-I then acts as docking protein for several signalling proteins including PI3-K, which forms part of the mammalian target of rapamycin (mTOR) signalling cascade (Glass, 2003a, Glass, 2003b, Fig. 1-7), leading to an increase in the activity of the ribosomal machinery (Baar, 2006). The activation of this signalling cascade is highly induced by SkM overload, stretch as seen in a lapine model (McKoy, et al., 1999) and resistance exercise in humans (Adams and Haddad, 1996, Allen, et al., 1997).

However, evidence has been presented to suggest a functional IGF-I receptor is not needed for the activation of mTOR following SkM overload (Spangenburg, et al., 2008). This is supported by fact that IGF-I is expressed at far later time points than mTOR following overload in mice (Spangenburg, et al., 2008).

This seemingly unclear evidence for the role of IGF-I signalling in stimulating hypertrophy, may reside in the potential role of IGF-I in myogenesis. The myogenic role for IGF-I in embryonic and postnatal growth is undisputed (as discussed previously) and the acquisition of nuclei following resistance exercise is well documented in humans (Petrell, et al., 2006, Petrella, et al., 2008). The notion of a 'ceiling size' to which a muscle fibre can hypertrophy exists, due to the nuclei only being able to control a finite amount of cytoplasm (myonuclear domain, Harridge, 2007). The incorporation of activated SC's into existing muscle fibres (myonuclear addition) following resistance exercise and overload may provide an explanation for the early or acute protein synthesis and delayed myogenic response (myonuclear addition) stimulated independently or dependently on IGF-I.

1.7.2 IGF-I Binding Proteins (IGFBP's)

The complexity of IGF-I signalling is amplified through the control by IGFBP's, proteins that act to carry IGF-I in either the blood or bind it to the ECM (Clemmons, 1998). IGFBP's also regulates the interaction of IGF-I with its receptor (Hwa, et al., 1999a, Hwa, et al., 1999b) whilst increasing the half of the protein and therefore plays a major role in modulating its action.

There have been six IGFBP's cloned and sequenced, with their differential effects in different tissues studied extensively (Stewart and Rotwein, 1996). IGFBP's in high concentrations inhibits growth (Wolf, et al., 2005) and a transgenic mouse overexpressing IGFBP-2 displays reduced myofibre size (Rehfeldt, et al., 2010). Furthermore, the ability of myoblasts to proliferate is also hindered in IGFBP-2 (Rehfeldt, et al., 2010). There is evidence that IGFBP-2 and -5 have extensive effects on SkM studied *in vivo* and *in vitro*. This is exemplified when increased circulating serum concentrations of IGFBP-2, relates to disability and reduced muscle strength in elderly men (van den Beld, et al., 2003). Additionally an increase in IGFBP-2 mRNA has been shown to underpin the reduced myogenesis of parent C2 vs. daughter C2C12 myoblasts *in vitro* (Sharples, et al., 2011).

IGFBP-5 mRNA has been shown to decrease in a model of overload induced hypertrophy in rats (Awede, et al., 2002), whilst unloading of the overloaded hind limb resulted in atrophy coupled with an increase in IGFBP-5 mRNA (Awede, et al., 1999). The interplay between IGFBP-5 and the action of IGF-I is illustrated when a temporal effect of decreasing IGFBP-5 mRNA and increasing IGF-I mRNA was found (Awede, et al., 1999). Also, using a model of multiple population doublings of C2C12's an increase in IGFBP-5 mRNA was shown to support reductions in myogenesis and myotube diameter (Sharples, et al., 2011). These data together provide evidence for the clear role of IGFBP's in regulating the action of IGF-I, contributing to the modulation of muscle mass and myogenesis.

The data surrounding the interaction of IGFBP's with IGF-I is evident in both *in vivo* and *in vitro*, as described above. With evidience to suggest the mechanical regulation of IGF-I *in vitro* (Cheema, et al., 2005), experiments are yet to be conducted surrounding the influence of mechanical signals on IGFBP expression. Such experiments conducted in a more representative model of SkM *in vitro* (in terms of macroscopic and microscopic structure) would allow for an isolated approach to investigate these putuative key genes in regulating muscle mass.

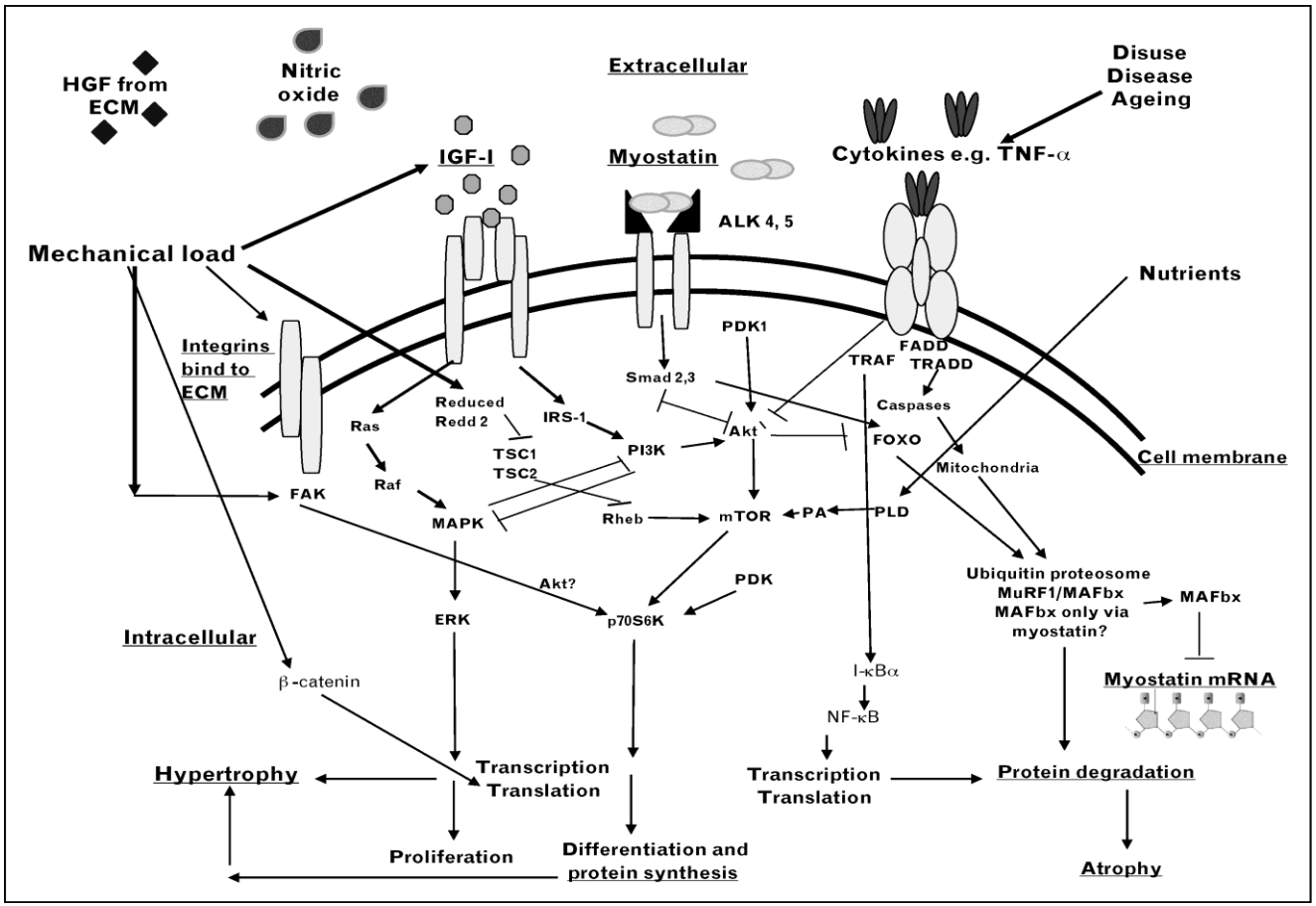

Figure 1-9. The molecular regulation of SkM mass. Protein signalling and gene transcriptional mechanisms associated with protein synthesis and protein ubiquination. (From Sharples and Stewart, 2011).

1.7.3 Matrix Metalloproteinases (MMP's)

MMP's are zinc dependent metallo-peptidases which serve to remodel the ECM (Lewis, et al., 2000) as a physiological process of adaptation, degeneration and regeneration following muscle cell trauma. This cycle of degeneration and regeneration can present itself in a pathophysiological manner, as evident in Duchenne muscular dystrophy (DMD) and in the *mdx* mouse (Bulfield, et al., 1984), whereby the absence of the dystrophin protein prevents myofibre stability with the ECM. These enzymes are categorised into four classes based upon structure and substrate specificity, are synthesised in a latent form and require activation by peptidases to function (Lewis, et al., 2000).

The MMP's -2 and -9 (Gelatinases –A and –B respectively) have been shown to form a major part of the regeneration process, degrading components of the ECM required to facilitate activated SC migration and fusion into the site of trauma (Kherif, et al., 1999). This is supported by *in vivo* (Kherif, et al., 1999) and *in vitro* data (Lewis, et al., 2000), demonstrating the activity of MMP's -2 and -9 in the migratory and fusion phases of myoblasts. Moreover, this data provides clear evidence that the secretion of MMP's from inflammatory activated cells (leukocytes) and SkM cells follows a temporal expression pattern. MMP-9 is expressed in the acute inflammation and activation of SC's, whereas MMP-2 is expressed during myoblast fusion (Kherif, et al., 1999, Lewis, et al., 2000, Dahiya, et al., 2011).

Data to support the role of MMP's in regeneration and adaptation of SkM is further underpinned by extensive hypertrophy that is evident in mice overexpressing an active mutant muscle specific MMP-9 (Dahiya, et al., 2011). Increases in fibre cross sectional area, contractile apparatus protein and isometric force production were all consequences of this overexpression (Dahiya, et al., 2011), providing a clear indication of the extent to which MMP-9 can regulate hypertrophy.

However, the inhibition of MMP-9 using a specific antibody demonstrates the increased regeneration and reduced fibrosis following induced trauma (Zimowska, et al., 2008). These data together suggest there may be a physiological balance of MMP activity required to facilitate sufficient remodelling, whilst ensuring minimal fibrosis.

Furthermore, MMP's have been shown to increase the bio-availability and hence action of growth factors required for SC activation, fusion and hypertrophy. MMP's activate IGF-I through the proteolysis of the IGFBP's (Coppock, et al., 2004), increasing its action and stimulating signalling through Akt and mTOR.

The response of MMP's has also been shown following both endurance (Carmeli, et al., 2002, Rullman, et al., 2007) and resistance-based (Madden, et al., 2011) exercise, despite high within and between subject variability. The response of MMP's in this manner to different modes of exercise illustrates the generalised activation following different contraction types and exercise duration. Thus, the measurement of MMP's in response to SkM contraction forms an indication of a physiological response to ensure satisfactory adaptation and regeneration.

1.7.4 Myostatin and the Ubiquitin Proteasome Pathway

SkM mass is also negatively regulated through pathways that serve to inhibit protein synthesis or increase proteolysis. The most studied pathways involved in these processes are the myostatin and ubiquitin proteasome pathways (UPP). It is acknowledged that there are multiple pathways that contribute to SkM proteolysis, including oxidative stress, nuclear factor κβ (NF-κβ) and tumour necrosis factor-α (TNF-α, Jackman and Kandarian, 2004), however it is beyond the scope of this thesis to review these areas. The increase of these genes and proteins has been shown to be present in the aging population (Gumucio and Mendias, 2012) as well as in conditions of cachexia (McFarlane, et al., 2006). Conversely, a reduction in their expression has been shown as a response to resistance exercise to stimulate hypertrophy (Roth, et al., 2003, Louis, et al., 2007).

Myostatin forms part of the transforming growth factor-β (TGFβ) superfamily of proteins and serves to negatively regulate SkM mass through various mechanisms. The discovery of myostatin was coupled with the identification of naturally occurring mutations, whereby excessive muscle growth leads to a hypertrophic phenotype (e.g. Belgian Blue Cattle, McPherron and Lee, 1997). This discovery has led to a wealth of research to investigate the mechanisms whereby myostatin has its influence.

One potential mechanism for myostatin in preventing SkM hypertrophy or stimulating a reduction in muscle mass is through inhibition of SC activation and proliferation. A dose dependent reduction in myoblast proliferation is seen when incubating C2C12 myoblasts with myostatin, through the inhibition of *Pax7* and MyoD co-localisation (Thomas, et al., 2000, Langley, et al., 2002). The inhibition of MyoD by myostatin further prevents the fusion of myoblasts (Langley, et al., 2002). Data also demonstrates the effect of myostatin on the expression of 'atrogenes' MuRF-1 (muscle RING finger-1) and muscle atrophy factor box (MAFBx) that form part of the UPP, a mechanism that is dependent on the expression of forkhead box O-1 (FoxO-1, McFarlane, et al., 2006). Myostatin also inhibits the Akt-mTOR pathway of protein synthesis (Amirouche, et al., 2009), a mechanism that is distinct from interactions with the atrogenes (Trendelenburg, et al., 2009, Goncalves, et al., 2010).

The activation of MuRF-1 and MAFBx leading to a proteolysis, is partly controlled by the ubiquination and subsequent degradation of proteins at the lysosome that have been marked by these E3 ligases (Yang, et al., 2006, Baehr, et al., 2011). The deletion of MuRF-1 leads to the sparing of SkM tissue breakdown following denervation or glucocorticoid treatment (Baehr, et al., 2011), illustrating the effect of this gene in regulating muscle mass in response to these traumas.

These proteins and genes have been shown to be modulated by both endurance and resistance modes of exercise (Coffey, et al., 2006, Nedergaard et al, 2007), with MAFBx playing a significant part in regenerating muscle following damaging exercise (Okada, et al., 2008). A temporal effect has also been shown with MuRF-1 and MAFBx mRNA expression, with an increase after an acute bout, with a reduction in proceeding bouts of exercise (Mascher, et al., 2008).

The effect of myostatin, MuRF-1 and MAFBx on SkM mass is evident in the basal and exercised conditions, elucidating a potent effect upon proteolysis. Investigating the manner in which these genes are activated following exercise, specifically with particular modes and contraction types, will enable the development of targeted therapies for the alleviation of SkM wasting diseases. Furthermore, investigating the role of mechanical signals in the activation or suppression of these genes will provide mechansistic evidence as to the mechano-transcrioptional profile following exercise. Moreover, the instrinsic regulation of these genes following exercise or overload has not been investigated, providing rationale for the investigation in an isolated system indepdent of systemic factors and supporting tissues. *In vivo* models of SkM and exercise are limited in being able to investigate the mechanisms discussed above, with the limitation being explored further below.

1.8 Limitations of *in vivo* testing to study cellular and molecular responses to exercise

Notwithstanding the importance of human investigations for understanding of the adaptation of SkM following exercise, methodological limitations preclude many questions from being answered. The inherent variability in SkM response to exercise in humans often masks the identification of a particular protein or gene which may have a role in regulating adaptation. This has often lead to the use of animal genetic clones in exercise studies, which allows for a greater amount of experimental control, along with permitting the development of dominant/negative mutant animals to investigate the role of a particular gene.

The use of such animals in research does however prevent translation to human physiology due to the obvious anatomical distinctions between rodents and human beings. Of particular concern with both human and animal studies are the ethical constraints surrounding the experimental design, which often relate to the type of exercise or stimulation protocol and sampling of the tissue. In many cases human studies are limited in the number of biopsy procedures that can be performed on one individual, whilst animals are most commonly sacrificed following the experiment.

Recently, evidence has been reported concerning the variability in the expression and phosphorylation of proteins highly implicated in protein synthesis; proteins that have received widespread attention in the field of exercise physiology in recent years. Caron et al., (2011) reported an 83 % increase in Akt and P70 S6K phosphorylation between biopsy samples taken from the *vastus lateralis* (VL) of the right leg in the morning (R1) and the left leg in the afternoon (AF). However, it was found that a second rested biopsy in the right leg (R2) did not affect the expression or phosphorylation of any of the proteins investigated, compared to (R1). These authors also found a significant effect of low intensity mobilisation on P70 S6K phosphorylation compared to R2 ($p < 0.05$, Caron, et al., 2011). Due to the nature of multiple biopsies with respect to sequential samples being taken from sites certain distances away from the previous biopsy, it is also conceivable that the fundamental anatomy and physiology of multiple samples may differ.

The data presented here clearly demonstrates the necessity to standardise biopsy protocols, in the rested and exercising conditions, in order obtain valid results relating to the proteins of interest. The effect of multiple biopsy sampling has also been shown to affect the transcriptional response of particular genes (Friedmann-Bette, et al., 2012). In a crossover design experiment, 11 subjects undertook standardised squatting exercise or vibration exercise, with biopsies being obtained from the VL pre and at three time-points post exercise.

As a control group, 8 non-exercising control participants were subjected to four biopsies at equivalent time points. Similar changes (increased or decreased) in the gene expression of interleukin 6, interleukin 6-receptor and IGF-I amongst others, were found between the control group and the exercising group (Friedmann-Bette, et al., 2012). The authors concluded from this data that multiple biopsy sampling can influence the expression of the genes investigated, with no additive or supressive effect of exercise. As such, it is difficult to make a judgement upon the influence of the exercise condition upon the expression and regulation of these genes. It is important to consider however, that the exercise protocol used may not have been potent enough to induce the activation of the investigated genes. Moreover, other variables including the sample sizes, the training staus and heterogeneity of the population sample used and the tissue processing methodologies may all confound the observed response. The necessity for large sample sizes to generate required statistical power in human investigations is also a product of human heterogeneity, a limitation that does not translate to cell line-based *in vitro* experiments. The use of a cell line, whereby all the cells are genetically identical allow for the highly controlled investigation of putative regulatory genes or proteins.

The inherent variation in human repsonses to exercise plays a significant role in observed effects and may often confound data. Recent evidence has provided support for such a notion, whereby individuals respond to a large extent in response aerobic (Timmons, et al., 2010) and resistance (Phillips et al., 2013) exercise. Such variability is governed by the expression of key genes, which are dysregulated in non-adaptive phenotypes (Timmons et al., 2010, Phillips et al., 2013). This variation makes it difficult to ascertain the roles of particular genes in humans and poses the question as to why an exercise stimulus can or cannot activate certain genes and what the upstream mechanisms are.

These data also provide strong evidence for the use of a system that does not rely upon a traumatic biopsy procedure, which has been demonstrated to influence the expression of proteins and genes which may have vital roles in the adaptation of SkM to exercise. Furthermore, the use of an isolated *in vitro* system allows for the investigation of the individual stimuli (mechanical, metabolic, etc.) which contribute to the expression of key genes regulating phenotypic adaptation.

When seeking to understand the adaptation of SkM to exercise, it is important to delineate between intrinsic and systemic regulation of proteins and genes. *In vivo* investigations permit the investigation of the integration between SkM and the systemic environment, however the influence of individual systemic factors and the intrinsic environment in isolation are not possible. Of particular interest is a recent investigation that demonstrated the requirement of intact adipocytokine signalling for the activation of PGC-1α following exercise (Li, et al., 2011). Utilising the obese ob/ob mice (which display dysregulated adiponectin and leptin mediated AMPK signalling), responses to exercise training in terms of signals that mediate mitochondrial biogenesis were absent (Li, et al., 2011). In order that the authors could ascertain a causal relationship between the reduced adipocytokine signalling and the effect upon mitochondrial biogenesis, *in vitro* experiments were conducted treating the cells with adiponectin and leptin confirming the positive influence of these proteins (Li, et al., 2011).

Such data can be considered proof of concept and requires further investigation to analyse the influence of intrinsic stimuli and proteins/genes that regulate PGC-1α expression. Current monolayer *in vitro* approaches to do not allow for such investigation, providing evidence for the use of 3D tissue engineered SkM. The multiple stimuli that effect SkM physiology and function, including neural activation and blood flow, means isolating the effect of mechanical signals alone extremely challenging.

Taking these limitations of *in vivo* exercise together, provides a strong rationale for the use of an *in vitro*, isolated system to further understand the role of mechanical signals on SkM physiology. The use of such systems to-date is extensively discussed below, however it is important to note there is currently no *in vitro* model of SkM that recapitulates *in vivo* tissue and that is also amenable to stimulation to model exercise or SkM loading.

Taking into consideration the limitations of current *in vivo* investigations and the requirement for the development of an *in vitro* system, the following research questions are proposed;

1. Can an *in vitro* model of SkM recapitulate the biochemical and molecular response seen with *in vivo* exercise?
2. What contribution do mechanical signals play in the regulation of key adaptative genes?
3. What is the intrinsically regulated response of genes required for adaptive phenotypes?

To be able to address these research questions, the development and utilisation of current cell culture-based systems will be discussed and critiqued.

1.9 Culture of Muscle Cells *In Vitro*

SkM cells have been cultured *in vitro* for many years, with early studies identifying the spontaneous contraction of muscle cells derived from the patella region of a rat (Murray and Pogogeff, 1946, Pogozelski, et al., 2009). These pioneering experiments developed a field of cell biology which would contribute not only to the understanding of SkM development (myogenesis) and physiology, but also cell biology in general.

1.9.1 Primary Muscle Cell Cultures

The use of primary tissue for the isolation of SkM cells has taken the form of two main isolation procedures. Firstly, explant cultures rely on the tissue maintaining the ability for SC activation, migration and commitment to the myogenic lineage; a technique which has been successfully used for many years (Pogogeff and Murray, 1945, Murray and Pogogeff, 1946). Secondly, enzymatic digestion of SkM tissue relies on the dissociation of the SC's from the basal membrane, which has been achieved using various enzymes (collagenase, dispase, trypsin to name a few). These methods display various amounts of success in isolating myogenic cells, with the inability to serially passage to obtain large cell numbers for experiments being one the main disadvantages of primary cells (Machida, et al., 2004).

However, isolating primary cells ensures a heterogeneous population of cells is obtained. This is an important factor when studying SkM *in vitro* considering the heterogeneous population of cells *in vivo*. Moreover, the influence of the non-myogenic population of cells has been demonstrated to influence the myogenic potential and mechano-contractile phenotype of muscle derived cells (MDC's) *in vitro* (Brady, et al., 2008). Conversely a myogenic only population of cells allows for the investigation of intrinsically regulated mechanisms of SkM cells.

1.9.2 SkM Cell Lines

The inherent variability and limitations of using primary sources for MDC's contributed to the development of cell lines that display similar genotype and phenotype characteristics of primary cells, with increased control and homogeneity. The original myogenic cell lines were the L8, L84 and the C2 lines (Yaffe and Saxel, 1977). A further sub-clone of the original C2 cell line was characterised by Blau et al., (1985) termed the C2C12 sub-clone, which is the most well used myogenic cell line cited in the literature (Blau, et al., 1985).

These cell lines were based upon the differentiation characteristics of cells isolated from primary sources and have been used to study myogenesis and postnatal muscle physiology. The control and reproducibility associated with these cells lines, has contributed to a greater understanding of the intrinsic molecular mechanisms associated with particular physiological and pathophysiological conditions within SkM.

1.9.3 Monolayer Cell Culture

MDC's and muscle cell lines have most commonly been cultured in a monolayer environment. Despite the relative simplicity of this technique, this environment does not recapitulate the 3D nature of SkM. Undeniably, the morphology of cells cultured in monolayer does not represent that of *in vivo* SkM (Smith, et al., 2012).

The ability of the cells to receive physical cues from attachment to a matrix in 3D seems to be the key influencing factor in obtaining a morphological and physiological representation of *in vivo* SkM. Furthermore, as one of the main functions of SkM is to produce force for mechanical movement (Baar, 2005), a monolayer culture system does not allow for such measurement. This notion has led to the development of tissue engineered SkM constructs.

1.10 SkM Tissue Engineering

3D SkM culture systems have successfully been developed, using various methods to develop fused SkM cells displaying *in vivo*-like morphology and function. The use of these tissue engineered models in basic physiological research is emerging (Khodabukus, et al., 2007), however the goal of tissue engineering as a field is to ultimately provide a replacement for damged or diseased tissue (Machingal, et al., 2011, Corona, et al., 2012,).

For successful 3D *in vitro* culture, the composition of the extra cellular matrix (ECM) used needs to promote the alignment and fusion of seeded myoblasts (Klumpp, et al., 2010).

This has been achieved using both synthetic (Acarturk, et al., 1999, Saxena, et al., 1999, Shah, et al., 2005) and naturally derived polymers (Vandenburgh and Kaufman, 1979, Vandenburgh, 1988, Vandenburgh, et al., 1989, Vandenburgh, et al., 1991, Powell, et al., 2002, Cheema, et al., 2003, Cheema, et al., 2005, Huang, et al., 2005, Brady, et al., 2008, Khodabukus and Baar, 2009, Mudera, et al., 2010, Khodabukus and Baar, 2012, Smith, et al., 2012).

It has been suggested that the rigidity of synthetic polymers may affect the contractile properties and function of the developed myotubes and if the polymer is bio-degradable this may affect the alignment of cells achieved (Bian and Bursac, 2009, Bian and Bursac, 2008, Thorrez, et al., 2008). Moreover, the proteins required for cell-matrix interaction via integrin-mediated cell attachment are coated onto the scaffold to ensure cell attachment and viability (Bacakova, et al., 2003).

The use of naturally derived polymers (including fibrin and collagen) has been shown to overcome these issues. The rapid polymerisation allows for an even distribution of the cells seeded, and the nano-structure allows for multiple attachment sites for the cells (Bian and Bursac, 2008). The alignment of cells within the 3D matrix has also been shown in the early stages of development (Cheema, et al., 2003). Another advantage of the use of naturally derived polymers is the ability to easily stimulate, both mechanically and electrically, due to the mechanical compliance of the polymerised tissue (Powell, et al., 2002, Cheema, et al., 2005).

The use of collagen hydrogels for SkM tissue engineering is increasingly popular and the fact that collagen is a large component of the ECM *in vivo* (Lewis, et al., 2001), provides a rationale for its use. The use of a 3D collagen based model to study SkM development is well characterised in the literature (Cheema, et al., 2003, Cheema, et al., 2005, Brady, et al., 2008, Mudera, et al., 2010, Smith, et al., 2012) and provides a good model to investigate SkM adaptation to mechanical stimuli.

The use of static mechanical signals, promotes the alignment and fusion of the seeded cells (Smith, et al., 2012), promoting morphology, gene expression and passive contractile phenotype that represents *in vivo* SkM (Mudera, et al., 2010, Brady, et al., 2008, Smith, et al., 2012). A summary table of current collagen-based matrices for SkM tissue engineering is presented overleaf.

Table 1-1. Tissue Egineered SkM models

System	**References**
Chamber slide long term model	Smith et al., (2010), Sharples et al., (2012)
Culuture Force Monitor (CFM) acute (24 hr) model	Cheema et al., (2003), Cheema et al (2005), Brady et al., (2008), Mudera et al., (2010)
Engineered muscle bundles	Rhim et al., (2007), Hinds et al., (2011)
Pre-clinial drug screening *in vitro* muscle tissue	Vandenburgh et al., (2008)
Bioartificical Muscle	Gawlitta et al. (2008), Boonen et al. (2010), Langelaan et al. (2011)
Organoids	Vandenburgh et al. (1996)

Adapted from Smith et al., (2010)

With the main goal for tissue engineering to develop artificial tissues for the regeneration and replacement of injured or diseased tissue, efforts were placed towards the improvement of *in vitro* constructs to be able to function within the *in vivo* environment upon implantation. In recent times, the use of such models to understand *in vivo* physiology and function has been explored (Khodabukus, et al., 2007).

To this end, the phrase 'pre-clinical models' has been given to tissue engineered musculoskeletal tissues, for the testing of pharmacological, genetic and exercise therapies (Gibbons, et al., 2012).

1.11 Stimulating SkM *In Vitro*

During voluntary movement, SkM is activated and responds to electrical and mechanical stimuli. When seeking to mimic these stimuli *in vitro* electrical and mechanical stimulation models have been employed, to further understand the molecular responses that govern adaptation. Stimulating cultured human myotubes *in vitro* (electrical pulse stimulation, EPS) has revealed an increase in metabolic parameters including glucose uptake, lactate production, ATP turnover and citrate synthase activity (Nikolic, et al., 2012). Additionally, an increase in key genes regulating adaptation to exercise were also modulated including PGC-1α, glucose transporter-4 (GLUT-4) and interleukin-6 (IL-6) expression (Nikolic, et al., 2012).

Another study utilising EPS showed an increase in AMPK and MAPK activity, whilst also confirming the expression and release of IL-6 into the culture media (Nedachi, et al., 2008). These data confirm the metabolic response of SkM cells following electrical-mediated stimulation, demonstrating activated mechanisms to increase ATP generating efficiency and substrate utilisation.

Using a 3D fibrin self-assembling model of SkM Khodabukus et al., (2007) articulately showed that electrical stimulation produced a similar response in S6K1 phosphorylation to that seen in an *in vivo* exercise protocol (Khodabukus, et al., 2007). More recently it has been shown that 24 hrs of continuous electrical stimulation resulted in an increase in force, partly dependent on the activation of the anabolic signalling protein mTOR (Khodabukus and Baar, 2012). Data concerning the electrical stimulation of SkM cells, illustrates the activation of both metabolic and hypertrophic pathways, providing key mechanistic data as to the adaptation of SkM to increase contractile activity.

Clearly SkM experiences mechanical stresses *in vivo* during contraction and as a passive effect (gravity, opposing external forces etc.). Studying the effect of these stresses *in vitro*, provides a highly controlled environment whereby direct quantifiable external forces can be applied to the cell. Using *ex vivo* SkM fibre preparations has revealed the increased active tension in response to mechanical stretch (Mutungi, et al., 2003)(Ramsey, et al., 2010). Increases in Ca^{2+} and consequential active tension have also been shown in smooth muscle cells in response to stretch (Ito, et al., 2006, Yadid and Landesberg, 2010). This increase in activate force as a consequence of mechanical strain is thought to be dependent on the stretch activated channels (SAC's). This hypothesis is confirmed when using streptomycin (an SAC inhibitor), whereby there is no evidence for active force in response to stretch of bioengineered cardio-myocyte cells compared to a large increase in control (Birla, et al., 2008).

These data indicate the potential for cardio-myocyte active tension in response to mechanical stretch, a response that warrants further investigation in SkM cells particularly in a 3D environment. Nevertheless, stretching SkM *in vitro* induces a passive mechanical response with a possible active resultant component. Relating to the addressed research questions presented in this Thesis, these data provide rationale that passive mechanical signals may contribute to active tension observed *in vivo*. As such the use of a SkM model of passive mechanical stretch will provide evidence as to the role of mechanical signals in regulating a molecular, depdent or independent of active tension.

Vandenburgh and Kaufman (1979) were the first authors to demonstrate the hypertrophic response to mechanical stretch of avian isolated SkM cells *in* vitro. Following continuous cyclic stretch, it was shown that the rate of amino acid uptake, protein synthesis and the total protein were all elevated compared to control (Vandenburgh and Kaufman, 1979). This was amongst earliest experiments to illustrate the mechanical sensitive nature of mechanisms that are associated with increasing SkM cell size and force generating capacity.

Data using a cell line, also demonstrates a reduction in protein synthesis immediately post stretch, despite increases in the molecular signals governing hypertrophy (Atherton, et al., 2009) data which supports *in vivo* findings of reduced protein synthesis immediately post exercise (Dreyer, et al., 2006). A potential autocrine mechanism for increases in anabolic signalling was demonstrated by the use of conditioned media from stretched myotubes onto control cells, illustrating an increase in anabolic signalling (Baar, et al., 2000). These *in vitro* data provided novel evidence for the role of direct mechanical signals in mediating an increase in anabolic protein signalling.

The mechanical stimulation of cells in monolayer also results in an increased CK efflux in the first few hrs of stretch, suggesting an increase in cellular metabolism (Vandenburgh, et al., 1989). It is important however, to consider that the increased CK activity could be a result of cell membrane damage as a consequence of stretch. On the contrary, *in vivo* data demonstrates an increased CK activity in human plasma reflective of tissue enzyme activity (Thompson, Scordilis et al. 2006). The measurement of CK as a marker of tissue damage or increased metabolism is particularly amendable to investigation *in vitro* and relates to the proposed research questions. An increase in glucose metabolism was also seen with *in vitro* stretch signifying an effect of mechanical activation on glucose uptake (Hatfaludy, et al., 1989).

Notwithstanding the novel data that has been generated from the extant *in vitro* SkM literature, the bio-mimicity of the *in vitro* systems discussed must be examined; these systems that are often monolayer in nature and random the alignment of the cells does not represent *in vivo* muscle tissue. There is evidence to suggest the differential regulation of signalling pathways that mediate myogenesis and hypertrophy in response to uniaxial and multi-axial stretch *in vitro* (Hornberger, et al., 2005). Indeed, when using stretch systems to study SkM adaptation it is important to consider both the morphology of the construct used, but also mechanical forces applied.

To overcome this issue the 3D *in vitro* culture systems amenable to mechanical stretch have been developed, which more greatly represent *in vivo* tissue morphology and function, compared to monolayer models. These systems are more advanced than current electrically stimulated monolayer systems, with regards to how the cells interact with the ECM. This interaction is vital for SkM integrity as the transmission of vector force and has been postulated to contribute to mechano-transduction (Klossner et al., 2009, Crossland et al. 2013). This provides evidence for the development and utilisation of an *in vitro* model which incorporates a representative ECM and has the ability to be stimulated, both mechanically and electrically, whilst investigating the response of genes that regulate SkM adaptation. Specifically relating to this Thesis, the role of the integrated ECM in the response to mechanical signals can only be invesgated in a 3D model.

The extant literature demonstrates the use of such models to investigate SkM physiology. Powell et al., (2002) demonstrated that the dynamic stretch of *in vitro* muscle tissue resulted in myofibre hypertrophy and an increase in passive force, a response similar to that seen *in vivo* (Holm, et al., 2008, Powell, et al., 2002). The mechanical stimulation of a 3D collagen based constructs also produced an increase in mechano-growth factor (MGF, Cheema, et al., 2005), similar to the response seen following resistance exercise (Hill and Goldspink, 2003). However it is important to consider that this study was modelling the development of SkM in culture, as the mechanical stimulation occurred immediately post the synthesis of the construct. The effect of mechanical overload on primary dystrophic and normal SkM cells MGF expression, demonstrated no apparent effect in a 3D tissue engineered model (Evans, et al., 2010). This surprising finding may reflect the inability of the overload protocol used, to induce a continuous cyto-mechanical response due to cell stress shielding.

The role of MMP's in the response to mechanical stretch has also been investigated in a 3D gelafoam model of SkM, establishing an increase in MMP-2 at 6 hrs of stretching (Auluck, et al., 2005). Increases in MMP-2 are seen chronically with *in vivo* exercise (Rullman, et al., 2007), suggesting an accelerated nature of the *in vitro* system. The monolayer and 3D SkM models that have been used to investigate the effects of mechanical cues on SkM cell response and adaptation have provided a foundation for research in this area. Much focus has been placed on the hypertrophic protein signalling and transcriptional response, with minimal attention on the molecular pathways that regulate metabolic adaptation.

The development of a SkM model which morphologically replicates *in vivo* tissue, with regards to gross architecture, cell morphology, myoblast fusion, ECM composition and stimulation modality will provide a key tool in further delineating the influence mechanical signals that mediate muscle cellular response and in particular metabolic and hypertrophic adaptation. Furthemore, the use of this model will allow for the specific identification of the stimuli required for the required adaptive phenotype (aerobic or hypertrophic) in a highly controlled environment. Such a model will prove useful in the identification of key genes and proteins regulating adaptation to exercise and will provide a pre-clinical test bed for the screening of exercise, pharmacological and genetic therapies for SkM disease. These data will allow for a more targeted approach to human investigations, minimising required resources and allowing for a more targeted scientifc approach.

1.12 Thesis Aims

Taking the above rationale forward, the following Thesis aims were set to address specific research questions undertaken in each experimental chapter.

1. Extensively characterise the development of a previously published 3D SkM model using the C2C12 cell line, with regards to the cell culture conditions required to develop a bio-mimetic tissue.

2. Utilise this model to investigate the effect of mechanical stimulation on the molecular responses which are known to occur with *in vivo* exercise or increased SkM load.

2 Methods

2.1 Cell Culture Procedures

All cell culture work was carried out using a Class II Heraeus Biological Safety cabinet in aseptic conditions. Cells were incubated at 37°C and 5% CO_2 in a Heracell 240 (Thermo Fisher Scientific, Rosklide, Denmark) incubator for both sub-culture and experimentation.

2.2 The C2C12 Cell Line

C2C12 Mouse C3H muscle myoblasts were sourced from the Health Protection Agency Culture Collections (HPA Cultures, Salisbury, UK). C2C12 cells are a sub-clone of the C2 parental cell line that was obtained from crush injuring the leg of the C3H mouse to induce SC activation and proliferation (Yaffe and Saxel, 1977). The C12 sub-clone was isolated for the apparent proliferative and fusion capacity (Blau, et al., 1985). In order to ensure the specific sub-clone that was purchased displayed the published characteristic fusion potential of C2C12's, an experiment was conducted as detailed (Fig. 2-1).

2.3 Resuscitation of Frozen Cells

Cells were plated at a density of 1500/cm^2 (see Cell Counting 2.4.1) in T75 tissue culture flasks (Nunc, Fisher Scientific, Loughborough, UK) in accordance with the data sheet recommendation. During the counting process, cells were counted for viability in order to ascertain the level of cell death following cryopreservation. Vials with greater than 25% cell death (trypan blue positive) were discarded. Furthermore, non-viable cells do not have the ability to attach the the tissue culture plastic substate and as such, can be removed following viable cell attachement. If a 50% confluence (as subjectively deemed by light microscopy) was not achieved in the following 24 hrs after seeding, the flask was discarded due to the extent of non-viable cel present.

Cells were cultured in 20ml Growth Media (GM) [Dulbecco's Modified Eagle's Medium (DMEM, Sigma-Aldrich, Gillingham, UK) supplemented with 20% foetal bovine serum (FBS; PAA Laboratories, Somerset, UK), penicillin (100 U/ml; Invitrogen, Paisley, UK) and streptomycin (100 µg/ml; Invitrogen)]. Cells were then sub-cultured in order to develop a cryopreserved stock of cells.

2.4 The Passaging (Sub-culturing) of Adherent Cells

A relative passage assignment was used upon obtaining the cells and as such the first passage was deemed passage 1 (P1). For all experimentation cells were cultured in T175 tissue culture flasks (Nunc), due to the large number of cells required. Cells were used between passages 3-8 for all experiments as previous research has indicated the reduced myogenic potential of C2C12's upon multiple population doublings (synonymous with passages, Sharples, et al., 2011). This is despite the well documented immortalised view of the cell line. Passaging took place once cells had reached between 60-70% confluence, in order to prevent the fusion and differentiation of the myoblasts to myotubes, but increase the number of cells required for experimentation.

Growth media (GM) was removed from the culture flasks and discarded. The monolayer of cells was then washed twice with the appropriate amount of calcium and magnesium-free Phosphate Buffered Saline (PBS; Fisher Scientific). This process removes the majority of the proteins found in the serum of the GM, which have an inhibitory effect on the activity of Trypsin. 1 ml/25 cm^2 of 0.05 % Trypsin/EDTA (Sigma-Aldrich) was added to the culture flasks. Following the agitation of the flask to allow the solution to cover the entire cell monolayer, the flask was incubated for 2-5 min depending on cell detachment. Cells were viewed under an inverted light microscope (Ceti, Medline, Oxon, UK) at 10x magnification in order to identify whether the cells had detached. Once all the cells were detached, GM medium was added in double volumes to the Trypsin/EDTA, in order to terminate the digesting and sequestering effect.

The cell suspension was then mixed by inversion and transferred to a conical centrifuge tube for centrifugation at 2000 rpm for 5 min at 4°C. Following centrifugation, the supernatant was carefully discarded so not disturb the pellet of cells. The pellet was re-suspended in an appropriate amount of GM, in order to count the cells using a haemocytometer (see Cell Counting 2.4.1). Cells were plated into the appropriate number of flasks at a density of 1500 cells/cm^2, or used for experimentation.

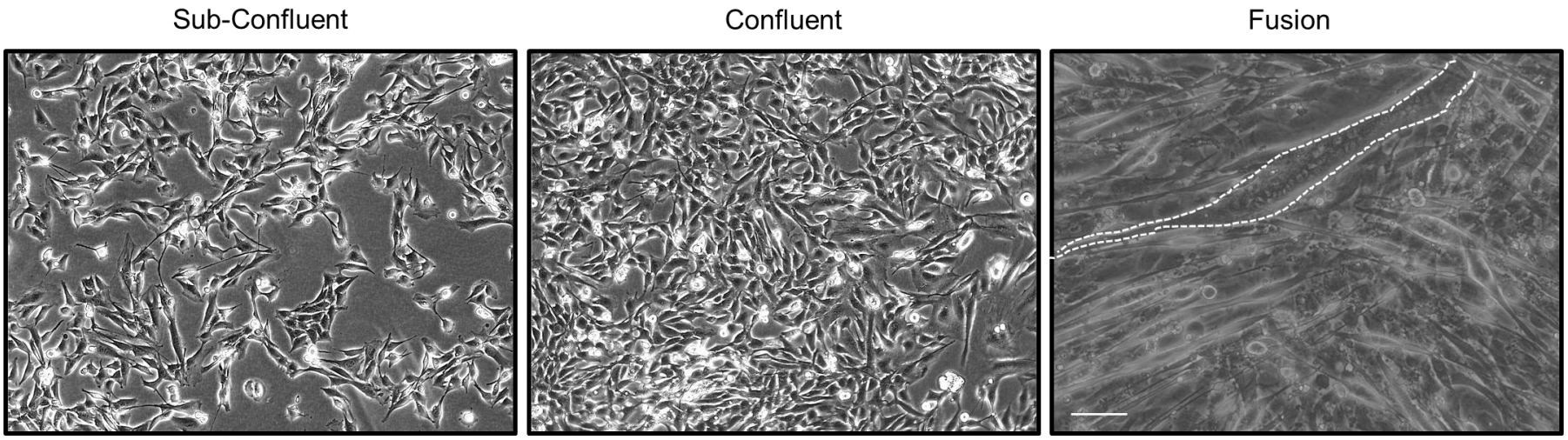

Figure 2-1. The fusion of C2C12 myoblasts. C2C12's were plated at a density of 1500 cells/cm2 and maintained in GM until confluency. Media was subsequently changed to differentiation media (DM, DMEM supplemented with 2% Horse serum [PAA] and 1% penicillin/streptomycin [Invitrogen]). Note the extent of fusion and number of nuclei within the single highlighted myotube (highlighted by the dotted line with) Scale bar = 50 µm.

2.4.1 Cell Counting

Specific cell numbers were needed for experimentation so a method for cell counting was employed using a haemocytometer. 10 µl of a cell suspension was added to 10 µl of Trypan Blue solution (Gibco, Invitrogen, UK), in order to determine viable and non-viable cells. 10 µl of this solution was pipetted under each end of the haemocytometer's coverslip to fill the chamber by capillary action.

Using a light microscope at x10 magnification, the numbers of cells present were counted in each of the four divided corners of haemocytometer (Fig. 2-2). The following equation was used to determine the total viable cell number:

Equation 2-1 Cell Counting

Total cell number = (four chamber viable cell number/4) x 2 x 10,000 x volume of cell suspension

Where; '2' is the multiplication for the dilution factor and '10,000' is the multiplication for the correction factor for the haemacytometer.

To work out the required volume for a particular number of cells for sub-culture, cryopreservation or experimentation, the following equation was used;

Equation 2-2 Required Cell Number

Volume of cell suspension for required cell number (ml) = (required cell number/actual total cell number) x volume of actual total cell suspension

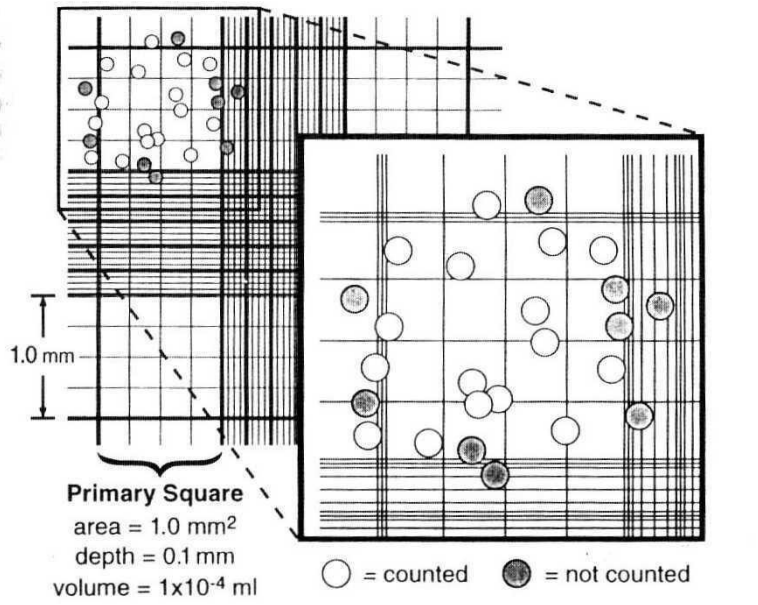

Figure 2-2. Schematic diagram of the counting chambers of a haemacytometer. Cells were diluted 1:1 with Trypan Blue (Gibco) and loaded into a Neubeur haemamacytometer. Cells stained blue were deemed non-viable. (Obtained from; **http://www.cf.ac.uk/biosi/staffinfo/kille/Methods/Cellculture/HAEMO.html**, accessed 15.9.09).

2.5 Cryopreservation of Cells

Stocks of C2C12's were cryopreserved at multiple passages between P3-P6 for future use in experimentation. Cells were Trypsinised as per the sub-culturing of adherent cells (2.4) and counted accordingly (2.4.1). Cells were then frozen at a concentration of 1 x10^6/ml in freezing media (FM) containing 90% FBS and 10% di-methylsulphoxide (DMSO, Fisher Scientific, UK).

2.6 Cell Seeded 3D Collagen Constructs

2.6.1 Material preparation

The collagen constructs used throughout this project were based upon a previously published protocol (Smith, et al., 2012). The 3D culture model involves seeding cells in a collagen based solution and allowing it to polymerise within a mould between two fixed points.

The fixed points were custom made structures termed floatation bars and A-frames (Fig. 2-3). Depending on the experiment, the type of A-frame constructed was different; the CFM and t-CFM frames provide attachment to a strain gauge and fixed point, whereas the frames for the glass chamber system were constructed to fit around the short axis ends of the chamber. Constructs were cast in glass chambers for maturation experiments (detailed in experimental chapters). The floatation bars were constructed using polyethylene plastic mesh (Darice Inc, Strongsville, Ohio, US) and stainless steel wire of 0.3 mm diameter (Scientific Wire Company, Great Dunmow, UK, Fig. 2-3). Three 5 x 3 mm sections of mesh were bound by two lengths of 0.3 mm wire. The A-frames for both the CFM and t-CFM systems, along with the glass chamber system, were constructed using 0.7 mm wire (Scientific Wire Company). All floatation bars and A-frames, along with the glass chambers and CFM moulds were sterilised before experimentation using 70% ETOH and a UV function on the biological safety cabinet.

2.6.2 Collagen Gel Preparation

0.3 ml of 10 x MEM (Gibco) was added to 2.6 ml of type 1 rat-tail collagen (First Link, Birmingham, U.K.; in 0.1 M acetic acid, protein concentration *n* =2.035 mg/ml). Sodium hydroxide (NaOH, Fisher Scientific) was used in 5 M and 1 M concentrations to neutralise the solution in a drop-wise fashion until a colour change (yellow to cirrus pink) was observed. Following neutralisation, a cell suspension of the correct number of C2C12 cells for experimentation, were added in a volume of 0.1 ml GM.

The resulting solution was set in either a Chamber Slide (Lab-Tek, Fisher Scientific, UK) or a Derilin mould (G.W. Cowler Ltd, Mead Lane, Hertford, UK), between two polyethylene mesh flotation bars ('A-frames'), placed in a 37°C humidified incubator with 5% CO_2 and allowed to gel for 30 min. Once set, the compliant construct was physically detached from the base of the mould and floated in standard growth medium.

The ‘A-frames’ provided two attachment points which lead to the development of lines of longitudinal isometric strain. The result was a 3D tissue possessing uni-axially aligned myoblasts capable of differentiating and performing directed contraction, analogous to *in vivo* SkM (Fig. 3-5).

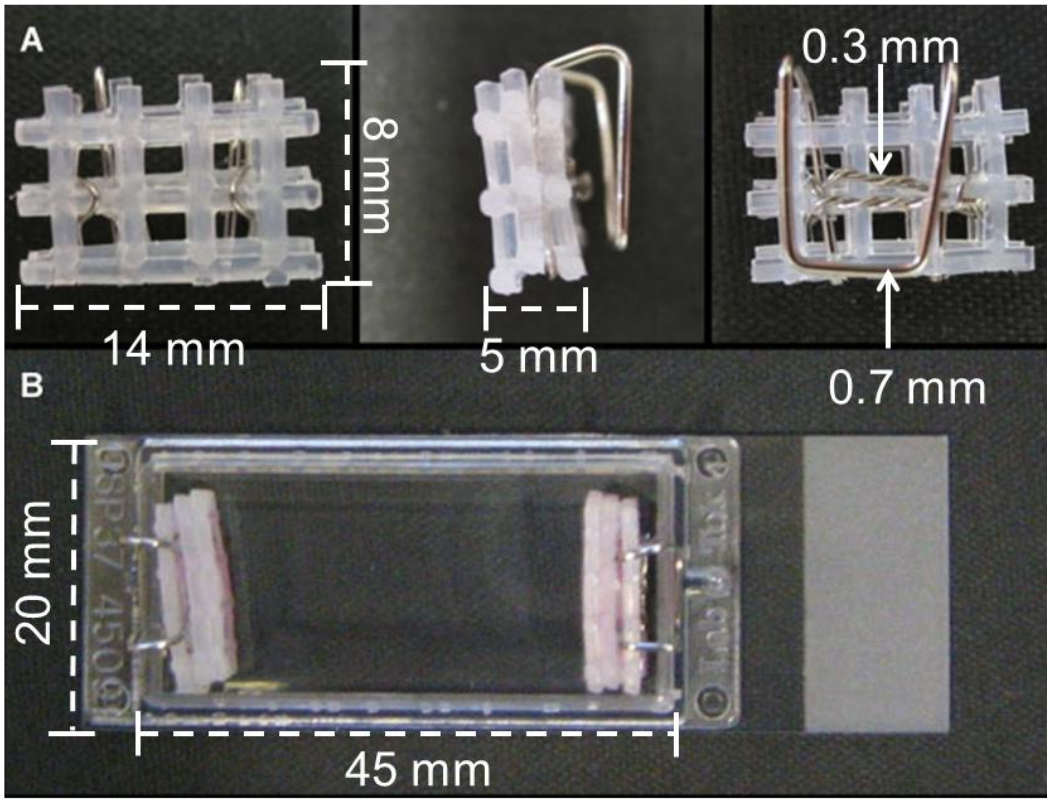

Figure 2-3. Floatation bar and A-frame set-up for collagen constructs. A) Custom made floatation bars with A-frames. B) Positioning of floatation bars and A- frames within a chamber slide. Note how the A-frames fit over the short axis perimeter to provide axial tension. Dimensions of the chamber and flotation bars are annotated with a dashed line. The blocked arrow lines annotate the grades of wire used for the A-frames. Adapted from (Smith, et al., 2012).

2.7 The Culture Force monitor (CFM)

The Culture Force Monitor (CFM) is an apparatus whereby real-time force contraction of 3D cellular collagen constructs can be accurately measured. The original CFM is now well documented in the literature (Eastwood, et al., 1996) however this system used 5ml larger gels requiring greater numbers of cells.

A new CFM system was set up using smaller gels in order to reduce the number of cells required and increase the cost effectiveness of the system.

2.7.1 Rig construction

A rig which could support all the required components of the CFM was constructed using a PTFE base and glass fibre poles (G.W. Cowler), cut to specification. The rig allowed for the positioning of the force transducer and opposing fixed point in a single plane, to accurately measure the force generated as a consequence of contraction of the gel. During experiments, the alignment of the force transducer and the opposing fixed point was achieved through the measurement of distances along the rig using digital calipers (Silverline, UK). This accurate measurement allowed for the controlled set up of the system between experiments, to minimise variation in the alignment and forces transduced.

2.7.2 The Force Transducer

The central measuring beam (Fig. 2-4) of the CFM was manufactured from a 0.15 mm thick Copper-Beryllium sheet (Goodfellow Metals Ltd, Cambridge, UK) cut into strips of 100 x 10 mm. Transducer class strain gauges (Wellyn Strain Measurement, Basingstoke, Hants, UK) were attached to the Copper-Beryllium beam in a full bridge electrical network at 20 mm from one end, to give a maximum lever arm for maximum sensitivity. A hook was soft soldered onto the opposite end of the measuring beam to facilitate connection to the culture through the custom made stainless steel wire A-frame. The force transducer was attached through a wired mechanism to the Model P3 Strain Indicator and Recorder (Vishay, Basingstoke, UK) connected to a computer via USB. This unit acted as a bridge amplifier, static strain indicator, and digital data logger. Micro-strain (με) and time data was collected at a rate of 1 Hz (one reading per second) for all measurements.

2.7.2.1 Calibration of the Force Transducers

Before each experiment the force transducers need to be calibrated, in order to check the integrity of the force transducer and also to provide an equation to convert the micro-strain (μƐ) reading to micro-Newton's (μN). Prior to calibration the force transducers were left in the incubator for a period of 24 hrs to thermally adjust to the normal operational temperature, humidity and CO_2 content.

The force transducers were calibrated against known masses which ranged between 0.5 g and 0.03 g (Table 2-1). Using the output software the correct channel was 'zeroed'. Each mass was attached to the force transducer via the attachment hook and then data was recorded for a period of 10 mins. The collected data was averaged and this value was recorded as the output for the particular mass. This process was repeated for each of the masses on the force transducers. Each of the average readings in micro-strain were plotted against theoretical value of force that each of the known masses would produce, in accordance with acceleration due to gravity (Table 2-1).

Table 2-1. CFM Force Calibration

g	kg	Expected Force (N)	Expected Force (μN)	μƐ
0.5	0.0005	0.004905	4905	244.2433
0.3	0.0003	0.002943	2943	139.222
0.2	0.0002	0.001962	1962	92.79642
0.05	0.00005	0.000491	491	25.96563
0.03	0.00003	0.000294	294	24.09446

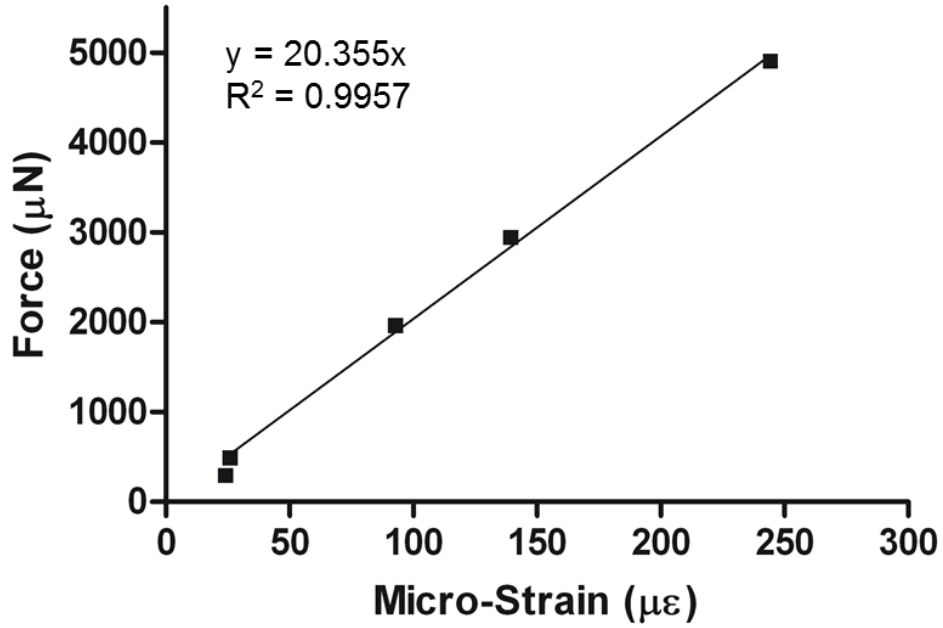

Figure 2-4. Typical CFM Calibration Curve. This curve allows for the conversion of recorded micro-strain (μƐ) to μN. It also allows for the assessment of the integrity of the strain gauge electrical bridge network on the transducer.

The r^2 value represents the extent to which the two variables are correlated. If a value any less than 0.95 is observed, the force transducer should be returned to the manufacturer for testing, as the accuracy and/or sensitivity of the force transducer is no longer effective. If the r^2 value in ≥ 0.95, the equation obtained from the trend line can be used for experimentation when converting the raw data in micro-strain to micro-Newton's.

Equation 2-3 Conversion of data from micro-strain (μƐ) to micro-Newton's (μN)

Force (μN) = 20.355 x μƐ

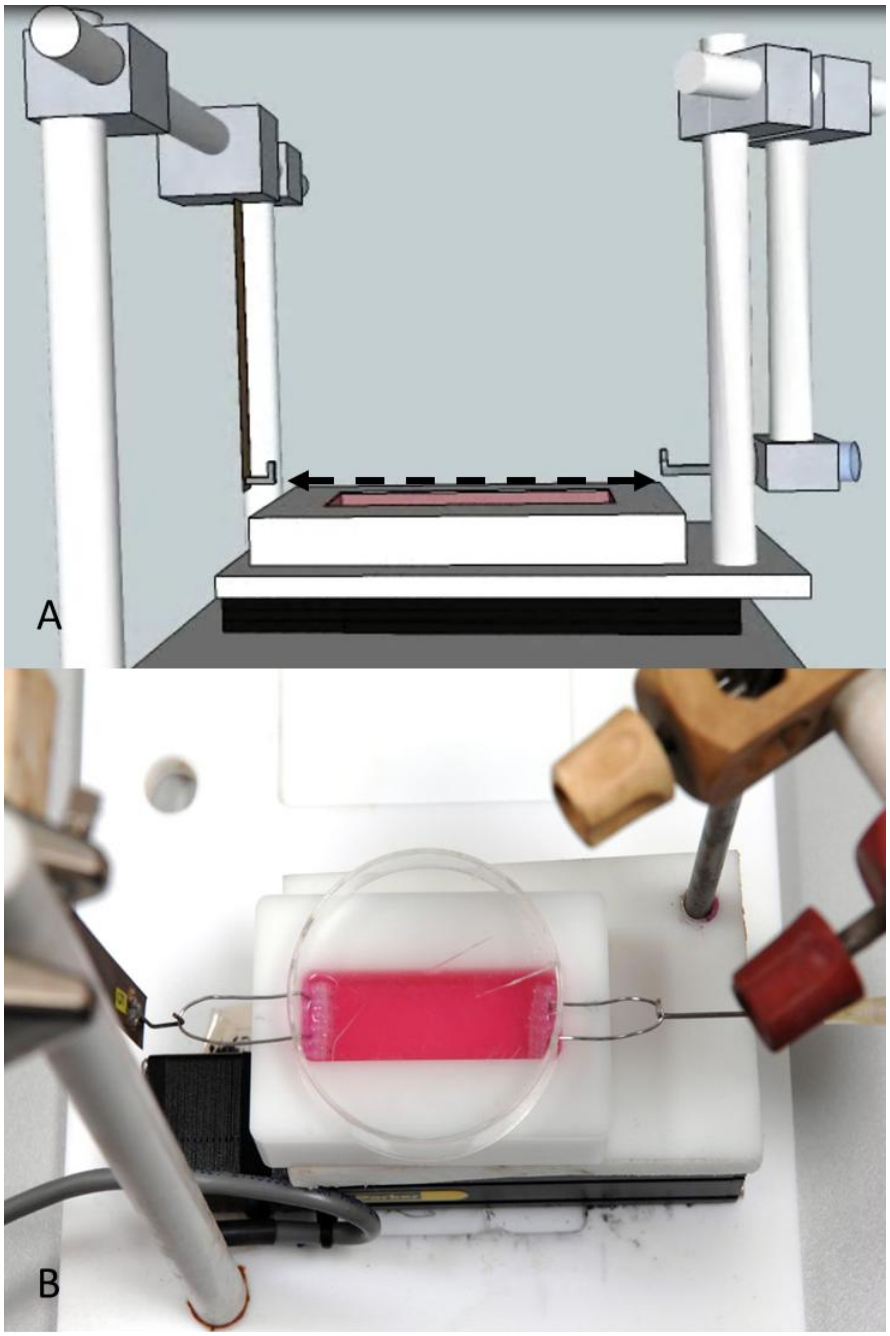

Figure 2-5. The Culture Force Monitor (CFM). A) Schematic of the CFM illustrating the constructed rig to hold the force transducer (left) and fixed point (right). The dashed arrowed line between the force transducer and fixed point illustrates the requirement for alignment B) Image of the actual CFM set-up with a collagen construct tethered ready for experimentation. The alignment of the A-frames in all planes is of paramount importance to allow for the transfer of longitudinal force to be accurately detected by the force transducer.

2.7.3 Tethering the Construct to the CFM

Stainless steel wire 'A-frames' attached to the flotation bars facilitated a connection between the construct and the CFM. The force measurement system for the CFM is extremely sensitive, therefore when tethering the construct to both the fixed point and the measuring beam, it is important that the mechanics are correct. If not, the force output may not represent the contraction from the construct. The two A-frames must be aligned in both a superior view along with a lateral view when looking into the incubator.

2.7.4 CFM Data Analysis

The raw data collected at 1 Hz was processed in Microsoft Excel in order to obtain a mean reading for each minute of experimentation. This data was then converted to micro-Newton's and plotted on a graph to represent the force-time contraction profile of the constructs (Fig. 3-1). Data was also analysed for initial rate of force development for each minute up to 60 min of contraction (µN/min). Data was also analysed for peak force and relative peak force according to cell seeding density. For compairsons in generated force between seeding densities or other conditions detailed in expiermental chapters, inferential statistical analysis was performed. Data was analysed for normal distrubtion and compliance to test assunmptions prior to presentation of data.

2.8 The Tensioning Culture Force Monitor (t-CFM)

2.8.1 Background and Set-Up

Essentially the t-CFM is an addition to the CFM, in that the setup is the same apart from the collagen gel PTFE mould sits upon a stage attached to a programmable motor. The stepper motor (Parker-Hannifin, Poole, UK) is connected to a Four Axis Motor Control Cabinet (Micromech Systems Ltd, Braintree, UK) which in turn is connected to a computer via an RS232 cable. Parker EASI-V software (Parker-Hannifin) was used to program the regimes.

2.8.2 Stretching Regimes

Regimes of mechanical stretch were devised using available commands on the Parker EASI-V software (Parker-Hannifin) within the command terminal (Fig. 2-6). The basic commands and an example of program development are detailed below.

DECLARE = Declare a new program

D = Distance (to program strain, defined below)

A = Acceleration

V = Velocity

T = Time Delay

LOOP = Loop selected program

K = Stop program or command

SV = Save program

When mechanically stimulating *in vitro* tissue the term 'strain' is often used to quantify the amount of displacement the construct is subjected to. Strain is defined as;

Strain (ε) = $\Delta l/l$

Where l is length and Δl is the change in length (final length-original length).

Equation 2.4 Definition of Strain

Cultures subjected to mechanical stretch were cast and matured in the glass chamber or chamber slide systems (longitudinal length = 45 mm). Therefore, to initiate a strain the distance of motor movement was programmed accordingly. The EASI-V software commands distance in motor steps, where 10,000 motor steps = 1 mm.

Hence to induce a 10% strain;

10% Ɛ = Δl/45 mm

Δl = 45 mm x 10% Ɛ

Δl = 4.5 mm

∴ Distance in motor steps = 45,000

Equation 2.5. To calculate 10% strain

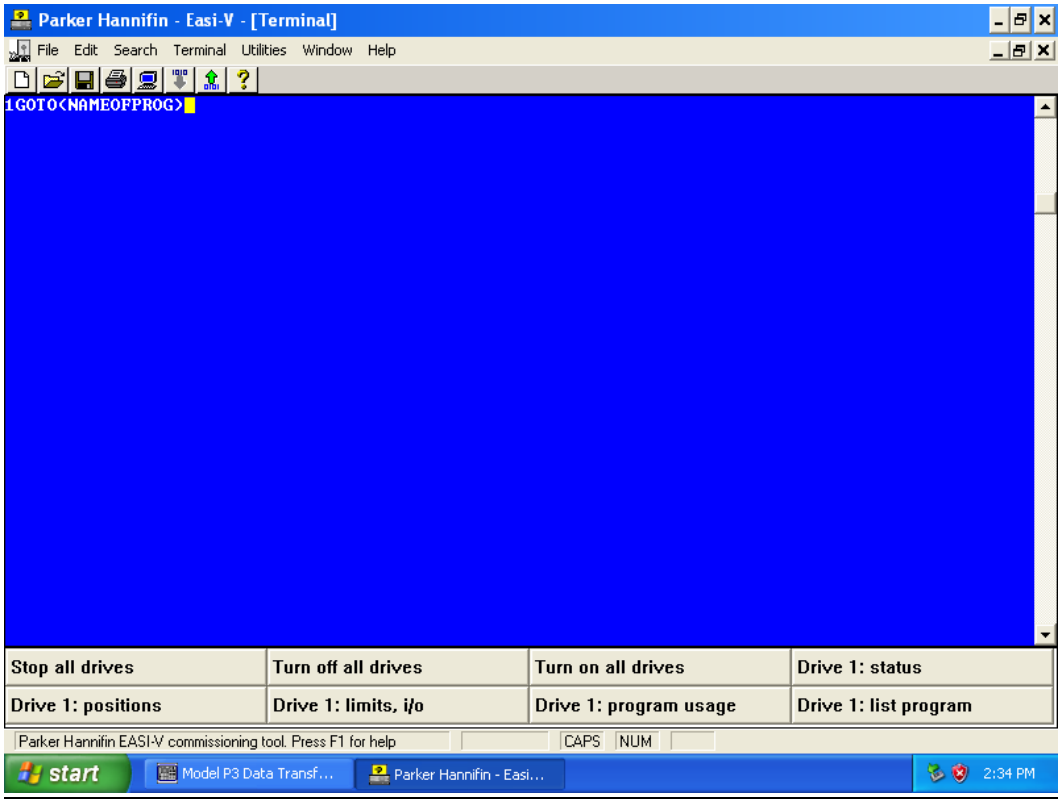

Figure 2-6. Axis terminal of EASI-V software. This software terminal was used to programme the mechanical stimulation regimes.

2.9 Analytical Procedures

2.9.1 Conditioned Media Lactate and Glucose Analysis

2.9.1.1 Principle

The analysis of plasma Lactate and Glucose have been used extensively in Exercise Physiology to characterise bouts of exercise with regards to the energy systems utilised. Various methods of measuring these substrates have been used; however the most commonly available methods take advantage of a basic chemical reaction. Using the Analox (P-GL5; London, UK) system Lactate and Glucose concentrations are determined by amperometric measurement of an oxido-reductase enzyme reaction (van Someren, et al., 2005). This device is a quick and cost effetctive way to obtain metabolite data and has been shown to produce data with a high degree agreement to standard spectrophotometric measures detailed below (van Someren, et al., 2005).

In the presence of oxygen, Lactate is oxidised by the enzyme Lactate oxidase to pyruvate and hydrogen peroxide;

$$L-Lactate + O_2 \xrightarrow[(LOD)]{L-Lactate\ Oxidase} Pyruvate + H_2O_2$$

Equation 2.6. Oxidation of Lactate

In the presence of oxygen, Glucose is oxidised by the enzyme glucose oxidase to gluconic acid and hydrogen peroxide;

$$\beta\text{-}D\text{-}Glucose + O_2 \xrightarrow[(GOD)]{Glucose\ Oxidase} D\text{-}Gluconic\ Acid + H_2O_2$$

Equation 2.7. Oxidation of Glucose

Therefore, under these reaction conditions, Oxygen consumption is directly proportional to Lactate and glucose concentration respectively.

2.9.1.2 Procedure

The Analox Analyser P-GL5 (Analox, London, UK) was utilised for the assessment of Lactate and Glucose concentrations within conditioned media samples. The manufacturers have validated the use of this method against standard spectrophotometric methods. It has been demonstrated that similar analysers from the same manufacturer (Analox GM-7, Analox, UK) utilising the amperometric principle, that the covariance of lactate measurements is very low (0.8-1.1 %, van Someren, et al., 2005).

The analyser was appropriately setup and calibrated using 8 mmol.L standards for both lactate and glucose. 10 µL samples were loaded and all reactions were performed in triplicate for each experimental sample, with final presented values representing a mean of the three triplicate reactions. Samples were always analysed within 24 hrs of sampling in order to preserve the concentrations of the substrates in question.

2.9.2 Immunohistochemistry (IHC)

2.9.2.1 Principle

The reagent used for fixation of the specimen is of importance, in order to retain the cytoskeletal structure and cellular architecture, whist identifying a suitable permeablisation buffer will allow for a great specificity for the antibody (Leong et al., 2010). The immunolocalisation of antigens within cells or a tissue is a common technique used in cell and molecular biology (Wheatley and Wang, 1998) and relies on the development of epitope specific antibodies, raised either *in vivo*, or more recently developed, *in vitro*. The use of a primary antibody raised in a particular species dictates the use of a secondary antibody, which must target the appropriate immunoglobulin of the primary species (Wheatley and Wang, 1998), Figure 2-7). Secondary antibodies conjugated to fluorophores allow for the detection of the antibody using fluorescence microscopy, by absorbing light at specific wavelengths and emitting light at a greater wavelength.

Many fluorophores are now available, thus allowing for the detection of multiple proteins simultaneously.

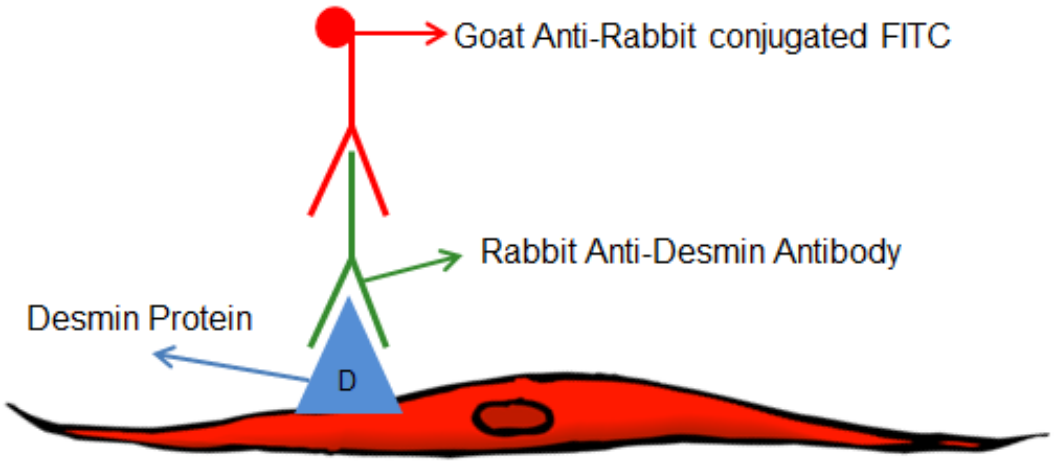

Figure 2-7. Principle of IHC for analysing Desmin protein expression on SkM cells.

2.9.2.2 Procedure

2.9.2.2.1 Gel Fixation

The following protocol was based upon that described in (Smith, et al., 2012). GM was removed from the glass chamber and the constructs were rinsed twice with 3 ml of PBS to remove and media and serum. 2 ml of PBS was left in the chamber and a 2 ml solution of Methanol/Acetone diluted 1:1 (100 Methanol, Company; 100% Acetone, Fisher-Scientific) was added and left at room temperature (RT) for 15-20 min. The solution was then removed and further 2 ml of the Methanol/Acetone fixative was used for 15-20 min. The constructs were removed from their chamber and A-frames and mounted upon polylysine coasted microscope slides (Fisher-Scientific), before being ringed with a PAP pen (Sigma-Aldrich) in order to prevent any staining reagents from dispersing from the tissue on the slide.

2.9.2.2.2 Immunostaining

The constructs were blocked for 1 hr using TBS (+ 5 % Goat serum [Sigma-Aldrich] and 0.2 % Triton X-100 [Fisher-Scientific]). Two further 5 min washes with TBS preceded treatment with the primary antibody (Rabbit Polyclonal to Mouse Desmin, Abcam, Cambridge UK) diluted 1:200 in TBS (+ 2 % goat serum and 0. 2 % Triton X-100). The sections were then incubated overnight at RT.

The constructs were again washed twice with TBS before being treated with the secondary antibody (Goat anti-Rabbit FITC, Stratech, Newmarket, UK) diluted 1:200 in TBS (+ 2 % serum, 0.2 % Triton X-100). The samples were incubated for 1 hr at RT in a darkened humidified chamber before being washed 3 times with TBS. SYTOX Green Nuclear stain (Invitrogen) was diluted 1:300 in water and applied to the samples for 30 mins. A cover glass was used to mount the slide using a drop of MOWIOL mounting medium (Sigma-Aldrich).

2.9.3 Confocal Microscopy

The mounted slides were visualized using a Zeiss LSM-510 fluorescence confocal microscope with associated software. Cell-associated fluorescence was visualized by epifluorescence, using the following filters; FITC (excitation at 485 nm and emission at 520 nm) and SYTOX® Green (excitation at 504nm and emission at 523nm). Images were exported to ImageJ (National Institutes of Health, US).

2.9.4 Gene expression using Quantitative Reverse transcription Polymerase Chain Reaction (qRT-PCR)

QRT-PCR was used in order to investigate the expression of genes involved in the myogenic programme along with those acutely regulated following SkM contraction and overload.

2.9.4.1 Principle

The blueprint for all proteins takes the form of messenger ribonucleic acid (mRNA), which is transcribed from a DNA sequence.

In order that the expression and identity of any gene transcript can be explored, a reverse transcription (RT) procedure must be completed. An RT enzyme often takes the form of an RNA virus enzyme, with a role *in vivo* to transcribe the viral RNA genome into a template for host transcription systems (Bartlett, 2002). The reverse transcribed mRNA (termed copy DNA, cDNA) can then be amplified in a PCR reaction.

The principle of the PCR reaction is based upon the rapid multiplication of a specific cDNA segment, performed by a polymerase enzyme originally isolated from the species *Thermus Aquaticus*. The unique characteristic of this enzyme is the ability to withstand high temperatures required for the denaturation step of PCR, without denaturing (Spurway and Wackerhage, 2006). There are three main stages to a PCR cycle; 1) annealing, 2) extension and 3) denaturation. The thermal cycling protocol (2.9.4.4) allows for these processes to occur. Quantitative PCR is a method for analysing the amplification of the product during the PCR reaction using fluorescent dye technology.

The most common forms of such technologies include probe based dyes and SYBR Green I. SYBR Green I was used throughout this thesis and the chemistry of how the dye works is illustrated in Figure. 2-8 below. SYBR Green only fluoresces when bound to double stranded DNA (dsDNA, Kubista, et al., 2006). An inbuilt flourometer within the real time PCR machine will quantify the fluorescence at the end of the extension step. Upon the sufficient amplification of the target sequence, fluorescence will develop above the threshold line, termed the cycle threshold (C_T).

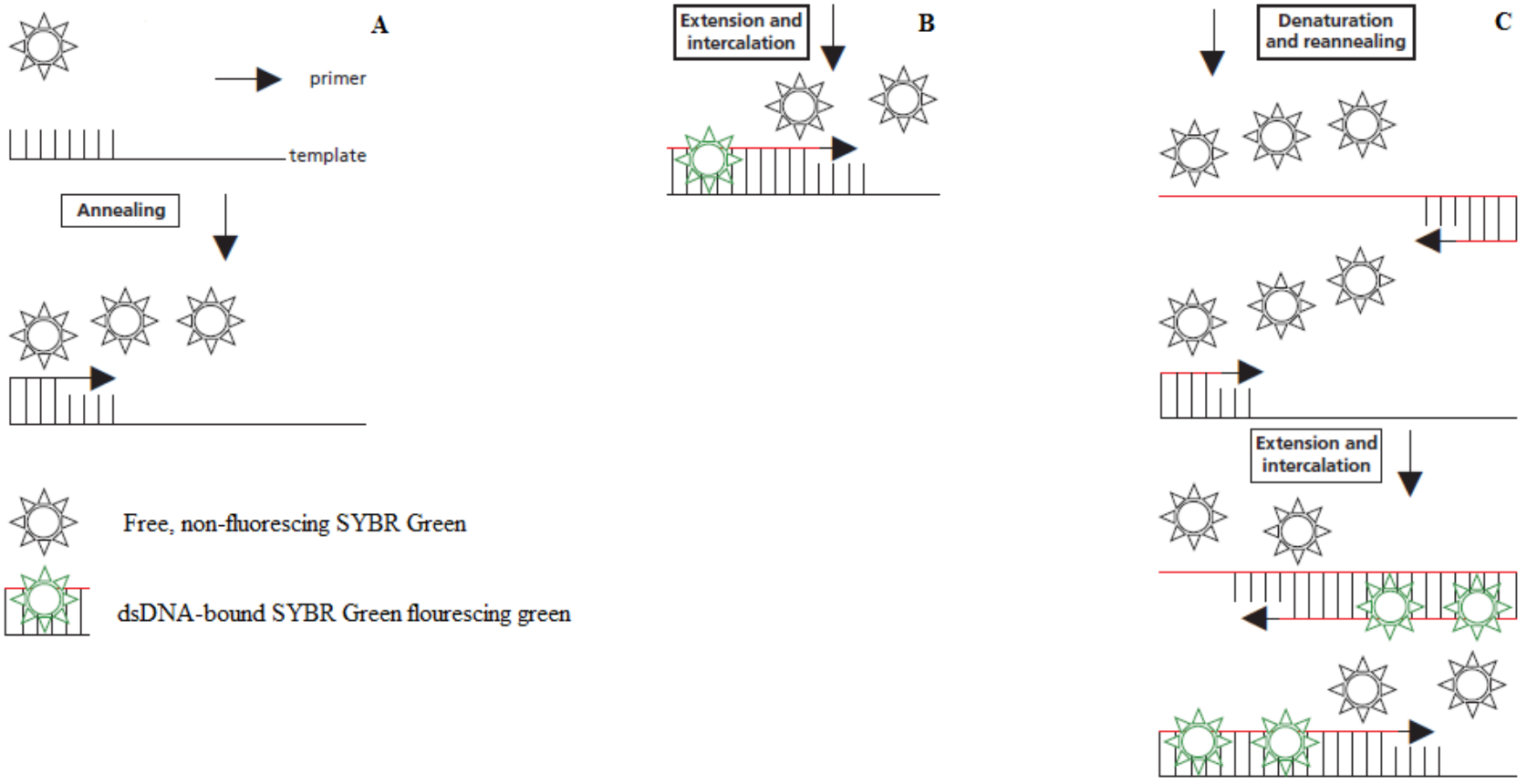

Figure 2-8. Principle of qPCR using SYBR Green (Amended from Qiagen, UK).

2.9.4.2 RNA extraction

The following protocol is based upon the recommendations from the manufacturer of TRIzol® (Sigma-Aldrich), with modifications in order to obtain the highest RNA yield. In order to prevent the degradation of the RNA, all materials used were cleaned using RNase Zap®(Sigma-Aldrich).

GM was removed from the mould and the construct was rinsed twice with 3ml of PBS to remove and media and serum. Gels were removed from the 'A-Frames' using a scalpel blade and transferred into a 50ml centrifuge tube. 500 µl TRIzol® was added to the tube and vortexed for 20 sec. A homogeniser (IKA T10, Fisher-Scientific) was cleaned using 70% ETOH, dried and then used to break up the collagen gel. Once most of the gel has broken down, triturating with a pipette was sufficient to break down the last fragments. The solution was then transferred into a 1.5 ml RNAse free tube (Fisher-Scientific).

Samples were first treated with 100 µl chloroform (Sigma-Aldrich) and were shaken vigorously for 15 sec and allowed to incubate at room temperature for 2-3 min. Samples were spun for 15 min at 4^{o}C at a speed of 12000 g. Following centrifugation, the solution appears in phases; the upper aqueous phase containing the RNA. This phase was carefully transferred to a fresh 1.5 ml RNAse free tube; the other phases contain DNA and protein which will contaminate the sample if disturbed.

250 µl isopropyl alcohol (Fisher-Scientific) was then added to the aqueous solution containing RNA. The samples were incubated at room temperature for 10 min before being spun for 10 min at 4^{o}C at a speed of 12000 g. The supernatant was removed, being careful not to dislodge the RNA pellet. The tube was blotted onto tissue paper in order to remove as much of the isopropyl alcohol as possible. 100 µl of 75% ETOH (diluted in nuclease-free water) was then added to the sample and incubated at room temperature for 5 min.

Samples were spun for 5 min at 4^{o}C at a speed of 7500 g; the supernatant was removed and any further ethanol was left to evaporate for 15 min. The isolated purified RNA was then re-suspended in 50 µl nuclease-free water. RNA quantity and quality was determined using a Fisherbrand Nanodrop 3000 (Thermo Fisher) spectrophotometer at 260 and 280 nm absorbance.

2.9.4.3 Primer Design

When designing oligonucleotide primers for PCR, there are some important considerations to account for to achieve accurate and reliable gene expression data. The common considerations discussed in the literature are displayed in the following table.

Table 2-2. Considerations for the design of qRT-PCR Primers

Consideration	Solution	Description
Primer Length	18-24 bp	Primer length generally controls specificity of the target sequence
Amplicon Length	50-150 bp	Allows for a more efficient amplification during each thermal cycle
Genomic DNA Amplification	Design primers crossing Exon-Exon boundaries	Primer sets homologous within an Exon can increase genomic DNA amplification
GC Nucleotide Content	Approximately 50%	GC nucleotide content relates to annealing temperature. 50% GC content with allow for a sufficient thermal window for the annealing phase of the PCR reaction
Annealing Temperature	50-62˚C	Optimal thermal temperature for the amplification of
Primer-Dimer	Ensure no complementary nucleotides in opposing primers, particularly at the 3' end	Primer-dimer will inhibit the efficient of the amplification of the target sequence

Primer design considerations based upon recommendations from (Dieffenbach, et al., 1993). All designed primer sets were assessed against all possible cross-matches using a Basic Local Alignment Search Tool (BLAST) available online (http://blast.ncbi.nlm.nih.gov/). All primers used within experiments presented in this thesis are displayed in Table 2-3. During each PCR experiment a melt curve analysis was used to determine the melting temperature of the final synthesised product. Primers were deemed to have synthesised a single specific target if a single peak was evident on the melt curve analysis (Fig.2-9).

Table 2-3. qPCR Primer Sequences

Target Gene	Forward Sequence (5' to 3')	Ref. Seq. Number
RPII-B	F:GGTCAGAAGGGAACTTGTGGTAT	NM_153798.2
	R:GCATCATTAAATGGAGTAGCGTC	
Myogenin	F: CCAACTGAGATTGTCTGTC	NM_031189.2
	R: GGTGTTAGCCTTATGTGAAT	
MMP-9	F: CTGGCAGAGGCATACTTG	NM_013599.2
	R: GCCGTAGAGACTGCTTCT	
PGC-1α	F: GAAGGGAATGGGAAAGGTAGA	NM_008904.2
	R: AACAGGACATGGAAAGCAGAT	
Tfam	F: CACGCTTTACCCTTCGTTCT	NM_009360.4
	R: CTCATTTCCCTGCCATTCTCTA	
Cytochrome C	F: GCCGACTAAATCAAGCAACA	NM_007808.4
	R: CAATGGGCATAAAGCTATCG	
NRF-1	F: CCTCAGCCTCCATCTTCT	NM_010938.4
	R: CTTAACACTTCTGTCACCTTCA	
NRF-2	F: TCCCGCTACACCGACTAC	NM_008065.2
	R: TCTGACCATTGTTTCCTGTTCTG	
COX-II	F: GAAGCGATTCTAGGGAGCAG	NM_ 010339.1
	R: GGAGCAGCGATTCTGAGTAGA	

β-Globin	F: GAAGCGATTCTAGGGAGCAG	NM_008220.4
	R: GGAGCAGCGATTCTGAGTAGA	
IGF-I	F: GCTTGCTCACCTTTACCAGC	NM_010512
	R: TTGGGCATGTCAGTGTGG	
MMP-9	F: CTGGCAGAGGCATACTTG	NM_013599.2
	R: GCCGTAGAGACTGCTTCT	
IGFBP-2	F: AGTGCCATCTCTTCTACAA	NM_008342.3
	R: GCTCAGTGTTGGTCTCTT	
IGFBP-5	F: GAAGAGGTGGTGACAGAG	NM_010518.2
	R: TGACAACAAGATCGGGAA	
MuRF-1	F: CCAAGGAGAATAGCCACCAG	NM_001039048.2
	R: CGCTCTTCTTCTCGTCCAG	
MAFBx	F: GTCGCAGCCAAGAAGAGAA	NM_026346.3
	R: CGAGAAGTCCAGTCTGTTGAA	
Myostatin	F: TACTCCAGAATAGAAGCCATAA	NM_010834.2
	R: GTAGCGTGATAATCGTCATC	

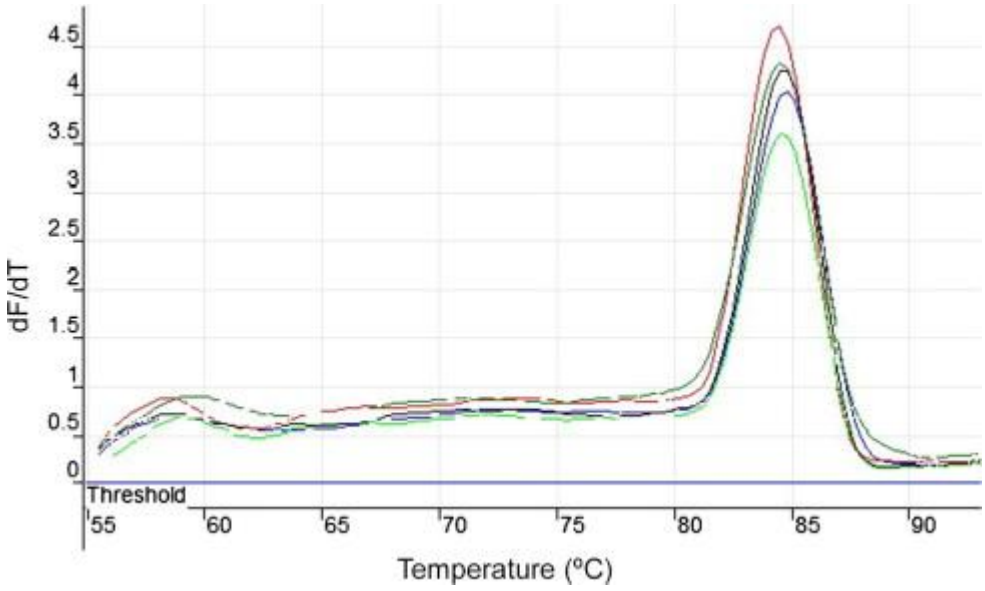

Figure 2-9. Example of a melt curve from the Qiagen Rotogene. The appearance of a single peak, relates to the amplification of a specific product. This provides evidence for the specificity of primer annealing.

2.9.4.4 Quantitative Reverse Transcription Polymerase Chain Reaction (qRT-PCR)

A single step reaction chemistry was used for the qRT-PCR for all experiments. This allows for the reverse transcription (RT) and the PCR to occur one after the other in the same sample tube and as such saving time and reducing potential contamination from handling samples. Due to the nature of the chemistry and thermo-cycling protocol, the reverse transcriptase enzyme in the RT Mix (Qiagen, West Sussesx, UK) is inactivated following the initial thermal protocol.

Following the manufacturers guidelines for the reverse transcription chemistry, 70ng reactions were used for each sample. A dilution was made from the stock RNA concentration, in order to have 70ng in 9.5µl, for however many reactions were being conducted. The Qiagen Qiagility Robot was used to perform all 'master mix' and sample preparations, using programmable software.

The 20 µl reaction volume consisted of the following; 9.5 µl RNA, 0.15 µl forward primer, 0.15 µl reverse primer, 10 µl Quantifast SYBR Green Mix (Qiagen) and 0.2 µl of the RT-Mix (Qiagen). Once the sample preparation was complete the samples were loaded into a Rotogene 3000Q (Qiagen) for the one step reaction. The PCR thermo-cycling was as follows; RT Step (Hold at 50°C for 10 mins, Hold 95°C for 5 mins) and PCR Step (Cycling 95°C for 10 sec, 60°C for 30 sec). Fluorescence at the end of each extension step was measured using the Green Channel at excitation 470 nm emission 510 nm. An example amplification plot is represented in Figure 2-10.

2.9.4.4.1 Data analysis

The mean C_T values for duplicates for each sample were used to calculate relative mRNA expression of the genes of interest (GOI) compared to an experimental control and endogenous control gene (RPII-B). A threshold was added to the PCR amplification curve within the lower third of the exponential phase, in order to obtain a CT value for each sample.

The relative gene expression levels were calculated using the comparative CT ($\Delta\Delta C_T$) equation otherwise known as the Livak method (Schmittgen and Livak, 2008) for determining normalised expression ratios, where the relative expression is calculated as $2^{-\Delta\Delta CT}$, where C_T represents the threshold cycle. An example equation for calculating a normalised gene expression is displayed below.

Table 2. Calculation of normalised gene expression using the comparative $\Delta\Delta C_T$ method. Where; GOI = gene of interest, C_T = cycle threshold, HKG = house-keeping gene. The ΔC_T is the C_T of the GOI minus the C_T of the HKG. The $\Delta\Delta C_T$ represents the ΔC_T of the sample minus the ΔC_T of the control sample (in this example Sample 1).

Name	GOI	C_T	HKG	C_T	ΔC_T	$\Delta\Delta C_T$	$2^{-\Delta\Delta C_T}$
Sample 1	Myogenin	20.2	RP2B	18.67	1.655	0	1
Sample 2	Myogenin	21.34	RP2B	18.77	2.55	0.9	0.538

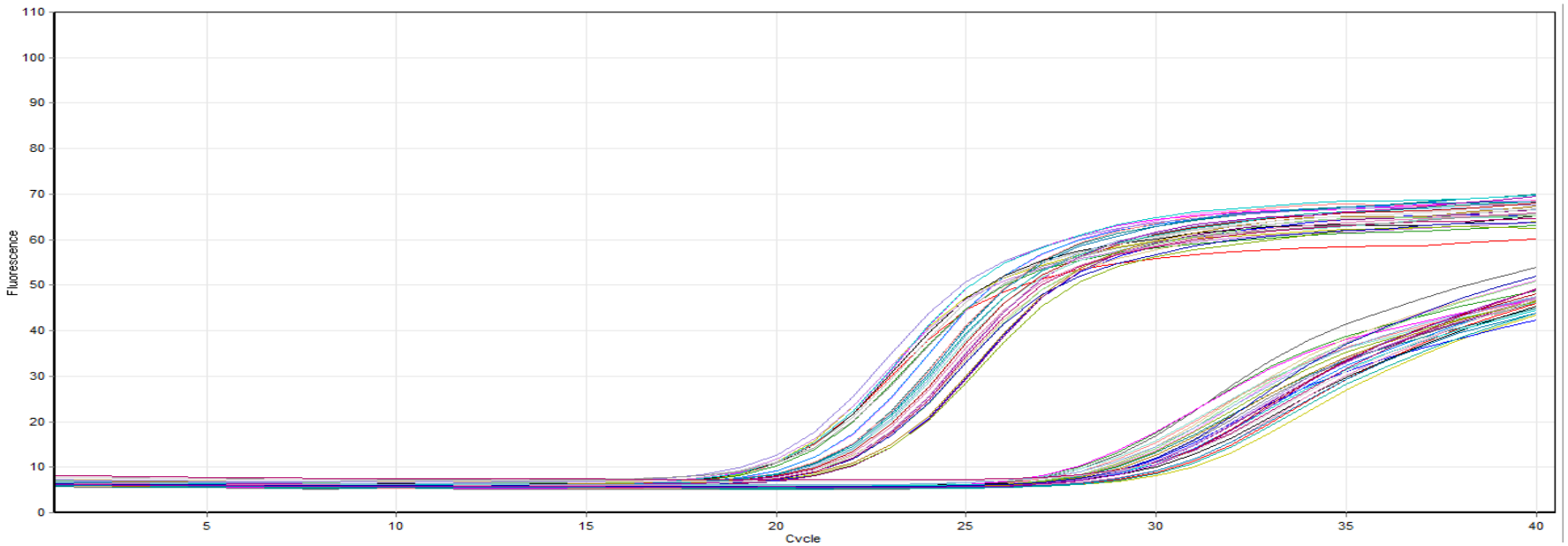

Figure 2-10. qRT-PCR Amplification plot using the Rotogene 3000. Note the exponential increase in fluorescence, followed by linear and plateau phases.

2.9.5 DNA Trizol reagent

2.9.5.1 Procedure

2.9.5.1.1 DNA Isolation, Purification and Quantification

DNA was isolated from the phenol-chloroform phase separated during the initial step of RNA extraction. Removal of any of the aqueous phase was carefully conducted prior to the addition of 150 µL of 100% ETOH. Samples were then mixed by inversion and incubated at RT for 2-3 min, before centrifugation at 2,000 g for 5 min to pellet the DNA. The phenol-ETOH supernatant was removed and transferred to another tube for protein isolation. The DNA pellet was then washed in 500 µL of wash solution containing 0.1 M sodium citrate (Fisher-Scientific) in 10% ethanol, pH 8.5. Samples were incubated for 30 min at RT and mixed periodically be inversion. The sample was centrifuged at 2,000 g for 5 min before a further 2 washes for 30 mins. 750 µL of 100% ETOH (Fisher-Scientific) was added to each sample and incubated for 20 min at RT, with periodic mixing to ensure the precipitation of the entire DNA sample. A 5 min centrifugation preceded the air drying of the DNA pellet for approximately 30 min, following the removal of all the ETOH.

The DNA pellet was then re-suspended in 8 mM sodium hydroxide (NaOH, Fisher-Scientific), with insoluble material being pelleted at 12,000 g for 10 min. DNA was immediately quantified using a Fisherbrand Nanodrop 3000 (Thermo Fisher) spectrophotometer at 230 nm and 260 nm absorbance. DNA was stored at -80˚C overnight prior to use in mtDNA experiments. The isolated DNA is not stable in 8 mM NaOH and therefore cannot be stored for prolonged periods of time. Hence all mtDNA analyses were performed within 48 hrof DNA isolation.

2.9.5.1.2 RNA:DNA Ratios

Upon isolation, purification and quantification of protein and DNA, ratios were calculated. RNA:DNA ratios have previously been used to quantify the level of transcription occurring within the tissue. Ratios were calculated as; µg.µL/µg.µL.

3 Experimental Chapter 1: The extensive characterisation of a 3D *in vitro* Skeletal Muslce model using the C2C12 cell line

3.1 Introduction

In order to understand the physiology of SkM further, the necessity for experimental control has driven the development of *in vitro* SkM culture systems (Baar, 2005). Experiments in monolayer including the use of primary sourced SkM cells and SkM cell lines, have been utilised to examine the cellular and molecular physiology of *in vivo* muscle tissue. Muscle cells *in vivo* develop and grow in a three dimensional (3D) environment, receiving many important physiological cues from the surrounding extra-cellular matrix (ECM, (Smith, et al., 2010) and as such, monolayer investigations may not reflect true *in vivo* physiology. Moreover, recent evidence has suggested the enhanced fusion of cells seeded in a 3D matrix and displaying similar gene expression of a marker of differentiation compared to monolayer cultures (Smith, et al., 2012).

A collagen based model, which has been shown to initiate the required mechanical signals for uni-axial tension, is now extensively published within the literature (Brady, et al., 2008, Mudera, et al., 2010, Smith, et al., 2012). Data demonstrates the development of lines of principle strain, as evidenced using finite element analysis (Eastwood, et al., 1998) along the longitudinal axis with this collagen-based culture system. This facilitates the alignment of seeded cells in a single plane and has been shown to be sufficient in promoting the alignment (Cheema, et al., 2003) and fusion myoblasts or muscle derived cells (MDC's, Brady, et al., 2008, Mudera, et al., 2010, Smith, et al., 2012).

The early work in this system carried out by Cheema et al (2003) examined the seeding density and force characteristic response of C2C12's compared to other primary sourced cells including human dermal fibroblasts and rabbit smooth muscle cells. This data illustrated the stark differences in cell-matrix interaction and contraction between each cell type (Cheema, et al., 2003), with a delayed 8 hr lag phase evident for C2C12's.

There was also confirmation of early myoblast fusion within the C2C12 constructs, however the open nature of the CFM system contributes to contamination and prevents long term culture for enhanced maturation. Additionally, these constructs were 5 ml collagen preparations with 20 x 10^6 cells, requiring long monolayer sub-culturing. This limiting factors, prevent the use of the model proposed by (Cheema, et al., 2003) in longer term physiological experiments.

Recently, Smith et al., (2012) published additional characterisation and optimisation of this model using 3 ml constructs, to enable the longer term culture of primary rat MDC's. The longer term culture of this model allows for the enhanced maturation of the seeded MPC's to attain architecture greatly similar to that of *in vivo* tissue (Smith, et al., 2012). Moreover, the histological analysis provides further evidence for the increased bio-mimicity of 3D culture systems over conventional monolayer culture.

Characterising the culture conditions required for the long term culture of a cell line within this system, would combat experimental and ethical issues surrounding of the previous 5 ml CFM model and the use of primary cells as presented in (Smith, et al., 2012). Furthermore, data has previously shown the high seeding density required to achieve fusion within this model (Smith, et al., 2012, Cheema, et al., 2003). Achieving this high cell number with primary cells is methodologically challenging, due to the limited myogenic potential of MDC's with multiple divisions; even as low three passages (Machida, et al., 2004). Therefore, developing the Smith, et al., (2012) model further for use with a cell line that enables long term culture will increase experimental productivity due to reduced cell isolation and characterisation from primary sources. Further, an increase in control will be achieved due to the homogeneity and sustained myogenic potential with cell lines.

In addition, developing precise control procedures within specific cell lines, will allow for the detailed and controlled investigation of key genes and proteins involved in SkM adaptation, regeneration and degeneration. In the context of the aims of this Thesis, the further development and characterisation of this model will provide a foundation from which the effects of mechanical signals on cell response can be investigated.

3.1.1 Aims

1. To characterise the use of C2C12 cells in 3 ml collagen constructs with respect to seeding density, culture period, macroscopic and histological parameters in the development of a bio-mimetic SkM construct.

2. To set up the mechanical stimulation system and to provide preliminary evidence for the acute regulation of genes implicated in SkM adaptation utilising characterised *in vitro* SkM constructs.

3.1.2 Hypotheses

It was hypothesised that with increased seeding density, the ability for the cells to attach and contract the matrix will be enhanced. Furthemore, the expression pattern of the key myogeninc gene myogenin would display a pattern similar to that witnessed in previous experiments in collagen constructs (Smith, et al., 2012). It is also hypothesised that following evidence of this gene expression pattern, the histological confirmation of myotubes would be achieved. Following this characterisation, it was hypothesised that an acute regimen of mechanical stretch would increase the expression of genes similar to that seen with *in vivo* exercise.

3.2 Methods

3.2.1 Cell Culture

The C2C12 SkM cell line was cultured according to methods detailed (Methods 2.4).

3.2.2 Cell seeded 3D Compliant Collagen Constructs

Collagen constructs were prepared as previously described (Methods2.6). Constructs were made identically for CFM and Chamber Slide experiments. However it is important to note the A-frame structures were prepared differently for CFM and Chamber Slide experiments (see section 2.6.1).

3.2.3 CFM Experiments

Recent data has revealed the necessity for 14 day culture for the fusion of MDC's within collagen constructs (Smith, et al., 2012); however it is clear that the immediate 24 hrs post seeding is vital for cell attachment and survival of seeded cells. The force characteristics of myoblasts and MDC's within these constructs has previously been used to provide data regarding cell-matrix and cell-cell interaction (Mudera, et al., 2010, Brady, et al., 2008, Cheema, et al., 2003), key determinants of cell survival and potential fusion. Therefore, investigating the CFM force profiles of seeded cells is an important factor in defining the myogenic potential.

The endogenous force characteristics associated with the seeded cells remodelling the collagen matrix over a 24 hr period is now comprehensively illustrated in the literature (Mudera, et al., 2010, Brady, et al., 2008, Cheema, et al., 2003, Eastwood, et al., 1998). Data has provided evidence for the use of 4 x 10^6 C2C12 cells/ml for a 5 ml construct to achieve a high cell density for attachment and fusion of the seeded myoblasts (Cheema, et al., 2003).

The current investigation aimed to characterise whether this seeding density would remain optimal for use in 3 ml constructs. Reducing construct volume will reduce sub-culture time to obtain required cell numbers and reduce financial expense, associated with engineering the constructs. Prior to any experimentation the CFM was set-up and calibrated accordingly (see section 2.7). n = 3 collagen constructs were prepared for each seeding density as follows; 1 x 10^6, 2 x 10^6, 3 x 10^6 and 4 x 10^6 cells/ml.

A preliminary seeding density of 5 x 10^6 cells/ml was used, however the force generation was sufficient to pull the construct away from the floatation bar and therefore this seeding density was discarded.

Following the polymerisation, the constructs were floated in GM and were immediately tethered to the CFM. There was no more than 30 min between the seeding of the myoblasts and the beginning of force measurement.

Micro-strain (με) and time data was collected at a rate of 1 Hz for all measurements (sees section 2.7). Raw data from the CFM was converted into μN and analysed as follows. Peak force was taken as the greatest value of force obtained over the 24 hr period. In order to assess the whether peak force was dependent upon cell density and to further ascertain cell-cell and cell-matrix interactions, peak force was also calculated relative to total seeded cell number. Rate of force development (RFD) was calculated as a mean increase in μN/min for the first 60 min of experimentation. Representative force traces for n = 3 constructs is graphically represented (Fig. 3.1).

Previous data had provided evidence for a 5 day culture period necessary to induce C2C12 myoblast fusion within the 5 ml constructs, therefore no histology was performed on the 24 hr CFM experiments

3.2.4 Chamber Slide Experiments

Following the definition of the optimal seeding density for use in experiments, the investigation of the macroscopic contraction of cell seeded collagen constructs was performed over 14 days. n = 4 constructs per time-point were seeded at 4 x 10^6 cell/ml for 5, 7 and 14 days in chamber slides. Scaled images of the constructs were measured throughout the time-course of culture using Image J software (NIH Image, US). Analysis of myogenin and PGC-1α mRNA was also conducted over the 14 day culture period, in order to evaluate the expression of these genes essential for the myogenic programme.

The expression pattern of these genes would provide essential information as to the required culture period for the differentiation of the seeded myoblasts into multinucleated myotubes, as previous data using human MDC's has shown the induction of myogenin mRNA expression only in multinucleated myotubes (Mudera, et al., 2010).

At each time-point constructs were removed from their chamber and A-frames for RNA extraction. Previous published data has suggested 14 days is adequate for the formation of primary rat MDC's (Smith, et al., 2012), however it was important to define a time-course of gene expression for the C2C12 cell line.

To examine whether the 14 day culture period was sufficient for the development of multinucleated myotubes, n = 3 collagen constructs were seeded at 4 x 10^6 cell/ml for 14 days. Following 14 days experimentation, the constructs were removed from the chamber slides and fixed using methanol and acetone (see methods section 2.9.2). Constructs were mounted onto polylysine-coated microscope slides for immunostaining. The constructs were stained to investigate the presence of intermediate filament protein Desmin, an early marker of commitment to the myogenic lineage (see 2.9.2). This protein has commonly been used to identify myoblasts and multinucleated myotubes in this model (Brady, et al., 2008, Smith, et al., 2012). Images were taken using a Zeiss LSM 510 confocal microscope with associated software. Cell-associated fluorescence was visualized by epifluorescence, using; FITC to detect Desmin (excitation at 485 nm and emission at 520 nm) and SYTOX® Green to detect nuclei (excitation at 504 nm and emission at 523 nm).

3.2.5 Tensioning Culture Force Monitor (T-CFM) Experiments

Following the definition of the seeding density and culture time required for the development of constructs with multinucleated myotubes, the effect of mechanical stimulation on genes which have been implicated in the adaptation of SkM to increase load were investigated.

This preliminary investigation aimed to ensure the new mechanical stimulation system was operated correctly, whilst also investigating the response of genes that would be examined in future experiments. n = 3 control constructs (CON) and n = 3 stretch constructs (STR) were seeded and matured for 14 days in culture before being transferred to the t-CFM for experimentation.

A previous investigation has used a 7.5 % substratum strain to investigate the response of seeded MDC's to cyclical mechanical strain (Auluck, et al., 2005). This loading pattern is also similar to continuous loading that would be evident with *in vivo* SkM contraction. Hence, a 7.5 % cyclic continuous strain was applied to the constructs for 60 mins. CON constructs were tethered to the t-CFM for 60 mins without stretch. At the 60 min time-point, constructs were immediately removed from the t-CFM, detached from the A-frames and submerged in 500 μL TRIzol for RNA extraction.

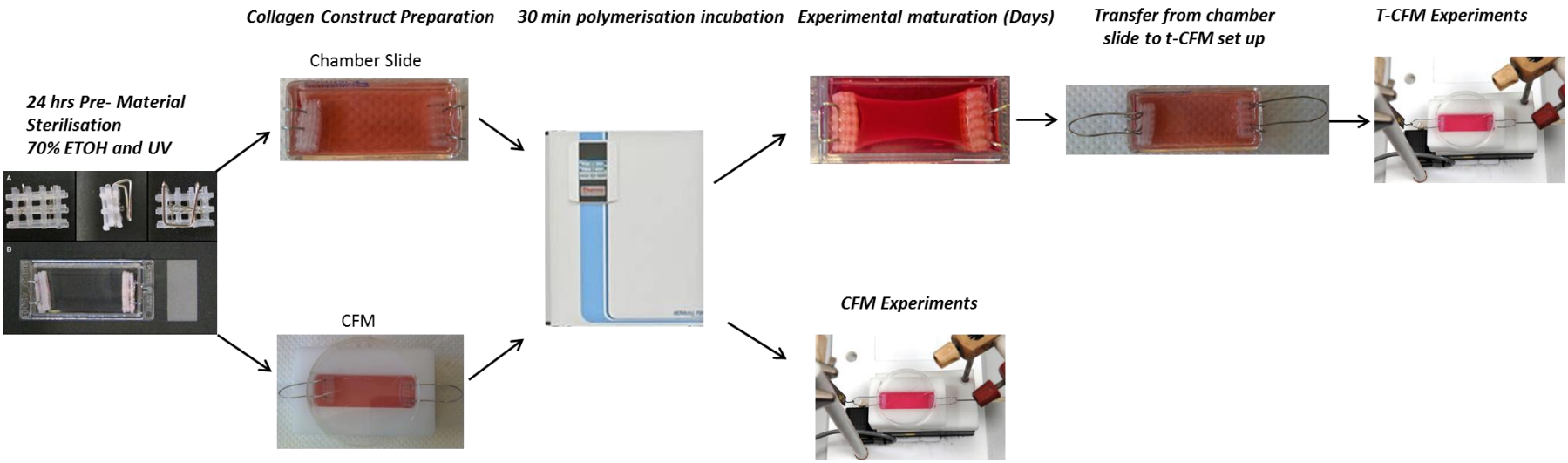

Figure 3-1. Schematic representation of collagen construct preparation and experimentation

3.2.6 Construct Macroscopic Contraction, Isolated RNA and Gene Expression Analysis Experiments

In order to analyse the effect of construct macroscopic contraction upon RNA isolation and gene expression n = 9 constructs were seeded in chamber slides with 4 x 10^6 cells/ml for 14 days maturation. At 14 days, image analysis of the extent of contraction was performed and the constructs were sampled for RNA extraction. The expression of genes associated with SkM development, differentiation and adaptation were investigated using RT-qPCR.

3.2.7 RNA Isolation and Purification

At each experimental sample time-point, constructs were removed from their chamber and RNA was extracted using the TRIzol method according to the manufacturer's protocol (Invitrogen Life Technologies, Carlsbad, CA, USA, see section 2.9.4.2). RNA quantity and quality were assessed by UV spectroscopy at O.Ds of 260 and 280 nm using a Nanodrop 3000 (Fisher Brand, Thermo Fisher Scientific, Rosklide, Denmark) spectrophotometer. 70 ng of RNA was used per RT-qPCR reaction.

3.2.8 RT-qPCR Primers

Primers (see section 2.9.4.3) were designed and synthesised by Sigma-Aldrich, without the requirement of further purification. Primers were designed to meet standard quality criteria; yield products spanning exon–intron boundaries to prevent any amplification of genomic DNA and minimal secondary structure or inter-molecular/intra-molecular interactions (hairpins, self-dimer and cross-dimer).

3.2.9 RT-qPCR and Data Analysis

Once the sample preparation was complete (2.9.4), the samples were loaded into a Rotogene 3000Q (Qiagen) for the one step reaction using the Quantifast SYBR Green Mix (Qiagen). Fluorescence at the end of each extension step was measured using excitation at 470 nm and emission at 510 nm.

The mean C_T values for duplicates were used to calculate relative mRNA expression of the genes of interest (GOI) compared to an internal normaliser and an endogenous housekeeping gene (HKG, RPII). The relative gene expression levels were calculated using the comparative CT ($\Delta\Delta C_T$) equation otherwise known as the Livak method (Schmittgen and Livak, 2008) for determining normalised expression ratios, where the relative expression is calculated as $2^{-\Delta\Delta CT}$, where C_T represents the threshold cycle.

3.2.10 Statistical Analyses

All statistical analysis was performed using SPSS software version 17 (SPSS INC, Chicago, IL, USA) and Graphpad Prism 6 (California, USA). All data analysis and out is detailed in Appendix 2 (8.2.1), where normal distribution and tests assumption statistics are presented. Significant differences between variables were analysed using independent t-tests and one way analysis of variance (ANOVA). For ANOVA, data was tested for homogeneity of variance (Levene's test) to comply with the assumptions of this form of analysis, where all test assumptions were met. A pair-wise comparison post-hoc test was performed with a Bonferroni adjustment for any data with significant F values. Analysis of relationships between variables was conducted using linear regression (Pearson's correlation). The two tailed alpha value of significance was set at $p \leq 0.05$ for all analyses. All data is presented as mean ± standard error of the mean (SEM).

3.3 Results

3.3.1 Constructs seeded with 4 x 10^6 cells/ml represent the greatest potential for the formation of a bio-mimetic SkM model

Increases in peak force were observed in the 3 x 10^6 and 4 x 10^6 seeding densities compared to 1 x 10^6 and 2 x 10^6 constructs despite no statistical main effect ($p = 0.405$, Fig. 3.2 A). The 4 x 10^6 cells/ml constructs displayed the greatest mean RFD compared to all other seeding densities, despite no main effect being observed for this variable reaching statistical significance ($p = 0.063$, Fig. 3.2 B).

In order to ascertain the cell behaviour associated with seeding density and peak force, data was calculated for relative peak force. A significant main effect for relative peak force was observed ($p = 0.009$). A reduction in relative peak force for 2 x 10^6 cells/ml ($p = 0.029$) and 4 x 10^6 cells/ml ($p = 0.014$) compared to 1 x 10^6 cells/ml constructs was observed for this variable, with the reduced relative peak force in the 3 x 10^6 cells/ml constructs approaching significance (Fig. 3.2 B). This data demonstrates a differential effect on peak force, when accounting for seeding density.

Table 3-2. 24 hr Force characteristics of collagen constructs seeded with 1, 2, 3 and 4 x 10^6 cells/ml.

Seeding Density	Peak Force (µN)	Rate of Force Development (µN/min, Initial 60 min)	Relative Peak Force (µN/Total seeded cell number
1 x 10^6/ml	619 ± 92	5 ± 2	206 ± 30
2 x 10^6/ml	570 ± 182	1 ± 1	95 ± 30
3 x 10^6/ml	1008 ± 222	2 ± 4	112± 24
4 x 10^6/ml	917 ± 362	9 ± 2	76 ± 30
Main Effect for Seeding Density (p value)	P = 0.405	P = 0.063	P = 0.009

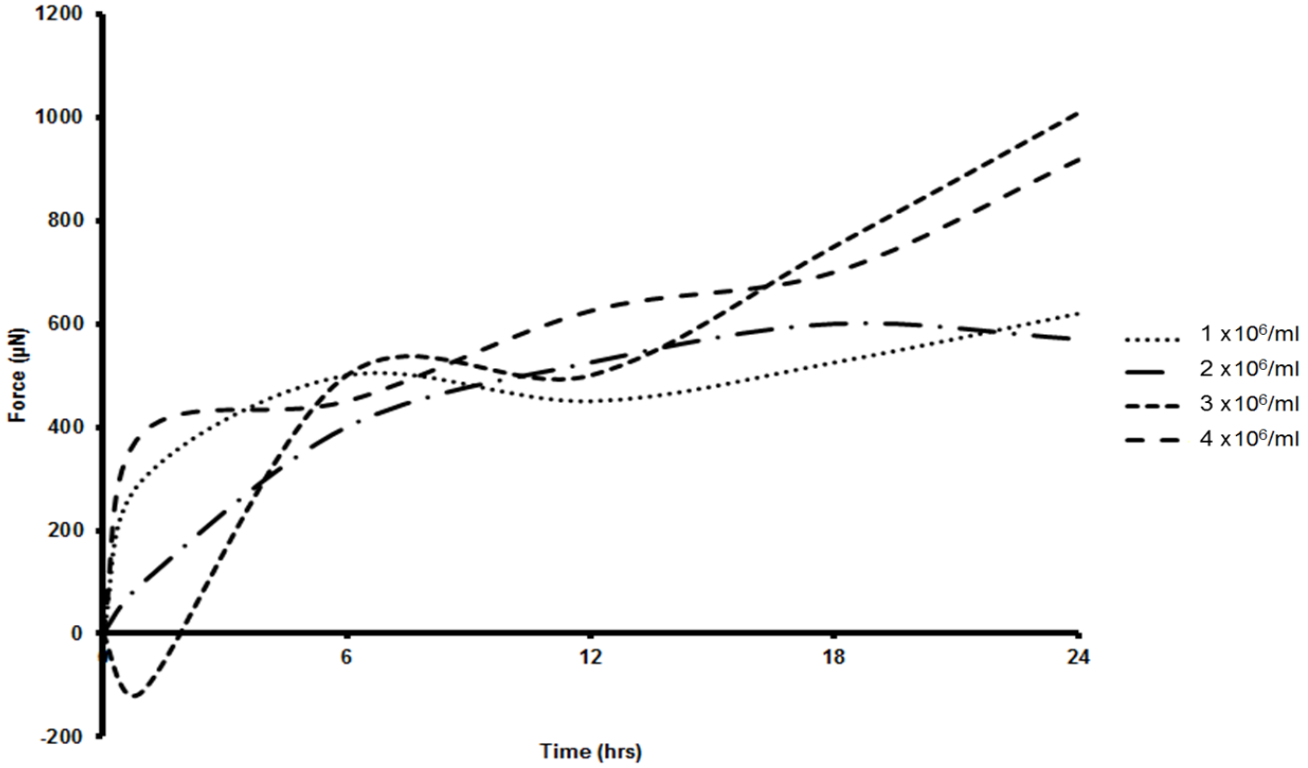

Figure 3-2. <u>Representative</u> mean force trace profiles from CFM experiments conducted over a 24 hr culture period. n = 3 experiments for all seeding densities were conducted with data collected and processed at 1 Hz. Constructs were seeded at 1 x 10^6/ml, 2 x 10^6/ml, 3 x 10^6/ml and 4 x 10^6/ml. Data presented is representative of data collected due to the large volume of data geneeated for each experiment.

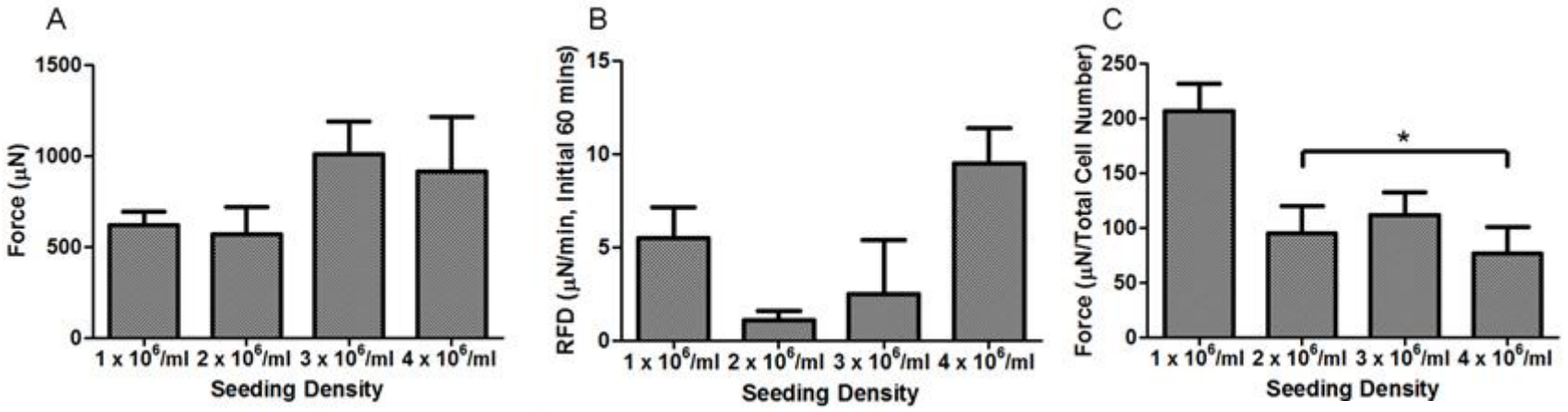

Figure 3-3. CFM data analysis following 24 hr experimentation. Data was collected at 1 Hz and analysed for the following parameters to identify differences between seeding densities. n = 3 experiments were conducted for each seeding density. A) Peak force; data was analysed based upon the highest force recorded over the 24 hr experiment. ($p = 0.405$). B) Rate of Force Development (RFD); data was analysed as a mean increase in force produced per minute for the initial 60 mins of each experiment. ($p = 0.063$). C) Relative peak force displayed per million seeded cells (both $*p < 0.05$ compared to 1 x 10^6 cells/ml). Data is presented as mean ± SEM.

3.3.2 Construct diameter reduces over time in culture

A significant main effect for construct diameter (p = 0.000) was further revealed sharp decline in gel diameter over the first week in culture, with a significant reduction by 3 days compared to 24 hrs (p = 0.016, Fig. 3-4). The second week in culture resulted in a mean, but non-significant further reduction in gel width compared to 5 and 7 days, reaching a final width of 9.10 ± 0.43 mm (p = 1, Fig. 3-4).

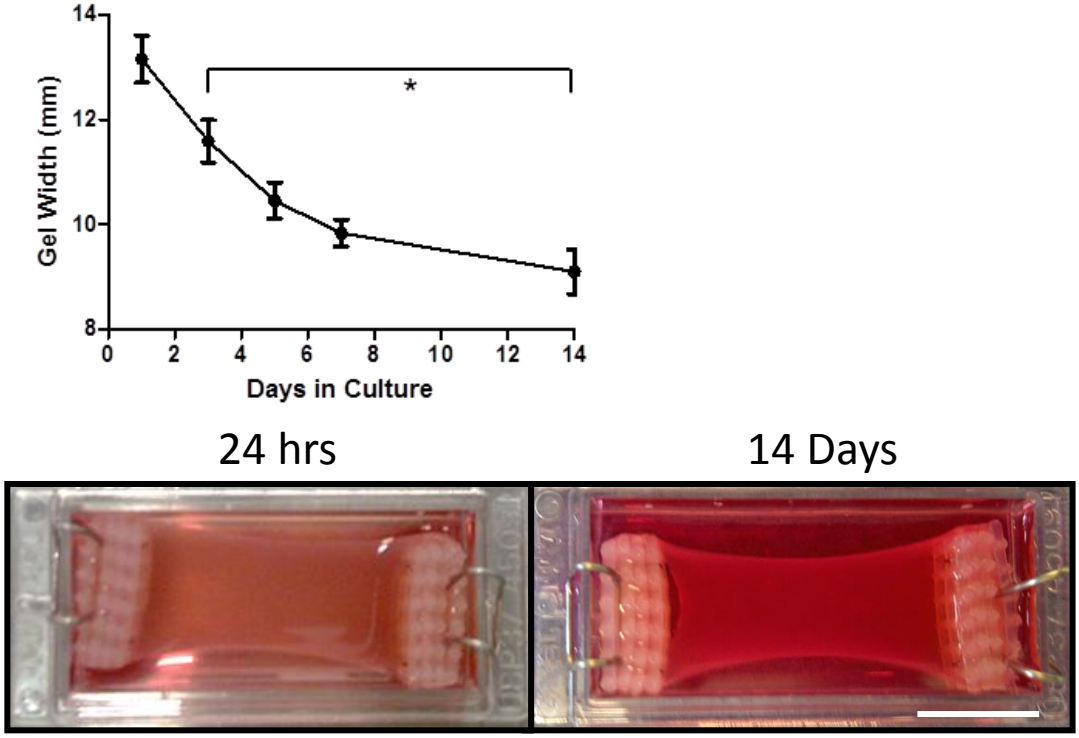

Figure 3-4. Time-course of macroscopic contraction of collagen constructs seeded with 4 x 10^6 cells/ml for 14 days. A significant reduction in gel with at 3 days in culture (p = 0.016) compared to the 24 hr time-point. No significant further reduction in gel width was observed beyond 5 days. *all p < 0.05 compared to 24 hrs. N = 3+ constructs were analysed. Data is presented as mean ± SEM. Scale bar = 10 mm.

3.3.3 A culture time of 14 days is required for the expression of the myogenic programme

Following evidence for the remodelling of the collagen matrix of a 14 day culture period, it was important to investigate whether the single seeded cells has fused within the constructs. Studying the pattern of myogenin mRNA provides evidence for the time course of the myogenic programme within the constructs and has previously been used within this model as an indicator for differentiation (Mudera, et al., 2010, Smith, et al., 2012). However it was important to demonstrate a similar expression pattern as a transcriptional indicator of fusion of C2C12's in this model.

Data presented here illustrates a higher to lower expression pattern of myogenin mRNA across the 14 day culture period in the chamber slide system. Mean reductions from 0.98 ± 0.35 at 5 days to 0.74 ± 0.43 at 7 days, falling to 0.57 ± 0.38 at 14 days (no significant main effect p =0.072, Fig. 3-5 A), demonstrate a reduction in the transcript required for differentiation. This provides evidence from a transcriptional perspective that the induction and potential fusion of seeded myoblasts to multinucleated myotubes has occurred within this time course of experimentation.

The process of myoblast fusion requires vast amount of ATP to supply the energy required during this developmental process. Indeed PGC-1α has been shown to play a pivotal role in co-ordinating mitochondrial biogenesis, to stimulate a greater oxidative potential for ATP production during the regeneration of SkM (Duguez, et al., 2002). The expression pattern of PGC-1α mRNA demonstrates variable expression, with mean reductions at 7 and 14 days compared to 5 days (main effect p = 0.132, Fig. 3-5 B).

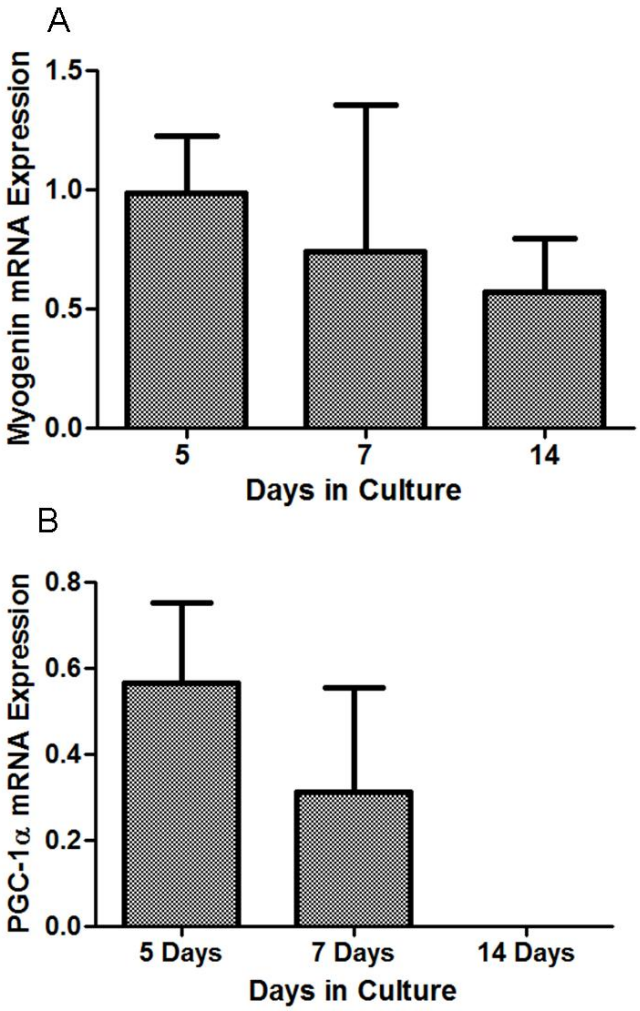

Figure 3-5. Time-course of gene expression of genes required for the myogenic programme. Collagen constructs were seeded with 4 x 10^6 cell/ml. n = 3 constructs per time-point were used. A) Reductions in myogenin mRNA at 7 and 14 days compared to 5 days culture (p = 0.072). B) Reductions in PGC-1α mRNA expression at 7 and 14 days compared to 5 days in culture (p = 0.132). Data is presented as mean ± SEM.

With transcriptional evidence for the development of myotubes within the collagen constructs by 14 days at 4 x10^6 cells/ml, it was important to determine histologically whether myotubes had formed. Collagen constructs were immunostained for cytoskeletal intermediate filament protein Desmin, a specific marker of cells of the myogenic lineage.

Images did indeed reveal the alignment and fusion of myoblasts to multinucleated myotubes in a single plane (Fig. 3-5). Images also revealed the development of myotubes in multiple axes, as demonstrated by myotubes present in different focal planes. This data further supports previous immuno-histological analyses of SkM cells in this system (Smith, et al., 2012) and demonstrates the conserved nature of myotube development and orientation in an alternative cell type.

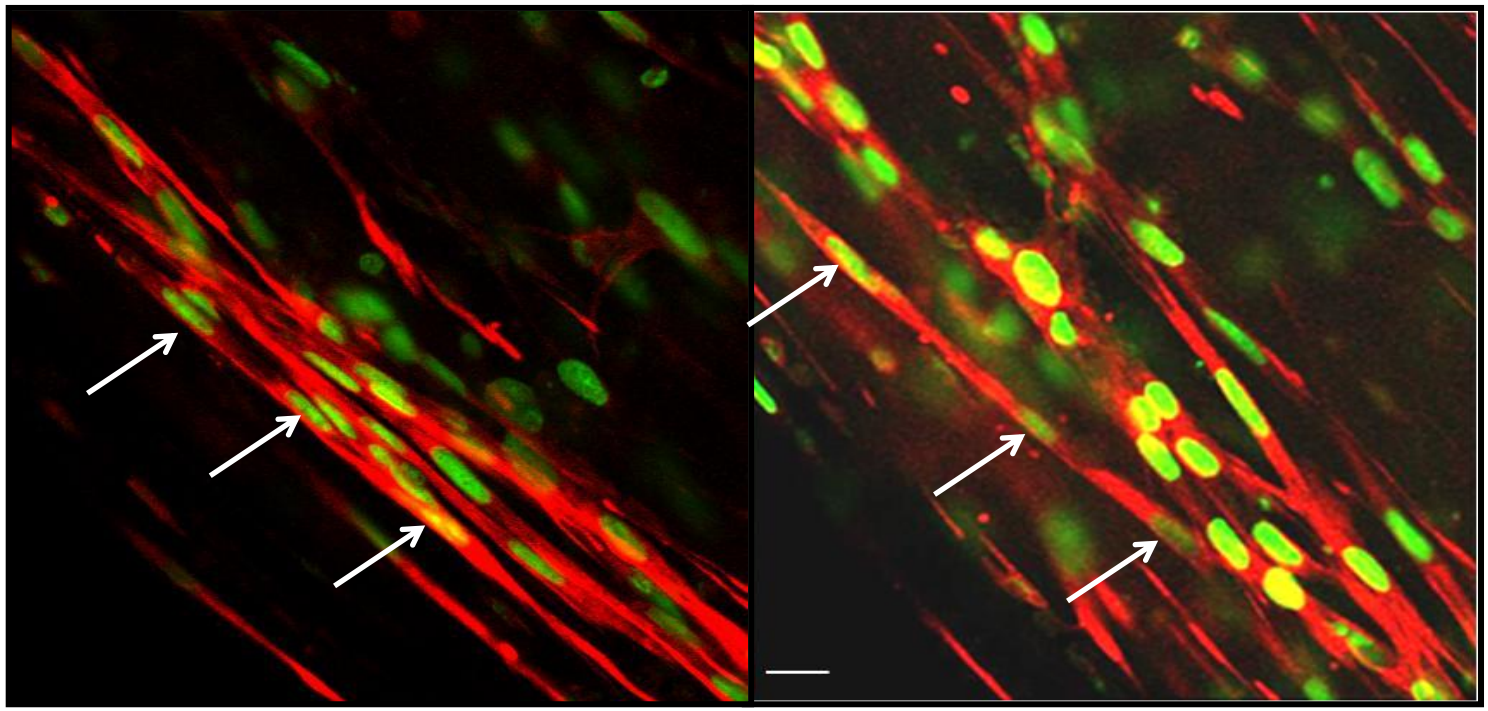

Figure 3-6. Collagen constructs seeded with 4 x 10^6 cells/ml for 14 days. Fixed constructs were immunostained with Desmin (Red) and SYTOX Green (Nuclei). Scale bar = 20 µm. Note the high level of orientation of the cells and the myotubes present with multiple nuclei as indicated by arrows.

3.3.4 Cyclic mechanical stretch of characterised constructs identifies large variation in gene expression response

Following the characterisation of the required seeding density and the duration of culture to develop a construct with multinucleated myotubes, the use of these constructs for mechanical stetch experiments was sought. In order to test the mechanical stimulation system developed within the laboratory a preliminary cyclic mechanical stretch experiment was conducted. This experiment sought to examine the effect of 60 mins continuous cyclic stretch at 7.5 % strain, upon the regulation of genes that would be investigated in greater detail in future experiments. This strain and stimulation mode has been shown to be effective in inducing a mechano responsive of MDC's (Auluck, et al., 2005).

Surprisingly, gene expression analysis showed a high degree of variation in the response of the stretched constructs (STR) compared to static controls (CON, Fig 3-7). A significant difference in reduction in Tfam mRNA expression was observed between STR and CON ($p < 0.001$). This finding is unanticipated considering the role Tfam plays in response to mechanical and metabolic signals to stimulate mitochondrial biogenesis *in vivo*. Evidently, there were no other significant changes in gene expression, with no apparent pattern indicative of a physiological response. This variation appeared to reside in variation in the expression of the genes of interest (GOI), as there was stability in the expression of the HKG (C_T's, 18.56 ± 0.49, CON vs. 18.86 ± 0.78, STR). As such the significant effect for Tfam may represent an error in variability, which may change with increased statistical power.

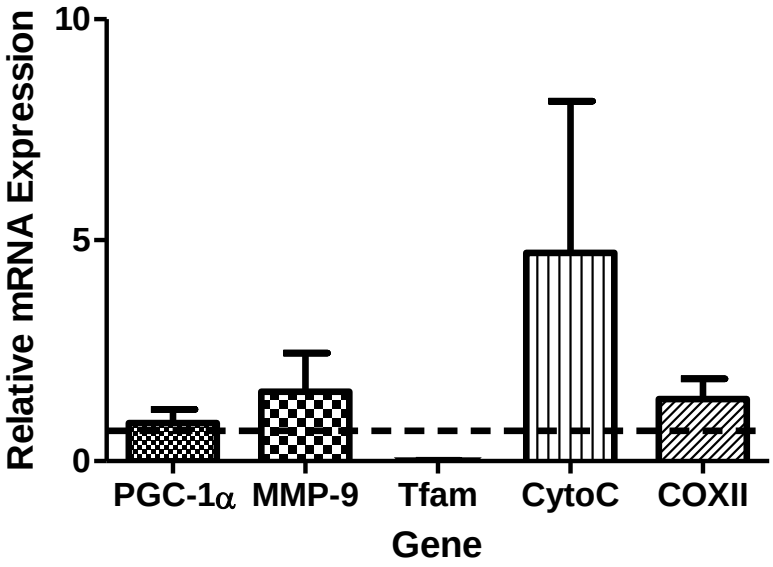

Figure 3-7. Acute mRNA regulation in response to cyclic mechanical stretch relative to static controls. n = 3 collagen constructs were seeded at 4 x 10^6 cells/ml for 14 days for both conditions. PGC1-α = Peroxisome proliferator-activated receptor gamma coactivator 1-alpha; MMP-9 = matrix metalloproteinase-9; Tfam = mitochondrial transcription factor A; CytoC = Cytochrome C; COXII = cytochrome C oxidase subunit II. Data is presented as a relative increase above control (CON, dotted line). Data is presented as mean ± SEM.

Table 1. Significance values for differences between STR and CON constructs subjected to 7.5% continuous cyclic strain.

Gene	P Value (Significance, STR vs CON)
PGC-1α	0.683
MMP-9	0.548
Tfam	0.000
CytoC	0.341
COXII	0.433

3.3.5 Construct bowing correlates to isolated RNA concentration and gene expression; a <10 mm construct width experimental control required for future experimentation

The inherent variation within the constructs was evident from the CFM data and the gene expression data from both the time-course and mechanical stimulation experiments. This demonstrates a variation in cell behaviour between construct samples, despite the same culture conditions. It was also witnessed that the macroscopic contraction (construct diameter) was variable between cultures. It was hypothesised that these variations would contribute to a difference in basal gene expression of the constructs and in this light would manifest a high level of variation during post stretch gene expression analysis. In order to develop a method to control for such variations, the expression of genes known to regulate differentiation, maturation and metabolism were investigated in relation to the extent of contraction of the constructs over a 14 day culture period.

The extent of construct contraction significantly predicted the amount of total RNA isolated from the constructs ($R^2 = 0.7788$, $p < 0.01$, Fig 3-8 A), demonstrating a potential increased level of transcription with a greater amount of bowing.

The expression of an endogenous proposed housekeeping gene (HKG, RPII), was also found to be highly dependent on the extent of the construct bowing (R^2 = 0.945, $p < 0.0001$, Fig. 3-7 B). The amount of isolated RNA also significantly negatively predicts the C_T of RPII (R^2 = 0.87, p= 0.0002, Fig. 3-8 C), despite the amount of template RNA for the RT-PCR reaction remaining the same. This level of variability proposes significant problems when using the comparative delta delta C_T method (Schmittgen and Livak, 2008) for gene expression analysis. This method is dependent on the stability of the endogenous control gene, to reliably and validly investigate gene expression.

A moderate positive relationship was found between the extent of construct bowing and myogenin mRNA C_T (R^2 = 0.459, $p > 0.05$, Fig 3-8 D), suggesting a modulation of the potential for differentiation. Furthermore, the extent of contraction positively correlated to the C_T of IGF-I, a gene highly implicated in SkM differentiation and hypertrophy (R^2 = 0.459, p = 0.0449, Fig 3-8 E). A significant positive correlation was also found between construct diameter and the C_T of PGC-1α (R^2 = 0.695, p = 0.0053, Fig 3.7 F). This suggests that the extent of the bowing of the constructs affects the potential to stimulate mitochondrial biogenesis, a necessity to increase mitochondrial content for ATP synthesis required for fusion and cell survival. As such this will contribute to increased cell survival, attachment to the matrix and potential for fusion, increasing the bio-mimicity of the model.

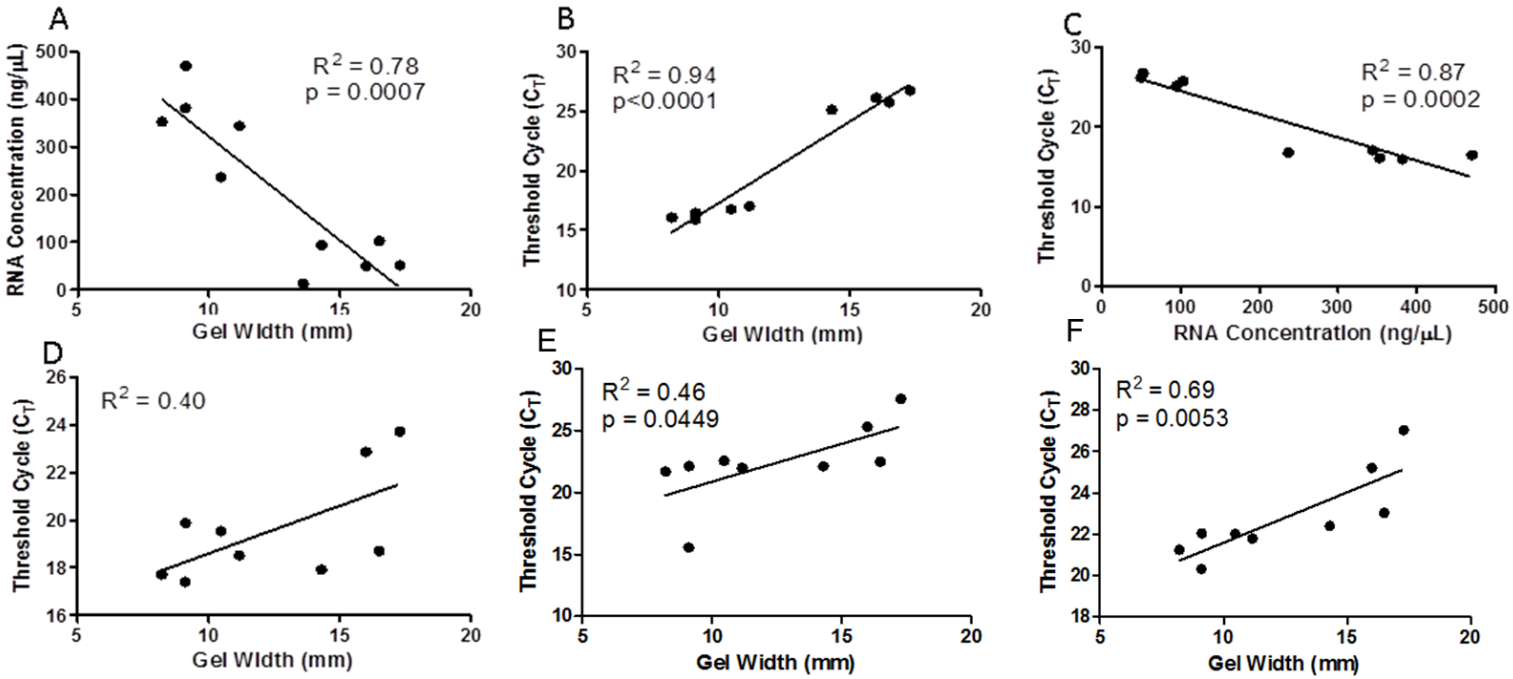

Figure 3-8. Linear regression analyses between construct contraction (gel width), isolated RNA and consequential gene expression. n = 9 collagen constructs seeded at 4 x 10^6 cells/ml were cultured for 14 days prior to images analysis and RNA extraction. A) There is a significant negative relationship between construct width and isolated RNA. B) Construct width significantly positively correlates to RPII C_T. C) Isolated RNA concentration significantly negatively correlates to the observed C_T of RPII. D) There is a moderate positive linear relationship between construct width and myogenin C_T. E) Construct width significantly predicts the C_T of IGF-I. F) There is a significant relationship between construct width and PGC-1α C_T.

3.4 Discussion

The aim of the current investigation was to further characterise the use of an established 3D model of SkM *in vitro*. The requirement to characterise the use of a cell line in this system for long term culture, will allow for the investigation of a homogenous population of seeded cells without the requirement of primary tissue sources. Moreover, the use of a homogenous cell populated tissue will combat experimental issues surrounding the inherent variability between primary and particularly human cells. This increased control will provide a model to analyse the molecular mechanisms that govern *in vivo* SkM and particularly myogenic cell physiology.

3.4.1 CFM Data

Previous investigations have used the CFM to investigate the cytomechanical properties of cells within this model of SkM. Data reported here provides evidence for the use of 4 x 10^6 cells/ml 3 ml C2C12 collagen constructs a reduction in volume from previous published data (Brady, et al., 2008, Mudera, et al., 2010, Smith, et al., 2012). This data demonstrates differential cytomechanical characteristics for each seeding density investigated (Fig. 3-2), further suggesting that the initial RFD may not relate to the peak force achieved (Fig. 3-3, Mudera, et al., 2010). This may reflect the complex nature of the cell-matrix and cell-cell interactions that are modulated dependent on seeding density, as demonstrated by calculating relative peak force (Fig. 3-3 C). Furthermore, seeding 5 ml collagen constructs at 1 x 10^6 cells/ml results in an 8 hr lag phase of force development, compared to constructs seeded at 4 x 10^6 cells/ml that show a similar profile to that presented here (Cheema, et al., 2003).

The force profiles for each seeding density used in the current investigation, demonstrate the development of traction, contraction and force plateau, characteristic of cells within collagen matrices (Fig. 3-2, Eastwood, et al., 1998). This therefore illustrates that reducing the gel volume and consequential cell number does not affect the cytomechanical characteristics of cells within this system.

Previous data has demonstrated the importance of the aspect ratio of the long and short axes in determining cell behaviour within collagen matrices (Eastwood, et al., 1998). The aspect ratio of constructs seeded in 5 ml and the 3 ml constructs presented here is the same. This further supports the notion of aspect ratio as an important determinant in cell behaviour, rather than construct volume.

3.4.2 Construct Width

Once a seeding density of 4 x 10^6 cells/ml was defined for the use in further experiments, the extent of the characteristic bowing within this model was investigated. Previous data has established a significant reduction in the construct surface area throughout a time course of culture (Smith, et al., 2012). Data presented here, further demonstrates a significant reduction ($p < 0.01$, Fig. 3-4) in the construct width over 14 days in culture. This demonstrates in this myoblast only model, that the cells are capable of remodelling the matrix, a phenomenon that was thought to be mainly driven by the non-myogenic component of primary cell seeded constructs (Smith, et al., 2012). However it is important to note the magnitude of the bowing in this current investigation is not as great as reported in Smith et al., (2012), suggestive that the non-myogenic component of primary cell cultures have the ability to remodel the matrix to a greater extent. Furthermore, previous work has suggested a synergistic role for the non-myogenic cells in the development of these constructs (Brady, et al., 2008).

Notwithstanding a role for the non-myogenic cells, it is demonstrated here that C2C12 myoblast only constructs remodel the collagen matrix promoting an increased cellular density to enhance the potential for myoblast fusion. The increased cell density will also promote an increased cell to matrix ratio, developing a tissue that more greatly represents *in vivo* SkM. Following the identification of matrix remodelling, it was necessary to ensure that single seeded myoblasts fused into post-mitotic multinucleated myotubes.

3.4.3 Fusion of seeded myoblasts

The expression of both myogenin and PGC-1α mRNA were found to follow a high to low pattern (Fig. 3-4), suggestive that the transcriptional signals required for differentiation were switched on at 5 days then down-regulated throughout the rest of the culture period. The expression of myogenin marks the entry of myoblasts into the differentiation process (Hawke and Garry, 2001); whilst myogenin and PGC-1α have been demonstrated to play a pivotal role in the regenerative process of SkM *in vivo* (Duguez, et al., 2002). These data provide support that the model developed here recapitulates the developmental and regenerative processes that occur with SkM *in vivo*, in terms of myogenin and PGC-1α expression patterns.

The data presented here also follows a similar pattern to that seen in this model using primary rat MDC's, whereby myogenin follows a high to low expression over a 14 day culture period (Smith, et al., 2012) sufficient to induce myoblast fusion. Experiments presented later in this thesis aimed to investigate the role of PGC-1α in response to mechanical stretch and therefore it was important to ensure its expression was completely down-regulated before experiments could begin. Coupled with the myogenin data, a 14 day maturation period prior to mechanical stretch experiments would be necessary to meet this requirement.

Analysis of the cellular architecture within this model was also necessary to confirm the presence of differentiated cells in this system at 14 days in culture. Previous data has showed the alignment of cell from multiple cell types, which is highly dependent on the predictable lines of strain throughout the matrix (Eastwood, et al., 1996, Cheema, et al., 2003, Smith, et al., 2012). This mechanical cue has been shown to be sufficient to encourage the alignment and fusion of seeded myoblasts (Sharples, et al., 2011, Smith, et al., 2012). This current investigation confirmed the presence of highly orientated myotubes, morphologically similar to *in vivo* SkM (Fig. 3-5).

Additionally, the 3D environment and mechanical tension generates cellular architecture which is improved above standard monolayer cultures, whereby the presence of branched myotubes is often found in this cell line (Sharples, et al., 2011). Despite evidence for myoblast fusion, it was not possible to quantify the extent of the process, due in part to the 3D nature of the constructs. In particular, the presence of myotubes and nuclei in multiple focal planes prevents the objective measurement of fusion, due to the limitation of microscopy to a single plane of focus at any one time. Future work using confocal microscopy and automated image analysis software may overcome this problem.

3.4.4 Mechanical stretch

Following the confirmation of the presence of myotubes with the culture conditions discussed, a preliminary investigation was conducted using mechanical stretch. It was found that the expression of genes that have previously been shown to be implicated in the acute response of SkM to increased load (Hood, 2001, Rullman, et al., 2007) was highly variable in this system (Fig. 3-6). This variability resulted in no statistical and physiological pattern of expression from being attained, giving rise to questions over reproducibility of culture in this model. It was evident from construct observations used in the mechanical stretch experiment, that there were inherent differences in the extent to which the constructs macroscopically contracted.

3.4.5 Gel width as a control measure

To this end, the extent to which the constructs bow over 14 days in culture was investigated in relation to expression of genes associated with myogenesis, hypertrophy and metabolic plasticity. Of particular interest was the positive association between construct contraction and the amount of total RNA isolated from the constructs (Fig. 3-7 A). Myogenesis is highly dependent on the expression of a magnitude of genes to co-ordinate the determination and fusion of myoblasts.

Early work demonstrated the increased half-life of synthesised RNA species at the fusion process (Buckingham, et al., 1974) and that hypertrophy is characterised by an increase in total RNA (Goldberg, 1967). These data suggest the muscle adaptation and regeneration is co-ordinated to a great extent by a transcriptional mechanism required for myoblast fusion and hypertrophy. It could therefore be hypothesised that the increase in total isolated RNA associated with the constructs that have contracted the greatest, have the greatest potential for fusion and hypertrophy.

The stable expression of an endogenous control gene is required for use in qPCR analysis using the comparative C_T method (Schmittgen and Livak, 2008). Data presented here demonstrates the variability in the house keeping gene used (RPII C_T expression) which is highly dependent on the extent of construct bowing (Fig 3-7 B). Thus, using these data in experiments to infer the regulation of particular genes will not provide insightful and meaning data.

The expression of the myogenic regulatory factors (MRF's) is indispensable for myogenesis, both embryonically and post-natally (Hawke and Garry, 2001). Myogenin augments the differentiation programme leading to myotube formation (Berkes and Tapscott, 2005). Evidence presented here suggests that the extent of bowing the constructs moderately relates to the expression of myogenin mRNA (C_T, Fig. 3-7 D). The pattern of expression may reflect the increased density of cells within the matrix, as cells in closer proximity to each other will co-ordinate the expression of myogenin to induce fusion.

Additionally increases in myogenin have been associated with increased fusion within this cell line (Sharples, et al., 2010). The positive association between construct width and the expression of IGF-I C_T also provides evidence for an altered potential for differentiation and hypertrophy (Fig 3.7 E). IGF-I has been reported to play a significant role in mediating myoblast differentiation (Allen and Boxhorn, 1989), regulated in part through the PI3K pathway (Coolican, et al., 1997).

Indeed, IGF-I has also been suggested underpin the morphological and biochemical differentiation observed within the C2C12 cell line (Sharples, et al., 2010). A muscle specific knock out of the IGF-I receptor (IGF-IR, MKR), demonstrates an essential role for IGF-I in myoblast differentiation (Heron-Milhavet, et al., 2010) whereby isolated MKR muscle precursor cells showed impaired differentiation compared to wild type controls following muscle damage (Heron-Milhavet, et al., 2010). This data therefore suggests that increased IGF-I mRNA expression associated with construct bowing may result in increased fusion, developing a tissue that is more characteristic of *in vivo* SkM.

PGC-1α has been suggested to be the master regulator of mitochondrial biogenesis, stimulating the co-ordinated expression of mitochondrial and nuclear encoding genes to increase mitochondrial DNA and protein content (Hood, 2001). Investigating the metabolic control within the constructs revealed a significant linear relationship between construct bowing and PGC-1α mRNA expression (C_T, Fig. 3-7 F, $R^2 = 0.69$, $p = 0.0053$). This data suggests the increased potential for mitochondrial biogenesis in constructs that have remodelled the matrix to a greater extent. Evidence has also suggested the increased expression of PGC-1α mRNA and mitochondrial transcription factor protein expression during the onset of satellite cell differentiation (Duguez, et al., 2002) increasing the ATP generating potential to support the myogenic process.

Additionally, using a specific inhibitor against mitochondrial protein synthesis reduced the differentiation of C2C12's as evident by a reduction in muscle creatine kinase (Hamai, et al., 1997). These data suggest that the increased expression of PGC-1α seen in the constructs that have bowed to a greater extent, may promote increased fusion compared to constructs with reduced PGC-1α mRNA expression.

Drawing upon this data, it is proposed that a control over the extent of bowing of the constructs should be in place for future expeirments. As such, constructs that do not contract the matrix beyond a 10 mm width should be excluded from further experimentation. This control will allow for the reduced variability in basal gene expression, in order that any regulation of particular genes by an experimental condition may be analysed in reliable and valid conditions. This would contribute to approximately a 75 % seed-experiment conversion rate, increasing the level of control for mechanical stimulation experiments.

3.5 Conclusions

Data presented here demonstrates the proposed use of a seeding density of 4 x 10^6 C2C12 cells/ml in a 3 ml collagen-based model of SkM. Further a culture period of 14 days is required for the development of multinucleated myotubes, with displaying morphology representative of *in vivo* SkM. Variation in gene expression following mechanical stimulation resulted in the investigation of construct macroscopic contraction as a control measure.

Altered regulation of genes implicated in the development and maturation of SkM have been shown to be dependent on the cytomechanical properties of the seeded cells, as evident by the differential amount of construct bowing. Controlling for this variability using a construct contraction cut-off point, will allow for the controlled investigation of SkM physiology and pathophysiology in a bio-mimetic *in vitro* model. Moreover the characterisation of this model using a cell line in an isolated system permits the investigation of intrinsic mechanisms that regulate SkM plasticity.

4 Modelling Contrasting Regimes of Skeetal Muscle Loading Using Bio-Engineered Skeletal Muscle: Metabolic and Transcriptional Responses

4.1 Introduction

Following the extensive characterisation of the SkM constructs in the previous chapter, the utilisation of this model to investigate responses to cyclical stretch were investigated. SkM is often described as diapplying a high degree of plasiticity, as it adapts readily to the physiological demands placed upon it, whether mechanical or metabolic, or both (Pilegaard, et al., 2000). Endurance based exercise has the ability to increase the oxidative capacity and metabolic efficiency of SkM (Holloszy, 1967) and as such, endurance exercise and training represents a key mode of physical activity in the fight against many pathologies including ageing, cancer and metabolic disorders such as, obesity, hypertension and diabetes (Rockl, et al., 2007).

Despite the widely accepted benefits of endurance exercise, the molecular mechanisms underpinning the responses are still poorly understood (Coffey, et al., 2006). It has been suggested that phenotypic adaptations are regulated by transient and temporal changes in key genes which are activated following a bout of exercise (Hood, 2001). Such changes can occur within hrs of an exercise stimulus, driven mainly by post-translational modifications of key signalling proteins. As a consequence, these changes have been thought to govern the adaptations observed in oxidative capacity and substrate utilisation via increases in mitochondrial number and content (Olesen, et al., 2010). Much focus has been placed upon understanding the mechanisms and consequences of the activation of the master regulator of mitochondrial biogenesis, PGC-1α. This gene and protein forms a major part of the network that controls mitochondrial plasticity.

In spite of an increase in research into some of the molecular signals that govern this process, methodological limitations associated with *in vivo* testing including muscle biopsy sampling method, complex temporal gene expression, ethical considerations and inter-individual differences, have hindered a greater understanding of the complex molecular pathways (Caron, et al., 2011, Friedmann-Bette, et al., 2012).

The use of *in vitro* systems allows for the controlled investigation of endogenous metabolic and molecular responses, controlling for the influence of systemic factors that would be present in the circulatory system *in vivo*. The notion of the use of 'pre-clinical models of exercise intervention' provides a more high-throughput analytical tool for the investigation of potential exercise and pharmacological therapies for disease.

To date the use of controlled *in vitro* SkM systems, have commonly taken the form of electrically stimulated models in an attempt to replicate contractile activity which stimulates mitochondrial adaptation (Nedachi, et al., 2008, Nikolic, et al., 2012). Conversely, the use of mechanically stimulated models to investigate mitochondrial dynamics has received little attention, despite a recent review suggesting the *in vivo*-like metabolic adaptations that can be observed using *in vitro* stretch systems (Passey, et al., 2011). Moreover, *in vivo* skeletal movement and muscle contraction results in a significant mechanical stimulus upon SkM cells. This stimulus has not been fully investigated with respect stimulating a mitochondrial and metabolic response and therefore provides an interesting area of research.

Previously published data utilising a monolayer and multi-axial SkM cell stretch model system has demonstrated stretch-induced glucose uptake, providing evidence for a mechanical signal in regulating this fundamental homeostatic process (Iwata, et al., 2007). This data provides a clear foundation for further work to be conducted surrounding the influence of mechanical stretch on metabolic parameters in SkM. However *in vitro* stretch systems such as that used by Iwata et al. (2008) lack structural and mechanical comparison to *in vivo* tissue, with many of these limitations discussed previously (see section 1.11). Importantly, many stretch paradigms currently used lack *in vivo*-like comparisons in terms of the variables manipulated including; duration, load and velocity of stimulation.

Therefore, the current investigation sought to address many of these issues to investigate the influence of mechanical stretch upon muscle cell metabolism and mitochondrial DNA replication. Following the characterisation of the SkM model in the previous chapter, these variables could be investigated in a highly controlled environment which recapitulates much of the *in vivo* SkM niche.

4.1.1 Aims and Hypotheses

1. Characterise the acute biochemical responses to two distinct modes of mechanical stretch, which represent *in vivo* modes of SkM loading.
2. Analyse the acute transcriptional response regulating mitochondrial biogenesis and mtDNA synthesis.

It was hypothesised that the distinct mechanical stetch regimes would contribute to a differential metabolic response, due to the differences cell-matrix response to the workload. Furthemore, it was hypothesised that these biochemical metabolic differences wouls translate to a distinction in the transcriptional response of the genes of interest.

4.2 Methods

4.2.1 Cell Culture

For all experimentation cells were used below passage 8. Monolayer cell culture was performed to increase cell numbers required for expeirments (see section 2.4).

4.2.1.1 Cell seeded 3D compliant collagen constructs

N = 9 collagen constructs were prepared as previously described in the Methods section (2.6). Following 4 days of culture in GM the medium was changed to differentiation medium (DM), to stimulate maximal levels of fusion, according to a previously published protocol (Smith et al., 2012). DM was changed every 48 hrs. A subsequent 10 days of culture allowed for the differentiation of singled seeded myoblasts into multinucleated myotubes aligned in a single plane, as characterised in the previous chapter.

4.2.2 Mechanical stimulation experiments

Following this 14 day developmental period, constructs were removed from the chamber slides and transferred to polyethylene moulds. A-frames for attachment to the t-CFM were fixed into the floatation bars and 6 ml DM was added to the mould. Constructs were then mounted upon the t-CFM for mechanical strain experimentation. N = 3 static controls (no mechanical stretch) were used as controls. An *in vivo* equivalent of such a control would take the form of a non-exercised group of participants or animals. The following stimulation protocols were conceived to investigate whether contrasting regimes of external mechanical load could induce a differential intrinsic cellular response, similar to that seen with *in vivo* exercise (Gibala, et al., 2006, Burgomaster, et al., 2008, Bartlett, et al., 2012).

4.2.2.1 Continuous Cyclic Mechanical Stimulation Protocol

In order to model a lower intensity strain of mechanical load, a stimulation protocol was developed to replicate the mechanical nature of such a regime *in vivo*; continuous moderate intensity exercise. To this end, a continuous cyclic load of 7.5 % (0.4 Hz; Fig. 4-1 A) was applied to the constructs for 60 mins.

4.2.2.2 Intermittent Cyclic Mechanical Stimulation Protocol

Similarly, a stimulation protocol was developed to model the mechanical nature of a bout of higher intensity and increased load. As such, the following protocol was used; 10 % intermittent cyclic load for 10 repetitions (0.3 Hz; Fig. 4-1 A) was followed by a 90 sec rest period (1 repetition). 3 further repetitions proceeded, with a 3 min rest period following the final repetition. The set of four repetitions was classed as an interval. Four intervals were completed in total. Previous literature has indicated that these strain and stimulation modalities can induce acute responses to SkM cells *in vitro*, further providing justification for their use (Powell, et al., 2002, Auluck, et al., 2005, Sasai, et al., 2010).

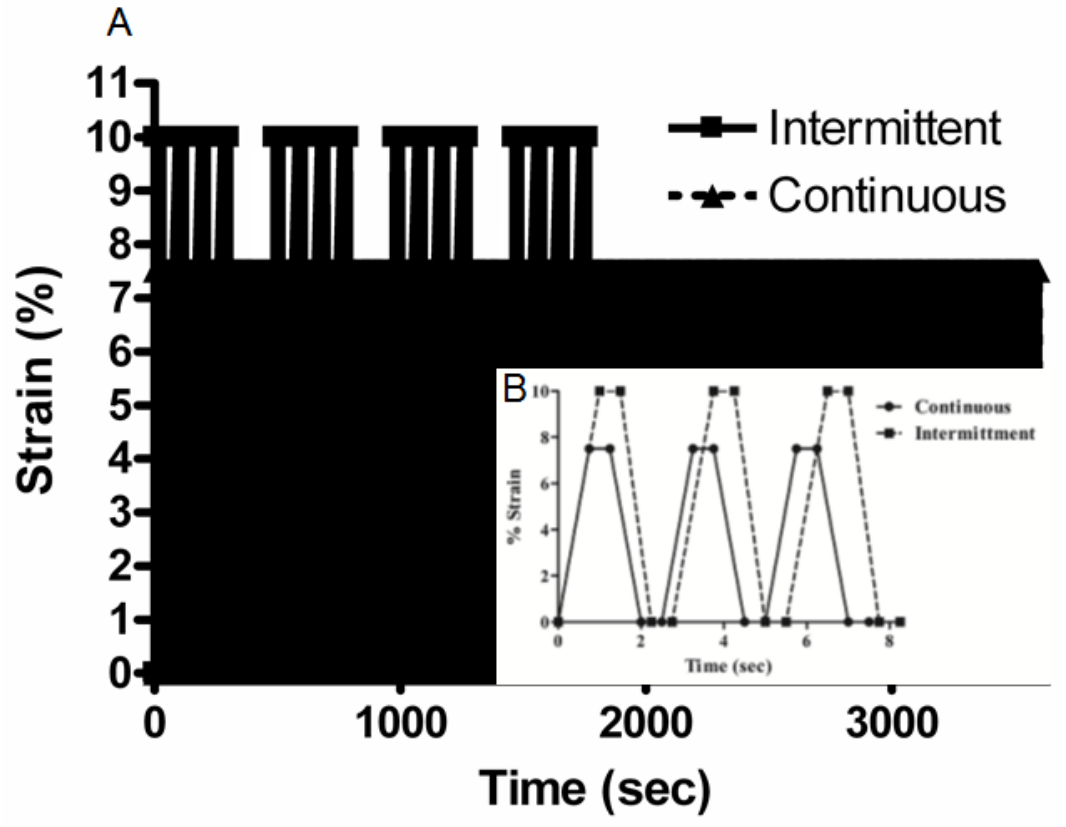

Figure 4-1. Continuous and Intermittent Cyclic mechanical stretch regimes. A) Graphical representation of the pattern of stretch used over the 60 minute expeirmentation. The clear constant workload in the Continuous condition is denoted by the insense black block up to 7.5 % strain. It is also clear to see the individual repetitions and intervals in the Intemrittent condition. B) Insert of the cyclical nature of the mechanical strain employed for 3 cycles for each condition.

4.2.3 Substrate Analysis

In order to analyse the metabolism of lactate and the uptake of glucose during the mechanical stretch protocols, conditioned media sampled from the media contained within the polyethylene moulds, was sampled post experimentation. An Analox Analyser P-GL5 (Analox) was appropriately calibrated and used to analyse both [lactate] and [glucose] within the conditioned media. To test whether the collagen gel was acting as a sponge with respect to absorbing and releasing lactate at any stage of the stimulation protocol, an a-cellular construct was tested for media lactate concentration during mechanical stretch.

No differences in media lactate were observed for either stretch regime (data not shown).

4.2.4 Construct Sampling and Extraction Protocol

Immediately following the end of the stretch protocol, the construct was removed from the t-CFM and the 'A-frames' and immersed in TRIzol (Invitrogen). RNA and DNA were extracted using the TRIzol method (see 2.9.4.2). RNA:DNA ratios were calculated as μg/μL:μg/μL.

4.2.5 Quantitative Reverse Transcriptase Real-Time PCR (qRT-PCR)

A one step reaction chemistry was used for the qRT-PCR for all experiments (Quantifast, Qiagen). Samples were prepared as described previously (see methods, 2.9.4). The mean C_T values for duplicates were used to calculate relative mRNA expression of the genes of interest (GOI) compared to an experimental control and endogenous control gene (RPII-B). The relative gene expression levels were calculated using the comparative C_T ($\Delta\Delta C_T$) equation (Schmittgen and Livak, 2008). All individual samples were normalised to sample CT= 1 for analysis of all gene expression.

Table 2. qPCR Primer Sequences

Target Gene	Forward Sequence (5' to 3')	Ref. Seq. Number
RPII-B	F:GGTCAGAAGGGAACTTGTGGTAT	NM_153798.2
	R:GCATCATTAAATGGAGTAGCGTC	
MMP-9	F: CTGGCAGAGGCATACTTG	NM_013599.2
	R: GCCGTAGAGACTGCTTCT	
PGC-1α	F: GAAGGGAATGGGAAAGGTAGA	NM_008904.2
	R: AACAGGACATGGAAAGCAGAT	

Tfam	F: CACGCTTTACCCTTCGTTCT	NM_009360.4
	R: CTCATTTCCCTGCCATTCTCTA	
Cytochrome C	F: GCCGACTAAATCAAGCAACA	NM_007808.4
	R: CAATGGGCATAAAGCTATCG	
NRF-1	F: CCTCAGCCTCCATCTTCT	NM_010938.4
	R: CTTAACACTTCTGTCACCTTCA	
NRF-2	F: TCCCGCTACACCGACTAC	NM_008065.2
	R: TCTGACCATTGTTTCCTGTTCTG	
COX-II	F: GAAGCGATTCTAGGGAGCAG	NM_ 010339.1
	R: GGAGCAGCGATTCTGAGTAGA	
β-Globin	F: GAAGCGATTCTAGGGAGCAG	NM_008220.4
	R: GGAGCAGCGATTCTGAGTAGA	

4.2.6 mtDNA Analysis

mtDNA copy number was assessed based upon a previously published protocol (Philp, et al., 2011, Safdar, et al., 2011). Briefly, mtDNA copy number, relative to the nuclear diploid chromosomal DNA content, was quantitatively analysed using qPCR.

Primers were designed within the COX-II region of the mitochondrial genome along with a nuclear encoding gene β-Globin (Table 4.1). qPCR was performed using isolated DNA using a Quantifast SYBR Green (Qiagen) qPCR kit on the Rotogene 3000 (Qiagen). Serial dilutions of DNA to create standards of known quantities of DNA were used in conjunction with the Rotogene associated software to generate standard curves and representative DNA copies. Data is represented as mtDNA copy number per nuclear diploid genome.

4.2.7 Statistical analyses

All statistical analysis was performed using SPSS software version 17 (SPSS INC, Chicago, IL, USA) and Graphpad Prism 6 (California, USA). Significant differences between variables were analysed using one way repeated measures ANOVA's. Normal distribution and homogeneity of variance were calculated to display compliance to statistical assumptions (see appendix 2). A pair-wise comparison post-hoc test was performed with a Bonferroni adjustment for any data with significant F values. The alpha value of significance was set at $p \leq 0.05$. All data is presented as mean ± standard error of the mean (SEM).

4.3 Results

4.3.1 Responses of lactate production and glucose uptake reveal an effect of Continuous and Intermittent stretch modalities

Data analyses revealed significant differences in peak Lactate concentration between conditions (Control = 1.733 ± 0.18, Continuous = 6.63 ± 0.50, Intermittent = 7.50 ± 0.15 mmol.L, $p < 0.000$, Fig. 4-2 A). Post-hoc analysis revealed significant differences between Control and Continuous ($p = 0.000$) and also Control and Intermittent stretch ($p = 0.000$). There was however, no significant difference between stretch modalities ($p = 0.175$).

Furthermore, significant differences in peak glucose concentration was observed between conditions (Control = 23.47 ± 0.26, Continuous = 20.13± 0.64, Intermittent = 19.07 ± 0.19 mmol.L, $p = 0.001$, Fig. 4-2 B). Post-hoc analysis revealed significant differences between Control and Continuous ($p = 0.008$) and also Control and Intermittent stretch ($p = 0.000$). There was no significant difference in peak glucose concentration between stretch modalities ($p = 0.183$).

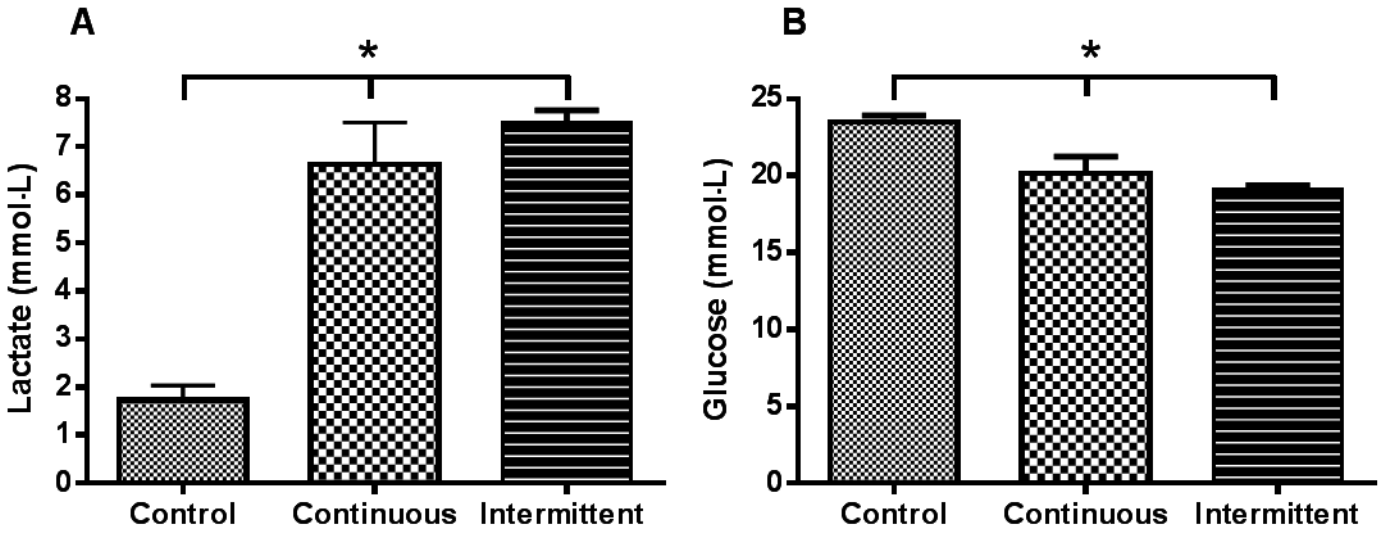

Figure 4-2. Conditioned media analysis. N = 3 replicate constructs per condition were subjected to Continuous and Intermittent mechanical stretch. All assays were performed in duplicate. A) Conditioned media lactate response to stretch. Significant increases in peak lactate production for Continuous and Intermittent stretch compared to Control (main effect, *p= 0.000).B) Media glucose response to stretch. Significant reduction in peak glucose concentration for Continuous and Intermittent stretch compared to Control (main effect, *p= 0.000).A significant difference existed following 1 complete interval of stretch (*p= 0.001). Data is presented as mean ± SEM.

4.3.2 A gross molecular output provides evidence for a transcriptional response to Continuous and Intermittent stretch

Both of the stretch protocols induced mean increases (approaching significance) in RNA:DNA ratio (Fig. 4-3), suggesting an increase in the level of transcription compared to Control (Control = 0.23 ± 0.08, Continuous = 2.14 ± 0.34, Intermittent = 3.77 ± 1.74, p = 0.065). This data provides evidence that the mechanical stretch protocols are initiating acute molecular adaptations alongside biochemical substrate regulation. Results from the investigation of specific RNA transcripts are detailed below.

4.3.3 MMP-9 mRNA expression following Continuous and Intermittent stretch

As an acute marker of transcriptnioal acitivity MMP-9 mRNA was measured as this gene has previously been shown to be activtated following a single bout of continuous cyclical loading of SkM *in vivo* (Rullman, et al., 2007). No significant differences were observed for MMP-9 mRNA between conditions (p = 0.094). Intermittent stretch protocol increased MMP-9 mRNA above Control (Intermittent = 6.63 ± 3.49 fold, Fig. 4-4), whilst the CC protocol produced a minimal effect on stimulating MMP-9 transcription (Continuous= 1.97 ± 0.91 fold, Fig. 4-4). Such data provides corroborating evidence for *in vivo*-like responses to MMP-9 in the Intermittent condition, similar to that seen with muscle contraction in the form of acute endurance exercise (Rullman, et al., 2007).

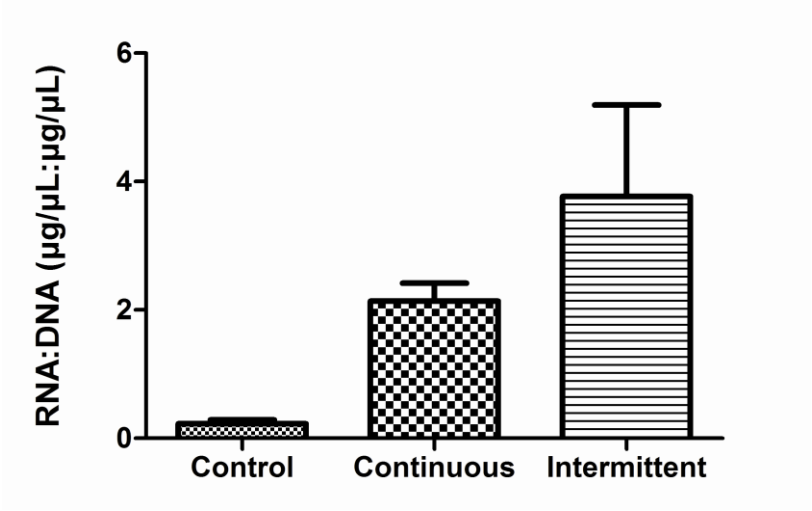

Figure 4-3. Continuous and Intermittent stretch induce an acute transcriptional response. N = 3 replicate constructs per condition were subjected to Continuous and Intermittent mechanical stretch. All assays were performed in duplicate. Increases in the RNA:DNA ratio demonstrates an increased level of gene transcription above un-stretched control constructs (p = 0.065). Data is presented as mean ± SEM.

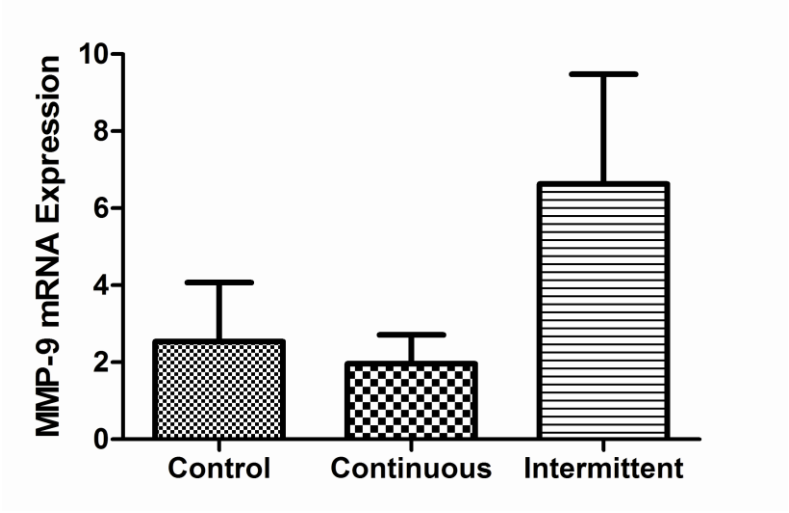

Figure 4-4. MMP-9 mRNA expression following Cyclic Stretch. Intermittent stretch induces a mean but non-significant increase in MMP-9 mRNA above Control. No significant differences were observed between conditions (main effect, p = 0.094). N = 3 replicate constructs per condition. Data is presented as mean ± SEM.

4.3.4 Higher Strain Intermittent and Lower Strain Continuous Cyclic Mechanical stretch results in increased mtDNA Copy Number

The current investigation utilised a qPCR based method for quantifying mitochondrial content by analysing mtDNA copy number. Continuous stretch caused a mean increase in mtDNA copy number compared to Control despite no statistical effect (617.46 ± 231.36 vs 415.72± 176.36, p = 0.188, Fig. 4-5). However the Intermittent protocol gave rise to a significantly greater mtDNA copy number compared to Control (1107.15± 399.40 vs 415.72± 176.36, p = 0.04, Fig. 4-5), suggesting a rapid increase in mitochondrial DNA content following this stretch protocol.

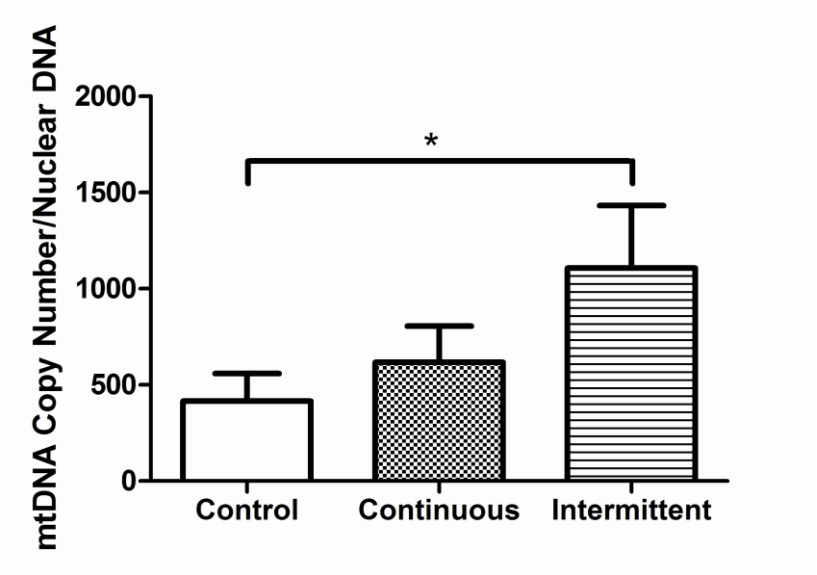

Figure 4-5. Continuous and Intermittent stretch and condequential mtDNA copy number. N = 3 replicate constructs per condition were subjected to Continuous and Intermittent mechanical stretch. No effect of Continuous stretch on mtDNA copy number above Control (p = 0.18). Intermittent stretch significantly increased mtDNA copy number above Control (*p = 0.04). Data is presented as mean ± SEM.

4.3.5 Increased mtDNA Copy Number are partially underpinned by the regulation of PGC-1α, NRF-1, NRF-2 and Cytochrome C

In the attempt to model the mechanical stimulus associated with SkM contraction *in vivo*, it was necessary to quantify genes that have been associated with increasing the oxidative potential of SkM. The Intermittent stretch protocol significantly increased the expression of PGC-1α compared to Control (5.6 ± 3.54 vs. 0.75 ± 0.2, p = 0.043, Fig. 4-6 A). However, the Continuous protocol did not induce any change in the expression of this gene (p = 0.9, Fig. 4-6 A). A significant difference was however observed between the Continuous and Intermittent in the expression of PGC-1α (p = #0.045). The increased expression of PGC-1α mRNA in the Intermittent condition, suggests the protocol is activating the mechanisms associated with inducing PGC-1α transcription.

The mitochondrial transcription factor A (mTFA, Tfam), a gene closely associated with PGC-1α in the mechanism of mitochondrial biogenesis, was not significantly altered in either of the protocols (p = 0.323, Fig. 4-6 B), despite a trend towards a reduction in expression in the Continuous condition. However Cytochrome C, a gene and protein often used as a representative measure of mitochondrial content, saw significant regulation (main effect, p = 0.002) in Intermittent (3.81 ± 0.20 fold, *p = 0.004) and trending towards a reduction in Continuous (p = 0.077) stretch, compared to Control (Fig. 4-6 C). There was also a signicant difference between stretch modalities (#p = 0.001).

The co-ordinated expression of the nuclear respiratory factors NRF-1 and -2 is required for an increase in mtDNA content (Hood, 2001) and as such the regulation of these genes in the current experiment provides a mechanism for the increased mtDNA content. A significant increase (p = 0.005) in NRF-1 mRNA was observed following stretch, with post-hoc analysis revealing a significant effect for Continuous stretch (1.78 ± 0.12 fold, p = 0.021, Fig. 4-6 D) whilst a physiological trend was found for Intermittent stretch (8.34 ± 1.82 fold, p = 0.059, Fig. 4-6 D).

No significant statistical effect was found NRF-2 mRNA expression for Continuous (2.79 ± 1.25 fold) and Intermittent (2.77 ± 0.24 fold) conditions compared to Control ($p = 0.356$, Fig. 4-6 E). These data suggest that the proposed mechanism for NRF-1 expression required for mtDNA synthesis is being modulated within this model of mechanical stimulation.

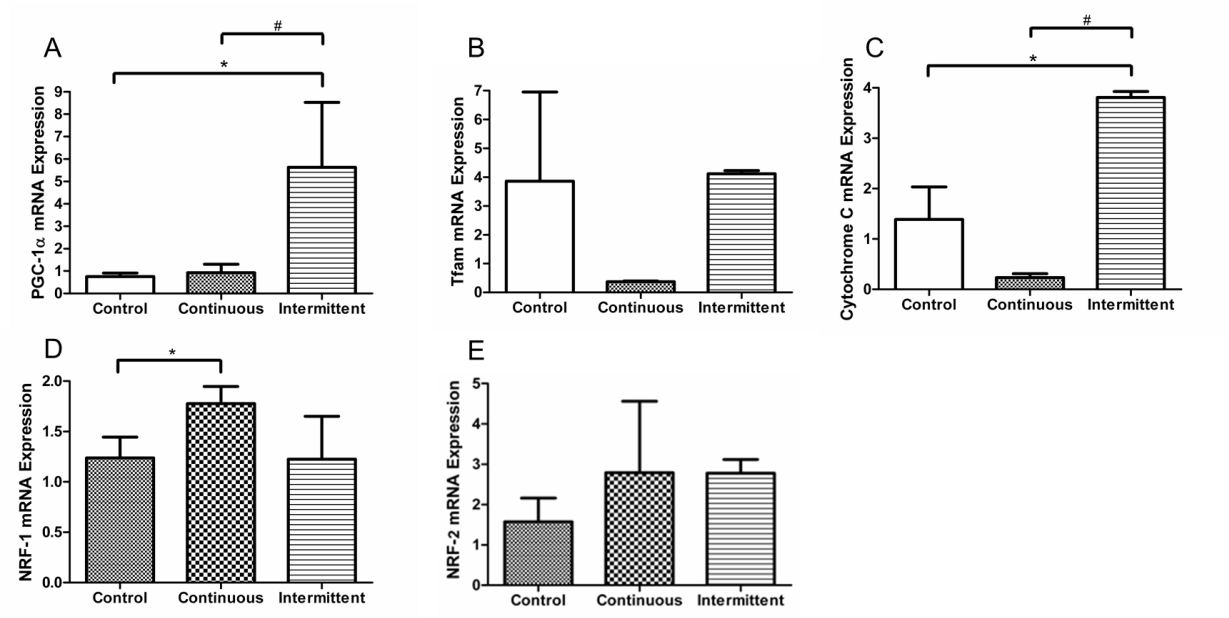

Figure 4-6. Regulation of genes implicated in mtDNA synthesis and mitochondrial biogenesis. N = 3 replicate constructs per condition were subjected to Continuous and Intermittent mechanical stretch. Control constructs were tethered to the t-CFM without stretch. A) Significant increase in PGC-1α mRNA in the IC condition compared to Control (*p = 0.043) and Continuous (#p = 0.045) conditions. B) Tfam mRNA in Continuous compared to Control and Intermittent conditions (p = 0.323). C) Significant increase in Cytochrome C mRNA in the Intermittent condition compared to Control (*p = 0.004) and Continuous (#p = 0.001) conditions. D) Significant increase in NRF-1 mRNA in Continuous stretch above Control (*p = 0.021) and approaching significance in Intermittent stretch (p = 0.059). E) No effect in NRF-2 mRNA in Continuous and Intermittent conditions compared to Control (p = 0.356). Data is presented as mean ± SEM.

4.4 Discussion

The aim of the current investigation was to test the acute metabolic and transcriptional responses to two diverse mechano-stimulation protocols. Data presented here demonstrates the development of two distinct mechanical stretch protocols, predictably producing responses both in terms of acute biochemical responses (lactate and glucose) and with respect to mtDNA copy number and the underpinning mRNA regulation, displayed in section 3.3. These data putatively show similar responses that are seen with *in vivo* exercise both acutely (biochemical and transcriptional) and chronically (mtDNA, Gibala, et al., 2006, Gibala, et al., 2009, Burgomaster, et al., 2008, Gibala, et al., 2009, Perry, et al., 2010, Bartlett, et al., 2012).

When analysing the lactate present in the conditioned media, it was found that both protocols induced significant increases following the stretch protocols. It has been suggested that the net increase in lactic acid production is a consequence of the mass of the working muscle and the intensity of the activation of the tissue (Billat, et al., 2003). In light of this hypothesis, the responses in lactate production may represent different cellular workloads within the engineered tissue, compared to Control.

Previous data has shown a significant increase of 46% above control, in media lactate production following 4-6 hrs of *in vitro* mechanical stretch of monolayer cultures (Hatfaludy, et al., 1989). However this is the first investigation to show the acute increase in Lactate production following mechanical stretch in a 3D bio-mimetic model, with the magnitude similar to that seen *in vivo* (Faude et al., 2009). It seems likely that the *in vivo*-like response is due to the nature of the model with respect to the alignment of the myotubes and the attachment and deformation of the cells in a 3D environment. The nature of the stimulation itself with regards to the frequency and duration may also contribute to the surprising commonality of data compared to SkM in response to contiuous and intermittent exercise *in vivo* (Zafeiridis, et al., 2010).

Both stretch protocols significantly reduced media glucose concentration ($p < 0.001$), showing similarities to moderate intensity continuous and intermittent exercise *in vivo* whereby a decrease in blood Glucose concentration of approximately 1 mmol.L is evident compared to pre-exercise conditions ($p < 0.05$, (Mackenzie, et al., 2011). Further, evidence has suggested the beneficial effect of intermittent contraction in glycaemic control both acutely (Mackenzie, et al., 2012) and hours post exercise (Iscoe and Riddell, 2011).

Hatfaludy et al., (1989) also observed increases in [3H] deoxy-D-glucose uptake by 34% compared to pre stretch conditions, in muscle cultures subjected to stretch-relaxation protocols using a monolayer *in vitro* stretch system. In another monolayer stretch model, data has also shown a calcium-dependent and IGF-I independent mechanism for glucose uptake by SkM cells following *in vitro* stretch (Iwata, et al., 2007).

These *in vitro* systems have provided fundamental evidence that mechanical load and stretch of SkM cells, results in up-take of glucose, independent of mechanisms that are regulated by systemically acting insulin. The precise mechanism whereby increases in calcium are achieved with SkM stretch are yet to be fully elucidated, however calcium increases may in part be regulated by active contraction. Data generated from the current investigation, provides evidence for the use of this system to examine the stretch induced-glucose uptake mechanisms in a more physiologically representative *in vitro* tissue.

4.4.1 An Increase in MMP-9 mRNA Provides Further Evidence for the *In Vivo* Nature of the Response to the Mechno-Stimulation

Data presented here showed a trend towards an increase in MMP-9 mRNA following (Fig. 4-5) Intemrittent stretch. With no statistical significance achieved, furutre experiments should seek to determine whether this trend could be reproduced. Previous *in vivo* data provides further support for the *in vivo*-like nature of the stimulation protocols in regulating MMP-9 mRNA.

Rullman et al., (2007) demonstrated that following 65 mins of continuous cycling exercise MMP-9 mRNA was elevated immediately post, reaching significance by 120 mins post exercise ($p < 0.05$, Rullman, et al., 2007). Matrix metalloproteinases (MMP's) play a significant role in extra cellular matrix (ECM) remodelling and have been shown to be activated during the migratory phase of activated satellite cells (myoblasts, (Lewis, et al., 2001, Zimowska, et al., 2008, Zimowska, et al., 2012), during SkM regeneration from damage). The activation and enhancement of the satellite cell pool has recently been shown to be dependent on the intensity rather than the duration of endurance exercise (Kurosaka, et al., 2011), with data presented here providing a potential mechanism for this response with an enhanced transcription of MMP-9 in the Intermittent condition.

4.4.2 A Role for PGC-1α, NRF-1, NRF-2 and Cytochrome C in the Increase in mtDNA

Results presented here show a significant increase in mtDNA copy number in the Intermittent condition (Fig. 4-6), illustrating a rapid increase in mtDNA content when controlling for nuclear DNA. This is the first investigation to show an increase in mtDNA copy number following mechanical stretch of bio-mimetic *in vitro* SkM.

Conversely, Safdar et al., (2011) showed increases in transcripts associated with mitochondrial biogenesis and mtDNA replication, despite no overall increase in mtDNA copy number, following acute endurance-based exercise *in vivo*.

The authors suggested that an increase in mtDNA copy number may result from multiple bouts of contractile activity that causes transient increases in the required transcripts (Safdar, et al., 2011). This view is supported by Perry et al (2010), who found a significant increase in mtDNA ($p < 0.05$) 24 hrs following three bouts of high intensity interval training (Perry, et al., 2010).

The increase in mtDNA copy number compared to Control following Intermittent stretch, may be a result of the accelerated nature of the mechanisms activated within the *in vitro* system. This rapid increase in mtDNA provides an ideal system to delineate the mechanisms controlling this vastly complex cellular process. Allowing for multiple sampling of the constructs throughout finite time periods, investigating the roles of intrinsic and extrinsic factors independently and utilising a clonal cell line are all advantages of the system described here above *in vivo* experiments.

When seeking to understand the mechanisms whereby an increase in mtDNA occurs following mechano-stimulation, it is necessary to investigate the responses to genes associated with increasing the oxidative potential of the tissue. Here, it has been shown that Intermittent stretch can up-regulate PGC-1α mRNA (Fig. 4-7 A), a master regulator of mitochondrial biogenesis, which is one of the mechanisms required to increase oxidative metabolism of SkM (Fernandez-Marcos and Auwerx, 2011).

Importantly, in the context of the data presented here, *in vivo* data has shown increases in PGC-1α following high intensity (greater strain or load) interval based SkM contraction (Gibala, et al., 2009, Little, et al., 2011). This therefore provides a context for the data presented here, suggesting an interval mode of exercise training can induce PGC-1α mRNA expression *in vivo* and *in vitro*. This data suggests the importance of the strain and load type upon SkM in activating PGC-1α mRNA, illustrating that primary mechanical load can induce such a response.

A recent study has demonstrated the requirement of an intact adipocytokine system for the activation of PGC-1α mRNA following SkM contraction (Li, et al., 2011), suggesting the necessity of a systemic environment. The novel finding presented here shows an increase in PGC-1α mRNA following Intermittent stretch in an isolated bio-mimetic model of SkM.

As such, this data provides evidence for the intrinsic regulation of PGC-1α transcriptional control in this system. An increase in NRF-1 mRNA reported here (Fig. 4-7 D) following Continuous mechanical strain provide further evidence for an activated mechanism towards increasing the oxidative potential of the construct. An increase in NRF-1 mRNA despite no increase in NRF-2 mRNA in the Continuous condition proposes a greater role for NRF-1 in the acute response to Continuous stretch in this system. The NRF's are transcriptional regulators of many genes encoding subunits of the oxidative phosphorylation (OXPHOS) system along with mtDNA replication (Moraes, 2001), including the transcription of mtTFA (Scarpulla, 2011). Moreover, it has been shown that a dominant negative allele of NRF-1 prevents the ability of PGC-1*α* to induce mitochondrial proliferation, defining the role of NRF-1 in PGC-1α activated mitochondrial biogenesis (Scarpulla, 2008). Increases in both PGC-1α (5.6-fold, $p = 0.04$) and NRF-1 (1.78-fold, $p = 0.021$) mRNA's found following in the current investigation ($p < 0.05$), provides evidence for the dependent role of the NRF's in increasing the mtDNA content observed in this current investigation.

PGC-1α is a transcriptional co-activator which has been associated with the indispensible expression of Tfam, a protein required for mtDNA transcription (Scarpulla, 2008, Scarpulla, 2011). Recently it has been reported how Tfam is in a complex with PGC-1α in the D-loop region of mtDNA, which is modulated by acute contractile activity (Safdar, et al., 2011).

The data for Tfam expression is considierably varied (Fig. 4-7 B), with greater sample numbers required to make a judgement on the response of this gene to mechanical load. The variability in expression mRNA of Tfam found in this investigation may reflect complex temporal regulation and inherent differnces in up-stream cell signalling required for its transcription, a hypothesis which requires investigation.

The RNA primer generated from the L-strand promoter required for mtDNA replication is dependent on Tfam (Hood, 2001), therefore investigating the protein expression of this essential protein warrants experimentation in this model and may provide more insightful data. Recently, the notion of mRNA half-life with respect to genes that regulate mitochondrial biogenesis has been investigated. Data proposed how the half-life of particular mRNA's (including Tfam) was particularly unstable and in particular in contracted muscle cells (Lai, et al., 2010). Moreover, the half-life of Tfam has been shown to be shorter in slow twitch muscle fibres (D'souza, et al., 2012), which may have pertinence for the *in vitro* constructs used in the current investigation. Furthermore, the expression of Tfam protein is thought to be 1700-3000 times more than mtDNA, levels which are thought to wrap human mtDNA entirely (Takamatsu, et al., 2002).

This therefore suggests, the requirement for transcription seems limited. These hypotheses should be tested within the proposed model, to test whether the initial stimulus may have been sufficient to induce Tfam mRNA expression; however the degradation of the transcript contributed to a minimal effect being found. The time-course of Tfam mRNA half-life investigated previously also supports this notion (Lai, et al., 2010). This hypothesis could also be readily tested in the mechano-stimulation model proposed here.

Intermittent stretch significantly increased the level of Cytochrome C mRNA (3.81-fold, $p = 0.004$, Fig. 4-7 C), a gene and protein required for oxidative phosphorylation (OXPHOS). Cytochrome C mRNA has been shown to be activated acutely following endurance based exercise *in vivo* (Wright, et al., 2007, Leick, et al., 2008, Safdar, et al., 2011) as a compensatory mechanism to induce homoeostatic recovery and enhance ATP production potential for future exercise bouts (Mahoney, et al., 2005).

It has been demonstrated *in vitro* (Wu, et al., 1999) and *in vivo* (Lin, et al., 2002) SkM that over-expression of PGC-1α protein results in increases in Cytochrome C mRNA and oxidative metabolism, providing evidence for the role of PGC-1α protein as transcriptional co-activator for this gene. An interesting finding of the current investigation is the reduction in Cytochrome C mRNA expression following Continuous stretch (Fig. 4-7 C). Such a finding again suggests a contrasting response to this form of stimulation compared to Intermittent stretch.

4.4.3 A Metabolic Threshold Required for Increases in Oxidative Associated Molecular Responses

Data presented here suggests a greater metabolic transcriptional response in the Intermittent (higher strain) than in the Continuous (lower strain) condition, as represented by increased mtDNA copy number (Fig. 4-6) and transcripts associated with such a response (Fig. 4-7). It is postulated therefore, that a mechano-metabolic transcriptional threshold may be required to initiate the mtDNA response observed. Future experiments should seek to establish whether the mean increase in lactate and reduction in glucose in the media observed between stretch modalities (Fig. 4-2), is indeed strain and workload dependent.

This is supported by extant published data indicating an increase in PGC-1α mRNA following just 60 mins exposure of exogenous lactate to L6 myotubes (Hashimoto, et al., 2007). Furthermore, this hypothesis has recently has been tested successfully *in vivo* (Tobina, et al., 2011), whereby exercise above lactate threshold induced greater increases in PGC-1α mRNA expression compared to below lactate threshold. The production of lactate is thought to signal to activate redox sensitive and calmodulin kinase sensitive PGC-1α transcription (Fig. 4-8).

Further investigations into metabolically activated proteins and transcription factors would be required to support such a hypothesis in this *in vitro* system.

Incrementally increasing the load placed upon the *in vitro* constructs, would also provide an ideal model to investigate this hypothesis in a controlled, biomimetic model such as that described here.

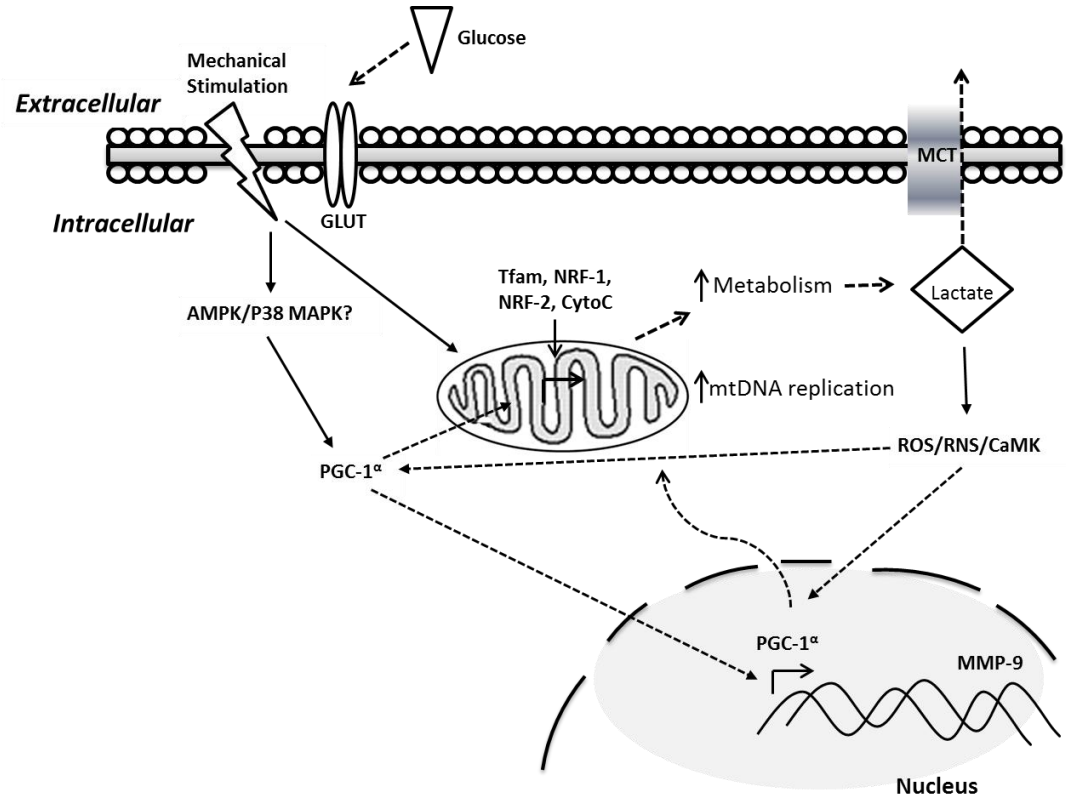

Figure 4-7. Cellular overview of the acute biochemical and transcriptional responses to cyclical stretch presented within the chapter. GLUT (glucose transport protein), MCT (monocarboxylate transporter protein), AMPK (AMP activated protein kinase), p38 MAPK (p38 mitogen activated protein kinase), PGC-1α (Peroxisome proliferator-activated receptor gamma coactivator 1-alpha), ROS/RNS (reactive oxygen/nitrogen species), CaMK (calmodulin kinase), Tfam (mitochondrial transcription factor A), NRF-1/2 (nuclear respiratory factor 1/2), CytoC (cytochrome C oxidase), MMP-9 (matrix metalloproteinase -9).

4.4.4 Increases in metabolism and mitochondrial adaptation: relevance to SkM tissue engineering?

The clear influence of mechanical signals during embryonic development of SkM is clear (Christ and Brand-Saberi, 2002), which has inspired the use of mechanical loasding to stimulate the development of tissue engineered SkM. Previously published data illustrates the improved contractile phenotype of tissue engineered constructs following stimulation (Moon du, et al., 2008, Boonen, et al., 2010, Corona, et al., 2012).

There is however limited data surrounding the influence of mechanical loading on metabolic response (Hatfaludy, et al., 1989, Iwata, et al., 2007) and mitochondrial adaptation, with respect to improving tissue engineered models. Data presented here supports the role of mechanical signals in increasing metabolism and stimulating a mitochondrial transcriptional response. With respect to developing a more bio-mimetic SkM model *in vitro*, stimulating metabolism and mitochondrial adaptation is a key finding with regards to the characterised response to contraction *in vivo*. As such the model presented here demonstrates a key finding with respect to developing *in vivo*-like tissue *in vitro*.

The research goal for SkM tissue engineering is to successfully implant the constructs *in vivo* to repair damaged or diseased tissue (Machingal, et al., 2011, Corona, et al., 2012). Increasing metabolism and stimulating mitochondrial biogenesis will improve cell survival, whilst also providing the machinery for ATP synthesis to support maturation. This provides evidence for the use of cyclic mechanical loading in the pre-conditioning of tissue engineered constructs prior to implantation.

4.5 Conclusions

Data reported in this current invesitgation provides evidence for the characterisation of two models of *in vitro* mechanical stimulation. Continuous and Intermittent stretch result in *in vivo*-like responses to lactate production and glucose uptake (Fig. 4-3), whilst stretch in part leads to the transcription of genes associated with the acute metabolic response to *in vivo* exercise (Fig. 4-7). Moreover, it is demonstrated a rapid increase in mtDNA following a single bout of Intermittent stretch, which will be invaluable for ascertaining the molecular signals that mediate this response. Future investigations to aim to further characterise the transcriptional regulation of certain metabolic 'candidate genes' (PGC-1α, Tfam, NRF-1 and NRF-2) associated with adaptations to endurance exercise.

The intracellular protein signalling, including post translational modifications should also be investigated within this model to investigate the acute mechanism which regulates mtDNA replication. Using such models to inform of the cellular and molecular adaptation to SkM mechano-stimulation will be invaluable in delineating the mechanisms by which increased SkM load can increase aerobic potential. This understanding with be vital in developing pre-clinical understanding of potential exercise and pharmacological therapies for a multitude of metabolic pathologies. Furthermore, this data will provide mechanistic understanding for the potential of mechanical stimulation in the pre-conditioning of SkM constructs prior to *in vivo* implantation for disease therapy in the future.

5 Acute Mechanical Overload in 3-Dimensional Bioengineered SkM Induces a Hypertrophic Transcriptional Response

5.1 Introduction

SkM plays significant roles in movement and providing a large metabolic pool for substrate storage and utilisation. The previous chapter investigated the role of mechanical signals on stimulating metabolism and increasing mtDNA for increased aerobic potential, whilst the aim of the current chapter is to investigate the influence of mechanical signals on stimulating transcription of genes associated with the potential for increasing muscle mass.

SkM mass plays a pivotal role in overall health and wellbeing. A decline in SkM mass and contractile proteins with disease (cachexia, Lenk, et al., 2010) and ageing (sarcopoenia, Pillard, et al., 2011) contributes to an increased susceptibility to metabolic diseases including; obesity, diabetes and associated cardiovascular disease (Degens and Alway, 2006, Narici and Maffulli, 2010). Moreover, a decrement in muscle mass and strength with age contributes to increased morbidity and mortality (Carmeli, et al., 2002, Rantanen, et al., 2003).

The mechanisms that govern the response of SkM hypertrophy have stemmed from the seminal work of Goldberg (1967) who demonstrated the rapid hypertrophic response in the target muscle after only 24hrs post tenotomy of a synergistic muscle (Goldberg, 1967) . This method of work overload-induced hypertrophy has received much attention (Armstrong, et al., 1979, Kandarian, et al., 1992, Esser and White, 1995, Linderman, et al., 1996) and has resulted in a far greater understanding of the molecular mechanisms that regulate this response. Increase in amino acid transport (Goldberg and Goodman, 1969, Henriksen, et al., 1993) and satellite cell proliferation (Schiaffino, et al., 1972, Rosenblatt and Parry, 1992, McCarthy and Esser, 2007, O'Connor and Pavlath, 2007) have been shown in part to form the basis of hypertrophy.

A global increase in protein synthesis (Goldspink, 1977) along with increases in protein content of the sub-fractions within SkM (Cuthbertson, et al., 2006), also play significant roles in the increase of SkM mass to overload or stretch.

SkM hypertrophy is characterised by an increase in total RNA content, whether following *in vitro* stretch or stimulation (Carson, et al., 2002) or *in vivo* exercise (Bickel, et al., 2005). The necessity for an increase in RNA to initiate a hypertrophic response following tenotomy has been demonstrated by the addition of a DNA-dependent RNA synthesis inhibitor, Actinomycin D, which ablated any compensatory hypertrophic response from occurring (Goldberg and Goodman, 1969). Specific gene transcript evidence has demonstrated roles for myogenic and hypertrophic genes; Insulin-like growth factor I (IGF-I, (Adams and Haddad, 1996, Awede, et al., 2002, Awede, et al., 1999) and matrix metalloproteinase 9 (MMP9, Lewis, et al., 2000, Dahiya, et al., 2011, Mehan, et al., 2011), along with the regulation of genes involved in atrophy including Myostatin, muscle RING finger protein 1(MuRF-1) and muscle atrophy factor box (MAFBx, McPherron, et al., 1997, McPherron, et al., 1997, Trendelenburg, et al., 2009, Welle, 2009). Despite these relatively well characterised mechanisms involved in regulating SkM mass, the intrinsic regulation of these genes particularly in isolated *in vitro* models is less understood.

Developing a model of overload induced hypertrophy *in vitro*, would overcome many of the experimental and ethical issues surrounding human and animal studies. Additionally, the development of an *in vitro* model of mechanical overload would reduce the necessity to use animal models for this research area.

Previous published *in vitro* models have demonstrated a stretch-induced hypertrophic response, including the early work of Vandenburgh and Kaufmen (1979). Another model from the same laboratory developed a system for the computer programmable stretch regimens, extending the work to mimic loading modalities *in vivo* (Vandenburgh, 1988). Existing published models have often employed a monolayer culture technique with uniaxial stimulation (Hubatsch and Jasmin, 1997, Iwata, et al., 2007), a development on the previously published multi-axial strain.

Despite this advancement the *in vitro* models often lack bio-mimicity with regards to the cellular architecture, the dimension in which the cells are grown and the extra-cellular matrix composition. As such the development of 3D culture systems have tried to address these issues (Powell, et al., 2002, Cheema, et al., 2003, Auluck, et al., 2005, Cheema, et al., 2005, Mudera, et al., 2010,), including work from our laboratory.

Recently, further advancements have been made with the development of a system mimicking *in vivo* SkM in terms of histology and genotype, allowing for the long term and hence enhanced maturation of the constructs (Smith, et al., 2012). Furthermore, the characterisation of the purely myogenic cell seeded construct has been described earlier in Thesis (Chapter 3), providing an appropriate model to investigate the effect of mechanical signals on regulating SkM mass.

The isolated nature of such a system also allows of the analysis of the intrinsic mechanisms activated in response to mechanical stimuli, controlling for the influence of systemic factors. Notwithstanding the potential role for systemic factors, an *in vitro* model as described (Smith, et al., 2012) allows for the investigation of single or multiple systemically regulated proteins in involved in hypertrophy. It is important however, to characterise the proposed model with respect to the regulation of many of the hypertrophic and atrophic genes described, before further advanced mechanistic studies can be undertaken. To this end, the following aims were proposed.

5.2 Aims and Hypotheses

1. To develop loading modalities that recapitulate existing models of overload induced hypertrophy.

2. Use these models to investigate the regulation of genes involved in stimulating a hypertrophic response.

3. Investigate the regulation of genes that inhibit protein synthesis, or are involved in protein degradation at the lysosome.

Taking the existing literature into consideration, it was hypothesised that mechanically loading the characterised SkM constructs described in Chapter 3, would result in a compensatory modulation of genes implicated in hypertrophy. Particularly, it was hypothesised that an increase in protein synthetic genes IGF-I and MMP-9 and a reduction in genes suppressing protein synthesis or involved in proteolysis, MuRF-1, MAFBx and Myostatin would result from mechanical overload.

5.3 Methods

5.3.1 Cell Culture

For all experimentation cells were used below passage 8 and were grown to 80 % confluence before being trypsinised (Trypsin-EDTA, Sigma-Aldrich), prior to preparation for collagen constructs (see 2.4 for methods).

5.3.2 Cell seeded 3D compliant collagen constructs

Collagen constructs were prepared as previously described (4.2.1.1). The constructs were transferred to DM, following 4 days of culture in GM. A further 10 days of culture allowed for the maturation of the constructs and the differentiation of myoblasts into multinucleated myotubes.

5.3.3 Experimentation

For experimentation, constructs were removed from the chambers and transferred to polyethylene moulds, floated in DM and mounted upon the Tensioning Culture Monitor (t-CFM, Cheema, et al., 2005)for mechanical stretch. N = 3 static controls (no mechanical stretch) were used to compare all data. Overload regimes were programmed as follows; Static Load (n = 4) 10 % strain for 60 mins, Ramp Load (n = 3) continuous increasing load to achieve 10 % strain at 60 mins (Fig. 5-1). Constructs were sampled immediately at 60 mins for RNA extraction.

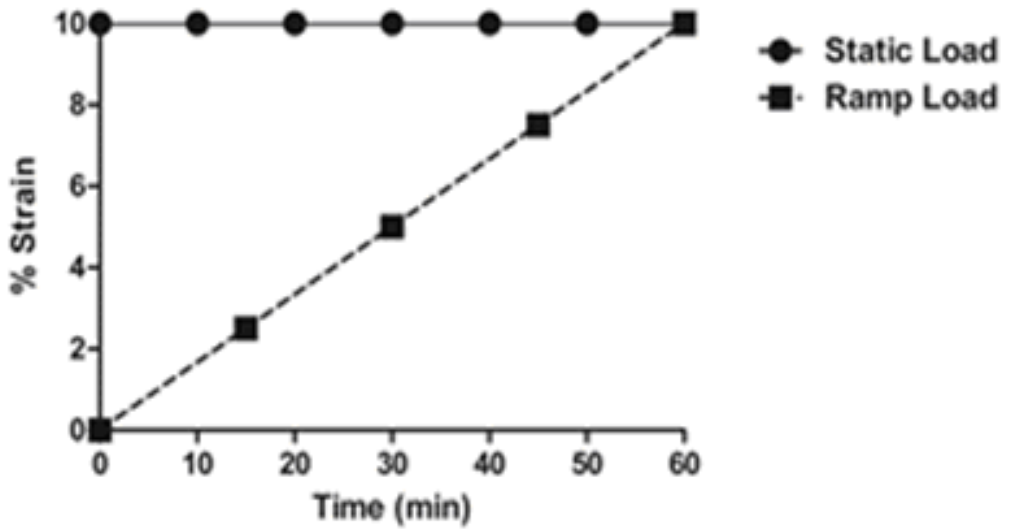

Figure 5-1. Graphical representation of mechanical overload regimes. Static load was achieved by applying a 10 % strain immediately to the constructs once they were tethered to the t-CFM. Ramp load was programmed to continually apply increasing load in order that 10 % strain was achieved at exactly 60 mins.

5.3.4 Lactate Analysis

In order to analyse the metabolic activity of the constructs and to test whether the different regimes were initiating a differential workload, the production of lactate during the mechanical stretch protocols was assessed (see 2.9.1).

5.3.5 Construct Sampling and Extraction Protocol

Immediately following the end of the stretch protocol, the constructs were removed from the t-CFM and submerged in TRIzol (Invitrogen), prior to homogenisation and RNA extraction (see section 2.9.4.2).

5.3.6 Primer Design and Synthesis

Primers (Table 5-1) were designed and synthesised by Sigma-Aldrich. Primer sequences were analysed for GC nucleotide content as well as being analysed using a 'Blast search' *(*www.ncbi.nlm.nih.gov/tools/primer-blast/*)* to check for target sequence specificity. Mean GC nucleotide content was 49.65 ± 3.94 % for all primers.

5.3.7 Quantitative Reverse Transcriptase Real-Time PCR (qRT-PCR)

A one step reaction chemistry was used for the qRT-PCR for all experiments (Quantifast, Qiagen, Crawley, UK). The Qiagen (Crawley, UK) Qiagility Robot was used to perform all 'master mix' and sample preparations, using associated programmable software (see section 2.9.4). Samples were loaded into a Rotogene 3000Q (Qiagen, Crawley, UK) for the one step RNA-CT reaction.

Samples were run in duplicate and the mean C_T (threshold cycle) values were used to calculate relative mRNA expression of the genes of interest (GOI). An experimental control (no overload) along with an endogenous control gene (RPII-B), were used to calculate the mRNA expression of each GOI. The relative gene expression levels were calculated using the comparative C_T ($\Delta\Delta C_T$) equation All individual samples were normalised to a single designated control sample, in order that the variation in control samples could be analysed.

Table 5-1. qPCR Primer Sequences

Target Gene	Forward Sequence (5' to 3')	Ref. Seq. Number
RPII-B	F:GGTCAGAAGGGAACTTGTGGTAT	NM_153798.2
	R:GCATCATTAAATGGAGTAGCGTC	
IGF-I	F: GCTTGCTCACCTTTACCAGC	NM_010512
	R: TTGGGCATGTCAGTGTGG	
MMP-9	F: CTGGCAGAGGCATACTTG	NM_013599.2
	R: GCCGTAGAGACTGCTTCT	
IGFBP-2	F: AGTGCCATCTCTTCTACAA	NM_008342.3
	R: GCTCAGTGTTGGTCTCTT	

IGFBP-5	F: GAAGAGGTGGTGACAGAG	NM_010518.2
	R: TGACAACAAGATCGGGAA	
MuRF-1	F: CCAAGGAGAATAGCCACCAG	NM_001039048.2
	R: CGCTCTTCTTCTCGTCCAG	
MAFBx	F: GTCGCAGCCAAGAAGAGAA	NM_026346.3
	R: CGAGAAGTCCAGTCTGTTGAA	
Myostatin	F: TACTCCAGAATAGAAGCCATAA	NM_010834.2
	R: GTAGCGTGATAATCGTCATC	

5.3.8 Statistical analyses

All statistical analysis was performed using SPSS software version 17 (SPSS INC, Chicago, IL, USA) and Graphpad Prism 6 (California, USA). Significant differences between variables were analysed using one way repeated measures ANOVA's. Normal distribution and homogeneity of variance were calculated to display compliance to statistical assumptions (see appendix 2). A pair-wise comparison post-hoc test was performed with a Bonferroni adjustment for any data with significant F values. The alpha value of significance was set at $p \leq 0.05$. All data is presented as mean ± standard error of the mean (SEM).

5.4 Results

5.4.1 A superior increase in lactate production in RL suggests an increased cellular metabolic demand and workload compared to SL

Confirming a continued increase in metabolic activity on the myotubes in the Ramp Load condition, peak Lactate was significantly greater compared to Control ($p = 0.003$) and Static Load conditions ($p= 0.000$, Ramp Load = 6.43 ± 0.08, Control = 1.73 ± 0.22, Static Load = 4.8 ± 0.32, Fig. 5-2).

The Static Load condition also induced a significantly greater peak lactate concentration compared to Control (p = 0.000). Together these data provide the evidence for an increased metabolic activity following the mechanical overload regimes employed here.

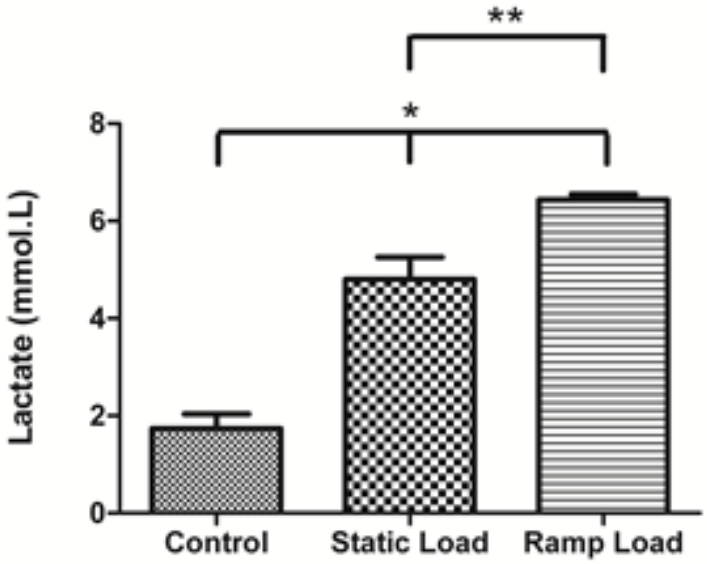

Figure 5-2. Conditioned media peak lactate analysis. N = 3+ constructs per condition analysed. Peak lactate concentration within conditioned media was immediately sampled at 60 mins of experimentation. Assays were performed in duplicate. A significant increase in peak lactate was observed for both Static Load and Ramp Load compared to Control (*p < 0.01). There was also a significant increase in peak lactate between Ramp Load and Static Load (**p < 0.001). Data is presented at mean ± SEM.

5.4.2 Increases in IGF-I and MMP9 mRNA's acutely following overload

Statistical analysis revealed significant modulation of IGF-I mRNA (p = 0.002), with Static Load significantly increasing IGF-I mRNA to 71.42 ± 16.42-fold compared to both Contorl (3.94 ± 3.88, p = 0.003) and Ramp Load (17.40 ± 7.77, p = 0.011, Fig. 5-3 A). There was no effect on IGF-I mRNA expression following Ramp Loading, compared to Control (Control = 3.94 ± 3.88 vs. Ramp Load = 17.40 ± 7.77, p = 0.603).

To illustrate the extent of IGF-I mRNA regulation in these conditions, the raw average C_T values for each sample for IGF-I and the housekeeping gene (RPII) have been displayed in Table 5-2. The clear reduction in C_T values demonstrates a clear up-regulation of this transcript.

A significant regulation in MMP-9 mRNA was also observed ($p = 0.013$) with increases found for both Static Load ($p = 0.027$) and Ramp Load ($p = 0.005$) compared to Control, whilst Ramp Load moderately increased MMP-9 mRNA compared to Static Load ($p = 0.234$, Static Load = 16.37 ± 6.69, Ramp Load = 22.70 ± 2.70, Control = 4.06 ± 2.37, Fig. 5-3 B). Increases in both IGF-I and MMP-9 mRNA for both SL and RL compared to Control, suggests the acute regulation of these genes following mechanical overload. The differential response in IGF-I and MMP-9 transcription to each stimulus, demonstrates a contrasting response dependent on the type of mechanical overload; SL has the ability to induce potential enhanced signalling through IGF-I, whilst RL demonstrates a greater ability to remodel the extra-cellular matrix through MMP-9.

Table 3. The extent of IGF-I transcription in response to mechanical overload. Raw C_T values for the housekeeping gene (RPII) and IGF-I demonstrates a clear increase in IGF-I mRNA.

Sample	***RPII***	***IGF-I***
Control	18.17	26.8
Static Load	17.24	19.3
Ramp Load	17.46	21.7

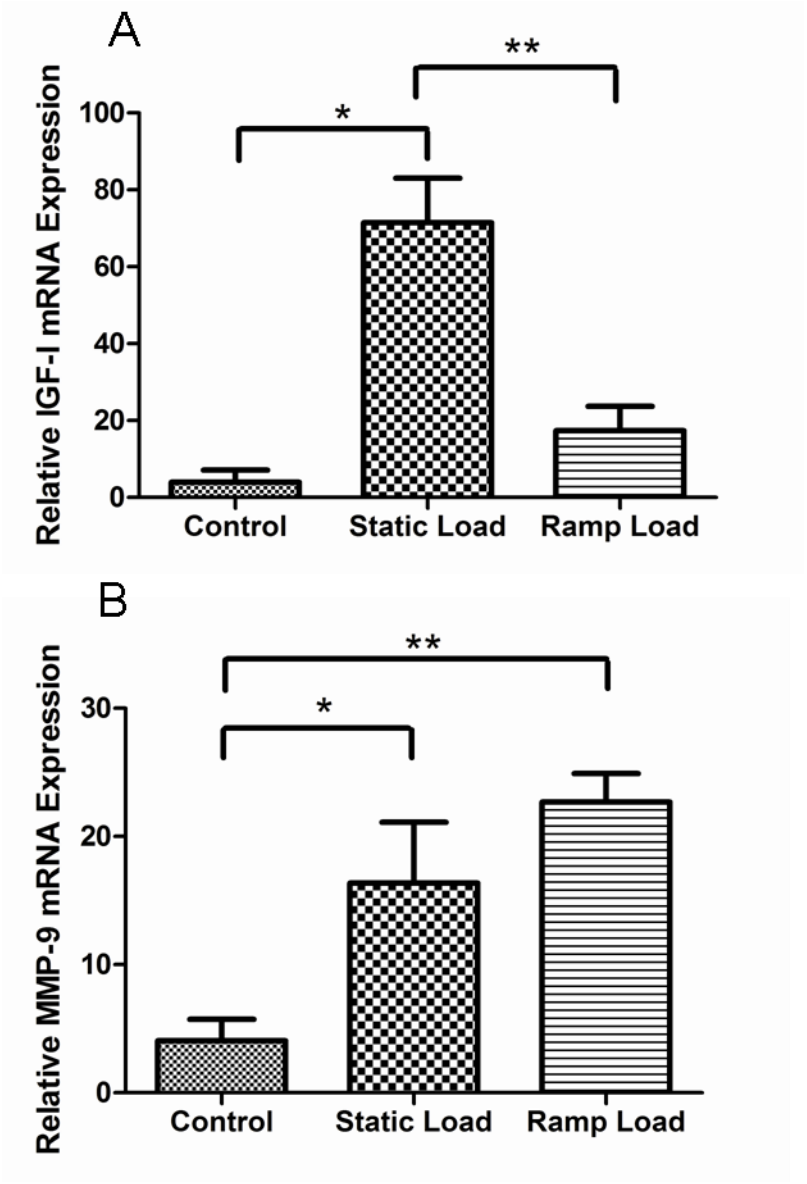

Figure 5-3. Increases in IGF-I and MMP-9 mRNA to Static Load and Ramp Load. N = 3+ constructs per condition were analysed. A) Increase in IGF-I mRNA following Static Load (*p = 0.003) and no significant modulation in Ramp Load (p = 0.603). IGF-I was also significantly increased in Static Load above Ramp Load (**p = 0.003). B). Significant increases in MMP-9 mRNA for Static Load (*p = 0.027) and Ramp Load (**p = 0.005), compared to Control. Data is presented at mean ± SEM.

5.4.3 A role for IGFBP2 and IGFBP5 in the acute response to mechanical overload

With enhanced transcription of IGF-I, it was logical to investigate any role IGF binding proteins may have in enhancing or impeding the action of IGF-I in response to mechanical overload and exercise (Severgnini, et al., 1999, Bickel, et al., 2003, van den Beld, et al., 2003, Rehfeldt, et al., 2010).

No statistical main effect was observed in IGFBP-2 mRNA expression, with a mean increase in the Static Load condition, with a non-significant reduction in Ramp Load, compared to Control ($p = 0.057$, Control = 1.03 ± 0.03, Static Load = 1.51 ± 0.52, Ramp Load = 0.44 ± 0.03, Fig. 5-4 A). A reduction in IGFBP-5 mRNA expression occurred following both overload regimes ($p = 0.018$), with significance in the Ramp Load condition compared to Control, and approaching significance in Static Load ($p = 0.027$ and 0.059 respectively, Control = 1.01 ± 0.01, Static Load = 0.46 ± 0.23, Ramp Load = 0.34 ± 0.12, Fig. 5-4 B). No difference in IGFBP-5 mRNA was found between overload conditions ($p = 1$).

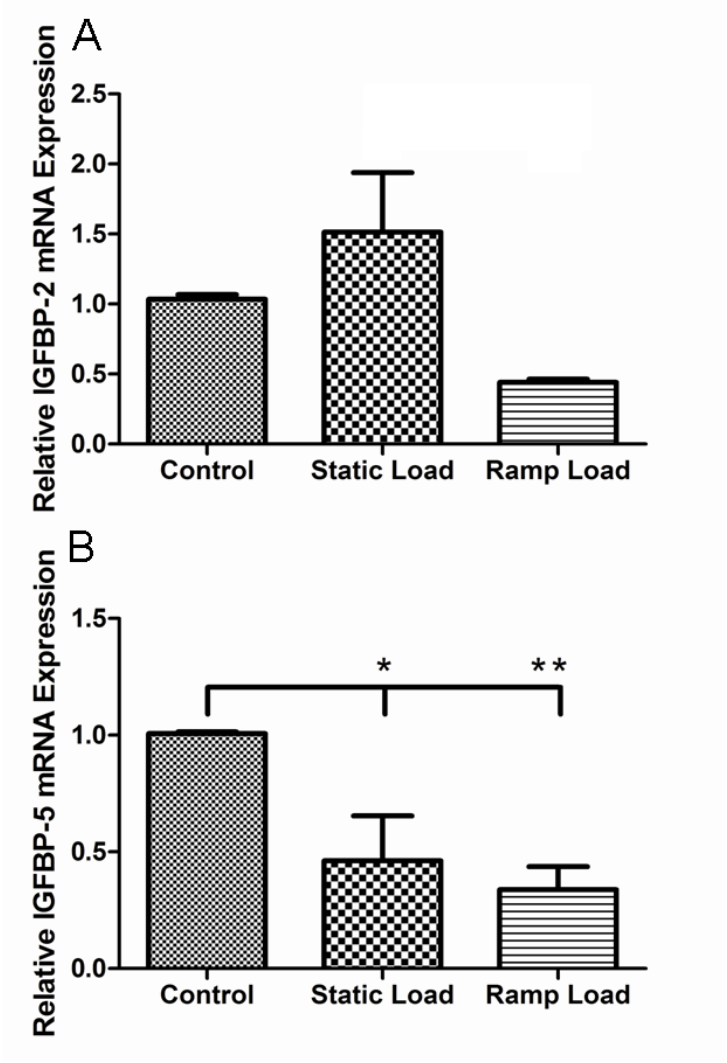

Figure 5-4. Modulation of IGFBP's in response to SL and RL. N = 3+ constructs per condition were analysed. A) IGFBP-2 mRNA following Static and Ramp Loading (p = 0.057). B) Significant modulation of IGFBP-5 mRNA (p = 0.018). Significant reductions in IGFBP-5 mRNA in Static Load (*p = 0.027) and approaching significance in Ramp Load (**p = 0.059) compared to Control. No differences were found between Static and Ramp Loading conditions. Data is presented at mean ± SEM.

5.4.4 No significant changes in either Myostatin mRNA or UPP associated transcripts following overload

Myostatin is a potent negative regulator of protein synthesis, whilst MuRF-1 and MAFBx enhance protein degradation via the ubiquitin proteasome pathway (UPP). As such, a reduction in these genes may contribute to enhanced protein synthesis and reduced protein breakdown leading to net protein accretion. Both overload regimes contributed to variable but mean reductions in Myostatin mRNA compared to Control (both $p = 0.572$, Control = 0.45 ± 0.35, Static Load = 0.15 ± 0.08, Ramp Load = 0.08 ± 0.06, Fig. 5-5 A). Further experimentation would be necessary to determine whether this effect was indeed true, with the variability in the Control samples leading to non-significant data. A Control expression value should be close to '1' and as such the mean expression of 0.45 ± 0.35, illustrates the varaiblity in this data set.

Additionally, no significant changes were apparent in MuRF-1 mRNA (Control = 1.24 ± 1.00, Static Load = 1.03 ± 0.22, Ramp Load = 1.87 ± 0.47) and MAFBx mRNA expression (Control = 1.07 ± 0.34, Static Load = 1.37 ± 0.39, Ramp Load = 1.13 ± 0.23, $p = 0.469$ and $p = 0.632$ respectively, Fig. 5-5 B and C).

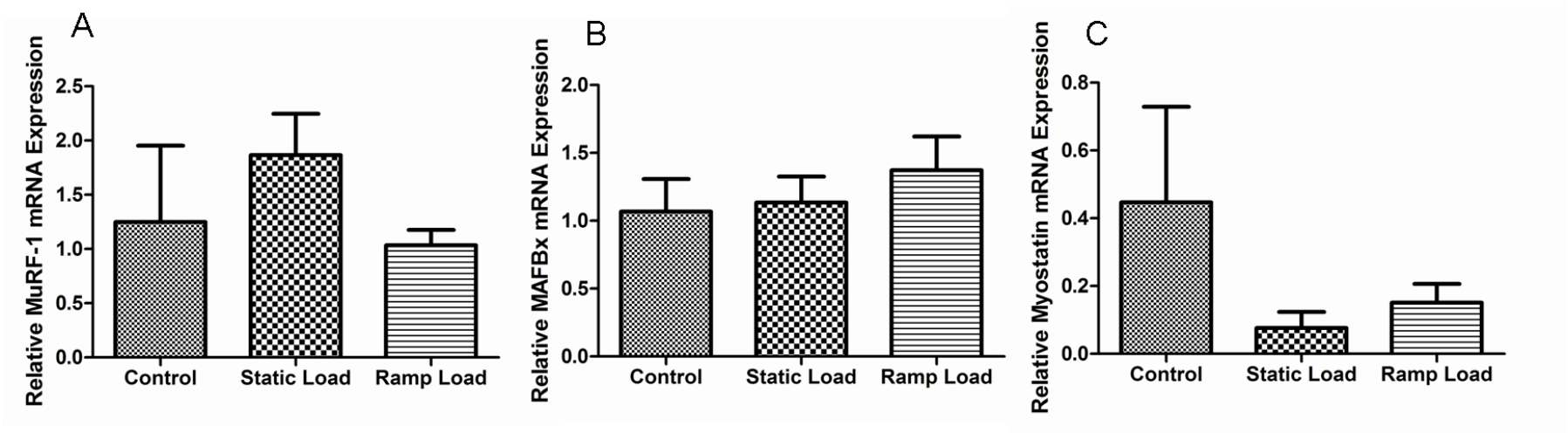

Figure 5-5. Modulations in genes associated with protein synthesis inhibition and degradation. N = 3+ constructs per condition were analysed. A) No changes in MuRF-1 mRNA in either Static Load or Ramp Load compared to Control ($p = 0.469$). B) No changes in MAFBx mRNA in Static Load or Ramp Load compared to Control ($p = 0.632$). C). Variable, but mean reductions in Myostatin mRNA in both Static Load and Ramp Load conditions compared to Control ($p = 0.572$). Data is presented at mean ± SEM.

5.5 Discussion

The aim of the current investigation was to analyse the acute metabolic and transcriptional responses of two mechanical overload regimens, to provide evidence for whether these models could be used in examining the cellular and molecular regulation of SkM mass.

5.5.1 Evaluating lactate production confirms the effect of mechanical overload on cellular metabolism

In order to analyse whether the mechanical overload regimes were in fact eliciting a cellular metabolic response above control and to assess the extent to which the different regimens moderated this response, media conditioned by the construct during stretch was analysed for lactate (Fig. 5-2). Despite a reduced total gross workload in the Ramp Load condition, the enhanced metabolic response in this condition (demonstrated by increases in peak media Lactate compared to Static Load, $p < 0.001$) could be explained in terms of an intricate cellular response to the mechanical strain. It has previously been postulated that cells in 3D matrices respond to minimise the perceived strain placed upon the extra-cellular matrix during tension (Eastwood, et al., 1998). This observation is supported by the change in shape of the cells associated with cytoskeletal rearrangements in accordance with the strain placed upon the extra-cellular matrix (Eastwood, et al., 1996). This data may provide evidence for the enhanced metabolic response in RL, as the cells will be continually reorganising themselves with the continuous increased load.

5.5.2 Differential mechano-responsive expression of hypertrophic genes IGF-I and MMP-9

With evidence to suggest a differential metabolic demand upon the cells in the Ramp Load condition compared to Static Load (Fig. 5-2), modulation in IGF-I mRNA was found to be independent of this metabolic demand. Static Load significantly increased IGF-I mRNA above Control T and Ramp Load (both $p < 0.05$), demonstrating the augmented acute regulation of this gene in response to this specific mode of overload.

Numerous *in vivo* models of mechanical overload have demonstrated increases in IGF-I, including models of synergistic ablation (Adams and Haddad, 1996, Adams, et al., 1999), mechanical overload (Awede, et al., 1999, McKoy, et al., 1999) or *in vitro* stretch (Goldspink, et al., 1995, McKoy, et al., 1999) induced hypertrophy.

IGF-I is a growth factor that has been implicated in the hypertrophic response of SkM and works at the endocrine, paracrine and autocrine levels with variations in protein structure and function arising from the alternate splicing of the IGF-I gene (Goldspink, 2005). Despite the liver supplying a large proportion of circulating IGF-I, it has been demonstrated that liver deficient IGF-I mice display similar gains in SkM strength to resistance exercise compared to control wild type mice (Matheny, et al., 2009). Moreover, localised infusion of IGF-I induces SkM hypertrophy in rats (Adams and McCue, 1998).

These findings provide support for the use and production of local IGF-I in the hypertrophic response in basal and exercise conditions *in vivo*. However, the use of *in vitro* experiments provides a means to investigate the role of locally produced IGF-I in response to overload or stretch. Stretch induced hypertrophy *in vitro* has been shown to be dependent upon the activation of PI3K/Akt and mTOR (Sasai, et al., 2010), signalling molecules that lie downstream of IGF-I.

Furthermore, mechanical stretch of bio-engineered developing SkM up-regulates IGF-Iea mRNA following an hr of ramp stretch (Cheema, et al., 2005). IGF-Iea (MGF) has been shown to influence the activation and proliferation of satellite cells (Ates, et al., 2007) and thus the regulation of this is more pertinent for developing or regenerating SkM tissue. Data presented here further supports this notion of the intrinsic regulation of IGF-I in the response to acute mechanical overload in a bio-mimetic model of SkM *in vitro*, in order to initiate the signalling mechanisms required for a compensatory hypertrophic response.

The mechanical overload regimes used in the current investigation increased the expression of MMP-9 mRNA to a similar extent compared to CT (both, $p < 0.05$). An increase in MMP-9 has been demonstrated to play a pivotal role in hypertrophy, satellite cell activation and migration, and the maintenance of SkM mass.

MMP's are a large family of Zinc (Zn^{2+}) containing endopeptidases causing proteolysis of selected extra cellular matrix (ECM) components (Carmeli, et al., 2002). MMP's are secreted in a pro-enzyme form which is not active until the propeptide is removed by proteolysis, with MMP-9 predominantly degrading collagen IV, the most abundant collagen in the basement membrane (Liu, et al., 2010). Not only does this degradation of the ECM allow for the enhanced action of growth factors (such as IGF-I), MMP's have been shown to enhance the bio-availability of IGF-I through the proteolysis of IGF binding proteins (Coppock, et al., 2004). Overexpression of an active mutant of MMP-9 in mice leads to increases in phenotypic (fibre cross-sectional area and contractile proteins) and functional (isometric force) characteristics of SkM (Dahiya, et al., 2011).

Upon the deletion of the MMP-9 gene fibre hypertrophy was reduced, underpinned by reductions in pAkt (Dahiya, et al., 2011), a signalling protein downstream of IGF-I. Collectively, these data provide the mechanistic evidence for the role of MMP-9 in the process of hypertrophy.

In this respect, the increases in the transcription of MMP-9 established in this investigation suggest an activated mechanism to induce the potential for hypertrophy.

5.5.3 Modulation of the gene expression of IGFBP's -2 and -5 illustrates a mechanism towards in the increased action of IGF-I

In order to investigate a potential enhancement in IGF signalling following the mechanical overload regimes, the roles of IGFBP's- 2 and -5 were investigated. Ramp Load reduced the expression of IGFBP-5 ($p = 0.008$), whilst Static Load moderately increased decreased IGFBP-5 ($p = 0.027$). IGFBP's regulate the action of IGF-I, working to inhibit or potentiate its action (Clemmons, 1998).

IGFBP's control growth and development through governing the bio-availability of IGF-I and the affinity to the IGF-IR, inhibiting growth in excess quantities (Wolf, et al., 2005). Consequently, in a transgenic mouse model overexpressing IGFBP-2, myofibre size is reduced and the ability for proliferating nuclei is hindered (Rehfeldt, et al., 2010). Moreover, increased circulating serum concentrations of IGFBP-2 *in vivo*, correlates with increased disability and muscle strength (van den Beld, et al., 2003) thus demonstrating a role for this protein the consequential function of SkM. The response of IGFBP-2 mRNA resported here, warrants further investigation to determine whether increased sample sizes would contribute to significant effects in the differential response to Static and Ramp Loading (Fig. 5-4).

The modulation of IGFBP-5 has also been shown in a model of overload induced hypertrophy, where IGFBP-5 mRNA reduced to a third of control levels (Awede, et al., 1999, Awede, et al., 1999). Interestingly, unloading of the overloaded hind limb resulted in atrophy coupled with an increase in IGFBP-5 mRNA (Awede, et al., 1999, Awede, et al., 1999). The regulation of IGFBP-5 mRNA is also evident following electrical stimulation of C2C12 myotubes, whereby modest reductions in expression compared to control are evident over a 3 day period (Bayol, et al., 2005).

Data presented here provides evidence that the regulation of IGFBP-5 mRNA is regulated in a mechano-mediated manner, which may provide evidence for a greater response compared to Bayol et al., (2005) where the mechanical response would only be secondary to the electrically evoked contraction.

Awede et al., (1999) also established a temporal relationship between decreasing IGFBP-5 mRNA and increasing IGF-I mRNA. Data surrounding the influence of IGFBP's on IGF-I action and hypertrophy are compelling, with data presented here providing further support for the functions of IGFBP-5 in the response to mechanical overload of SkM. These data support the research questions and hypotheses outlined for this investigation, whereby a hypertrophic transcriptional signature is evident. Future work using a timecourse model of mRNA expression, should seek to determine whether interactions between IGFBP-5 mRNA and consequential protein production contribute to increased IGF-I mRNA following overload.

5.5.4 Myostatin mRNA following mechanical overload

When investigating the molecular regulation of SkM mass, it is important to consider the mechanisms involved in inhibiting protein synthesis or increasing proteolysis. To this end, the effect of the mechanical overload regimes upon myostatin and members of the ubiquitin proteasome pathway were investigated. Despite no significant effect of mechanical overload being present for any of these genes, a mean but variable reduction was evident for myostatin (Fig. 5-5). Myostatin is a member of the TGFβ family of growth factors (Elkina, et al., 2011) and was discovered to have a profound effect on SkM mass in myostatin knockout models and naturally occurring myostatin null animals (McPherron and Lee, 1997). The influence of myostatin in directly inhibiting protein synthesis, or increasing protein tissue breakdown through MuRF-1 and MAFBx signalling is still disputed (Welle, 2009).

However there is evidence to suggest that myostatin directly inhibits signalling through the Akt/TORC1/P70S6K pathway of protein synthesis in C2C12 myotubes, independent of the activation of MuRF-1 or MAFBx (Trendelenburg, et al., 2009). However an alternative view, points towards myostatin activating MuRF-1 and MAFBx via upstream protein FoxO-1 (McFarlane, et al., 2006), which works to directly to breakdown contractile and structural proteins via ubiquination. As such the expression pattern of MuRF-1 or MAFBx following overload may reflect a complex temporal expression pattern, which warrants further investigation.

5.5.5 Stimulating the mechanisms for hypertrophy *in vitro*: application to SkM tissue engineering?

Previous literature detailed below, has demonstrated the positive influence of mechanical signals in contributing to enhanced maturation and development of tissue engineered SkM (Powell, et al., 2002, Cheema, et al., 2005, Moon du, et al., 2008, Corona, et al., 2012, 2005). However, there is evidence to suggest that cyclical mechanical stimulation may hinder maturation of C2C12's seeded in tissue engineered constructs (Boonen, et al., 2010). Data presented here supports the role of mechanical stimulation in the enhanced hypertrophic transcriptional response. Increasing the potential for myotube growth contributes to enhanced development of the construct, with respect to engineering a more *in vivo* representative tissue. Furthermore the ability to generate force, if implanted in vitro would be greater following hypertrophy of the embedded myotubes. In addition, the use of ramp and static mechanical overload compared to cyclical load (Boonen, et al., 2010) appears to contribute to enhanced maturation potential.

5.6 Conclusion

The data from the current investigation supports the experimental hypothesis surrounding the expression of key hypetrophic genes. Particulalry, this study demonstrates the intrinsic role of IGF-I and the IGFBP-5 in increasing the potential for IGF-I signalling to enhance protein synthesis.

Coupled with the reduction in Myostatin mRNA, the overload regimes have induced a transcriptional response known to induce compensatory hypertrophy. In addition, this study has provided evidence for the use of an animal-free bio-mimetic *in vitro* model to investigate the response of SkM to mechanical overload. Furthermore, the use of ramp and static loading of tissue engineered SkM will contribute to an enhanced maturation potential for use as pre-clinical or implantation models for disease.

Future experiments will seek to understand the acute protein signalling mechanisms (which are difficult to investigate *in vivo*) that are activated upon mechanical loading, which contribute to the transcription of the genes investigated here. The investigation into the consequences of the altered transcription of the genes discussed here is also warranted. The proposed effect of modulated mRNA of the genes investigated here is represented in Fig. 5-6. Furthermore, the effect of mechanical loading upon phenotypic adaptation should be explored with respect to myotube hypertrophy and myonuclear addition.

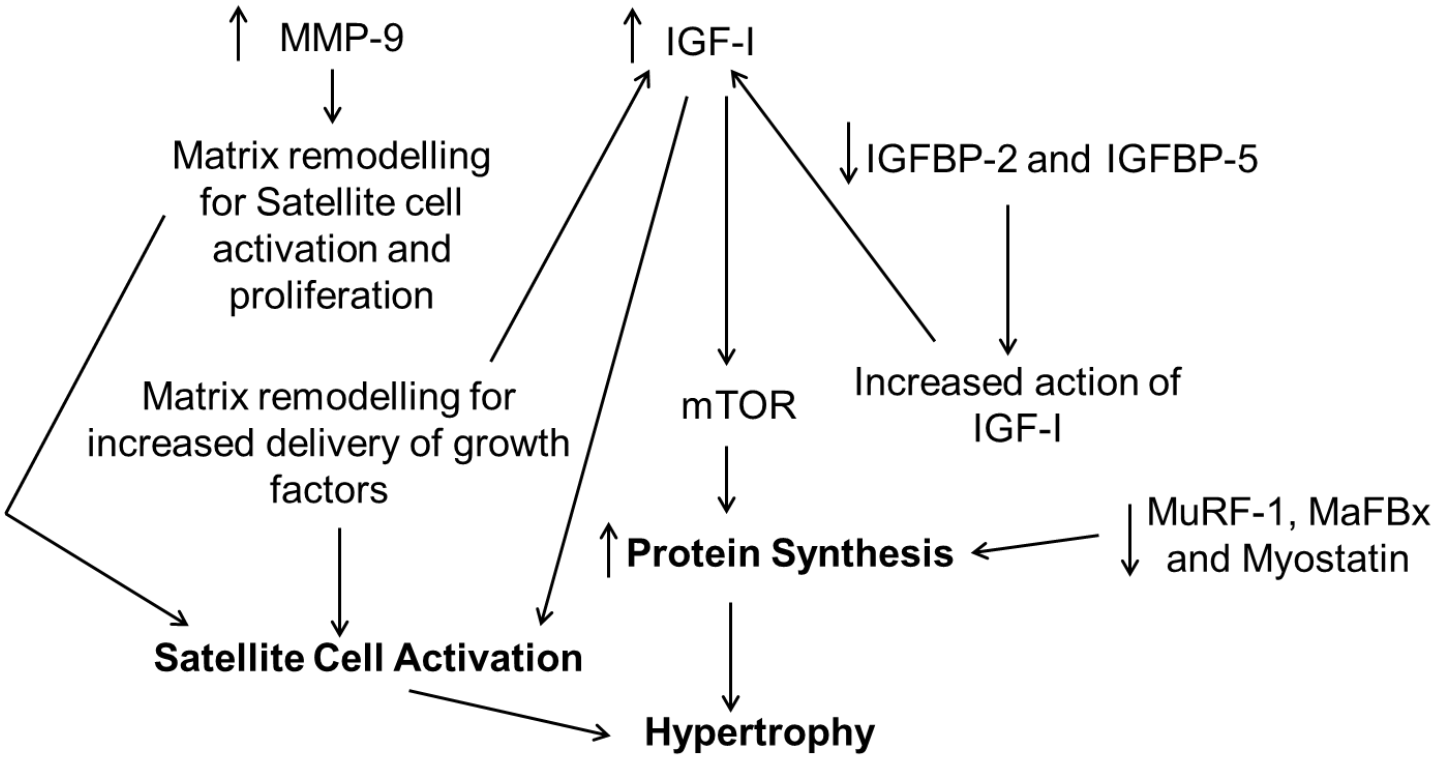

Figure 5-6. Schematic representation of the acute transcriptional responses and key potential mechanisms regulating consequential hypertrophy.

6 Thesis Discussion

6.1 Summary of Thesis Aims

The aim of this Thesis was to develop, characterise and utilise an *in vitro* model of SkM, to further understand the regulation of SkM adaptation to mechanical loading. The limitations of *in vivo* research has steered the development of *in vitro* models of mechanical loading, which often lack bio-mimicity with respect to the morphology of the cells, overlooking of the influence of a representative ECM and the vector nature of loading. Therefore, the experiments presented in this Thesis aimed to combat these issues to provide a model that could reflect *in vivo* physiology to a greater extent.

6.2 Novelty of Findings

Data presented within this Thesis provides novel evidence for the use of the proposed model to investigate SkM physiology.

6.2.1 Chapter 3

The development of a long term culture system, using small collagen constructs represents an advancement of previously published literature (see section 3.3, Cheema, et al., 2003, Cheema, et al., 2005). Moreover, the conserved behaviour of C2C12 myoblasts within 3 ml compared to 5 ml constructs ensures a reduced culture requirement and economic cost of reagents.

Novel data was also presented to illustrate the extent of matrix remodelling (macroscopic contraction, see section 3.3.2) and myoblast differentiation within an isolated population of myogenically determined seeded cells (see section 3.3.3). It had previously been postulated that a non-myogenic population of cells would be required for sufficient remodelling of the matrix to ensure myogenic cell-cell contact for fusion (Smith, et al., 2012). This data is significant with respect to investigating the intrinsic response of myoblasts within a representative niche (Sharples, et al., 2012). The uni-axial alignment and morphology of these fused cells conveys distinct similarity to *in vivo* SkM (Gillies and Lieber, 2011), an improvement of previously published monolayer culture systems.

Moreover, this model permits the study of other physiological and pathophysiological stimuli on SkM cells within a construct that is characteristic of *in vivo* tissue. These characterisation data supported the hypotheses that an utilising a high seeding density and recapitualing the in vivo SkM niche, would contribute to the development of a bio-mimetic SkM model.

6.2.2 Chapter 4

The precise effect of mechanical cues in stimulating SkM response to exercise *in vivo* is challenging to investigate, due to the influence of many other confounding factors including systemic circulation, neural influence and ethical limitations. Data presented in this Thesis advances previous *in vitro* studies with respect to the cell morphology, ECM and the modalities of stimulation investigated (Passey, et al., 2011).

Studies investigating the effect of mechanical strain on metabolism are limited, despite the clear mechanical component of SkM contraction. The development of an *in vitro* model to investigate this was presented in this Thesis. The execution of cyclic stimulation protocols that replicate continuous low strain and intermittent higher strain mechanical loads revealed a mode-dependent metabolic and transcriptional effect (see section 4.3). Previous studies have investigated the effect of mechanical signals on mediating glucose uptake (Iwata, et al., 2007), however this is the first investigation to characterise the metabolic effect following of mechanical strain of SkM cells in bio-mimetic culture. Furthermore, the response of the metabolic parameters measured (lactate and glucose) discovered similarities to that of *in vivo* exercise (Billat, et al., 2003, Mackenzie, et al., 2011). Investigating the molecular response to cyclical stimulation, confirmed a rapid increase in mtDNA content a response underpinned in part by the regulation genes involved in mitochondrial biogenesis (Hood, 2001, Safdar, et al., 2011, see sections 4.3.4 and 4.3.5).

This original data is the first to illustrate a mechanical influence on mitochondrial dynamics in SkM and challenges previously published hypotheses as to the systemic circulating adipokines required (Li, et al., 2011). This rapid effect of mechano-stimulation on mtDNA provides a highly controlled and efficient model to study mitochondrial dynamics in SkM. Additionally, this model represents a key adaptation to endurance-based exercise providing evidence for a mechano-metabolic influence on stimulating mtDNA synthesis. Together, the data presented in Chapter 4 supported the set hypotheses, demonstrating a metabolic and associated metabolic transcriptional response to cyclic mechanical strain.

6.2.3 Chapter 5

The molecular response of SkM to mechanical signals has been shown for over 50 years (Goldberg, 1967), providing the earliest mechanistic data regulating hypertrophy. Numerous *in vivo* models have been employed to investigate mechanical overload and hypertrophy, including synergistic ablation and resistance exercise.

There is also a body of research that have used *in vitro* models to characterise the molecular signals that co-ordinate compensatory hypertrophy (Vandenburgh, et al., 1989, Powell, et al., 2002, Hornberger, et al., 2005, Sasai, et al., 2010). Data presented in this Thesis establishes two models of mechanical overload, which show transcriptional modulation similar to that seen in previous models (increases in IGF-I, MMP-9 and decreases in IGFBP-5 mRNA, see section 5.4). Increases in the expression of genes associated with hypertrophy and a decrease in the expression of genes associated with atrophy supports the hypotheses generated and reflects a trend towards stimulating protein accretion in this model. The isolated nature and accurately defined stimulation of this system, allows for the investigation of the intrinsic muscle cell response to mechanical overload (Sharples, et al., 2012). The novelty of this data resides in the bio-mimicity of the constructs used, the uni-axial tension applied and the consequential pattern of gene expression.

In conclusion, the data presented in this Thesis describes the development and utilisation of a novel SkM model to investigate the effect of mechanical loading on the biochemical and molecular response of muscle cells. The data accumulated here will form the basis of future investigations to analyse the response and adaptation of SkM to increased loading. The application of the models to pathologies and particular myopathies will permit the pre-clinical investigation of potential exercise, pharmacological and genetic therapies to combat the diseases.

6.3 Limitations and Future Directions

The following sections will aim to outline the current limitations to the experimental design and procedures conducted within this Thesis. As such, it is hoped that future expeirments will be able to overcome these issues.

6.3.1 Experimental Design and Statistical Analysis

When designing experiments it is important to consider the number of samples required (sample size), to be able to observe a satistical effect between control and treatment groups. With this in mind, prospective power calculations to determine sample size are often performed for *in vivo* invesirgations, to ensure enough participants or animals are included in the study. *In vitro* experiments are often limited in sample size, largely due to resrource and time constraints, however can display enough statistical power to see an effect. Due to the novelty of the data presented in this Thesis, it was difficult to perform classical prospective power calculations. In this regard the 'Resource Equation' method for determining sample size could be considered as an alternative approach method (Mead, 1988).

An approximate sample size can be calculated by the number of degrees of freedom for the error term in the inferential statistical test (Festing, 2001). This is described by the formula;

$$E = N - T - B$$

Where E, N, T and B are the error, total, treatment and block degrees of freedom in the inferential test.

Equation 6.1

The suggestion is that E should be between 10 and 20 (Festing, 2001). Therefore for an experiment with a single indepedent variable with two levels, with a total of 6 observations the following equation would be true;

$E = 5 – 1 = 4$

Thus the experimental design described would be deemed under powered for determining a statistical effect, because the error term is less than 10. In the case of the experiments described in this Thesis, unfortunately using the method described would reveal insufficient sample sizes. However, it is important to consider that if a statistical effect has been shown there must be enough statistical power to show this effect. Future experiments utilising the model described herein, should perform prospective power calculations in order to ensure the chance of an effect of treatment can be witnessed. This will make sure the controlled *in vitro* model will indeed prove to be system whereby basic mechanisms can be investigated in a refined pre-clinical setting.

6.3.2 Advancement of the Model System

The data presented in this Thesis demonstrates the ability to investigate the development of 3D tissue engineered SkM. Following development, it has been demonstrated that these constructs can be used to examine the intrinsic muscle cell responses following mechanical overload. Despite the ability to analyse these intrinsic mechanisms, the presence of a systemic circulatory system limits the extrapolation of findings to *in vivo* SkM. Indeed, the existence of a vascularised SkM model promotes maturation of myotubes within a tissue engineered SkM model with the ability for electrical excitability (Borschel et al., 2007).

With this in mind, future work should aim to increase the bio-mimicity of the model by investigating the effect of systemically acting proteins on the response to mechanical stretch. The systematic investigation of proposed effector proteins such as adipocytokines (Li et al., 2011), would form a highly controlled system to examine intrinsic-extrinsic protein interaction. The integration of a basic perfusion flow system would also allow the continuous delivery of nutrients and growth factors, contributing to a more *in vivo*-like microenvironment.

Despite the objective of current Thesis to investigate the effect of mechanical stretch on SkM cells, it is important to consider the intrinsic and neural excitability that stimulates contraction *in vivo* prior to a mechanical response. Efforts have been made to incorporate motoneurons into SkM models, with encouraging signs of neuromuscular interaction (Das et al., 2010; Smith et al., 2012b). The functionality of these interactions in terms of whether a full neuromuscular junction is present is difficult to test due to the amount of extra-cellular collagen. The ability to test functional synapses relies on electro-physiological techniques, which to date have shown promising results in monolayer co-culture systems (Umbach et al., 2012).

The density of the collagen matrix within the model described here also reduces the resolution to be able to witness intrinsic excitation. The contraction of the collagen matrix has been attributed in part to originate from passive and active contraction of the myotubes (Smith et al., 2012a). The inability to observe any potential active contraction, particularly in response to stretch, has been ascribed to the innate stiffness of collagen (Khodabukus and Baar, 2009). The capacity to observe this phenomenon within this model would further increase its bio-mimicity. Studying cellular calcium dynamics during and following mechanical stretch would provide evidence as to whether an active contractile response was achieved, an occurrence that has been demonstrated in other cell types (Dalrymple et al., 2007, Iribe and Khol, 2008).

Furthermore, the staining of the myotubes present in the system with an antibody against myosin heavy chain or othe relevant proteins to provide indication as to the presence of contractile machinery, would offer data concerning the potential for active contraction of the developed myotubes. Additionally, the development of the model to increase the occurrence of neuromuscular interaction and reduce matrix volume and stiffness for electrophysiological analysis would provide an ideal model to study moto-neuromuscular interaction following stretch.

The transmission of mechanical force within SkM is controlled in part by the ECM and the myotendinous junctions (Larkin et al., 2012). The model presented here uses a matrix comprised of type I collagen, a major constituent of the ECM *in vivo*. However the transmission of mechanical force is facilitated by the A-frame structures which attach to the mechanical stimulation system. Future work should aim to attach the SkM model to a tissue engineered tendon, in order to further enhance the *in vivo* nature of the system. These tissue hybrids have been successfully engineered and tested *in vitro*, providing evidence for the interaction of the two tissue types with positive expression of specific muscle-tendon unit (MTU) protein paxillin (Larkin et al., 2006). Utilising an MTU system will enable the analysis of the response of SkM cells to mechanical signals in an environment similar to *in vivo* SkM tissue.

Furthermore, the transmission of external force through a more in vivo-like MTU system would allow for the dinlineation of the precise mechanical sgnals which regulate mechano-activation of SkM cellular mechanisms. Indeed, furutre investigations should also aim to define the influences of stretch activated channels (SAC's, Spangenburg and McBride, 2006, Butterfield and Best, 2009), integrins (Boppart, et al., 2011, Lueders, et al., 2011) and the dystrophin-dystroglycan complex (Parcell, et al., 2009) on the signal transduction following mechanical stimuli within the model presented here and fututure bio-mimetic systems.

The rationale for using the C2C12 cell line within the experiments presented here was based upon the requirement to investigate the intrinsic regulation of myogenic cells in response to mechanical stimulation. Although this provides a highly controlled environment for the study of myogenic cells, it is clear that non-myogenic cells regulate myogenic cell fate and behaviour (Brady et al., 2008; Stern et al., 2009; Brzoska et al., 2011). Future experiments should aim to characterise the effect of these two different cell types on the response to mechanical stimulation. There is evidence *in vivo* for the activation of mesenchymal stem cells other than satellite cells following eccentric exercise (mainly pericytes, Valero et al., 2012). The use of primary cell culture methodologies to identify these non-myogenic cell types, combined with mechanical stimulation would enable the controlled investigation of the mechanism whereby these cells are activated. The ability to examine the differential proportions of these cell types *in vitro*, will also contribute to a greater understanding of cell-cell interaction, particularly in response to mechanical strain.

The final methodological advancement that should be made for this model is the analysis of intra-cellular protein. The ability to successfully measure intra-cellular protein will be indispensible to understand the mechanisms that regulate responses to mechanical signals in SkM. The 'gold standard' method of protein quantification, Western Blotting, was used to investigate a potential intra-cellular mechanism (see appendix 1). However, limitiations surrounding protein isolation and purification prevented robust data from being generated. Future investigations should aim to use more sensitive methods of protein analysis, to overcome the limited cellular protein isolation possible in this system. An increasingly popular method of protein analysis is the cytometric bead array, which uses flow cytometric technology with antibody conjugated beads. This technology allows for the analysis of multiple proteins of interest, including post-transnationally modified proteins, with a very small amount of protein (Morgan et al., 2004, Sharples et al., 2012).

Developing a method to investigate proteins involved in converting mechanical signals into biochemical signals (putative mechano-chemical proteins), will enable a greater understanding of the mechano-transduction pathways.

The data presented in Chapter 4 shows a rapid increase in mtDNA content following cyclical mechanical stimulation. Future experiments should aim to address the underlying mechanism which is regulating this response. Efforts should be made to delineate whether the mechanism is mediated by mechanical or metabolic signals, by manipulating these two parameters. It seems likely that these two parameters are inextricably linked, however a cause and effect relationship as to the stimulating mechanism of mitochondrial biogenesis should be explored. The hypothesis of a metabolic threshold for mitochondrial biogenesis could be explored within this system using incremental strain, which may provide sustenance to the high intensity interval training principle surrounding increased mitochondrial biogenesis and aerobic metabolism.

The process of mitochondrial biogenesis and mtDNA replication is controlled by a multitude of proteins and genes, with the transduction network forming a highly complex system. In order to ascertain a direct effector mechanism for the influence of mechanical signals on mtDNA replication, the use of protein and/or gene overexpression or inhibition would allow for the investigation of single proteins and genes.

Data presented in Chapter 5 illustrates a hypertrophic transcriptional response to mechanical overload, exemplified increases in hypertrophic genes and a down regulation of genes involved in atrophy. Despite this evidence demonstrating an acute transcriptional response to mechanical overload, the acute protein signalling mechanisms associated with translation initiation at the ribosome. The advancement of the system that allows for long term culture without the development infection would enable the longer term stimulation of the constructs.

This would permit the study of multiple bouts of mechanical stimulation where particular focus could be placed upon adaptation; examining for myotube hypertrophy using histological techniques. The interplay between signalling mechanisms that regulate mitochondrial biogenesis and hypertrophy (particularly AMPK-mTOR) is complex in nature, with previous studies illustrating a mode specific activation of these two adaptive responses (Atherton et al., 2005). This led to the proposal of an intra-cellular switch mechanism which co-ordinates the divergent response. This hypothesis has recently been challenged with a highly controlled *in vivo* experiment (Vissing et al., 2011), however there is still limited molecular evidence as to the fibre type-fibre size (oxidative or hypertrophy) phenomenon (van Wessel et al., 2010).

6.3.3 Future Applications of the Model

The use of this model to investigate the cellular and molecular pre-dispositions to SkM injury is also a research theme that should be pursued with this model, particularly following the development of a model of mechanical overload presented in this Thesis. The application of this model to study the effect of mechanical stress on diseased cells will enable the 'pre-clinical' testing of potential exercise therapies. Furthermore, the model presented here will be able to identify the mechano-chemical signals that are impaired in diseased muscle cells. Particularly, the evidence for exercise as a therapy for muscular dystrophy is debated in the scientific community with much progress to be made regarding this matter (Yamada, et al., 2012). The use of pre-clinical models to 'screen' the response of dystrophic cells to mechanical stimulation will provide an invaluable to inform as to whether exercise may reduce the debilitation seen with this disease.

Finally, the application of this model to study the effect of mechanical stress on diseased cells will enable the 'pre-clinical' testing of potential exercise therapies. Furthermore, the model presented here will be able to identify the mechano-chemical signals that are impaired in diseased muscle cells.

Particularly, the evidence for exercise as a therapy for muscular dystrophy is debated in the scientific community with much progress to be made regarding this matter (Markert et al., 2012). The use of pre-clinical models to 'screen' the response of dystrophic cells to mechanical stimulation will provide an invaluable to inform as to whether exercise may reduce the debilitation seen with this disease.

6.4 Conclusion

This Thesis has presented novel data regarding the development and use of an *in vitro* SkM model to investigate the acute biochemical and molecular effect of mechanical stimulation. This model will be a valuable tool in delineating the mechanisms that regulate SkM cell response and adaptation to mechanical signals. Furthermore the use of this model as a pre-clinical tool will form a highly controlled environment to investigate various stimuli prior to *in vivo* testing.

7 References

Acarturk TO, Peel MM, Petrosko P, LaFramboise W, Johnson PC, DiMilla PA. 1999. Control of attachment, morphology, and proliferation of skeletal myoblasts on silanized glass. J Biomed Mater Res 44:355-370.

Adams GR, Haddad F. 1996. The relationships among IGF-1, DNA content, and protein accumulation during skeletal muscle hypertrophy. J Appl Physiol 81:2509-2516.

Adams GR, McCue SA. 1998. Localized infusion of IGF-I results in skeletal muscle hypertrophy in rats. J Appl Physiol 84:1716-1722.

Adams GR, Haddad F, Baldwin KM. 1999. Time course of changes in markers of myogenesis in overloaded rat skeletal muscles. J Appl Physiol 87:1705-1712.

Alegria-Schaffer A, Lodge A, Vattem K. 2009. Performing and optimizing Western blots with an emphasis on chemiluminescent detection. Methods Enzymol 463:573-599.

Allen DG, Kabbara AA, Westerblad H. 2002. Muscle fatigue: the role of intracellular calcium stores. Canadian Journal of Applied Physiology = Revue Canadienne De Physiologie Appliquee 27:83-96.

Allen DL, Linderman JK, Roy RR, Grindeland RE, Mukku V, Edgerton VR. 1997. Growth hormone/IGF-I and/or resistive exercise maintains myonuclear number in hindlimb unweighted muscles. J Appl Physiol 83:1857-1861.

Allen RE, Boxhorn LK. 1989. Regulation of skeletal muscle satellite cell proliferation and differentiation by transforming growth factor-beta, insulin-like growth factor I, and fibroblast growth factor. J Cell Physiol 138:311-315.

Allen RE, Rankin LL. 1990. Regulation of satellite cells during skeletal muscle growth and development. Proc Soc Exp Biol Med 194:81-86.

Al-Shanti N, Faulkner SH, Saini A, Loram I, Stewart CE. 2011. A semi-automated programme for tracking myoblast migration following mechanical damage: manipulation by chemical inhibitors. Cell Physiol Biochem 27:625-636.

Amirouche A, Durieux AC, Banzet S, Koulmann N, Bonnefoy R, Mouret C, Bigard X, Peinnequin A, Freyssenet D. 2009. Down-regulation of Akt/mammalian target of rapamycin signaling pathway in response to myostatin overexpression in skeletal muscle. Endocrinology 150:286-294.

Armstrong RB, Marum P, Tullson P, Saubert CWt. 1979. Acute hypertrophic response of skeletal muscle to removal of synergists. Journal of Applied Physiology: Respiratory, Environmental and Exercise Physiology 46:835-42.

Ates K, Yang SY, Orrell RW, Sinanan AC, Simons P, Solomon A, Beech S, Goldspink G, Lewis MP. 2007. The IGF-I splice variant MGF increases progenitor cells in ALS, dystrophic, and normal muscle. FEBS Lett 581:2727-2732.

Atherton PJ, Babraj J, Smith K, Singh J, Rennie MJ, Wackerhage H. 2005. Selective activation of AMPK-PGC-1alpha or PKB-TSC2-mTOR signaling can explain specific adaptive responses to endurance or resistance training-like electrical muscle stimulation. FASEB Journal : Official Publication of the Federation of American Societies for Experimental Biology 19:786-8.

Atherton PJ, Szewczyk NJ, Selby A, Rankin D, Hillier K, Smith K, Rennie MJ, Loughna PT. 2009. Cyclic stretch reduces myofibrillar protein synthesis despite increases in FAK and anabolic signalling in L6 cells. J Physiol 587:3719-3727.

Auluck A, Mudera V, Hunt NP, Lewis MP. 2005. A three-dimensional in vitro model system to study the adaptation of craniofacial skeletal muscle following mechanostimulation. Eur J Oral Sci 113:218-224.

Awede B, Thissen J, Gailly P, Lebacq J. 1999. Regulation of IGF-I, IGFBP-4 and IGFBP-5 gene expression by loading in mouse skeletal muscle. FEBS Lett 461:263-267.

Awede BL, Thissen JP, Lebacq J. 2002. Role of IGF-I and IGFBPs in the changes of mass and phenotype induced in rat soleus muscle by clenbuterol. Am J Physiol Endocrinol Metab 282:E31-7.

Baar K, Torgan CE, Kraus WE, Esser K. 2000. Autocrine phosphorylation of p70(S6k) in response to acute stretch in myotubes. Mol Cell Biol Res Commun 4:76-80.

Baar K. 2005. New dimensions in tissue engineering: possible models for human physiology. Exp Physiol 90:799-806.

Baar K. 2006. Training for endurance and strength: lessons from cell signaling. Med Sci Sports Exerc 38:1939-1944.

Bacakova L, Lapcikova M, Kubies D, Rypacek F. 2003. Adhesion and growth of rat aortic smooth muscle cells on lactide-based polymers. Adv Exp Med Biol 534:179-189.

Baehr LM, Furlow JD, Bodine SC. 2011. Muscle sparing in muscle RING finger 1 null mice: response to synthetic glucocorticoids. J Physiol 589:4759-4776.

Bailey AJ. 2001. Molecular mechanisms of ageing in connective tissues. Mech Ageing Dev 122:735-755.

Bailey AJ, Shellswell GB, Duance VC. 1979. Identification and change of collagen types in differentiating myoblasts and developing chick muscle. Nature 278:67-69.

Baird MF, Graham SM, Baker JS, Bickerstaff GF. 2012. Creatine-kinase- and exercise-related muscle damage implications for muscle performance and recovery. J Nutr Metab 2012:960363.

Baldwin KM, Klinkerfuss GH, Terjung RL, Mole PA, Holloszy JO. 1972. Respiratory capacity of white, red, and intermediate muscle: adaptative response to exercise. The American Journal of Physiology 222:373-8.

Baker JS, McCormick MC, Robergs RA. 2010. Interaction among Skeletal Muscle Metabolic Energy Systems during Intense Exercise. J Nutr Metab 2010:905612.

Bartlett JD, Hwa Joo C, Jeong TS, Louhelainen J, Cochran AJ, Gibala MJ, Gregson W, Close GL, Drust B, Morton JP. 2012. Matched work high-intensity interval and continuous running induce similar increases in PGC-1alpha mRNA, AMPK, p38, and p53 phosphorylation in human skeletal muscle. J Appl Physiol 112:1135-1143.

Bartlett JM. 2002. Approaches to the analysis of gene expression using mRNA: a technical overview. Mol Biotechnol 21:149-160.

Bayol S, Brownson C, Loughna PT. 2005. Electrical stimulation modulates IGF binding protein transcript levels in C2C12 myotubes. Cell Biochem Funct 23:361-365.

Beauchamp JR, Heslop L, Yu DS, Tajbakhsh S, Kelly RG, Wernig A, Buckingham ME, Partridge TA, Zammit PS. 2000. Expression of CD34 and Myf5 defines the majority of quiescent adult skeletal muscle satellite cells. J Cell Biol 151:1221-1234.

Bekedam MA, van Beek-Harmsen BJ, Boonstra A, van Mechelen W, Visser FC, van der Laarse WJ. 2003. Maximum rate of oxygen consumption related to succinate dehydrogenase activity in skeletal muscle fibres of chronic heart failure patients and controls. Clin Physiol Funct Imaging 23:337-343.

Beneke R, Leithauser RM, Ochentel O. 2011. Blood lactate diagnostics in exercise testing and training. Int J Sports Physiol Perform 6:8-24.

Berchtold MW, Brinkmeier H, Muntener M. 2000. Calcium ion in skeletal muscle: its crucial role for muscle function, plasticity, and disease. Physiological Reviews 80:1215-65.

Bergeron R, Ren JM, Cadman KS, Moore IK, Perret P, Pypaert M, Young LH, Semenkovich CF, Shulman GI. 2001. Chronic activation of AMP kinase results in NRF-1 activation and mitochondrial biogenesis. American Journal of Physiology Endocrinology and Metabolism 281:E1340-6.

Berkes CA, Tapscott SJ. 2005. MyoD and the transcriptional control of myogenesis. Semin Cell Dev Biol 16:585-595.

Bian W, Bursac N. 2008. Tissue engineering of functional skeletal muscle: challenges and recent advances. IEEE Eng Med Biol Mag 27:109-113.

Bian W, Bursac N. 2009. Engineered skeletal muscle tissue networks with controllable architecture. Biomaterials 30:1401-1412.

Bickel CS, Slade JM, Haddad F, Adams GR, Dudley GA. 2003. Acute molecular responses of skeletal muscle to resistance exercise in able-bodied and spinal cord-injured subjects. J Appl Physiol 94:2255-2262.

Bickel CS, Slade J, Mahoney E, Haddad F, Dudley GA, Adams GR. 2005. Time course of molecular responses of human skeletal muscle to acute bouts of resistance exercise. J Appl Physiol 98:482-488.

Billat VL, Sirvent P, Py G, Koralsztein JP, Mercier J. 2003. The concept of maximal lactate steady state: a bridge between biochemistry, physiology and sport science. Sports Med 33:407-26.

Birla RK, Huang YC, Dennis RG. 2008. Effect of streptomycin on the active force of bioengineered heart muscle in response to controlled stretch. In Vitro Cell Dev Biol Anim 44:253-260.

Bischoff R. 1986. A satellite cell mitogen from crushed adult muscle. Dev Biol 115:140-147.

Blau HM, Pavlath GK, Hardeman EC, Chiu CP, Silberstein L, Webster SG, Miller SC, Webster C. 1985. Plasticity of the differentiated state. Science 230:758-66.

Bogdanis GC, Nevill ME, Boobis LH, Lakomy HK. 1996. Contribution of phosphocreatine and aerobic metabolism to energy supply during repeated sprint exercise. J Appl Physiol 80:876-884.

Boonen KJ, Langelaan ML, Polak RB, van der Schaft DW, Baaijens FP, Post MJ. 2010. Effects of a combined mechanical stimulation protocol: Value for skeletal muscle tissue engineering. J Biomech 43:1514-1521.

Boppart MD, Burkin DJ, Kaufman SJ. 2011. Activation of AKT signaling promotes cell growth and survival in alpha7beta1 integrin-mediated alleviation of muscular dystrophy. Biochim Biophys Acta 1812:439-446.

Bouzakri K, Koistinen HA, Zierath JR. 2005. Molecular mechanisms of skeletal muscle insulin resistance in type 2 diabetes. Curr Diabetes Rev 1:167-174.

Brady MA, Lewis MP, Mudera V. 2008. Synergy between myogenic and non-myogenic cells in a 3D tissue-engineered craniofacial skeletal muscle construct. J Tissue Eng Regen Med 2:408-17.

Buckingham M. 2003. How the community effect orchestrates muscle differentiation. Bioessays 25:13-16.

Buckingham M, Bajard L, Chang T, Daubas P, Hadchouel J, Meilhac S, Montarras D, Rocancourt D, Relaix F. 2003. The formation of skeletal muscle: from somite to limb. J Anat 202:59-68.

Buckingham ME, Caput D, Cohen A, Whalen RG, Gros F. 1974. The synthesis and stability of cytoplasmic messenger RNA during myoblast differentiation in culture. Proc Natl Acad Sci U S A 71:1466-1470.

Bulfield G, Siller WG, Wight PA, Moore KJ. 1984. X chromosome-linked muscular dystrophy (mdx) in the mouse. Proc Natl Acad Sci U S A 81:1189-1192.

Buller AJ, Eccles JC, Eccles RM. 1960. Differentiation of fast and slow muscles in the cat hind limb. The Journal of Physiology 150:399-416.

Burgomaster KA, Howarth KR, Phillips SM, Rakobowchuk M, Macdonald MJ, McGee SL, Gibala MJ. 2008. Similar metabolic adaptations during exercise after low volume sprint interval and traditional endurance training in humans. J Physiol 586:151-160.

Butterfield TA, Best TM. 2009. Stretch-activated ion channel blockade attenuates adaptations to eccentric exercise. Med Sci Sports Exerc 41:351-356.

Carmeli E, Coleman R, Reznick AZ. 2002. The biochemistry of aging muscle. Experimental Gerontology 37:477-89.

Caron MA, Charette SJ, Maltais F, Debigare R. 2011. Variability of protein level and phosphorylation status caused by biopsy protocol design in human skeletal muscle analyses. BMC Res Notes 4:488.

Carson JA, Nettleton D, Reecy JM. 2002. Differential gene expression in the rat soleus muscle during early work overload-induced hypertrophy. FASEB J 16:207-209.

Centeno-Baez C, Dallaire P, Marette A. 2011. Resveratrol inhibition of inducible nitric oxide synthase in skeletal muscle involves AMPK but not SIRT1. Am J Physiol Endocrinol Metab 301:E922-30.

Cheema, Yang SY, Mudera V, Goldspink GG, RA. B. 2003. 3-D in vitro model of early skeletal muscle development. Cell Motil Cytoskeleton. 54:226-36.

Cheema U, Brown R, Mudera V, Yang SY, McGrouther G, Goldspink G. 2005. Mechanical signals and IGF-I gene splicing in vitro in relation to development of skeletal muscle. J Cell Physiol 202:67-75.

Chen G, Bressler BH, Quinn LS. 1994. Extracts from mdx and normal mouse skeletal muscle contain similar levels of mitogenic activity for myoblasts. Cell Biol Int 18:229-235.

Chen Y, Leask A, Abraham DJ, Kennedy L, Shi-Wen X, Denton CP, Black CM, Verjee LS, Eastwood M. 2011. Thrombospondin 1 is a key mediator of transforming growth factor beta-mediated cell contractility in systemic sclerosis via a mitogen-activated protein kinase kinase (MEK)/extracellular signal-regulated kinase (ERK)-dependent mechanism. Fibrogenesis Tissue Repair 4:9.

Chin ER. 2005. Role of Ca2+/calmodulin-dependent kinases in skeletal muscle plasticity. J Appl Physiol 99:414-23.

Choi J, Costa ML, Mermelstein CS, Chagas C, Holtzer S, Holtzer H. 1990. MyoD converts primary dermal fibroblasts, chondroblasts, smooth muscle, and retinal pigmented epithelial cells into striated mononucleated myoblasts and multinucleated myotubes. Proc Natl Acad Sci U S A 87:7988-7992.

Christ B, Jacob HJ, Jacob M. 1974. Experimental studies on the development of the thoracic wall in chick embryos. Experientia 30:1449-1451.

Christ B, Jacob HJ, Jacob M. 1977. Experimental analysis of the origin of the wing musculature in avian embryos. Anat Embryol (Berl) 150:171-186.

Christ B, Brand-Saberi B. 2002. Limb muscle development. Int J Dev Biol 46:905-914.

Clemmons DR. 1998. Role of insulin-like growth factor binding proteins in controlling IGF actions. Mol Cell Endocrinol 140:19-24.

Clemmons DR. 2009. Role of IGF-I in skeletal muscle mass maintenance. Trends Endocrinol Metab 20:349-356.

Coffey VG, Zhong Z, Shield A, Canny BJ, Chibalin AV, Zierath JR, Hawley JA. 2006. Early signaling responses to divergent exercise stimuli in skeletal muscle from well-trained humans. FASEB J 20:190-2.

Coolican SA, Samuel DS, Ewton DZ, McWade FJ, Florini JR. 1997. The mitogenic and myogenic actions of insulin-like growth factors utilize distinct signaling pathways. J Biol Chem 272:6653-6662.

Coppock HA, White A, Aplin JD, Westwood M. 2004. Matrix metalloprotease-3 and -9 proteolyze insulin-like growth factor-binding protein-1. Biol Reprod 71:438-443.

Corona BT, Machingal MA, Criswell T, Vadhavkar M, Dannahower AC, Bergman C, Zhao W, Christ GJ. 2012. Further development of a tissue engineered muscle repair construct in vitro for enhanced functional recovery following implantation in vivo in a murine model of volumetric muscle loss injury. Tissue Eng Part A 18:1213-1228.

Coppock HA, White A, Aplin JD, Westwood M. 2004. Matrix metalloprotease-3 and -9 proteolyze insulin-like growth factor-binding protein-1. Biol Reprod 71:438-443.

Costill DL, Fink WJ, Pollock ML. 1976. Muscle fiber composition and enzyme activities of elite distance runners. Med Sci Sports 8:96-100.

Crossland H, Kazi AA, Lang CH, Timmons JA, Pierre P, Wilkinson DJ, Smith K, Szewczyk NJ, Atherton PJ. 2013. Focal adhesion kinase is required for IGF-I- mediated growth of skeletal muscle cells via a TSC2/mTOR/S6K1-mediated pathway. Am. J. Physiol. Endocrinol. Metab. ul;305(2):E183-93. doi: 10.1152/ajpendo.00541.2012. Epub 2013 May 21.

Cuthbertson DJ, Babraj J, Smith K, Wilkes E, Fedele MJ, Esser K, Rennie M. 2006. Anabolic signaling and protein synthesis in human skeletal muscle after dynamic shortening or lengthening exercise. Am J Physiol Endocrinol Metab 290:E731-8.

D'souza DM, Lai RY, Shuen M, Hood DA. 2012. mRNA Stability as a Function of Striated Muscle Oxidative Capacity. Am J Physiol Regul Integr Comp Physiol

Dahiya S, Bhatnagar S, Hindi SM, Jiang C, Paul PK, Kuang S, Kumar A. 2011. Elevated levels of active matrix metalloproteinase-9 cause hypertrophy in skeletal muscle of normal and dystrophin-deficient mdx mice. Hum Mol Genet 20:4345-4359.

De Feo P, Di Loreto C, Lucidi P, Murdolo G, Parlanti N, De Cicco A, Piccioni F, Santeusanio F. 2003. Metabolic response to exercise. J Endocrinol Invest 26:851-854.

Degens H, Alway SE. 2006. Control of muscle size during disuse, disease, and aging. International Journal of Sports Medicine 27:94-9.

Dieffenbach CW, Lowe TM, Dveksler GS. 1993. General concepts for PCR primer design. PCR Methods Appl 3:S30-7.

Dietrich S, Abou-Rebyeh F, Brohmann H, Bladt F, Sonnenberg-Riethmacher E, Yamaai T, Lumsden A, Brand-Saberi B, Birchmeier C. 1999. The role of SF/HGF and c-Met in the development of skeletal muscle. Development 126:1621-1629.

Dreyer HC, Fujita S, Cadenas JG, Chinkes DL, Volpi E, Rasmussen BB. 2006. Resistance exercise increases AMPK activity and reduces 4E-BP1 phosphorylation and protein synthesis in human skeletal muscle. J Physiol 576:613-624.

Dreyfus JC, Schapira G, Resnais J, Scebat L. 1960. Serum creatine kinase in the diagnosis of myocardial infarct. Rev Fr Etud Clin Biol 5:386-387.

Duguez S, Feasson L, Denis C, Freyssenet D. 2002. Mitochondrial biogenesis during skeletal muscle regeneration. Am J Physiol Endocrinol Metab 282:E802-9.

Dulhunty AF. 2006. Excitation-contraction coupling from the 1950s into the new millennium. Clin Exp Pharmacol Physiol 33:763-772.

Eastwood M, Porter R, Khan U, McGrouther G, Brown R. 1996. Quantitative analysis of collagen gel contractile forces generated by dermal fibroblasts and the relationship to cell morphology. J Cell Physiol 166:33-42.

Eastwood M, Mudera VC, McGrouther DA, Brown RA. 1998. Effect of precise mechanical loading on fibroblast populated collagen lattices: morphological changes. Cell Motil Cytoskeleton 40:13-21.

Eastwood M, McGrouther DA, Brown RA. 1998. Fibroblast responses to mechanical forces. Proc Inst Mech Eng H 212:85-92.

Elkina Y, von Haehling S, Anker SD, Springer J. 2011. The role of myostatin in muscle wasting: an overview. J Cachexia Sarcopenia Muscle 2:143-151.

Esser KA, White TP. 1995. Mechanical load affects growth and maturation of skeletal muscle grafts. J Appl Physiol 78:30-7.

Evans MJ, Scarpulla RC. 1989. Interaction of nuclear factors with multiple sites in the somatic cytochrome c promoter. Characterization of upstream NRF-1, ATF, and intron Sp1 recognition sequences. The Journal of Biological Chemistry 264:14361-8.

Evans RM, Harridge SD, Velloso CP, Yang SY, Goldspink G, Orrell RW. 2010. Investigation of MGF mRNA expression in patients with amyotrophic lateral sclerosis using parallel in vivo and in vitro approaches. Amyotroph Lateral Scler 11:172-177.

Faude O, Kindermann W, Meyer T. 2009. Lactate threshold concepts: how valid are they?. Sports Med 39:469-90.

Fernandez-Marcos PJ, Auwerx J. 2011. Regulation of PGC-1alpha, a nodal regulator of mitochondrial biogenesis. Am J Clin Nutr 93:884S-90.

Festing M.F.W, 2001. Guidelines for the Design and Statistical Analysis of Experiments in Papers Submitted to ATLA. ATLA 29: 427-446.

Foster C, Costill DL, Daniels JT, Fink WJ. 1978. Skeletal muscle enzyme activity, fiber composition and VO2 max in relation to distance running performance. Eur J Appl Physiol Occup Physiol 39:73-80.

Freyssenet D, Di Carlo M, Hood DA. 1999. Calcium-dependent regulation of cytochrome c gene expression in skeletal muscle cells. Identification of a protein kinase c-dependent pathway. The Journal of Biological Chemistry 274:9305-11.

Friedmann-Bette B, Schwartz FR, Eckhardt H, Billeter R, Bonaterra G, Kinscherf R. 2012. Similar changes of gene expression in human skeletal muscle after resistance exercise and multiple fine needle biopsies. J Appl Physiol 112:289-295.

Gallagher S, Winston SE, Fuller SA, Hurrell JG. 2001. Immunoblotting and immunodetection. Curr Protoc Immunol Chapter 8:Unit 8.10.

Gibala MJ, Little JP, van Essen M, Wilkin GP, Burgomaster KA, Safdar A, Raha S, Tarnopolsky MA. 2006. Short-term sprint interval versus traditional endurance training: similar initial adaptations in human skeletal muscle and exercise performance. J Physiol 575:901-911.

Gibala MJ, McGee SL, Garnham AP, Howlett KF, Snow RJ, Hargreaves M. 2009. Brief intense interval exercise activates AMPK and p38 MAPK signaling and increases the expression of PGC-1alpha in human skeletal muscle. J Appl Physiol 106:929-34.

Gibbons MC, Foley MA, Cardinal KO. 2012. Thinking Inside the Box: Keeping Tissue-Engineered Constructs In Vitro for Use as Preclinical Models. Tissue Eng Part B Rev Epub

Gillies AR, Lieber RL. 2011. Structure and function of the skeletal muscle extracellular matrix. Muscle Nerve 44:318-331.

Glass DJ. 2003a. Molecular mechanisms modulating muscle mass. Trends Mol Med 9:344-350.

Glass DJ. 2003b. Signalling pathways that mediate skeletal muscle hypertrophy and atrophy. Nat Cell Biol 5:87-90.

Goldberg AL. 1967. Work-induced growth of skeletal muscle in normal and hypophysectomized rats. Am J Physiol 213:1193-1198.

Goldberg AL, Goodman HM. 1969. Amino acid transport during work-induced growth of skeletal muscle. Am J Physiol 216:1111-1115.

Goldspink DF. 1977. The influence of immobilization and stretch on protein turnover of rat skeletal muscle. J Physiol 264:267-282.

Goldspink DF, Cox VM, Smith SK, Eaves LA, Osbaldeston NJ, Lee DM, Mantle D. 1995. Muscle growth in response to mechanical stimuli. Am J Physiol 268:E288-97.

Goldspink G. 2005. Mechanical signals, IGF-I gene splicing, and muscle adaptation. Physiology (Bethesda) 20:232-238.

Gomes AV, Potter JD, Szczesna-Cordary D. 2002. The role of troponins in muscle contraction. IUBMB Life 54:323-333.

Goncalves MD, Pistilli EE, Balduzzi A, Birnbaum MJ, Lachey J, Khurana TS, Ahima RS. 2010. Akt deficiency attenuates muscle size and function but not the response to ActRIIB inhibition. PLoS One 5:e12707.

Gospodarowicz D, Weseman J, Moran JS, Lindstrom J. 1976. Effect of fibroblast growth factor on the division and fusion of bovine myoblasts. J Cell Biol 70:395-405.

Greenhaff PL, Nevill ME, Soderlund K, Bodin K, Boobis LH, Williams C, Hultman E. 1994. The metabolic responses of human type I and II muscle fibres during maximal treadmill sprinting. J Physiol 478 (Pt 1):149-155.

Green HJ, Thomson JA, Daub BD, Ranney DA. 1980. Biochemical and histochemical alterations in skeletal muscle in man during a period of reduced activity. Can J Physiol Pharmacol 58:1311-1316.

Green JD, Narahara HT. 1980. Assay of succinate dehydrogenase activity by the tetrazolium method: evaluation of an improved technique in skeletal muscle fractions. J Histochem Cytochem 28:408-412.

Griffin CA, Apponi LH, Long KK, Pavlath GK. 2010. Chemokine expression and control of muscle cell migration during myogenesis. J Cell Sci 123:3052-3060.

Gumucio JP, Mendias CL. 2012. Atrogin-1, MuRF-1, and sarcopenia. Endocrine xxx

Gundersen K. 2011. Excitation-transcription coupling in skeletal muscle: the molecular pathways of exercise. Biological Reviews of the Cambridge Philosophical Society 86:564-600.

Hamai N, Nakamura M, Asano A. 1997. Inhibition of mitochondrial protein synthesis impaired C2C12 myoblast differentiation. Cell Struct Funct 22:421-431.

Harridge SD. 2007. Plasticity of human skeletal muscle: gene expression to in vivo function. Exp Physiol 92:783-797.

Hashimoto T, Hussien R, Oommen S, Gohil K, Brooks GA. 2007. Lactate sensitive transcription factor network in L6 cells: activation of MCT1 and mitochondrial biogenesis. FASEB J 21:2602-2612.

Hatfaludy S, Shansky J, Vandenburgh HH. 1989. Metabolic alterations induced in cultured skeletal muscle by stretch-relaxation activity. Am J Physiol 256:C175-81.

Hawke TJ, Garry DJ. 2001. Myogenic satellite cells: physiology to molecular biology. J Appl Physiol 91:534-551.

Henriksen EJ, Schneider MC, Ritter LS. 1993. Regulation of contraction-stimulated system A amino acid uptake in skeletal muscle: role of vicinal sulfhydryls. Metabolism 42:440-445.

Heron-Milhavet L, Mamaeva D, LeRoith D, Lamb NJ, Fernandez A. 2010. Impaired muscle regeneration and myoblast differentiation in mice with a muscle-specific KO of IGF-IR. J Cell Physiol 225:1-6.

Hill DJ, Crace CJ, Nissley SP, Morrell D, Holder AT, Milner RD. 1985. Fetal rat myoblasts release both rat somatomedin-C (SM-C)/insulin-like growth factor I (IGF I) and multiplication-stimulating activity in vitro: partial characterization and biological activity of myoblast-derived SM-C/IGF I. Endocrinology 117:2061-2072.

Hill M, Goldspink G. 2003. Expression and splicing of the insulin-like growth factor gene in rodent muscle is associated with muscle satellite (stem) cell activation following local tissue damage. J Physiol 549:409-418.

Hoffman EP, Monaco AP, Feener CC, Kunkel LM. 1987. Conservation of the Duchenne muscular dystrophy gene in mice and humans. Science 238:347-350.

Holloszy JO. 1967. Biochemical adaptations in muscle. Effects of exercise on mitochondrial oxygen uptake and respiratory enzyme activity in skeletal muscle. J Biol Chem 242:2278-82.

Holloszy JO, Kohrt WM. 1996. Regulation of carbohydrate and fat metabolism during and after exercise. Annu Rev Nutr 16:121-138.

Holm L, Reitelseder S, Pedersen TG, Doessing S, Petersen SG, Flyvbjerg A, Andersen JL, Aagaard P, Kjaer M. 2008. Changes in muscle size and MHC composition in response to resistance exercise with heavy and light loading intensity. J Appl Physiol 105:1454-1461.

Hood DA. 2001. Invited Review: contractile activity-induced mitochondrial biogenesis in skeletal muscle. J Appl Physiol 90:1137-57.

Hopkins, PM. 2006. Voluntary Motor Systems- skeletal muscle, reflexes and control of movement in Foundations of Anesthesia, 2nd Edition, Mosby, USA.

Hornberger TA, Armstrong DD, Koh TJ, Burkholder TJ, Esser KA. 2005. Intracellular signaling specificity in response to uniaxial vs. multiaxial stretch: implications for mechanotransduction. Am J Physiol Cell Physiol 288:C185-94.

Huang YC, Dennis RG, Larkin L, Baar K. 2005. Rapid formation of functional muscle in vitro using fibrin gels. J Appl Physiol 98:706-713.

Hubatsch DA, Jasmin BJ. 1997. Mechanical stimulation increases expression of acetylcholinesterase in cultured myotubes. Am J Physiol 273:C2002-9.

Huxley AF, Niedergerke R. 1954. Structural changes in muscle during contraction; interference microscopy of living muscle fibres. Nature 173:971-973.

Huxley H, Hanson J. 1954. Changes in the cross-striations of muscle during contraction and stretch and their structural interpretation. Nature 173:973-976.

Huxley HE. 1957. The double array of filaments in cross-striated muscle. J Biophys Biochem Cytol 3:631-648.

Hwa V, Oh Y, Rosenfeld RG. 1999a. The insulin-like growth factor-binding protein (IGFBP) superfamily. Endocr Rev 20:761-787.

Hwa V, Oh Y, Rosenfeld RG. 1999b. Insulin-like growth factor binding proteins: a proposed superfamily. Acta Paediatr Suppl 88:37-45.

Iscoe KE, Riddell MC. 2011. Continuous moderate-intensity exercise with or without intermittent high-intensity work: effects on acute and late glycaemia in athletes with Type 1 diabetes mellitus. Diabet Med 28:824-32.

Ishihara A, Ohira Y, Roy RR, Nagaoka S, Sekiguchi C, Hinds WE, Edgerton VR. 2002. Succinate dehydrogenase activity in rat dorsolateral ventral horn motoneurons at L6 after spaceflight and recovery. J Gravit Physiol 9:39-48.

Ito S, Kume H, Oguma T, Ito Y, Kondo M, Shimokata K, Suki B, Naruse K. 2006. Roles of stretch-activated cation channel and Rho-kinase in the spontaneous contraction of airway smooth muscle. Eur J Pharmacol 552:135-142.

Iwata M, Hayakawa K, Murakami T, Naruse K, Kawakami K, Inoue-Miyazu M, Yuge L, Suzuki S. 2007. Uniaxial cyclic stretch-stimulated glucose transport is mediated by a ca-dependent mechanism in cultured skeletal muscle cells. Pathobiology 74:159-68.

Jackman RW, Kandarian SC. 2004. The molecular basis of skeletal muscle atrophy. Am J Physiol Cell Physiol 287:C834-43.

Johnston AP, Baker J, Bellamy LM, McKay BR, De Lisio M, Parise G. 2010. Regulation of muscle satellite cell activation and chemotaxis by angiotensin II. PLoS One 5:e15212.

Jones DA, Round JM, De Haan A. 2004. Skeletal muscle: A textbook of muscle physiology for sport, exercise and physiotherapy, Churchill Livingston, UK.

Jorgensen SB, Richter EA, Wojtaszewski JF. 2006. Role of AMPK in skeletal muscle metabolic regulation and adaptation in relation to exercise. The Journal of Physiology 574:17-31.

Kandarian SC, Schulte LM, Esser KA. 1992. Age effects on myosin subunit and biochemical alterations with skeletal muscle hypertrophy. J Appl Physiol 72:1934-9.

Kendall B, Eston R. 2002. Exercise-induced muscle damage and the potential protective role of estrogen. Sports Med 32:103-123.

Kherif S, Lafuma C, Dehaupas M, Lachkar S, Fournier JG, Verdiere-Sahuque M, Fardeau M, Alameddine HS. 1999. Expression of matrix metalloproteinases 2 and 9 in regenerating skeletal muscle: a study in experimentally injured and mdx muscles. Dev Biol 205:158-170.

Khodabukus A, Paxton JZ, Donnelly K, Baar K. 2007. Engineered muscle: a tool for studying muscle physiology and function. Exerc Sport Sci Rev 35:186-191.

Khodabukus A, Baar K. 2009. Regulating fibrinolysis to engineer skeletal muscle from the C2C12 cell line. Tissue Eng Part C Methods 15:501-511.

Khodabukus A, Baar K. 2012. Defined electrical stimulation emphasizing excitability for the development and testing of engineered skeletal muscle. Tissue Eng Part C Methods 18:349-357.

Kjaer M. 2004. Role of extracellular matrix in adaptation of tendon and skeletal muscle to mechanical loading. Physiol Rev 84:649-698.

Klumpp D, Horch RE, Kneser U, Beier JP. 2010. Engineering skeletal muscle tissue--new perspectives in vitro and in vivo. J Cell Mol Med 14:2622-2629.

Koubassova NA, Tsaturyan AK. 2011. Molecular mechanism of actin-myosin motor in muscle. Biochemistry (Mosc) 76:1484-1506.

Kubista M, Andrade JM, Bengtsson M, Forootan A, Jonak J, Lind K, Sindelka R, Sjoback R, Sjogreen B, Strombom L, Stahlberg A, Zoric N. 2006. The real-time polymerase chain reaction. Mol Aspects Med 27:95-125.

Kurosaka M, Naito H, Ogura Y, Machida S, Katamoto S. 2011. Satellite cell pool enhancement in rat plantaris muscle by endurance training depends on intensity rather than duration. Acta Physiol (Oxf) Epub 2011/11/02.

Lai RY, Ljubicic V, D'souza D, Hood DA. 2010. Effect of chronic contractile activity on mRNA stability in skeletal muscle. Am J Physiol Cell Physiol 299:C155-63.

Langley B, Thomas M, Bishop A, Sharma M, Gilmour S, Kambadur R. 2002. Myostatin inhibits myoblast differentiation by down-regulating MyoD expression. J Biol Chem 277:49831-49840.

Le Grand F, Rudnicki M. 2007. Satellite and stem cells in muscle growth and repair. Development 134:3953-3957.

Leick L, Wojtaszewski JF, Johansen ST, Kiilerich K, Comes G, Hellsten Y, Hidalgo J, Pilegaard H. 2008. PGC-1alpha is not mandatory for exercise- and training-induced adaptive gene responses in mouse skeletal muscle. Am J Physiol Endocrinol Metab. 294:E463-74.

Leick L, Fentz J, Bienso RS, Knudsen JG, Jeppesen J, Kiens B, Wojtaszewski JF, Pilegaard H. 2010. PGC-1{alpha} is required for AICAR-induced expression of GLUT4 and mitochondrial proteins in mouse skeletal muscle. American Journal of Physiology Endocrinology and Metabolism 299:E456-65.

Lenk K, Schuler G, Adams V. 2010. Skeletal muscle wasting in cachexia and sarcopenia: molecular pathophysiology and impact of exercise training. Journal of Cachexia, Sarcopenia and Muscle 1:9-21.

Lenka N, Basu A, Mullick J, Avadhani NG. 1996. The role of an E box binding basic helix loop helix protein in the cardiac muscle-specific expression of the rat cytochrome oxidase subunit VIII gene. The Journal of Biological Chemistry 271:30281-9.

Lewis MP, Tippett HL, Sinanan AC, Morgan MJ, Hunt NP. 2000. Gelatinase-B (matrix metalloproteinase-9; MMP-9) secretion is involved in the migratory phase of human and murine muscle cell cultures. Journal of Muscle Research and Cell Motility 21:223-33.

Lewis MP, Machell JR, Hunt NP, Sinanan AC, Tippett HL. 2001. The extracellular matrix of muscle--implications for manipulation of the craniofacial musculature. Eur J Oral Sci 109:209-221.

Li L, Pan R, Li R, Niemann B, Aurich AC, Chen Y, Rohrbach S. 2011. Mitochondrial biogenesis and peroxisome proliferator-activated receptor-gamma coactivator-1alpha (PGC-1alpha) deacetylation by physical activity: intact adipocytokine signaling is required. Diabetes 60:157-67.

Lieber RL, Shah S, Friden J. 2002. Cytoskeletal disruption after eccentric contraction-induced muscle injury. Clin Orthop Relat Res (403 Suppl):S90-9.

Lin J, Wu H, Tarr PT, Zhang CY, Wu Z, Boss O, Michael LF, Puigserver P, Isotani E, Olson EN, Lowell BB, Bassel-Duby R, Spiegelman BM. 2002. Transcriptional co-activator PGC-1 alpha drives the formation of slow-twitch muscle fibres. Nature. 418:797-801.

Linderman JK, Talmadge RJ, Gosselink KL, Tri PN, Roy RR, Grindeland RE. 1996. Synergistic ablation does not affect atrophy or altered myosin heavy chain expression in the non-weight bearing soleus muscle. Life Sciences 59:789-95.

Little JP, Safdar A, Cermak N, Tarnopolsky MA, Gibala MJ. 2010. Acute endurance exercise increases the nuclear abundance of PGC-1alpha in trained human skeletal muscle. Am J Physiol Regul Integr Comp Physiol 298:R912-7.

Little JP, Safdar A, Bishop D, Tarnopolsky MA, Gibala MJ. 2011. An acute bout of high-intensity interval training increases the nuclear abundance of PGC-1alpha and activates mitochondrial biogenesis in human skeletal muscle. American Journal of Physiology Regulatory, Integrative and Comparative Physiology 300:R1303-10.

Liu HH, Wang JW, Zhang RP, Chen X, Yu HY, Jin HB, Li L, Han CC, Xu F, Kang B, He H, Xu HY. 2012. In ovo feeding of IGF-1 to ducks influences neonatal skeletal muscle hypertrophy and muscle mass growth upon satellite cell activation. J Cell Physiol 227:1465-1475.

Liu X, Lee DJ, Skittone LK, Natsuhara K, Kim HT. 2010. Role of gelatinases in disuse-induced skeletal muscle atrophy. Muscle Nerve 41:174-178.

Louis E, Raue U, Yang Y, Jemiolo B, Trappe S. 2007. Time course of proteolytic, cytokine, and myostatin gene expression after acute exercise in human skeletal muscle. J Appl Physiol 103:1744-1751.

Lueders TN, Zou K, Huntsman HD, Meador B, Mahmassani Z, Abel M, Valero MC, Huey KA, Boppart MD. 2011. The alpha7beta1-integrin accelerates fiber hypertrophy and myogenesis following a single bout of eccentric exercise. Am J Physiol Cell Physiol 301:C938-46.

Machida S, Spangenburg EE, Booth FW. 2004. Primary rat muscle progenitor cells have decreased proliferation and myotube formation during passages. Cell Prolif 37:267-277.

Machingal MA, Corona BT, Walters TJ, Kesireddy V, Koval CN, Dannahower A, Zhao W, Yoo JJ, Christ GJ. 2011. A tissue-engineered muscle repair construct for functional restoration of an irrecoverable muscle injury in a murine model. Tissue Eng Part A 17:2291-2303.

MacPhee DJ. 2010. Methodological considerations for improving Western blot analysis. J Pharmacol Toxicol Methods 61:171-177.

Madden MC, Byrnes WC, Lebin JA, Batliner ME, Allen DL. 2011. Plasma matrix metalloproteinase-9 response to eccentric exercise of the elbow flexors. Eur J Appl Physiol 111:1795-1805.

McFarlane C, Plummer E, Thomas M, Hennebry A, Ashby M, Ling N, Smith H, Sharma M, Kambadur R. 2006. Myostatin induces cachexia by activating the ubiquitin proteolytic system through an NF-kappaB-independent, FoxO1-dependent mechanism. J Cell Physiol 209:501-514.

McPherron AC, Lee SJ. 1997. Double muscling in cattle due to mutations in the myostatin gene. Proc Natl Acad Sci U S A 94:12457-12461.

Magid A, Law DJ. 1985. Myofibrils bear most of the resting tension in frog skeletal muscle. Science 230:1280-1282.

Mahoney DJ, Parise G, Melov S, Safdar A, Tarnopolsky MA. 2005. Analysis of global mRNA expression in human skeletal muscle during recovery from endurance exercise. FASEB J. 19:1498-500.

Mascher H, Tannerstedt J, Brink-Elfegoun T, Ekblom B, Gustafsson T, Blomstrand E. 2008. Repeated resistance exercise training induces different changes in mRNA expression of MAFbx and MuRF-1 in human skeletal muscle. Am J Physiol Endocrinol Metab 294:E43-51.

Matheny RW, Merritt E, Zannikos SV, Farrar RP, Adamo ML. 2009. Serum IGF-I-deficiency does not prevent compensatory skeletal muscle hypertrophy in resistance exercise. Exp Biol Med (Maywood) 234:164-170.

Mauro A. 1961. Satellite cell of skeletal muscle fibers. J Biophys Biochem Cytol 9:493-495.

McArdle WD, Katch FI, Katch VL. 2004. Essentials of exercise physiology: Energy, Nutrition and Human Performance. Lippincott Williams and Wilkins, Baltimore, USA.

McCarthy JJ, Esser KA. 2007. Counterpoint: Satellite cell addition is not obligatory for skeletal muscle hypertrophy. J Appl Physiol 103:1100-2; discussion 1102-3.

McGee SL, Hargreaves M. 2004. Exercise and myocyte enhancer factor 2 regulation in human skeletal muscle. Diabetes 53:1208-14.

McKoy G, Ashley W, Mander J, Yang SY, Williams N, Russell B, Goldspink G. 1999. Expression of insulin growth factor-1 splice variants and structural genes in rabbit skeletal muscle induced by stretch and stimulation. J Physiol 516 (Pt 2):583-592.

McPherron AC, Lawler AM, Lee SJ. 1997. Regulation of skeletal muscle mass in mice by a new TGF-beta superfamily member. Nature 387:83-90.

Mehan RS, Greybeck BJ, Emmons K, Byrnes WC, Allen DL. 2011. Matrix metalloproteinase-9 deficiency results in decreased fiber cross-sectional area and alters fiber type distribution in mouse hindlimb skeletal muscle. Cells Tissues Organs 194:510-520.

Mole PA, Oscai LB, Holloszy JO. 1971. Adaptation of muscle to exercise. Increase in levels of palmityl Coa synthetase, carnitine palmityltransferase, and palmityl Coa dehydrogenase, and in the capacity to oxidize fatty acids. The Journal of Clinical Investigation 50:2323-30.

Moon du G, Christ G, Stitzel JD, Atala A, Yoo JJ. 2008. Cyclic mechanical preconditioning improves engineered muscle contraction. Tissue Eng Part A 14:473-482.

Moraes CT. 2001. What regulates mitochondrial DNA copy number in animal cells?. Trends Genet. 17:199-205.

Morgan JE, Partridge TA. 2003. Muscle satellite cells. Int J Biochem Cell Biol 35:1151-1156.

Mudera V, Smith AS, Brady MA, Lewis MP. 2010. The effect of cell density on the maturation and contractile ability of muscle derived cells in a 3D tissue-engineered skeletal muscle model and determination of the cellular and mechanical stimuli required for the synthesis of a postural phenotype. Journal of Cellular Physiology 225:646-53.

MURRAY MR, POGOGEFF IA. 1946. Observations on adult mammalian skeletal muscle cultivated in vitro. Anat Rec 94:484.

Musaro A, McCullagh K, Paul A, Houghton L, Dobrowolny G, Molinaro M, Barton ER, Sweeney HL, Rosenthal N. 2001. Localized Igf-1 transgene expression sustains hypertrophy and regeneration in senescent skeletal muscle. Nat Genet 27:195-200.

Mackenzie R, Maxwell N, Castle P, Brickley G, Watt P. 2011. Acute hypoxia and exercise improve insulin sensitivity (S(I) (2*)) in individuals with type 2 diabetes. Diabetes Metab Res Rev 27:94-101.

Mackenzie R, Maxwell N, Castle P, Elliott B, Brickley G, Watt P. 2012. Intermittent Exercise with and without Hypoxia Improves Insulin Sensitivity in Individuals with Type 2 Diabetes. The Journal of Clinical Endocrinology and Metabolism

McLoon LK, Thorstenson KM, Solomon A, Lewis MP. 2007. Myogenic precursor cells in craniofacial muscles. Oral Dis 13:134-140.

Mutungi G, Edman KA, Ranatunga KW. 2003. A mechanical stretch induces contractile activation in unstimulated developing rat skeletal muscle in vitro. J Physiol 551:93-102.

Nagata Y, Partridge TA, Matsuda R, Zammit PS. 2006. Entry of muscle satellite cells into the cell cycle requires sphingolipid signaling. J Cell Biol 174:245-253.

Nagatomo F, Fujino H, Kondo H, Kouzaki M, Gu N, Takeda I, Tsuda K, Ishihara A. 2012. The effects of running exercise on oxidative capacity and PGC-1alpha mRNA levels in the soleus muscle of rats with metabolic syndrome. J Physiol Sci 62:105-114.

Narici MV, Maffulli N. 2010. Sarcopenia: characteristics, mechanisms and functional significance. British Medical Bulletin 95:139-59.

Nedachi T, Fujita H, Kanzaki M. 2008. Contractile C2C12 myotube model for studying exercise-inducible responses in skeletal muscle. Am J Physiol Endocrinol Metab 295:E1191-204.

Nikolic N, Skaret Bakke S, Tranheim Kase E, Rudberg I, Flo Halle I, Rustan AC, Thoresen GH, Aas V. 2012. Electrical pulse stimulation of cultured human skeletal muscle cells as an in vitro model of exercise. PLoS One 7:e33203.

Noden DM. 1983. The role of the neural crest in patterning of avian cranial skeletal, connective, and muscle tissues. Dev Biol 96:144-165.

O'Connor RS, Pavlath GK. 2007. Point:Counterpoint: Satellite cell addition is/is not obligatory for skeletal muscle hypertrophy. J Appl Physiol 103:1099-1100.

Ojuka EO, Jones TE, Nolte LA, Chen M, Wamhoff BR, Sturek M, Holloszy JO. 2002a. Regulation of GLUT4 biogenesis in muscle: evidence for involvement of AMPK and Ca(2+). American Journal of Physiology Endocrinology and Metabolism 282:E1008-13.

Ojuka EO, Jones TE, Han DH, Chen M, Wamhoff BR, Sturek M, Holloszy JO. 2002b. Intermittent increases in cytosolic Ca2+ stimulate mitochondrial biogenesis in muscle cells. American Journal of Physiology Endocrinology and Metabolism 283:E1040-5.

Ojuka EO, Jones TE, Han DH, Chen M, Holloszy JO. 2003. Raising Ca2+ in L6 myotubes mimics effects of exercise on mitochondrial biogenesis in muscle. FASEB Journal : Official Publication of the Federation of American Societies for Experimental Biology 17:675-81.

Okada A, Ono Y, Nagatomi R, Kishimoto KN, Itoi E. 2008. Decreased muscle atrophy F-box (MAFbx) expression in regenerating muscle after muscle-damaging exercise. Muscle Nerve 38:1246-1253.

Olesen J, Kiilerich K, Pilegaard H. 2010. PGC-1alpha-mediated adaptations in skeletal muscle. Pflugers Arch 460:153-62.

Olson EN, Williams RS. 2000. Calcineurin signaling and muscle remodeling. Cell 101:689-92.

Oscai LB, Holloszy JO. 1971. Biochemical adaptations in muscle. II. Response of mitochondrial adenosine triphosphatase, creatine phosphokinase, and adenylate kinase activities in skeletal muscle to exercise. The Journal of Biological Chemistry 246:6968-72.

Oyedotun KS, Lemire BD. 2004. The quaternary structure of the Saccharomyces cerevisiae succinate dehydrogenase. Homology modeling, cofactor docking, and molecular dynamics simulation studies. J Biol Chem 279:9424-9431.

Parcell AC, Woolstenhulme MT, Sawyer RD. 2009. Structural protein alterations to resistance and endurance cycling exercise training. J Strength Cond Res 23:359-365.

Passey S, Martin N, Player D, Lewis MP. 2011. Stretching skeletal muscle in vitro: does it replicate in vivo physiology?. Biotechnol Lett

Perry CG, Lally J, Holloway GP, Heigenhauser GJ, Bonen A, Spriet LL. 2010. Repeated transient mRNA bursts precede increases in transcriptional and mitochondrial proteins during training in human skeletal muscle. The Journal of Physiology 588:4795-810.

Petrella JK, Kim JS, Cross JM, Kosek DJ, Bamman MM. 2006. Efficacy of myonuclear addition may explain differential myofiber growth among resistance-trained young and older men and women. Am J Physiol Endocrinol Metab 291:E937-46.

Petrella JK, Kim JS, Mayhew DL, Cross JM, Bamman MM. 2008. Potent myofiber hypertrophy during resistance training in humans is associated with satellite cell-mediated myonuclear addition: a cluster analysis. J Appl Physiol 104:1736-1742.

Phillips BE, Williams JP, Gustafsson T, Bouchard C, Rankinen T, Knudsen S, Smith K, Timmons JA, Atherton PJ. 2013. Molecular networks of human muscle adaptation to exercise and age. PLoS Genet. Mar;9(3):e1003389. doi: 10.1371/journal.pgen.1003389. Epub 2013 Mar 21.

Phillips SM. 2012. Nutrient-rich meat proteins in offsetting age-related muscle loss. Meat Sci 92:174-178.

Philp A, Belew MY, Evans A, Pham D, Sivia I, Chen A, Schenk S, Baar K. 2011. The PGC-1α-related coactivator promotes mitochondrial and myogenic adaptations in C2C12 myotubes. Am J Physiol Regul Integr Comp Physiol. 301:R864-72.

Pilegaard H, Domino K, Noland T, Juel C, Hellsten Y, Halestrap AP, Bangsbo J. 1999. Effect of high-intensity exercise training on lactate/H+ transport capacity in human skeletal muscle. Am J Physiol 276:E255-61.

Pilegaard H, Ordway GA, Saltin B, Neufer PD. 2000. Transcriptional regulation of gene expression in human skeletal muscle during recovery from exercise. Am J Physiol Endocrinol Metab 279:E806-14.

Pillard F, Laoudj-Chenivesse D, Carnac G, Mercier J, Rami J, Riviere D, Rolland Y. 2011. Physical activity and sarcopenia. Clinics in Geriatric Medicine 27:449-70.

Player DJ, Lewis, MP. 2012. Mechanisms activating PGC-1α and consequential transcriptional mechanisms following exercise: A mini review. CMEP 1:(1)xx.

Pogogeff IA, Murray MR. 1945. Regeneration of Adult Mammalian Skeletal Muscle in Vitro. Science 101:174.

Pogogeff IA, Murray MR. 1946. Form and behavior of adult mammalian skeletal muscle in vitro. Anat Rec 95:321-335.

Pogozelski AR, Geng T, Li P, Yin X, Lira VA, Zhang M, Chi JT, Yan Z. 2009. p38gamma mitogen-activated protein kinase is a key regulator in skeletal muscle metabolic adaptation in mice. PloS One 4:e7934.

Powell-Braxton L, Hollingshead P, Warburton C, Dowd M, Pitts-Meek S, Dalton D, Gillett N, Stewart TA. 1993. IGF-I is required for normal embryonic growth in mice. Genes Dev 7:2609-2617.

Powell CA, Smiley BL, Mills J, Vandenburgh HH. 2002. Mechanical stimulation improves tissue-engineered human skeletal muscle. Am J Physiol Cell Physiol 283:C1557-65.

Powers SK, Lieu FK, Criswell D, Dodd S. 1993. Biochemical verification of quantitative histochemical analysis of succinate dehydrogenase activity in skeletal muscle fibres. Histochem J 25:491-496.

Puigserver P, Wu Z, Park CW, Graves R, Wright M, Spiegelman BM. 1998. A cold-inducible coactivator of nuclear receptors linked to adaptive thermogenesis. Cell 92:829-39.

Ramsey KA, Bakker AJ, Pinniger GJ. 2010. Fiber-type dependence of stretch-induced force enhancement in rat skeletal muscle. Muscle Nerve 42:769-777.

Rantanen T, Volpato S, Ferrucci L, Heikkinen E, Fried LP, Guralnik JM. 2003. Handgrip strength and cause-specific and total mortality in older disabled women: exploring the mechanism. Journal of the American Geriatrics Society 51:636-41.

Rehfeldt C, Renne U, Sawitzky M, Binder G, Hoeflich A. 2010. Increased fat mass, decreased myofiber size, and a shift to glycolytic muscle metabolism in adolescent male transgenic mice overexpressing IGFBP-2. Am J Physiol Endocrinol Metab 299:E287-98.

Reznick RM, Shulman GI. 2006. The role of AMP-activated protein kinase in mitochondrial biogenesis. The Journal of Physiology 574:33-9

Robergs RA, Ghiasvand F, Parker D. 2004. Biochemistry of exercise-induced metabolic acidosis. Am J Physiol Regul Integr Comp Physiol 287:R502-16.

Rockl KS, Hirshman MF, Brandauer J, Fujii N, Witters LA, Goodyear LJ. 2007. Skeletal muscle adaptation to exercise training: AMP-activated protein kinase mediates muscle fiber type shift. Diabetes 56:2062-9.

Roecker K, Schotte O, Niess AM, Horstmann T, Dickhuth HH. 1998. Predicting competition performance in long-distance running by means of a treadmill test. Med Sci Sports Exerc 30:1552-1557.

Rosenblatt JD, Parry DJ. 1992. Gamma irradiation prevents compensatory hypertrophy of overloaded mouse extensor digitorum longus muscle. J Appl Physiol 73:2538-2543.

Roth SM, Martel GF, Ferrell RE, Metter EJ, Hurley BF, Rogers MA. 2003. Myostatin gene expression is reduced in humans with heavy-resistance strength training: a brief communication. Exp Biol Med (Maywood) 228:706-709.

Rullman E, Rundqvist H, Wagsater D, Fischer H, Eriksson P, Sundberg CJ, Jansson E, Gustafsson T. 2007. A single bout of exercise activates matrix metalloproteinase in human skeletal muscle. J Appl Physiol 102:2346-51.

Safdar A, Little JP, Stokl AJ, Hettinga BP, Akhtar M, Tarnopolsky MA. 2011. Exercise increases mitochondrial PGC-1alpha content and promotes nuclear-mitochondrial cross-talk to coordinate mitochondrial biogenesis. J Biol Chem 286:10605-17.

Saks V. 2008. The phosphocreatine-creatine kinase system helps to shape muscle cells and keep them healthy and alive. J Physiol 586:2817-2818.

Sasai N, Agata N, Inoue-Miyazu M, Kawakami K, Kobayashi K, Sokabe M, Hayakawa K. 2010. Involvement of PI3K/Akt/TOR pathway in stretch-induced hypertrophy of myotubes. Muscle Nerve 41:100-106.

Saxena AK, Marler J, Benvenuto M, Willital GH, Vacanti JP. 1999. Skeletal muscle tissue engineering using isolated myoblasts on synthetic biodegradable polymers: preliminary studies. Tissue Eng 5:525-532.

Scarpulla RC. 2002. Nuclear activators and coactivators in mammalian mitochondrial biogenesis. Biochim Biophys Acta 1576:1-14.

Scarpulla RC. 2006. Nuclear control of respiratory gene expression in mammalian cells. Journal of Cellular Biochemistry 97:673-83.

Scarpulla RC. 2008. Transcriptional Paradigms in Mammalian Mitochondrial Biogenesis and Function. Physiol Rev 88:611-638.

Scarpulla RC. 2011. Metabolic control of mitochondrial biogenesis through the PGC-1 family regulatory network. Biochimica Et Biophysica Acta 1813:1269-78.

SCEBAT L, RENAIS J, LENEGRE J. 1961. Serum creatine-kinase in the diagnosis of myocardial lesions. (Clinical and experimental study). Arch Mal Coeur Vaiss 54:721-731.

Schiaffino S, Bormioli SP, Aloisi M. 1972. Cell proliferation in rat skeletal muscle during early stages of compensatory hypertrophy. Virchows Arch B Cell Pathol 11:268-273.

Schmittgen TD, Livak KJ. 2008. Analyzing real-time PCR data by the comparative C(T) method. Nat Protoc 3:1101-8.

Schwander JC, Hauri C, Zapf J, Froesch ER. 1983. Synthesis and secretion of insulin-like growth factor and its binding protein by the perfused rat liver: dependence on growth hormone status. Endocrinology 113:297-305.

Sciote JJ, Morris TJ. 2000. Skeletal muscle function and fibre types: the relationship between occlusal function and the phenotype of jaw-closing muscles in human. J Orthod 27:15-30.

Severgnini S, Lowenthal DT, Millard WJ, Simmen FA, Pollock BH, Borst SE. 1999. Altered IGF-I and IGFBPs in senescent male and female rats. J Gerontol A Biol Sci Med Sci 54:B111-5.

Shah R, Sinanan AC, Knowles JC, Hunt NP, Lewis MP. 2005. Craniofacial muscle engineering using a 3-dimensional phosphate glass fibre construct. Biomaterials 26:1497-1505.

Sharples AP, Al-Shanti N, Stewart CE. 2010. C2 and C2C12 murine skeletal myoblast models of atrophic and hypertrophic potential: relevance to disease and ageing?. J Cell Physiol 225:240-250.

Sharples AP, Stewart CE. 2011. Myoblast models of skeletal muscle hypertrophy and atrophy. Curr Opin Clin Nutr Metab Care 14:230-6.

Sharples AP, Al-Shanti N, Lewis MP, Stewart CE. 2011. Reduction of myoblast differentiation following multiple population doublings in mouse C2 C12 cells: a model to investigate ageing?. J Cell Biochem 112:3773-3785.

Sharples AP, Player DJ, Martin NR, Mudera V, Stewart CE, Lewis MP. 2012. Modelling in vivo skeletal muscle ageing in vitro using three-dimensional bioengineered constructs. Aging Cell 11:986-995.

Sheehan SM, Allen RE. 1999. Skeletal muscle satellite cell proliferation in response to members of the fibroblast growth factor family and hepatocyte growth factor. J Cell Physiol 181:499-506.

Silva LA, Pinho CA, Scarabelot KS, Fraga DB, Volpato AM, Boeck CR, De Souza CT, Streck EL, Pinho RA. 2009. Physical exercise increases mitochondrial function and reduces oxidative damage in skeletal muscle. Eur J Appl Physiol 105:861-867.

Sinanan AC, Buxton PG, Lewis MP. 2006. Muscling in on stem cells. Biol Cell 98:203-214.

Sjogren K, Liu JL, Blad K, Skrtic S, Vidal O, Wallenius V, LeRoith D, Tornell J, Isaksson OG, Jansson JO, Ohlsson C. 1999. Liver-derived insulin-like growth factor I (IGF-I) is the principal source of IGF-I in blood but is not required for postnatal body growth in mice. Proc Natl Acad Sci U S A 96:7088-7092.

Smith AS, Passey S, Greensmith L, Mudera V, Lewis MP. 2012. Characterization and optimization of a simple, repeatable system for the long term in vitro culture of aligned myotubes in 3D. J Cell Biochem 113:1044-53.

Smith AST, Shah R, Hunt NP, Lewis MP. 2010. The Role of Connective Tissue and Extracellular Matrix Signaling in Controlling Muscle Development, Function, and Response to Mechanical Forces. Seminars in Orthodontics 16:135-142.

Spangenburg EE, McBride TA. 2006. Inhibition of stretch-activated channels during eccentric muscle contraction attenuates p70S6K activation. J Appl Physiol 100:129-135.

Spangenburg EE, Le Roith D, Ward CW, Bodine SC. 2008. A functional insulin-like growth factor receptor is not necessary for load-induced skeletal muscle hypertrophy. J Physiol 586:283-291.

Spurway M, Wackerhage H. 2006. Genetics and molecular biology of muscle adaptation: Advances in sport and exercise science

Srikanthan P, Karlamangla AS. 2011. Relative muscle mass is inversely associated with insulin resistance and prediabetes. Findings from the third National Health and Nutrition Examination Survey. J Clin Endocrinol Metab 96:2898-2903.

Stewart CE, Rotwein P. 1996. Insulin-like growth factor-II is an autocrine survival factor for differentiating myoblasts. J Biol Chem 271:11330-11338.

Tajbakhsh S, Rocancourt D, Cossu G, Buckingham M. 1997. Redefining the genetic hierarchies controlling skeletal myogenesis: Pax-3 and Myf-5 act upstream of MyoD. Cell 89:127-138.

Takamatsu C, Umeda S, Ohsato T, Ohno T, Abe Y, Fukuoh A, Shinagawa H, Hamasaki N, Kang D. 2002. Regulation of mitochondrial D-loops by transcription factor A and single-stranded DNA-binding protein. EMBO Rep 3:451-456.

Tatsumi R, Anderson JE, Nevoret CJ, Halevy O, Allen RE. 1998. HGF/SF is present in normal adult skeletal muscle and is capable of activating satellite cells. Dev Biol 194:114-128.

Tatsumi R, Wuollet AL, Tabata K, Nishimura S, Tabata S, Mizunoya W, Ikeuchi Y, Allen RE. 2009. A role for calcium-calmodulin in regulating nitric oxide production during skeletal muscle satellite cell activation. Am J Physiol Cell Physiol 296:C922-9.

Thomas M, Langley B, Berry C, Sharma M, Kirk S, Bass J, Kambadur R. 2000. Myostatin, a negative regulator of muscle growth, functions by inhibiting myoblast proliferation. J Biol Chem 275:40235-40243.

Thompson HS, Scordilis SP, De Souza MJ. 2006. Serum creatine kinase activity varies with ovulatory status in regularly exercising, premenopausal women. Horm Res 65:151-158.

Thorrez L, Shansky J, Wang L, Fast L, VandenDriessche T, Chuah M, Mooney D, Vandenburgh H. 2008. Growth, differentiation, transplantation and survival of human skeletal myofibers on biodegradable scaffolds. Biomaterials 29:75-84.

Timmons JA, Knudsen S, Rankinen T, Koch LG, Sarzynski M, Jensen T, Keller P, Scheele C, Vollaard NB, Nielsen S, Akerstrom T, MacDougald OA, Jansson E, Greenhaff PL, Tarnopolsky MA, van Loon LJ, Pedersen BK, Sundberg CJ, Wahlestedt C, Britton SL, Bouchard C. 2010. Using molecular classification to predict gains in maximal aerobic capacity following endurance exercise training in humans. J Appl Physiol 108:1487-1496.

Tobina T, Yoshioka K, Hirata A, Mori S, Kiyonaga A, Tanaka H. 2011. Peroxisomal proliferator-activated receptor gamma co-activator-1 alpha gene expression increases above the lactate threshold in human skeletal muscle. The Journal of Sports Medicine and Physical Fitness 51:683-8.

Trendelenburg AU, Meyer A, Rohner D, Boyle J, Hatakeyama S, Glass DJ. 2009. Myostatin reduces Akt/TORC1/p70S6K signaling, inhibiting myoblast differentiation and myotube size. Am J Physiol Cell Physiol 296:C1258-70.

Trieu EP, Gross JK, Targoff IN. 2009. Immunoprecipitation-western blot for proteins of low abundance. Methods Mol Biol 536:259-275.

van den Beld AW, Blum WF, Pols HA, Grobbee DE, Lamberts SW. 2003. Serum insulin-like growth factor binding protein-2 levels as an indicator of functional ability in elderly men. Eur J Endocrinol 148:627-634.

van Someren KA, Howatson G, Nunan D, Thatcher R, Shave R. 2005. Comparison of the Lactate Pro and Analox GM7 blood lactate analysers. Int J Sports Med 26:657-661.

Vandenburgh H, Kaufman S. 1979. In vitro model for stretch-induced hypertrophy of skeletal muscle. Science 203:265-268.

Vandenburgh HH. 1988. A computerized mechanical cell stimulator for tissue culture: effects on skeletal muscle organogenesis. In Vitro Cell Dev Biol 24:609-619.

Vandenburgh HH, Hatfaludy S, Karlisch P, Shansky J. 1989. Skeletal muscle growth is stimulated by intermittent stretch-relaxation in tissue culture. Am J Physiol 256:C674-82.

Vandenburgh HH, Hatfaludy S, Karlisch P, Shansky J. 1991. Mechanically induced alterations in cultured skeletal muscle growth. J Biomech 24 Suppl 1:91-99.

Wagenmakers AJ. 1998. Protein and amino acid metabolism in human muscle. Adv Exp Med Biol 441:307-319.

Wang G, Burczynski FJ, Hasinoff BB, Zhang K, Lu Q, Anderson JE. 2009. Development of a nitric oxide-releasing analogue of the muscle relaxant guaifenesin for skeletal muscle satellite cell myogenesis. Mol Pharm 6:895-904.

Welle SL. 2009. Myostatin and muscle fiber size. Focus on "Smad2 and 3 transcription factors control muscle mass in adulthood" and "Myostatin reduces Akt/TORC1/p70S6K signaling, inhibiting myoblast differentiation and myotube size". Am J Physiol Cell Physiol 296:C1245-7.

Wells GD, Noseworthy MD, Hamilton J, Tarnopolski M, Tein I. 2008. Skeletal muscle metabolic dysfunction in obesity and metabolic syndrome. Can J Neurol Sci 35:31-40.

Wheatley SP, Wang YL. 1998. Indirect immunofluorescence microscopy in cultured cells. Methods Cell Biol 57:313-332.

Wilkinson SB, Phillips SM, Atherton PJ, Patel R, Yarasheski KE, Tarnopolsky MA, Rennie MJ. 2008. Differential effects of resistance and endurance exercise in the fed state on signalling molecule phosphorylation and protein synthesis in human muscle. The Journal of Physiology 586:3701-17.

Wright DC. 2007. Mechanisms of calcium-induced mitochondrial biogenesis and GLUT4 synthesis. Applied Physiology, Nutrition, and Metabolism = Physiologie Appliquee, Nutrition Et Metabolisme 32:840-5.

Wolf E, Schneider MR, Zhou R, Fisch TM, Herbach N, Dahlhoff M, Wanke R, Hoeflich A. 2005. Functional consequences of IGFBP excess-lessons from transgenic mice. Pediatr Nephrol 20:269-278.

Wright DC, Han DH, Garcia-Roves PM, Geiger PC, Jones TE, Holloszy JO. 2007. Exercise-induced mitochondrial biogenesis begins before the increase in muscle PGC-1alpha expression. J Biol Chem. 282:194-9.

Wu Z, Puigserver P, Andersson U, Zhang C, Adelmant G, Mootha V, Troy A, Cinti S, Lowell B, Scarpulla RC, Spiegelman BM. 1999. Mechanisms controlling mitochondrial biogenesis and respiration through the thermogenic coactivator PGC-1. Cell. 98:115-24.

Wust RC, Degens H. 2007. Factors contributing to muscle wasting and dysfunction in COPD patients. Int J Chron Obstruct Pulmon Dis 2:289-300.

Wust RC, Myers DS, Stones R, Benoist D, Robinson PA, Boyle JP, Peers C, White E, Rossiter HB. 2012. Regional skeletal muscle remodeling and mitochondrial dysfunction in right ventricular heart failure. Am J Physiol Heart Circ Physiol 302:H402-11.

Xia Y, Buja LM, McMillin JB. 1998. Activation of the cytochrome c gene by electrical stimulation in neonatal rat cardiac myocytes. Role of NRF-1 and c-Jun. The Journal of Biological Chemistry 273:12593-8.

Xiao B, Sanders MJ, Underwood E, Heath R, Mayer FV, Carmena D, Jing C, Walker PA, Eccleston JF, Haire LF, Saiu P, Howell SA, Aasland R, Martin SR, Carling D, Gamblin SJ. 2011. Structure of mammalian AMPK and its regulation by ADP. Nature 472:230-3.

Yadid M, Landesberg A. 2010. Stretch increases the force by decreasing cross-bridge weakening rate in the rat cardiac trabeculae. J Mol Cell Cardiol 49:962-971.

Yaffe D, Saxel O. 1977. A myogenic cell line with altered serum requirements for differentiation. Differentiation 7:159-66.

Yamada AK, Verlengia R, Bueno Junior CR. 2012. Mechanotransduction pathways in skeletal muscle hypertrophy. J Recept Signal Transduct Res 32:42-44.

Yang D, Lu X, Zhang W, He F. 2002. Biochemical changes in primary culture of skeletal muscle cells following dimethoate exposure. Toxicology 174:79-85.

Yang Y, Jemiolo B, Trappe S. 2006. Proteolytic mRNA expression in response to acute resistance exercise in human single skeletal muscle fibers. J Appl Physiol 101:1442-1450.

Yarasheski KE, Zachweija JJ, Angelopoulos TJ, Bier DM. 1993. Short-term growth hormone treatment does not increase muscle protein synthesis in experienced weight lifters. J Appl Physiol 74:3073-3076.

Zafeiridis A, Sarivasiliou H, Dipla K, Vrabas IS. 2010. The effects of heavy continuous versus long and short intermittent aerobic exercise protocols on oxygen consumption, heart rate, and lactate responses in adolescents. Eur J Appl Physiol 110:17-2.

Zammit PS, Partridge TA, Yablonka-Reuveni Z. 2006. The skeletal muscle satellite cell: the stem cell that came in from the cold. J Histochem Cytochem 54:1177-1191.

Zhang Y, Ma K, Sadana P, Chowdhury F, Gaillard S, Wang F, McDonnell DP, Unterman TG, Elam MB, Park EA. 2006. Estrogen-related receptors stimulate pyruvate dehydrogenase kinase isoform 4 gene expression. The Journal of Biological Chemistry 281:39897-906.

Zimowska M, Brzoska E, Swierczynska M, Streminska W, Moraczewski J. 2008. Distinct patterns of MMP-9 and MMP-2 activity in slow and fast twitch skeletal muscle regeneration in vivo. The International Journal of Developmental Biology 52:307-14.

Zimowska M, Olszynski KH, Swierczynska M, Streminska W, Ciemerych MA. 2012. Decrease of MMP-9 activity improves soleus muscle regeneration. Tissue Eng Part A 18:1183-1192.

Zong H, Ren JM, Young LH, Pypaert M, Mu J, Birnbaum MJ, Shulman GI. 2002. AMP kinase is required for mitochondrial biogenesis in skeletal muscle in response to chronic energy deprivation. Proceedings of the National Academy of Sciences of the United States of America 99:15983-7.

8 Appendices

8.1 Appendendix 1

Towards the optimisation of biochemical and Western Blot analyses for the investigation of acute cellular responses to cyclic mechanical stretch

8.1.1 Introduction

The data from Chapter 3 revealed an increase in mtDNA content following cyclical stretch. The transcriptional mechanisms that underpin this response were proposed, with the particular focus on PGC-1α. The adaptation of SkM mitochondria to exercise is regulated by transient increases in both the transcription of key genes and post-translationally modified proteins (PGC-1α, Tfam, NRF-1 and -2). Identifying the precise way in which these mechanisms are transduced is an important and popular research theme within molecular exercise and SkM physiology.

Increased mechanical load of SkM (through physical exercise) forms another major part of the signal that is required to activate many signalling pathways associated with physiological adaptation. To this end, models of mechanical stretch have been used to investigate in isolation, the role of mechanical signals in transducing signalling mechanism. As previously described (see 1.11), these models have been commonly employed to examine mechanisms underpinning hypertrophy. Conversely, minimal attention has been given to the influence of mechanical signals in regulating metabolic adaptation of SkM. This is surprising considering the interaction between many signalling mechanisms that regulate hypertrophy and metabolic adaptation, including the interplay between mTOR signalling and AMPK signalling (Coffey, et al., 2006).

As such *in vitro* models have begun to be used to study mechano-transduction related to metabolic responses and adaptation. Stretching SkM cells in monolayer culture has been shown to increase glucose uptake (Iwata, et al., 2007), through a Ca2+/CaMK dependent mechanism (Iwata, et al., 2007).

Despite not identifying the upstream activating mechanism within this system, this data provides clear evidence as to the influence of mechanical stretch in glucose uptake. Surprisingly, investigating the influence of mechanical stretch upon activating mitochondrial biogenesis has not been considered to date, despite evidence to suggest the activation of proteins that regulate this response to *in vitro* stretch (Atherton, et al., 2009, Iwata, et al., 2007).

The model used by Iwata and colleagues is however basic in nature, taking the form of monolayer culture and multi-axial stretch. This system therefore negates the influence of cell-matrix interaction with regards to stretch and moreover does not reflect the vector movement of SkM *in vivo*. This provides a rationale for investigating the effect of *in vitro* stretch on the metabolic parameters of SkM, using a model which more greatly recapitulates the *in vivo* environment.

It Chapter 2 it was demonstrated that intermittent cyclic stretch increased mtDNA content and increased the transcriptional response of key genes involved in mitochondrial biogenesis. This data illustrated the influence of mechanical signals in mediating this rapid transcriptional response. In seeking to understand the acute metabolic and the upstream protein mechanisms potentially involved in this outcome, the current investigation aimed to optimise, characterise and utilise methods to this effect.

Due to the novelty of the model presented in this thesis, it was essential to assess whether particular methods and assays were compatible and feasible for use and as such this chapter aims to present important progress towards this end.

8.1.2 Aims

1. To investigate and characterise the use of SDS-PAGE and Western Blotting to assess acute protein signalling mechanisms as a consequence of cyclic mechanical loading.

2. To analyse the acute metabolic biochemical response to cyclic mechanical loading, investigating aerobic and anaerobic pathways of ATP production.

8.1.3 Methods

For all cell culture procedures please refer to Materials and Methods 2.1. In order to investigate the acute protein signalling mechanisms associated with activating PGC-1α, it was necessary to develop a Western Blotting protocol.

8.1.3.1 Protein expression using Sodium Dodecyl sulphate Polyacrylamide Gel Electrophoresis (SDS-PAGE) and western blotting

The analysis of intra-cellular protein signalling using Western Blotting has become a key feature of many *in vitro*-based SkM experiments in recent years. Standard monolayer culture techniques allow for the high extraction yield of protein in order to use in Western Blotting, however tissue engineered constructs pose methodological limitations, with respect to a high content of extra-cellular protein (matrix and serum proteins). This limitation has resulted in few studies (especially in SkM) investigating protein signalling. Western Blot data has been published using Fibrin-based matrices (Huang, et al., 2005, Khodabukus and Baar, 2009, Khodabukus and Baar, 2012), however the cells in model have the ability to remodel the matrix to a greater extent than in collagen based constructs. This increases the cellular: extra-cellular content enabling increased protein extraction. A recent investigation has been published providing a method for extraction of cellular protein from collagen gels (Chen, et al., 2011), from which the following method is based.

8.1.3.2 Western Blotting Principle

Western Blotting is based upon the electrophoretic separation of negatively charged proteins, the blotting of those proteins onto a membrane and the immuno-detection of a protein of interest. A standard method for Western Blotting is described below.

8.1.3.3 Procedure

8.1.3.3.1 Protein Extraction

Passage 5 C2C12's were used and following experimentation, GM was removed from samples (either 2D monolayer cultures, or 3D collagen gels) and rinsed with PBS. 3D samples were removed from their glass chambers and placed in a 50ml tube. Samples were then subjected to 500µL of a lysis buffer containing 8M Urea and 1 % SDS in TBS (Chen, et al., 2011). In monolayer cultures, a pipette tip was used to scrape the bottom of the well to remove cells, before being transferred to a 50ml tube. All samples were then subjected to homogenisation using a stick homogeniser (Ika T10), with 30 second blasts until the tissue or cells were completely dissolved. Protein concentration was then determined using the Pierce 660nm protein assay.

8.1.3.3.2 SDS-PAGE

The Bio-Rad Mini Protean system was used for the separation of the proteins within the sample. Two gels were cast simultaneously. A 12 % resolving gel (6.7 ml dH_20, 8 ml 3 0% w/v acrylamide (Sigma-Aldrich, UK) 5 ml 1.5 M Tris HCl pH 8.8, 200 µL 1% SDS, 100µL Ammonium Persulphate (APS) and 10µL TEMED) and 4% stacking gel (6.05 ml dH_20, 1.3 ml 30 % w/v acrylamide (Sigma-Aldrich, UK) 2.5 ml 1M Tris HCl pH 6.8, 100 µL 1 % SDS, 50 µL Ammonium Persulphate (APS) and 10 µL TEMED) were cast into the glass plates. The plates were transferred to the running tank and running buffer (10x running buffer; 30.3 g Tris Base, 144 g Glycine, 10 g SDS and 1 L dH_20) was added to cover 5 cm above the top of the gels.

Samples were prepared with 25 µg of protein diluted 1:1 in sample buffer (4 ml dH_20, 1 ml 1M TRIS HCl pH 6.8, 800 µL Glycerol, 1.6 ml 1 0% w/v SDS, 400 µL 2-β-mercaptoethanol and 200 µL 0.05 % w/v bromophenol blue) in a 1.5 ml tube and boiled for 10 mins along with a molecular weight (MW) standard (BioRad, UK).

The MW standard and samples were loaded and the gels were run for 30-40 mins at 80 V or until the bromophenol blue dye was at the 'stack line'.

At this point the voltage was increased to 120 V until the bromophenol blue was evident at the bottom of the gel. For analytical purposes, the gels were sometimes stained with Coomassie Brilliant Blue to view the separated proteins. Gels stained with Coomassie are longer suitable for electrophoretic transfer and therefore were dried and scanned, using a ChemiDoc XRS (BioRad, UK) scanner for imaging. The migration front of each SDS-PAGE gel was recorded against the molecular weight markers to ensure that the particular proteins of interest corresponded to their respective molecular weight.

8.1.3.3.3 Transfer and Western Blotting

Gels were prepared for transfer by immersing in transfer buffer (3.02 g Tris Base, 14.4 g Glycine, 200 ml Methanol and 800 ml dH_20) and allowed to equilibrate for 10 mins at 4˚C. Gels were then prepared in the transfer cassette with Nitrocellulose membranes (manufacturer) for transfer. The cassettes were loaded into the Bio-Rad™ mini Trans-Blot unit filled with transfer buffer, for transfer at 100 V for 60 min.

8.1.3.3.4 Immunoblotting

Following transfer the membranes were immediately washed in wash buffer (TBST, TBS plus TWEEN 20) for 5 min on a rocker, before being blocked (0.4 g BSA in 10 ml TBS) for 60 min at 4˚C. Membranes were then washed 3 x 5 mins in wash buffer before the addition of the Primary Antibody for 2 hr at RT.

Following 3 x 5 min washes, the HRP conjugated Secondary Antibody was added for incubation at RT for 1 hr. Finally, the membranes were washed prior to detection.

8.1.3.3.5 Detection Using Enhanced Chemiluminescence (ECL)

Membranes were prepared protein side up on sheet of acetate film, for the addition of the ECL reagents (1ml per membrane, mixed 1:1 peroxidase buffer and detection reagent, Thermo Scientific, UK). Following 5 min incubation at RT the membranes were transferred to the Bio-Rad Chemi Doc system for the detection of protein bands. Membranes were placed protein side up and positioned in the centre of the detection plate. A live acquire exposure programme was generated on the associated Quantity One software, to take 10 images with 5 sec exposures over a 60 second sampling time.

8.1.3.3.6 Quantification

Band intensities were quantified using the Quantity One densitometric analysis functions. A rectangle was drawn around the largest visible band, with the rectangle surface area being repeated for all other bands, along with the labelling of a background area. Densitometric data was calculated based upon the volume intensity of each band minus the calculated background intensity. Data is presented as a relative abundance of the protein of interest, appropriately calibrated and normalised depending on the experiment.

8.1.4 Succinate dehydrogenase (SDH) activity assay

The activity of succinate dehydrogenase was measured following a previously published protocol.

8.1.4.1 Principle

Various methods have been used to analyse the activity of SDH within *in vivo* SkM biopsy samples, or within cultured cells. The most commonly utilised method for SDH activity analysis with *in vivo* samples is concerned with the staining of frozen cross sections. The quantification of the activity is based upon the staining intensity using a particular microscope filter. Limitations of this semi-quantitative method are evident, with the necessity for all microscope imaging settings being consistent between samples.

Alternative methodologies utilising spectrophomtetric measurements are based upon the increased extinction of a reaction buffer (commonly nitroblue tetrazolium, NBT) at a particular wavelength. The principle behind this procedure involves the progressive reduction of NBT by NAD to an insoluble coloured compound (NBT-diformazan; NBT-dfz) which is used as a reaction indicator at 500 nm (Powers, et al., 1993). This modified quantitative method has proven to be useful in analysing the SDH activity on muscle cells cultured *in vitro* (Yang, et al., 2002) and hence was chosen for use in this investigation.

8.1.4.2 Procedure

Protein was extracted from samples using a lysis buffer containing 8 M Urea and 1% SDS. Quantification of the protein concentration of the lysates was performed using a Bio Rad DC protein assay, following the manufactures instructions. 250 µL of each lysate was then added to 24- well plate with the addition of the 100 µL of the reaction buffer containing 0.1 M sodium succinate, 0.1 M sodium phosphate buffer, 0.01 M NBT and 0.1 M DMSO. Samples were then incubated at 37˚C for 30 min, with the final reaction reagent being measured on a nanovue spectrophotometer at 500 nm. The activity of SDH was displayed as OD/µg of extracted protein.

8.1.5 Creatine Kinase Assay

8.1.5.1 Principle

The measurement of CK activity has been performed for many years on blood serum samples and has formed a key method in the diagnosis and analysis on myocardial infarctions and particular myopathies (Dreyfus, et al., 1960, Scebat, et al., 1961). The measurement of CK activity has also be used to mark the differentiation of myoblasts into multinucleated myotubes (Auluck, et al., 2005), with the particular kit used here (Catachem Inc., Connecticut, NE, USA) being previously used in differentiated muscle cell C2 and C2C12 lysates (Sharples, et al., 2011, Sharples, et al., 2010).

The biochemical reactions that the assay is formulated upon follow the phosphagen system for generating ATP as described in the literature review. The production of glucose-6-phosphate (G-6-P) from the hexokinase (HK) reaction is oxidised in the presence of nicotinaminde adenine dinucleotide (NAD) which forms 6-phosphogluconate (6-PG), a reaction that is catalysed by G-6-P dehydrogenase (G-6-PDH). The reduction of NAD to NADH during this oxidation reaction results in the increase in absorbance at the emission at 340 nm, which can be measured spectrophotometrically. The reduction of NAD to NADH is proportional to the activity of CK is this assay.

CK

PCr + ADP ==> Creatine + ATP

HK

ATP + Glucose ==> ADP + G-6-P

G-6-PDH

G-6-P + NAD ==> 6-PG + NADH ==> Increased absorbance at 340 nm

Equation 2. **The biochemical reactions of the CK assay.** The reactions are displayed with the catalysing enzymes above the arrow .

8.1.5.2 Prodecure

The assay was set up on a 96 well UV plate (BD Biosciences, San Jose, CA, USA). The correct amount of aqueous reagent (reagent A) and reagent powder (reagent B) from the CK kit from Catachem, Inc. (Connecticut, NE, USA), needs to be correctly weighed and pipetted to ensure the efficiency of the reaction meets the manufacturers recommendations. This is of particular importance when using the formula to calculate CK activity which has been developed based upon certain amounts of reagent used. Following the manufactures instructions, 200 µL of the working enzymatic reagent is required for each sample.

4 µL of sample was pipetted into the 96 well plate, with each sample being ran in duplicate. Blank samples were also loaded containing 4 µL of lysis buffer containing 8 M Urea and 10 % SDS. 200 µL of the working CK reagent was added using a multichannel pipette as quick and efficiently as possible. The 96 well plate was inserted into Varioskan plate reader (Thermo-Fisher), where readings at 340 nm were taken every 30 secs for up to 10 mins. CK activity was calculated using the following equation based upon the difference in absorption at 340 nm at two different time-points. CK activity was measured from the same time-points for each sample to ensure satisfactory comparison. Enzymatic activity for CK was normalised to total protein content following the manufacturers recommendations.

$\Delta A.min^{-1}$ = (Time-point 2 – Time-point 1)/ (Measure time 1 – Measure time 2)

CK activity ($U.l^{-1}$) = ($\Delta A.min^{-1}$ x 0.204 x 1000)/ (6.22 x 0.004)

Where:

$\Delta A.min^{-1}$ = change in absorbance per minute at 340 nm

0.204 = total reaction volume

1000 = conversion to ml

6.22 = constant of millimolar absorptivity of NADH at 340 nm

0.004 = sample volume in ml

Equation 3. Calculation of Creatine Kinase Activity

8.1.6 Results

In order to assess the protein extraction efficiency of cellular collagen constructs for use with Western Blotting analysis, monolayer cultures, a-cellular constructs and cellular constructs were lysed to analyse protein concentration (Table 1). The apparent lower concentration of protein evident in the monolayer cultures compared to collagen constructs reflects the extra-cellular protein content with collagen constructs, in the form of collagen and media serum proteins. Data also revealed an interesting phenomenon, in that there was no difference in the protein isolated from cellular constructs compared to a-cellular constructs ($p = 0.78$), despite the addition of 12×10^6 cells.

This therefore demonstrates an inability of the cellular fraction of protein content to be efficiently isolated and purified from the extra-cellular content.

Table 6.1 ***Protein Extraction Characterisation.*** Concentration of protein (mg.mL) isolated from 3 independent cultures of monolayer, a-cellular and cellular experiments. All samples were run in triplicate on the same microplate and protein concentration was determined against known BSA standards diluted in lysis buffer. Data is presented as individual sample concentrations, mean values and SE.

n	Monolayer	A-Cellular	Cellular
1	0.93	2.53	1.92
2	1.15	2.22	2.22
3	0.93	1.75	2.16
Mean	**1.00**	**2.17**	**2.10**
SEM	0.17	0.31	0.20

Following the isolation of protein and the evident poor extraction of cellular protein in the cellular constructs, it was important to optimise and analyse the ability of the lysates to run on SDS-PAGE. Following the optimisation of the necessary voltage required to ensure even running of all the samples throughout the SDS-PAGE gel, samples from the monolayer, a-cellular and cellular lysates were loaded and ran on SDS-PAGE and stained with Coomassie Blue.

The electrophoresis of isolated proteins was successful, with clear separation of protein identified in the monolayer samples (Fig. 6-1. A, lanes 1 and 2). The heavy and irregular banding on the gel (highlighted by continuous box) in lanes 3, 4, 5 and 6 (a-cellular and cellular construct samples) is likely to be a combination of collagen protein and albumin contained within the media serum.

There is evidence for the electrophoresis of cellular protein in the cellular construct samples (Fig. 6-1. A, lanes 5 and 6, identified by the dotted highlighted box), since there is no evidence of protein in the a-cellular samples at the same molecular weight. Notwithstanding the identification of minimal isolated cellular protein from the total protein concentrations between a-cellular and cellular constructs, evidence suggests the successful electrophoresis of cellular protein.

Following the identification of positive electrophoresis in the cellular construct samples, it was important to assess the transfer of protein from the SDS-PAGE gel to a nitrocellulose membrane for immuno-blotting. Following electro-transfer, the membrane was stained for Ponceau S a reversible non-specific protein stain. Figure 6-1., B demonstrates the extent to which the protein can transfer to the membrane, with the monolayer samples (lanes 1 and 2) appearing to transfer to the greatest extent. The irregular region which is speculated to contain collagen and serum protein, also transfers to the membrane (lanes 3, 4, 5, and 6) with little evidence for abundant cellular protein present.

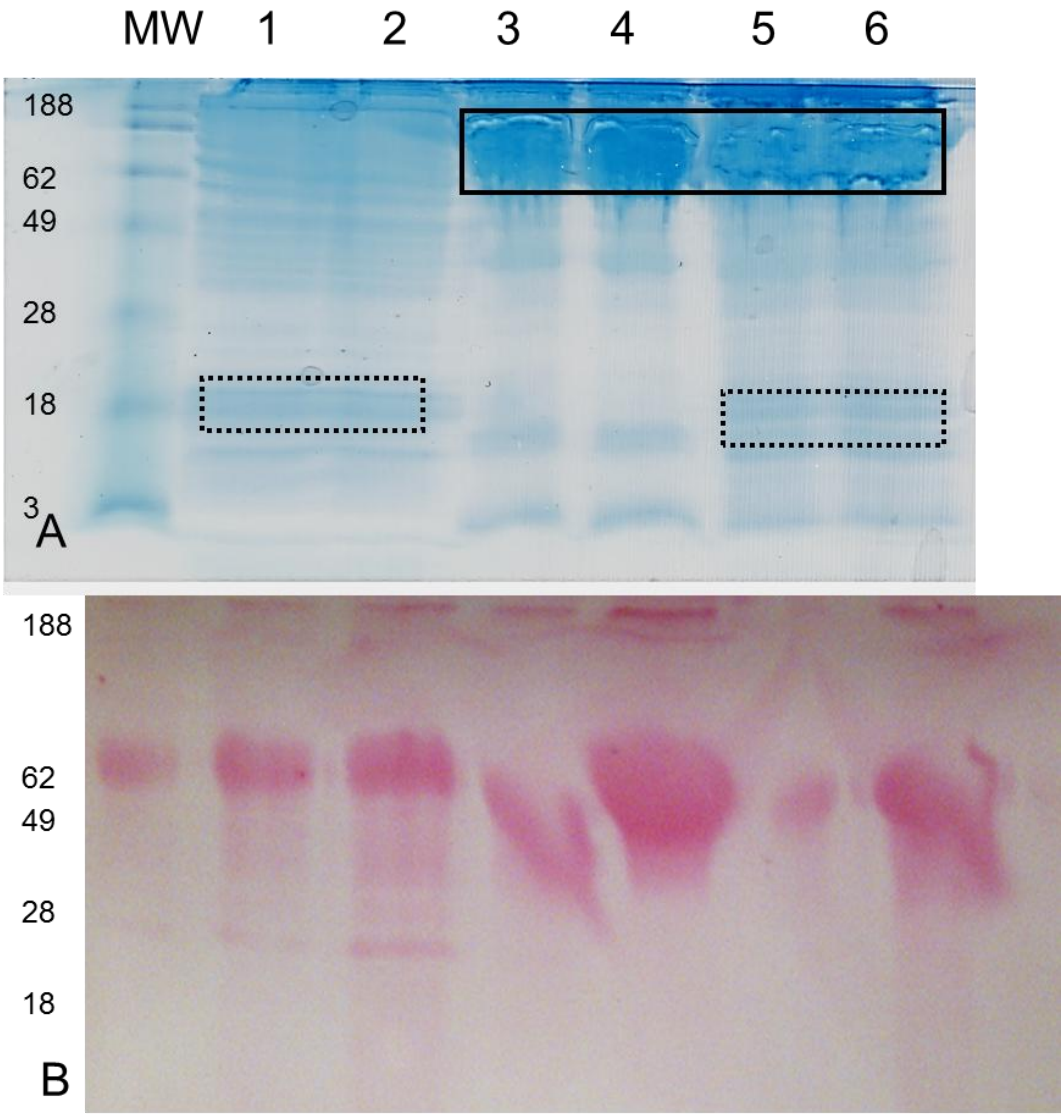

Figure 8-1 SDS-PAGE and Electro-transfer. A. SDS-PAGE gel stained with Coomassie Blue. MW = Molecular Weight marker. Lanes, 1 = monolayer culture sample 1, 2 = monolayer culture sample 2, 3 = a-cellular collagen construct sample 1, 4 = a-cellular collagen construct sample 2, 5 = cellular collagen construct sample 1, 6 = cellular collagen construct sample 2.

Following the transfer onto the nitrocellulose membrane it was important to evaluate whether immuno-blotting could be performed and in particular to assess the extent to which protein could be detected. The detection of β-Actin revealed a negative result for the a-cellular sample (Fig. 6-2., A, lane 1), with positive detection for cellular (lanes 2, 3 and 4) and monolayer (lanes 5, 6 and 7) samples confirming specificity of antibody detection at the correct molecular weight. In order to provide further evidence for the reduced cellular protein extraction from the cellular construct samples, the quantification of β-Actin was used. β-Actin is commonly used as a loading control protein, as it is a ubiquitously expressed cellular protein and has been demonstrated to reflect total cellular protein content. This analysis confirmed the significant reduced expression of β-Actin in construct samples compared to monolayer samples ($p = 0.0009$), suggesting the reduced content of cellular protein loaded in this condition. Despite this difference, the important observation was the positive detection in cellular construct samples, a finding which has proven difficult to achieve to date.

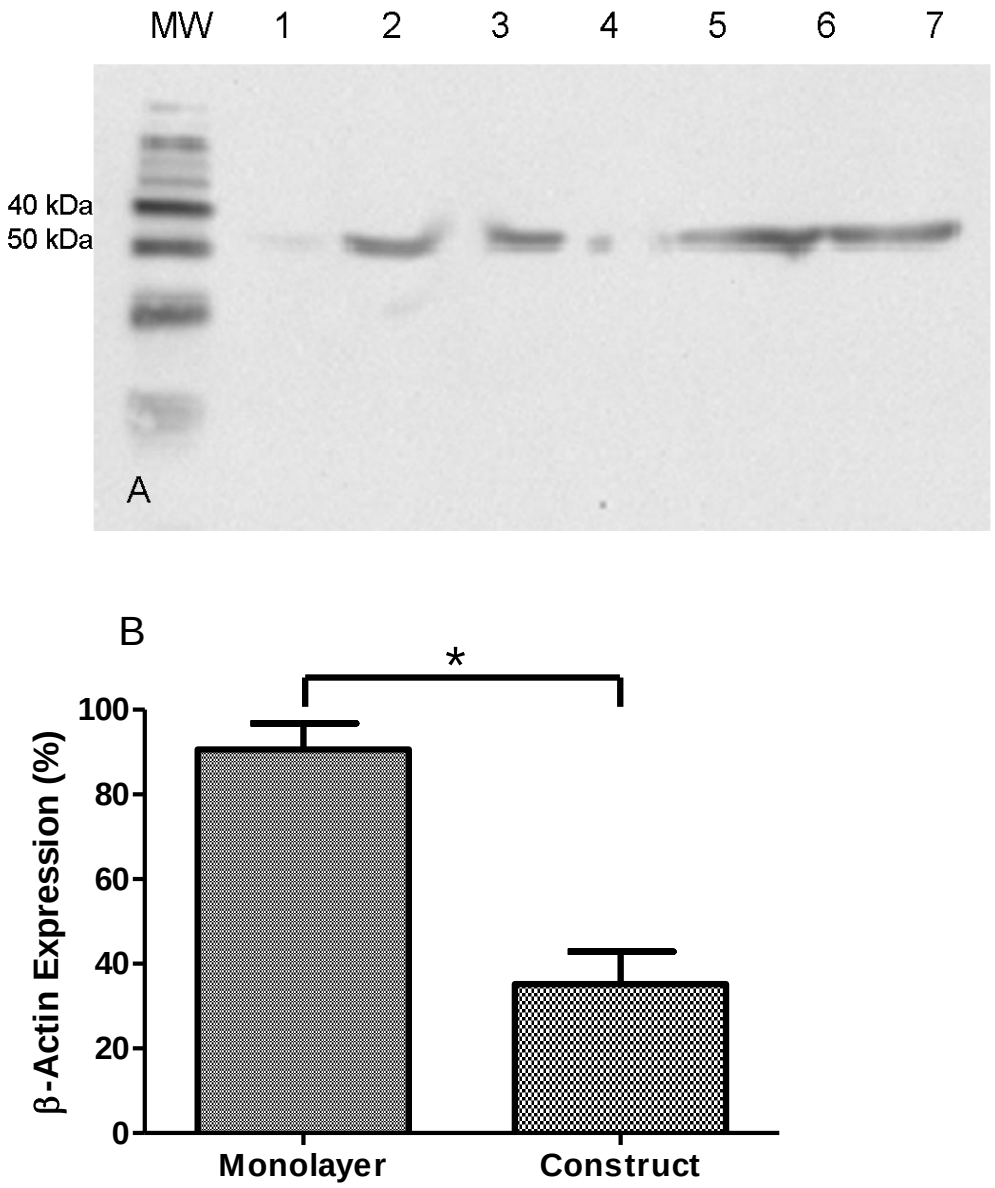

Figure 8-2 Western Blot for detection of β-Actin. A) Representative Western Blot for β-Actin. Lane 1 = a-cellular construct sample, lanes 2, 3 and 4 = cellular construct samples, lanes 5, 6 and 7 = monolayer samples. B) Densitometric quantification of β-Actin expression in monolayer and cellular construct samples. Data is presented as a mean ± SEM of duplicate samples across three separate Western Blots. Data is expressed as a % relative expression compared monolayer sample 1 replicate 1 in each run. *p = 0.0009.

In order to identify further if the cyclic stretch protocol was eliciting an acute biochemical stimulus as well as increasing the cellular metabolism rate above control, we aimed to characterise the activity of SDH as an indication of metabolic flux and Krebs' cycle activity.

Following a previous published method for analysing SDH activity in cell culture (Yang et al., 2002), analysis was performed on lysates MON1, MON2 and MON3 and also CT1, CT2 and CT3. The normalised SDH activity revealed a significant increase ($p = 0.0549$) in C samples (0.00022019 ± 0.005003) compared to M samples ($2.04461E\text{-}05 \pm 0.001481$, Fig. 6-3). Further, due to the activity being normalised to protein concentration, if the value was being normalised to only cellular protein within the cell construct samples the activity would be significantly greater. This data suggests in the basal state there is an increased metabolic flux associated with cells in a 3D environment compared to conventional monolayer culture. Moreover, this data demonstrates the use of this assay in identifying whether cyclic stretch of 3D constructs increases cellular aerobic metabolism.

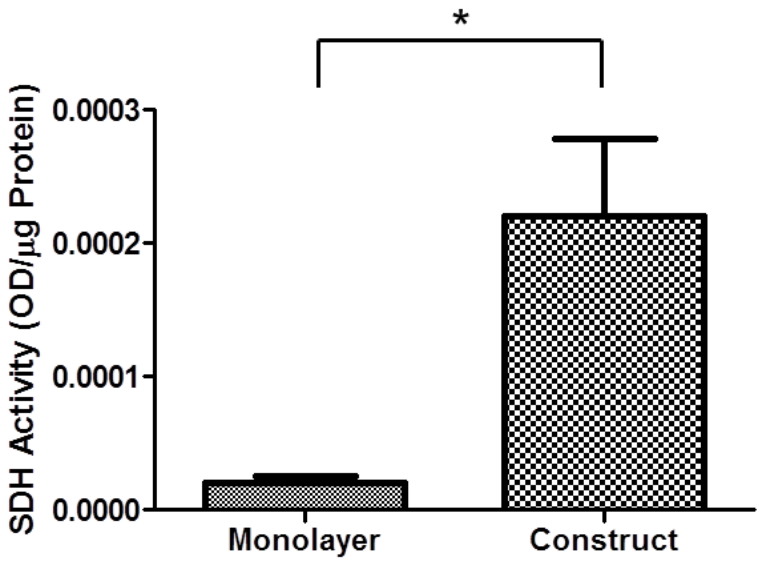

Figure 8-3. SDH activity between monolayer and cellular construct samples. Data is presented as mean ± SE of triplicate samples across two independent assays. Statistical analysis revealed a significant difference between conditions (p = .0549).

Following the characterisation and of the analytical procedures discussed previously an intermittent stretch protocol was performed as described in the chapter methods section (4.555). To provide a mechanistic rationale for an increase in PGC-1α mRNA, the analysis of pP38 MAPK (Tyr180/182) was performed. The phosphorylation of this residue has been demonstrated to activate phosphorylate and activate PGC-1α protein, which translates to the nucleus to auto-regulate the PGC-1α gene.

Figure 6-4 exhibits a representative Western Blot from CT and ST samples. This analysis unfortunately cannot provide the data required to inform upon the activation or suppression of pP38 MAPK (Tyr180/182) in the ST condition due to inconsistency in immuno-detection. The variation in band intensity and negative outcome in some samples seems likely to be due to the limited available cellular protein for antibody affinity.

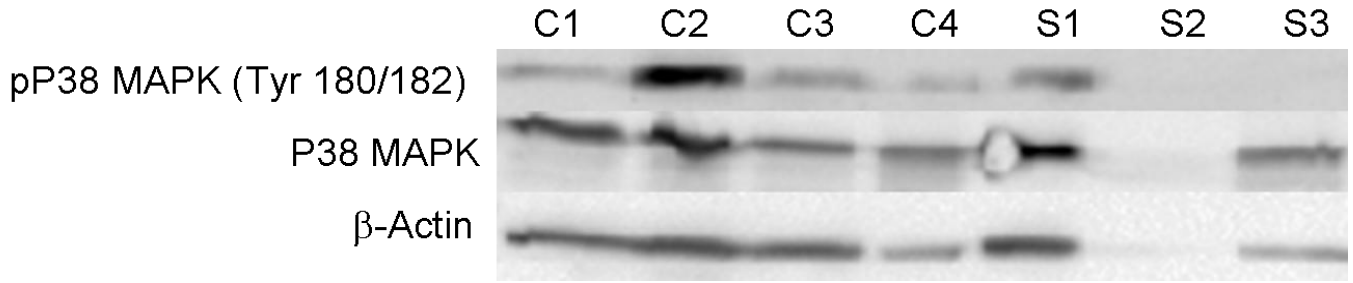

Figure 8-4. Representative Western Blots for pP38 MAPK (Tyr 180/182), Total P38 MAPK, and β-Actin. 'C' represents the control samples and 'S' represents the stretch samples. These representative blots were taken from two independent Western Blots.

Analysing SDH activity following stretch demonstrated no effect of SDH activity in ST (0.000809 ± 0.01567) compared to CT (0.000717 ± 0.007926, p = 0.88), suggesting no enhanced increase in Krebs' cycle activity. Despite a marginal increase, this data provides evidence that this mode of cyclic stretch in manipulating cellular metabolic activity, if further experiments were conducted and potentially for longer durations.

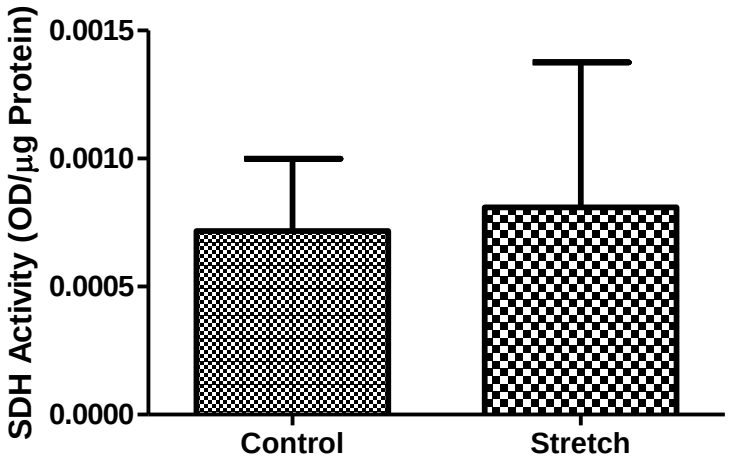

Figure 8-5. SDH Activity between Control and Intermittently Cyclic Stretched constructs. Data is represented as mean ± SEM for n = 4 CT samples and n = 3 ST samples. All sample assays were performed in duplicate and at the same time. Data is representative on two independent assays. Statistical analysis revealed a no significant difference between conditions (p = 0.88).

To further support the notion that cyclic stretch stimulates an intracellular metabolic response along with the stretch directly manipulating the structural components of the cell, the analysis of Creatine Kinase was performed. Measuring CK activity in both the conditioned media and construct lysates confirmed a mean increase between ST and CT samples. CK activity increased from 6.01 ± 0.98 in CT to 10.66 ± 1.63 in the conditioned media (Fig. 6-6. A, p = 0.516) indicative of an increased release of CK during the stretch programme.

This reflects the direct influence of the mechanical stretch upon the structural proteins of the muscle cells, providing evidence that the model employed here directly manipulates the cells with the matrix. Further, CK activity was found to be greater in the lysates of the ST condition (7.86 ± 0.97, Fig. 6-6. B) compared to CT (4.78 ± 0.93, p = 0.311). An increase in intracellular CK activity would provide additional support for the increase in metabolic activity from cyclic mechanical stretch.

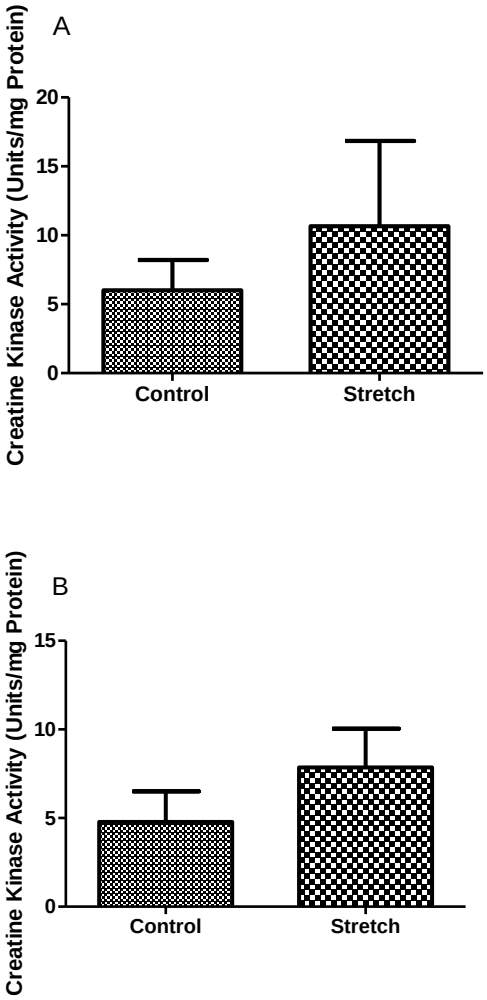

Figure 8-6. Creatine Kinase Activity between Control and Intermittently Cyclic Stretched constructs. A) Conditioned media analysis. B) Construct lysates analysis. Data is represented as mean ± SEM for n = 4 CT samples and n = 3 ST samples. All sample assays were performed in duplicate and at the same time. Data is representative on two independent assays.

8.1.7 Discussion

The aim of this chapter was to develop and utilise methods for the analysis of the acute biochemical and intra-cellular protein signalling responses to intermittent cyclic stretch. Through analysing these parameters, it was hypothesised that the mechanisms that underpinned the transcriptional response demonstrated in chapter 4 could be understood in greater detail.

8.1.7.1 The isolation of protein from collagen constructs reveals the limited extraction of cellular protein

The first important step in the analysis of intracellular metabolic reactions, along with protein signalling mechanisms is the high and consistent yield of protein following extraction. A study which has utilised a similar method to generate bio-engineered tissue to investigate cytomechanical forces successfully proposed an intra-cellular mediated mechanism for the main outcome measure (Chen, et al., 2011). The isolation of cellular protein to achieve positive and consistent Western Blot was clearly possible for this aforementioned experiment. However, it is important to consider the difference in cell type used between the current experiments and that performed by Chen et al., (2011). Fibroblasts (such as that used by Chen et al., 2011) have been demonstrated to have a distinct ability to attach, contract and remodel a collagen matrix (Brady, et al., 2008, Cheema, et al., 2003). In this respect it can be hypothesised that the ratio of cellular: matrix protein would be substantially greater in fibroblast seed collagen constructs compared to myogenic seeded constructs presented in this Thesis.

Tissue engineered SkM constructs using alternative matrix protein composition have the ability to isolate cellular protein for the investigation of contractile and intra-cellular signalling proteins (Khodabukus and Baar, 2009, Khodabukus and Baar, 2012). The extent of matrix remodelling within these models may reflect the ability to extract cellular protein however it is important to consider that these models do not represent *in vivo* SkM structure within respect to ECM structure, therefore negating for the influence of cell-matrix interaction within their experimental conditions.

8.1.7.2 Reduced and inconsistent expression of β-Actin in cellular constructs compared to monolayer samples

The detection of β-Actin was used to identify whether cellular protein could be successfully detected using Western Blotting. Quantification of the expression of β-Actin established a significant reduction in cellular constructs compared to monolayer samples. This further demonstrates the reduced cellular protein that can be effectively extracted from the cellular constructs. There was also a large variability in the expression of β-Actin, suggesting an inconsistency in the amount of cellular protein that was loaded. Additionally, the 'contaminating' influence of excess serum proteins and collagen may also contribute to reduced antibody-antigen interaction and thus may reflect the variations observed here (MacPhee, 2010, Gallagher, et al., 2001). Furthermore, considering the significant abundance of β-Actin within SkM samples (Lieber, et al., 2002), such inconsistency presents issues with regards to the comparability of samples from within a particular experimental condition. As Western Blotting is a semi-quantitative method for the analysis of protein expression, the consistency of protein loading between samples is extremely important (Spurway and Wackerhage, 2006).

8.1.7.3 Cellular constructs display increased SDH activity compared to monolayer samples

The activity of SDH, an enzyme complex of the Krebs' cycle has been investigated extensively within *in vivo* SkM. The activity of this enzyme has been demonstrated to reflect oxygen consumption (VO_2), when oxygen is not a rate limiting factor (Wust, et al., 2012).

Data presented here shows the increased activity of SDH in cellular constructs compared to monolayer samples, suggesting an increased aerobic metabolism of cells within a 3D environment. This finding is a logical one, with respect to the cells attachment and contraction of the matrix in a 3D environment requiring increased energy supply, compared to monolayer culture.

This data also provides further support of the use of 3D tissue engineered constructs compared to conventional monolayer culture to study muscle physiology, as the increased metabolic activity reflects the *in vivo* rate of SkM metabolism to a greater extent.

8.1.7.4 Methodological limitations prevent a mechanism of PGC-1α transcription from being presented

In order to investigate the mechanism whereby intermittent cyclic stretch increases the expression of PGC-1α mRNA, the activation of P38 MAPK was investigated using Western Blotting. P38 MAPK has been demonstrated to phosphorylate PGC-1α protein (Atherton, et al., 2005) which auto-regulates its own transcription (Scarpulla, 2002). Western Blotting for pP38 MAPK (Tyr 180/182) and total P38 MAPK exposed the inconsistent nature of using this method to investigate protein signalling within this model of SkM. Due to the apparent limited cellular protein that is extracted from cellular collagen constructs, the amount of protein of interest available for detection is low or present in varying amounts. This limitation has prevented the reliable and valid investigation into whether this key signalling mechanism is modulated following intermittent cyclic stretch.

Alternative methods for reliable detection of proteins of interest may serve as more appropriate methods for this analysis. Immuno-precipitation (IP) has been demonstrated to be effective in enriching the content of low abundant proteins compared to immuno-blotting of whole cell lysates (Trieu, et al., 2009). Additionally, Enzyme-Linked Immunosorbent Assays (ELISA's) also serve as a more precise method to detect proteins in low abundance (Alegria-Schaffer, et al., 2009). These methods may be more appropriate to investigate candidate signalling mechanisms within this model of SkM, where extracted cellular protein content is in low.

8.1.7.5 Increases in SDH and CK activity indicate a metabolic effect of intermittent cyclic stretch

Investigating the activity of SDH following stretch established the potential for an increase if the sample size was increased and also if the protocol was for a longer period. An increase would suggest the stretch protocol has the potential to increase in the metabolic flux through the Krebs' cycle and may therefore represent increased oxygen consumption. This is the first investigation to examine the effects of mechanical stretch upon the activity of SDH and provides evidence for the direct effect of mechanical perturbations of cell structure upon metabolic activity.

This finding has many implications for the understanding of the enhanced or impaired mitochondrial function witnessed in athletic and pathological population's respectively. It has been shown for many years that exercise can enhance aerobic capacity, which in part is due to increased mitochondrial function (Costill, et al., 1976, Foster, et al., 1978, Green, et al., 1980, Green and Narahara, 1980).

More recently, the impaired aerobic capacity and mitochondrial function associated with pathological conditions has been investigated. Such investigations have demonstrated the reduced activity of SDH, contributing to impaired ATP synthesis (Wust, et al., 2012)(Nagatomo, et al., 2012). Data presented here contributes to the understanding of mechanical signals in stimulating SDH activity, which provides novel evidence as to the enhanced or impaired SkM function in athletic and diseased populations. The increase in CK activity presented here provides evidence for the influence of the mechanical signal upon stimulating CK activity. The activity of CK is fundamental for the anaerobic synthesis of ATP through the utilisation of mitochondrial phosphor-Creatine (PCr, (Saks, 2008).

The increase in CK activity measured in the lysates following intermittent stretch provides evidence for the requirement of ATP synthesis from anaerobic sources, required to meet the energy demand of the cells in response to stretch. Moreover, this data supports the lactate data from chapter 4 further providing evidence that the mechano-stimulation causes a metabolic response within the myotubes.

The CK protein is bound to the M-Line of the sarcoplasmic reticulum of the myofibrils and the I-Band of the sarcomeres to provide ATP for actin-myosin interaction (Baird, et al., 2012). It is speculated to be released into the circulation following high specific force contractions and the loss of Ca^{2+} homoeostasis (Kendall and Eston, 2002). In this light, the detection of CK and CK activity within blood plasma has been used for many years as a marker of muscle damage, however the use of this marker has received much criticism due to the heterogeneity in response of individuals (Baird, et al., 2012). The increase in CK and CK activity in blood plasma has been postulated to reflect the tissue enzyme activity, with appearance in blood deemed to be a natural occurrence following regular SkM contraction (Thompson, et al., 2006). This evidence provides support that the increase in CK activity found within the conditioned media during the current investigation, may reflect an *in vivo*-like response to activation rather than muscle cell damage following mechano-stimulation.

8.1.8 Conclusions

Data presented in this chapter has demonstrated the isolation and characterisation of protein isolated from collagen SkM constructs. Methodological advancements were made with respect to the successful electrophoretic separation and electro-transfer of isolated proteins. Further, progress was made in the detection of intra-cellular proteins that regulate PGC-1α mRNA expression. Future experiments will seek to increase the sensitivity of protein detection in order to provide more definitive evidence as to the expression of these proteins of interest.

Of particular attention was the investigation of SDH and CK activity following intermittent cyclic stretch. Data provided further support that the mechano-stimulus is sufficient to induce a cellular metabolic response, supporting the lactate data presented in chapter 4. Future experiments should aim to explore the effect of manipulating the mechanical variables in order to investigate the contribution of aerobic and anaerobic metabolism. Moreover, the increased activity of the SDH complex warrants further experimentation to provide a model to study SkM aerobic metabolism *in vitro*.

8.2 Appendix 2

8.2.1 Statistical Analyses Summary

8.2.1.1 Statistical Analyses Chapter 3

8.2.1.1.1 Table 1 Normal Distribution Analysis

	Gel Width	Peak Force	RFD	RPF	PGC	MMP-9	Tfam	CytoC	COXII	Myog T/C	PGC-1a T/C
Normality test 1											
K2	0.9791	1.952	0.8877	1.396	N/A	N/A	N/A	N/A	N/A	6.345	3.142
P value	0.6129	0.3767	0.6416	0.4977						0.0419	0.2079
Passed normality test?	Yes	Yes	Yes	Yes						No	Yes
P value summary	ns	ns	ns	ns						*	ns
Normality test 2											
KS distance					0.1498	0.2399	0.3108	0.3711	0.239	0.1679	0.2665
P value					0.2	0.2	0.0718	0.0098	0.2	0.2	0.0184
Passed normality test?					Yes	Yes	Yes	No	Yes	Yes	No
P value summary					ns	ns	ns	**	ns	ns	*

See list of abreviations Page xii and Chapter 3 for details. T/C denotes Timecourse.

8.2.1.1.2CFM Data

Dependent Variable	(I) Condition	(J) Condition	Mean Difference (I-J)	Sig.	95% Confidence Interval	
					Lower Bound	Upper Bound
Peak_Force	1.00	2.00	115.68667	1.000	-835.3615	1066.7348
		3.00	-322.27000	1.000	-1273.3181	628.7781
		4.00	-231.37333	1.000	-1182.4215	719.6748
	2.00	1.00	-115.68667	1.000	-1066.7348	835.3615
		3.00	-437.95667	.887	-1389.0048	513.0915
		4.00	-347.06000	1.000	-1298.1081	603.9881
	3.00	1.00	322.27000	1.000	-628.7781	1273.3181
		2.00	437.95667	.887	-513.0915	1389.0048
		4.00	90.89667	1.000	-860.1515	1041.9448
	4.00	1.00	231.37333	1.000	-719.6748	1182.4215
		2.00	347.06000	1.000	-603.9881	1298.1081
		3.00	-90.89667	1.000	-1041.9448	860.1515
RFD	1.00	2.00	4.40667	.881	-5.1354	13.9487
		3.00	3.02333	1.000	-6.5187	12.5654
		4.00	-3.98333	1.000	-13.5254	5.5587
	2.00	1.00	-4.40667	.881	-13.9487	5.1354
		3.00	-1.38333	1.000	-10.9254	8.1587
		4.00	-8.39000	.094	-17.9321	1.1521

	3.00	1.00	-3.02333	1.000	-12.5654	6.5187
		2.00	1.38333	1.000	-8.1587	10.9254
		4.00	-7.00667	.204	-16.5487	2.5354
	4.00	1.00	3.98333	1.000	-5.5587	13.5254
		2.00	8.39000	.094	-1.1521	17.9321
		3.00	7.00667	.204	-2.5354	16.5487
Peak_Force_Relative	1.00	2.00	133.59056*	.029	13.3631	253.8180
		3.00	116.60481	.058	-3.6226	236.8322
		4.00	152.18306*	.014	31.9556	272.4105
	2.00	1.00	-133.59056*	.029	-253.8180	-13.3631
		3.00	-16.98574	1.000	-137.2132	103.2417
		4.00	18.59250	1.000	-101.6349	138.8199
	3.00	1.00	-116.60481	.058	-236.8322	3.6226
		2.00	16.98574	1.000	-103.2417	137.2132
		4.00	35.57824	1.000	-84.6492	155.8057
	4.00	1.00	-152.18306*	.014	-272.4105	-31.9556
		2.00	-18.59250	1.000	-138.8199	101.6349
		3.00	-35.57824	1.000	-155.8057	84.6492

8.2.1.1.3 Gel Width Timecourse

ANOVA

Gel_Width

	Sum of Squares	df	Mean Square	F	Sig.
Between Groups	30.320	4	7.580	17.436	.000
Within Groups	4.347	10	.435		
Total	34.667	14			

(I) Day	(J) Day	Mean Difference (I-J)	Sig.	95% Confidence Interval	
				Lower Bound	Upper Bound
1.00	3.00	1.56733*	.016	.3678	2.7668
	5.00	2.70167*	.001	1.5022	3.9012
	7.00	3.31767*	.000	2.1182	4.5172
	14.00	4.05700*	.000	2.8575	5.2565
3.00	1.00	-1.56733*	.016	-2.7668	-.3678
	5.00	1.13433	.061	-.0652	2.3338
	7.00	1.75033*	.009	.5508	2.9498
	14.00	2.48967*	.001	1.2902	3.6892
5.00	1.00	-2.70167*	.001	-3.9012	-1.5022
	3.00	-1.13433	.061	-2.3338	.0652
	7.00	.61600	.279	-.5835	1.8155
	14.00	1.35533*	.031	.1558	2.5548
7.00	1.00	-3.31767*	.000	-4.5172	-2.1182
	3.00	-1.75033*	.009	-2.9498	-.5508
	5.00	-.61600	.279	-1.8155	.5835
	14.00	.73933	.200	-.4602	1.9388
14.00	1.00	-4.05700*	.000	-5.2565	-2.8575
	3.00	-2.48967*	.001	-3.6892	-1.2902
	5.00	-1.35533*	.031	-2.5548	-.1558
	7.00	-.73933	.200	-1.9388	.4602

8.2.1.1.4 Myogenin Timecourse Data

ANOVA

Myogenin

	Sum of Squares	df	Mean Square	F	Sig.
Between Groups	5761421.871	3	1920473.957	3.021	.072
Within Groups	7627643.443	12	635636.954		
Total	13389065.314	15			

8.2.1.1.5 PGC-1 Timecourse Data

ANOVA

Expression

	Sum of Squares	df	Mean Square	F	Sig.
Between Groups	.899	3	.300	3.186	.132
Within Groups	1.129	12	.094		
Total	2.028	15			

8.2.1.1.6 Bowing CT Data

8.2.1.1.6.1 Regression- Myogenin CT

Variables Entered/Removed[b]

Model	Variables Entered	Variables Removed	Method
1	Gel_Width[a]	.	Enter

a. All requested variables entered.

b. Dependent Variable: Myogenin

Model Summary[b]

Model	R	R Square	Adjusted R Square	Std. Error of the Estimate
1	.631[a]	.40	.312	1.87413

a. Predictors: (Constant), Gel_Width

b. Dependent Variable: Myogenin

ANOVA[b]

Model		Sum of Squares	df	Mean Square	F	Sig.
1	Regression	16.268	1	16.268	4.632	.068[a]
	Residual	24.586	7	3.512		
	Total	40.854	8			

Model Summary[b]

Model	R	R Square	Adjusted R Square	Std. Error of the Estimate
1	.631[a]	.40	.312	1.87413

a. Predictors: (Constant), Gel_Width

b. Dependent Variable: Myogenin

Coefficients[a]

Model		Unstandardized Coefficients		Standardized Coefficients	t	Sig.	Collinearity Statistics	
		B	Std. Error	Beta			Tolerance	VIF
1	(Constant)	14.603	2.398		6.090	.000		
	Gel_Width	3.998	1.858	.631	2.152	.068	1.000	1.000

a. Dependent Variable: Myogenin

Collinearity Diagnostics[a]

Model	Dimension	Eigenvalue	Condition Index	Variance Proportions	
				(Constant)	Gel_Width
1	1	1.965	1.000	.02	.02
	2	.035	7.544	.98	.98

a. Dependent Variable: Myogenin

Residuals Statistics[a]

	Minimum	Maximum	Mean	Std. Deviation	N
Predicted Value	17.8852	21.5191	19.5856	1.42600	9
Residual	-2.49925	2.20094	.00000	1.75309	9
Std. Predicted Value	-1.192	1.356	.000	1.000	9
Std. Residual	-1.334	1.174	.000	.935	9

a. Dependent Variable: Myogenin

8.2.1.1.6.1.1 Charts

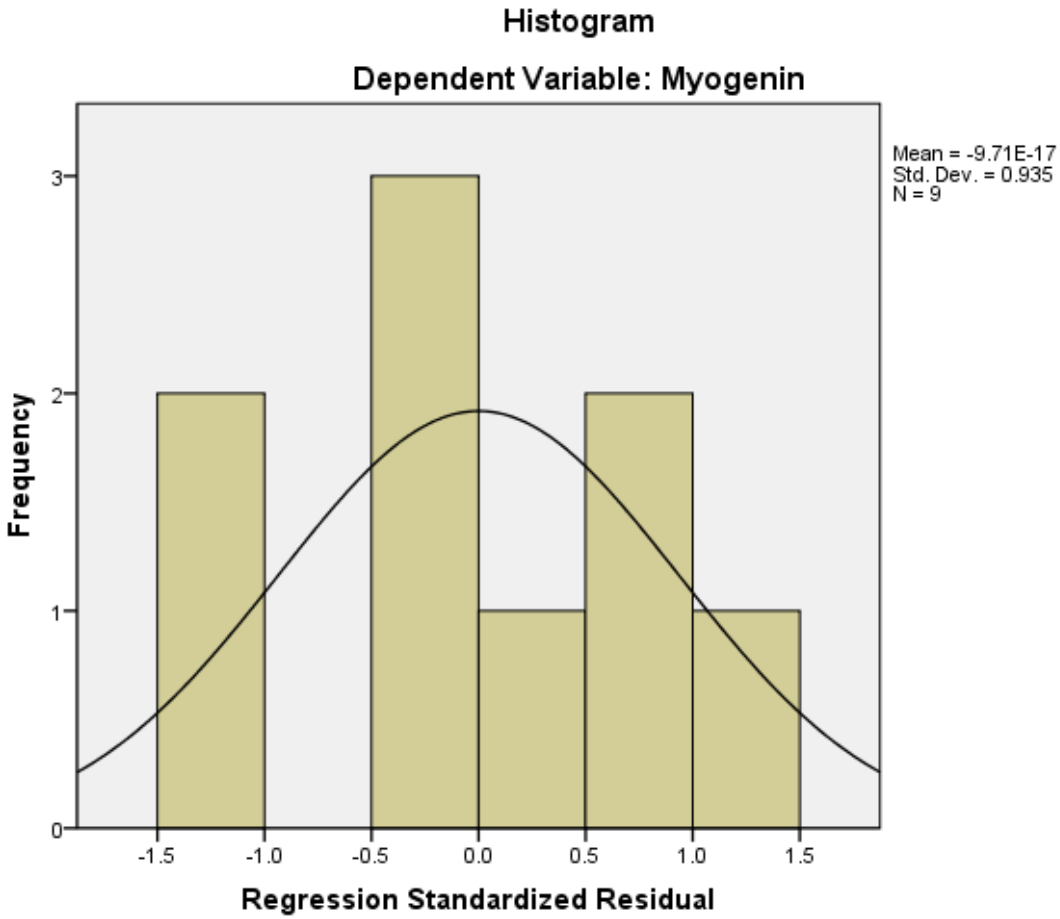

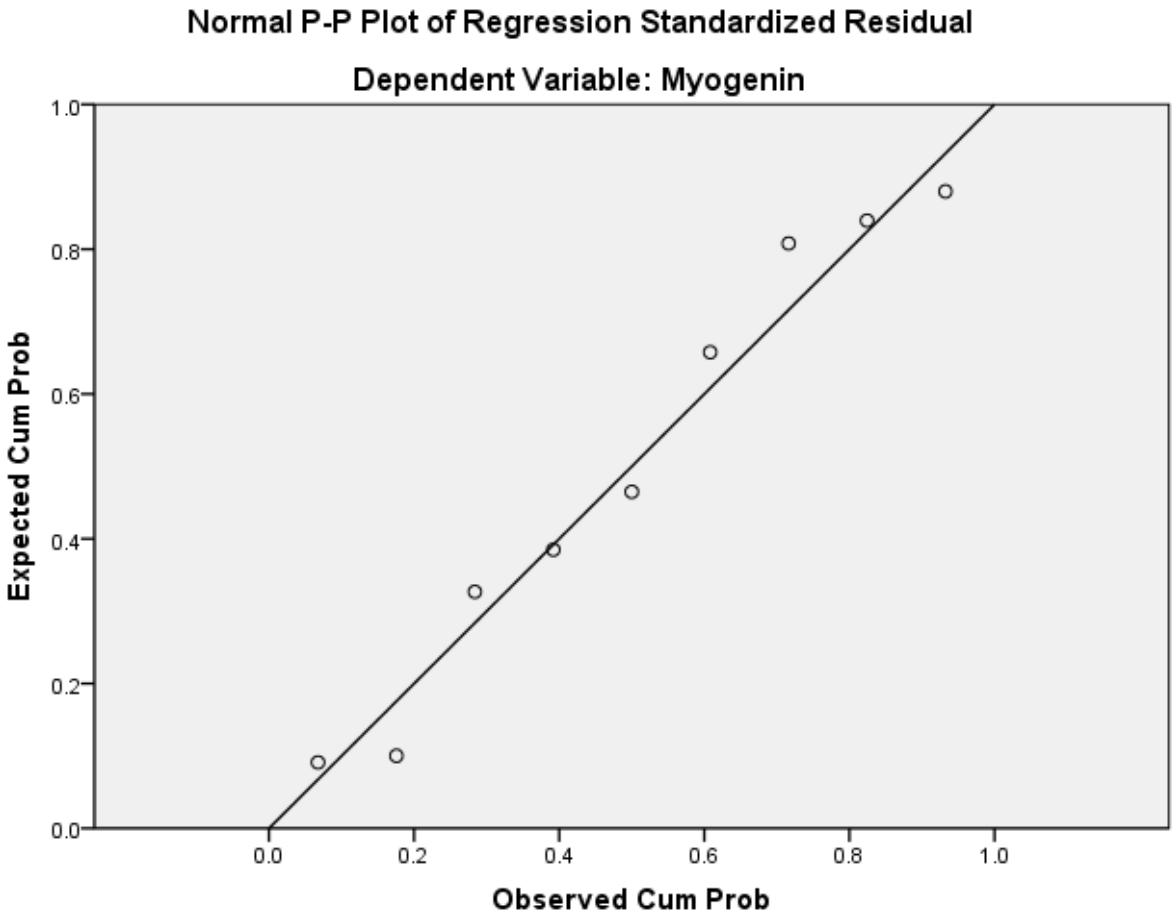
Normal P-P Plot of Regression Standardized Residual
Dependent Variable: Myogenin
Expected Cum Prob
Observed Cum Prob
0.0
0.2
0.4
0.6
0.8
1.0

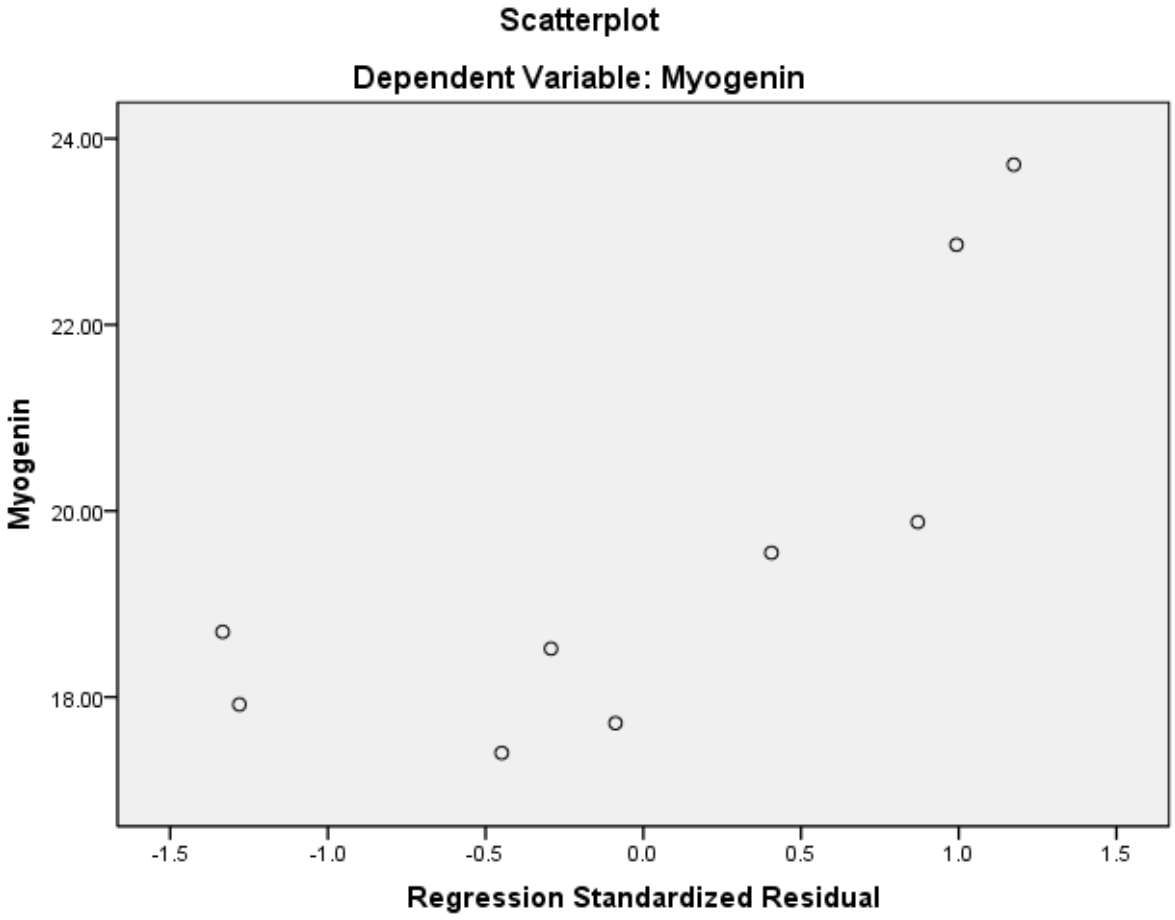
Scatterplot
Dependent Variable: Myogenin
Myogenin
24.00
22.00
20.00
18.00
-1.5
-1.0
-0.5
0.0
0.5
1.0
1.5
Regression Standardized Residual

8.2.1.1.6.2 Regression- RNA Concentration

Variables Entered/Removed[b]

Model	Variables Entered	Variables Removed	Method
1	Gel_Width[a]	.	Enter

a. All requested variables entered.

b. Dependent Variable: RNA

Model Summary[b]

Model	R	R Square	Adjusted R Square	Std. Error of the Estimate
1	.883[a]	.779	.751	83.18747

a. Predictors: (Constant), Gel_Width

b. Dependent Variable: RNA

ANOVA[b]

Model		Sum of Squares	df	Mean Square	F	Sig.
1	Regression	194953.539	1	194953.539	28.172	.000[a]
	Residual	55361.246	8	6920.156		
	Total	250314.785	9			

Model Summary[b]

Model	R	R Square	Adjusted R Square	Std. Error of the Estimate
1	.883[a]	.779	.751	83.18747

a. Predictors: (Constant), Gel_Width

b. Dependent Variable: RNA

Coefficients[a]

Model		Unstandardized Coefficients		Standardized Coefficients	t	Sig.	Collinearity Statistics	
		B	Std. Error	Beta			Tolerance	VIF
1	(Constant)	756.831	106.413		7.112	.000		
	Gel_Width	-435.144	81.983	-.883	-5.308	.001	1.000	1.000

a. Dependent Variable: RNA

Collinearity Diagnostics[a]

Model	Dimension	Eigenvalue	Condition Index	Variance Proportions	
				(Constant)	Gel_Width
1	1	1.969	1.000	.02	.02
	2	.031	7.965	.98	.98

Coefficients[a]

Model		Unstandardized Coefficients		Standardized Coefficients	t	Sig.	Collinearity Statistics	
		B	Std. Error	Beta			Tolerance	VIF
1	(Constant)	756.831	106.413		7.112	.000		
	Gel_Width	-435.144	81.983	-.883	-5.308	.001	1.000	1.000

a. Dependent Variable: RNA

Residuals Statistics[a]

	Minimum	Maximum	Mean	Std. Deviation	N
Predicted Value	4.0313	399.5775	209.5500	147.17848	10
Residual	-151.53473	110.02058	.00000	78.42990	10
Std. Predicted Value	-1.396	1.291	.000	1.000	10
Std. Residual	-1.822	1.323	.000	.943	10

a. Dependent Variable: RNA

8.2.1.1.6.2.1 Charts

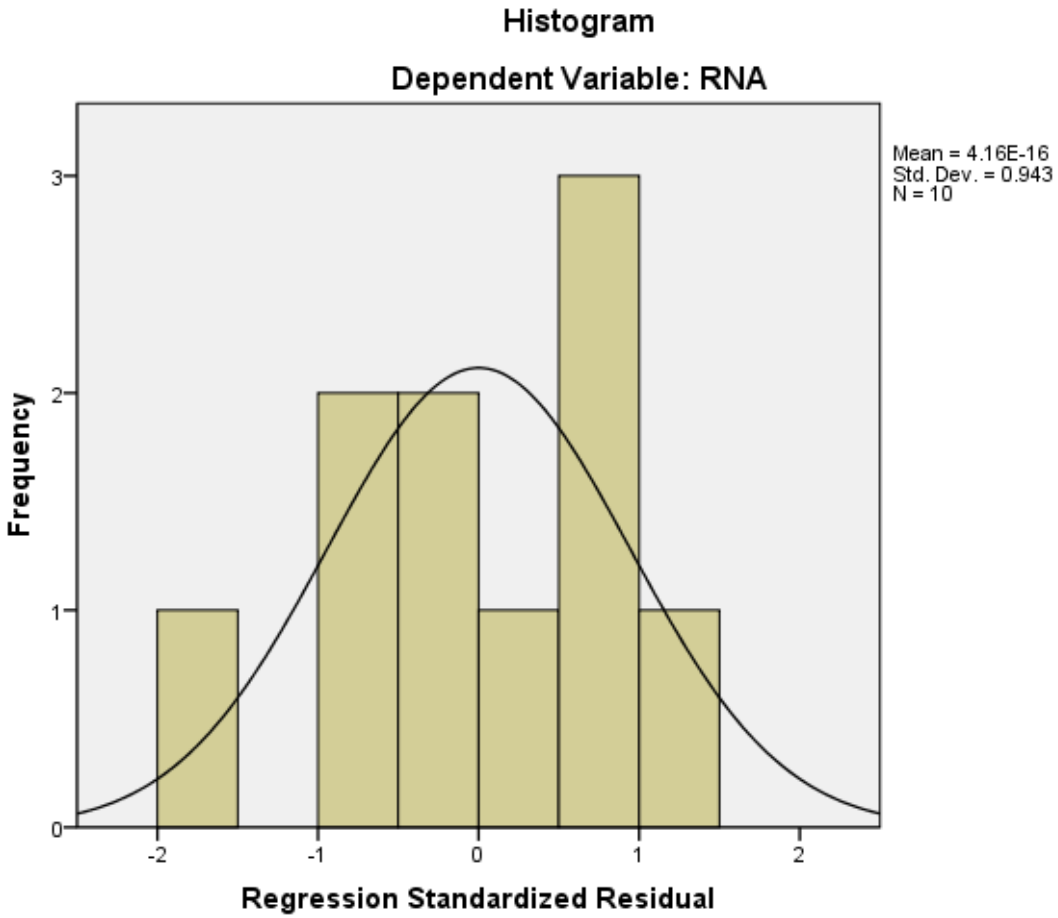

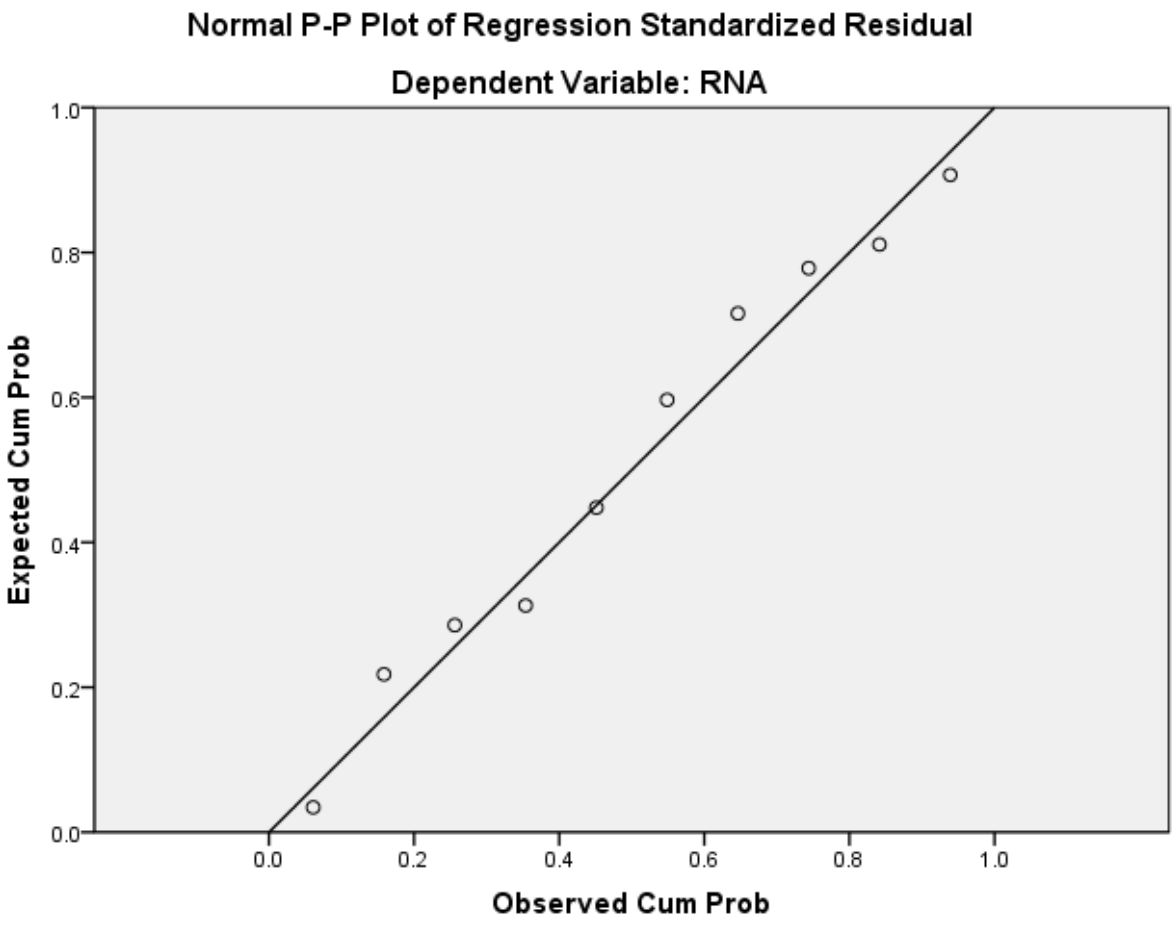
Normal P-P Plot of Regression Standardized Residual
Dependent Variable: RNA
Expected Cum Prob
Observed Cum Prob
0.0
0.2
0.4
0.6
0.8
1.0

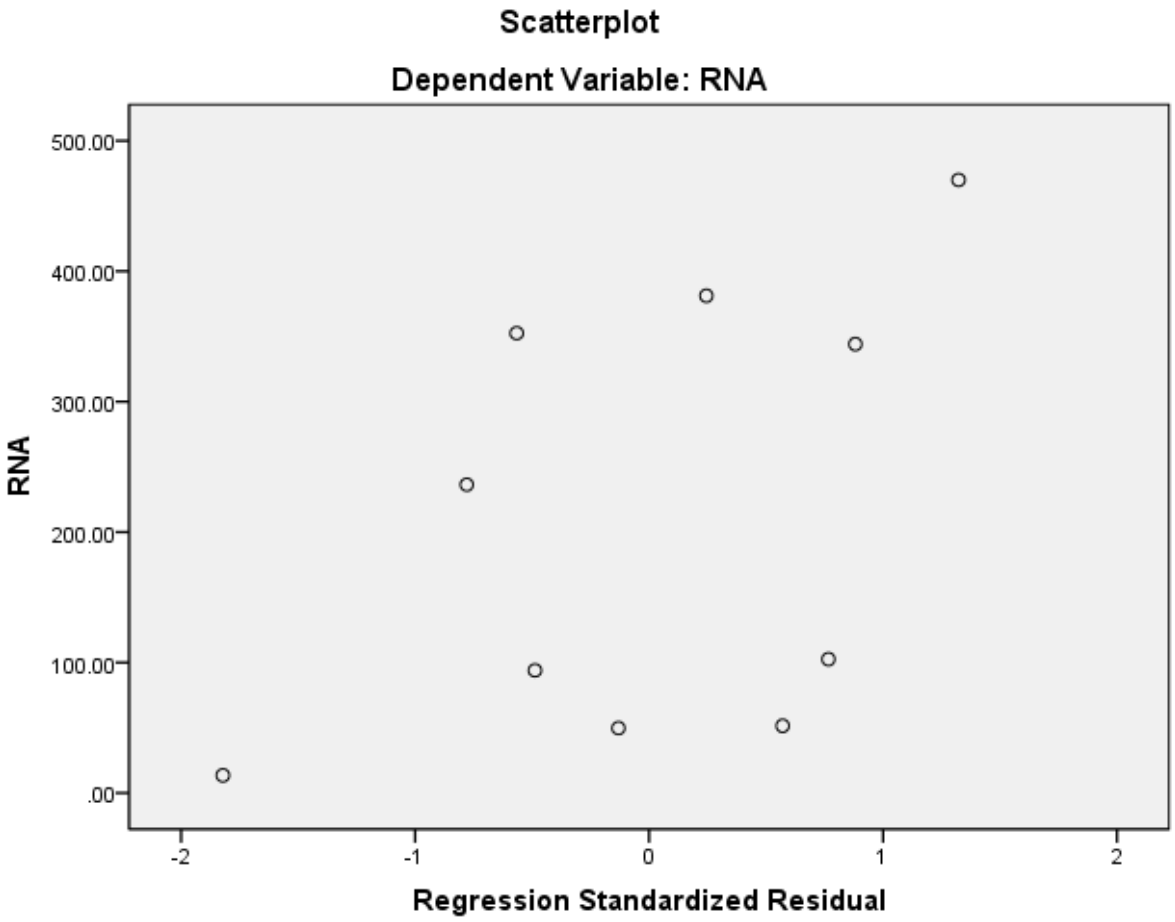
Scatterplot
Dependent Variable: RNA
500.00
400.00
300.00
200.00
100.00
.00
RNA
-2
-1
0
1
2
Regression Standardized Residual

8.2.1.1.6.3 Regression- RPII CT

Variables Entered/Removed[b]

Model	Variables Entered	Variables Removed	Method
1	Gel_Width[a]	.	Enter

a. All requested variables entered.

b. Dependent Variable: RPII

Model Summary[b]

Model	R	R Square	Adjusted R Square	Std. Error of the Estimate
1	.972[a]	.945	.937	1.26267

a. Predictors: (Constant), Gel_Width

b. Dependent Variable: RPII

ANOVA[b]

Model		Sum of Squares	df	Mean Square	F	Sig.
1	Regression	190.835	1	190.835	119.696	.000[a]

	Residual	11.160	7	1.594		
	Total	201.995	8			

a. Predictors: (Constant), Gel_Width

b. Dependent Variable: RPII

Coefficients[a]

Model		Unstandardized Coefficients		Standardized Coefficients	t	Sig.	Collinearity Statistics	
		B	Std. Error	Beta			Tolerance	VIF
1	(Constant)	3.593	1.616		2.224	.062		
	Gel_Width	13.692	1.251	.972	10.941	.000	1.000	1.000

a. Dependent Variable: RPII

Collinearity Diagnostics[a]

Model	Dimension	Eigenvalue	Condition Index	Variance Proportions	
				(Constant)	Gel_Width
1	1	1.965	1.000	.02	.02
	2	.035	7.544	.98	.98

a. Dependent Variable: RPII

Residuals Statistics[a]

	Minimum	Maximum	Mean	Std. Deviation	N

Predicted Value	14.8342	27.2801	20.6578	4.88409	9
Residual	-1.85696	1.93748	.00000	1.18112	9
Std. Predicted Value	-1.192	1.356	.000	1.000	9
Std. Residual	-1.471	1.534	.000	.935	9

a. Dependent Variable: RPII

8.2.1.1.6.3.1 Charts

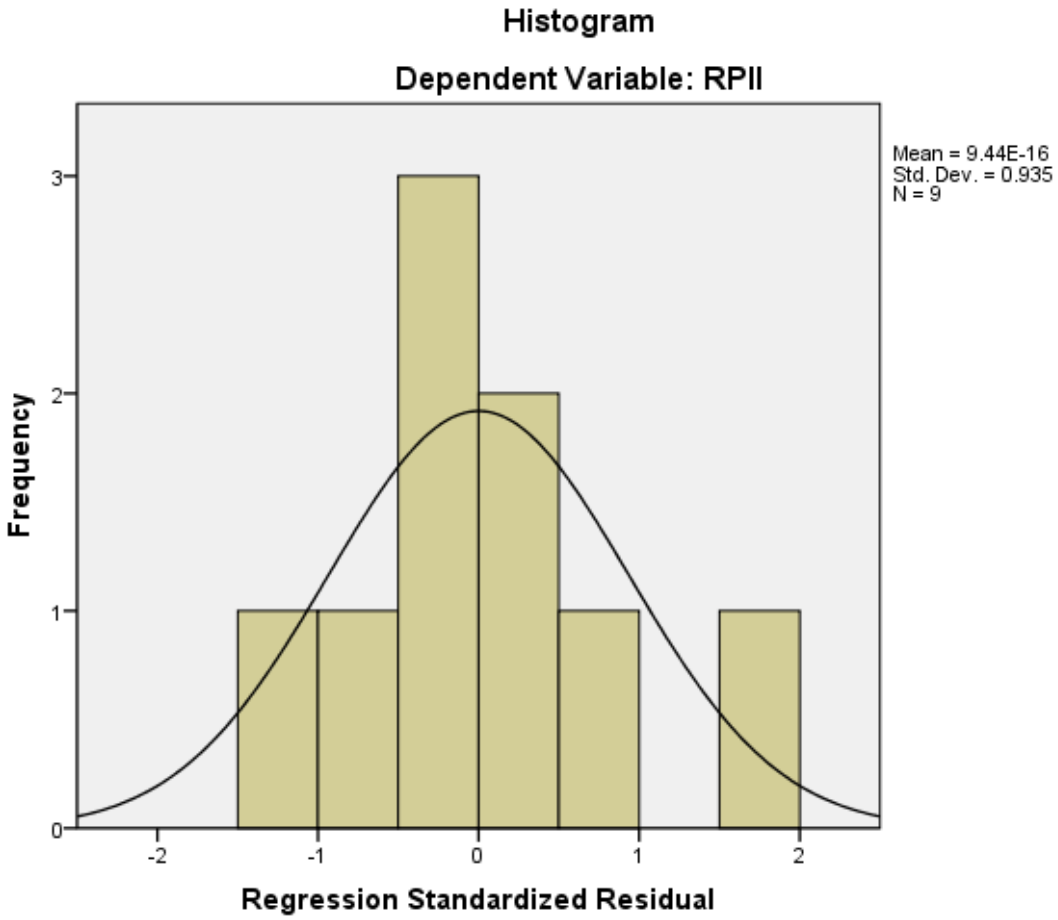

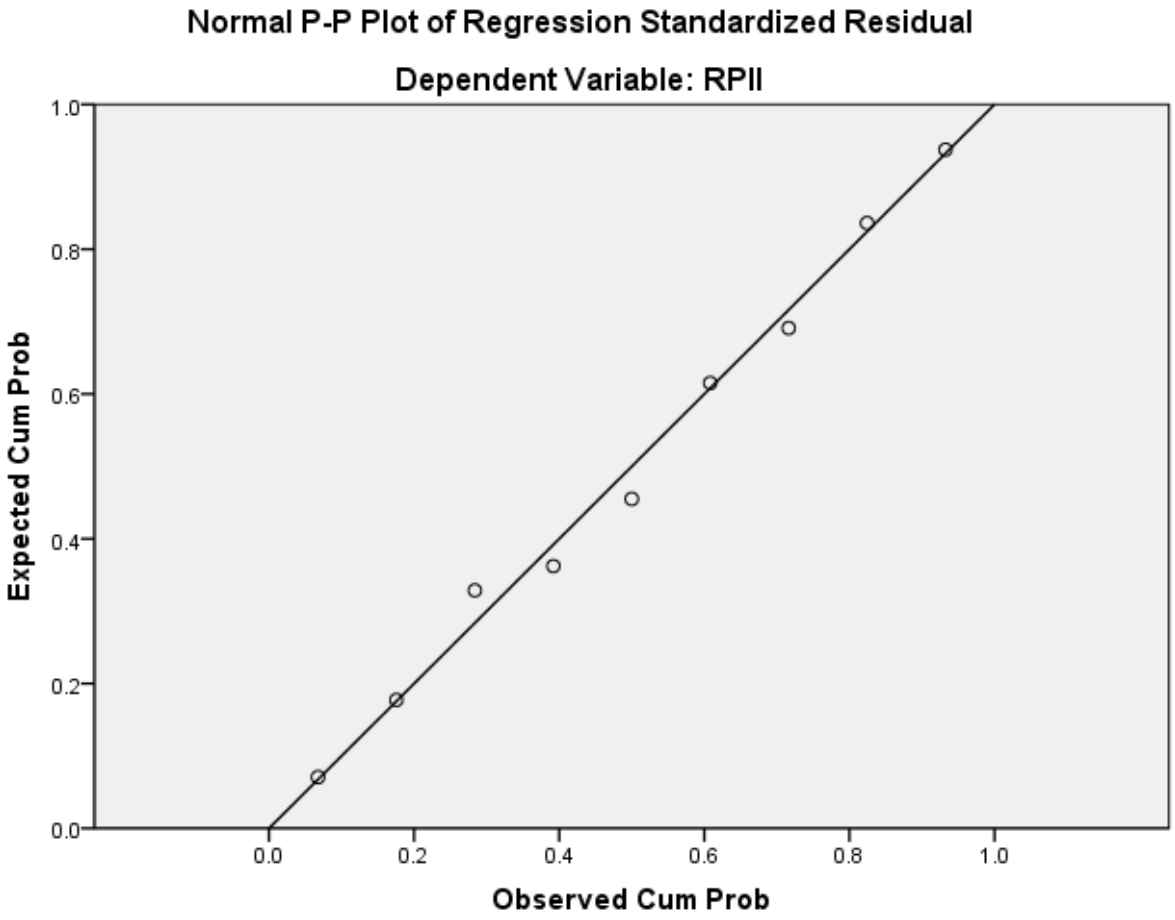
Normal P-P Plot of Regression Standardized Residual
Dependent Variable: RPII
Expected Cum Prob
Observed Cum Prob
0.0
0.2
0.4
0.6
0.8
1.0

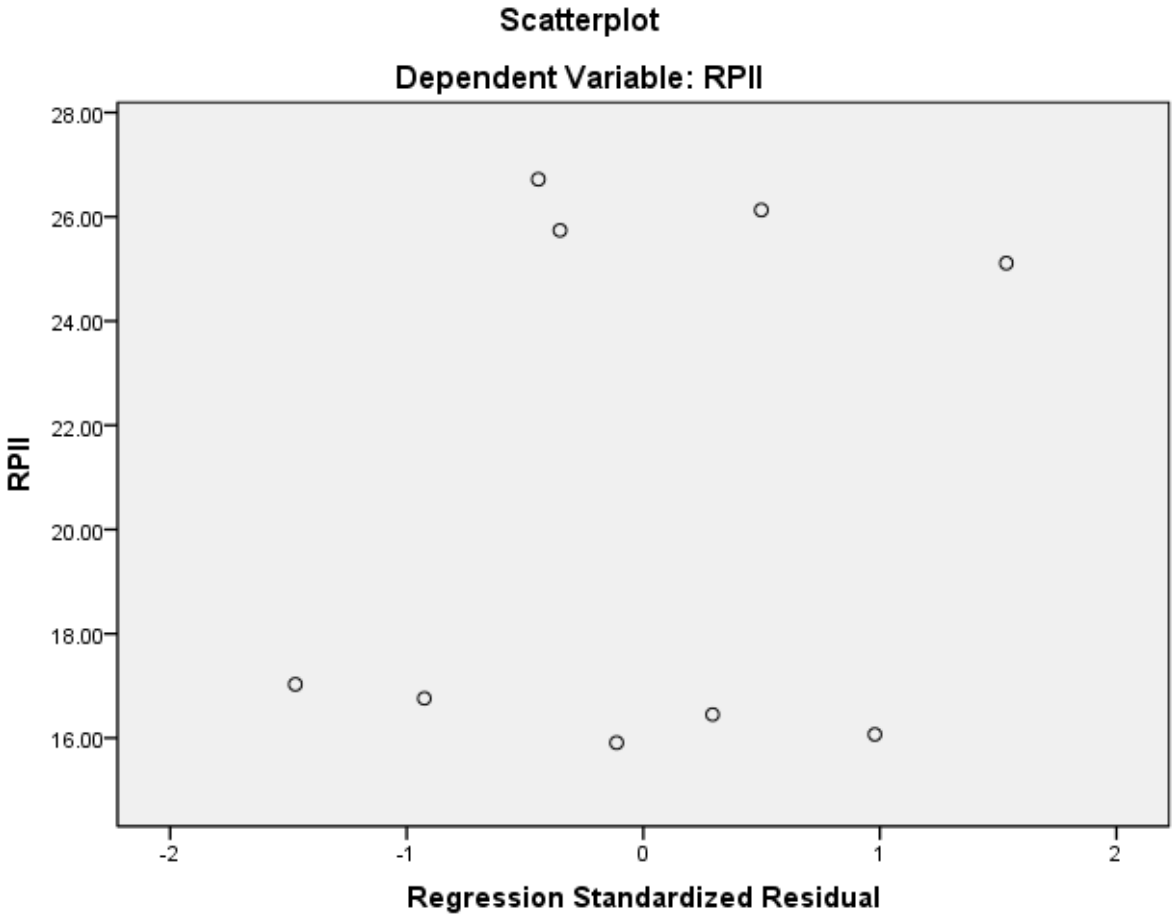
Scatterplot
Dependent Variable: RPII
28.00
26.00
24.00
22.00
20.00
18.00
16.00
RPII
-2
-1
0
1
2
Regression Standardized Residual

8.2.1.1.6.4 Regression- IGF-I CT

Variables Entered/Removed[b]

Model	Variables Entered	Variables Removed	Method
1	Gel_Width[a]	.	Enter

a. All requested variables entered.

b. Dependent Variable: IGF

Model Summary[b]

Model	R	R Square	Adjusted R Square	Std. Error of the Estimate
1	.678[a]	.459	.382	2.53363

a. Predictors: (Constant), Gel_Width

b. Dependent Variable: IGF

ANOVA[b]

Model		Sum of Squares	df	Mean Square	F	Sig.
1	Regression	38.127	1	38.127	5.939	.045[a]
	Residual	44.935	7	6.419		
	Total	83.062	8			

ANOVA[b]

Model		Sum of Squares	df	Mean Square	F	Sig.
1	Regression	38.127	1	38.127	5.939	.045[a]
	Residual	44.935	7	6.419		
	Total	83.062	8			

a. Predictors: (Constant), Gel_Width

b. Dependent Variable: IGF

Coefficients[a]

Model		Unstandardized Coefficients		Standardized Coefficients	t	Sig.	Collinearity Statistics	
		B	Std. Error	Beta			Tolerance	VIF
1	(Constant)	14.762	3.242		4.554	.003		
	Gel_Width	6.120	2.511	.678	2.437	.045	1.000	1.000

a. Dependent Variable: IGF

Collinearity Diagnostics[a]

Model	Dimension	Eigenvalue	Condition Index	Variance Proportions	
				(Constant)	Gel_Width
1	1	1.965	1.000	.02	.02
	2	.035	7.544	.98	.98

ANOVA[b]

Model		Sum of Squares	df	Mean Square	F	Sig.
1	Regression	38.127	1	38.127	5.939	.045[a]
	Residual	44.935	7	6.419		
	Total	83.062	8			

a. Dependent Variable: IGF

Residuals Statistics[a]

	Minimum	Maximum	Mean	Std. Deviation	N
Predicted Value	19.7870	25.3500	22.3900	2.18309	9
Residual	-4.78164	2.21996	.00000	2.36999	9
Std. Predicted Value	-1.192	1.356	.000	1.000	9
Std. Residual	-1.887	.876	.000	.935	9

a. Dependent Variable: IGF

8.2.1.1.6.4.1 Charts

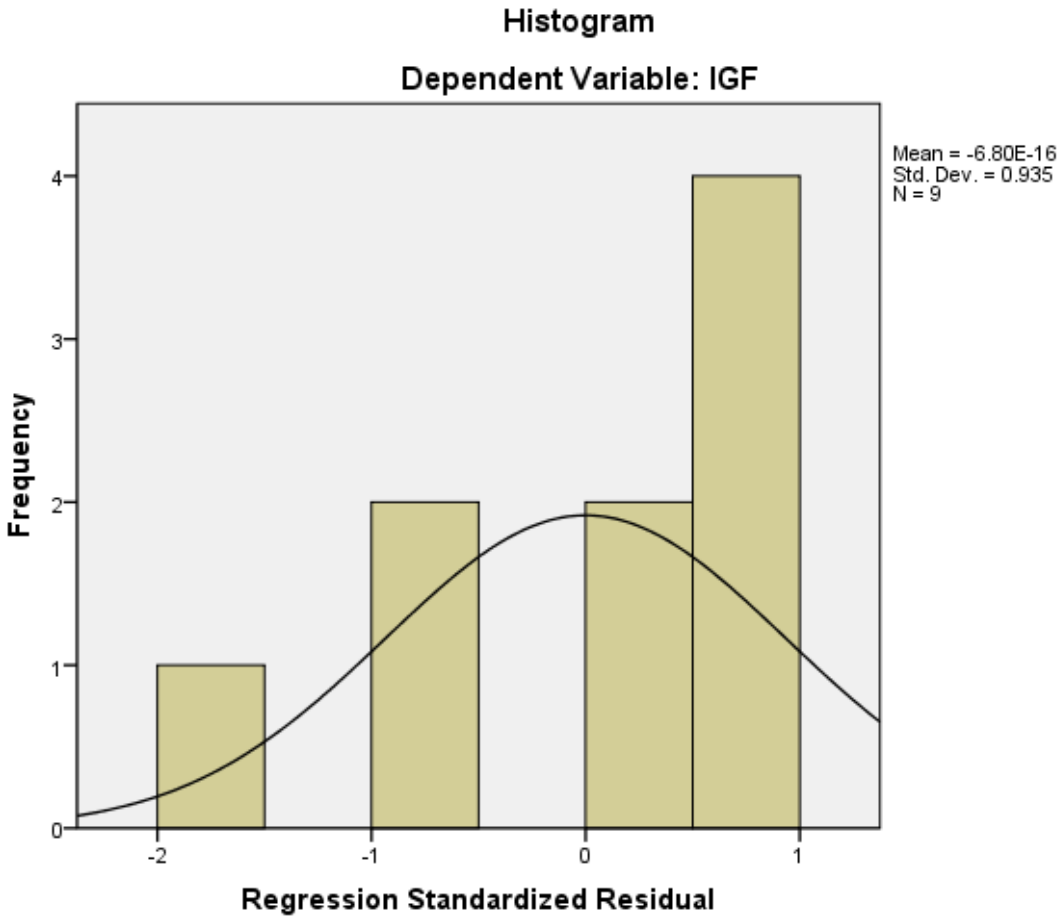

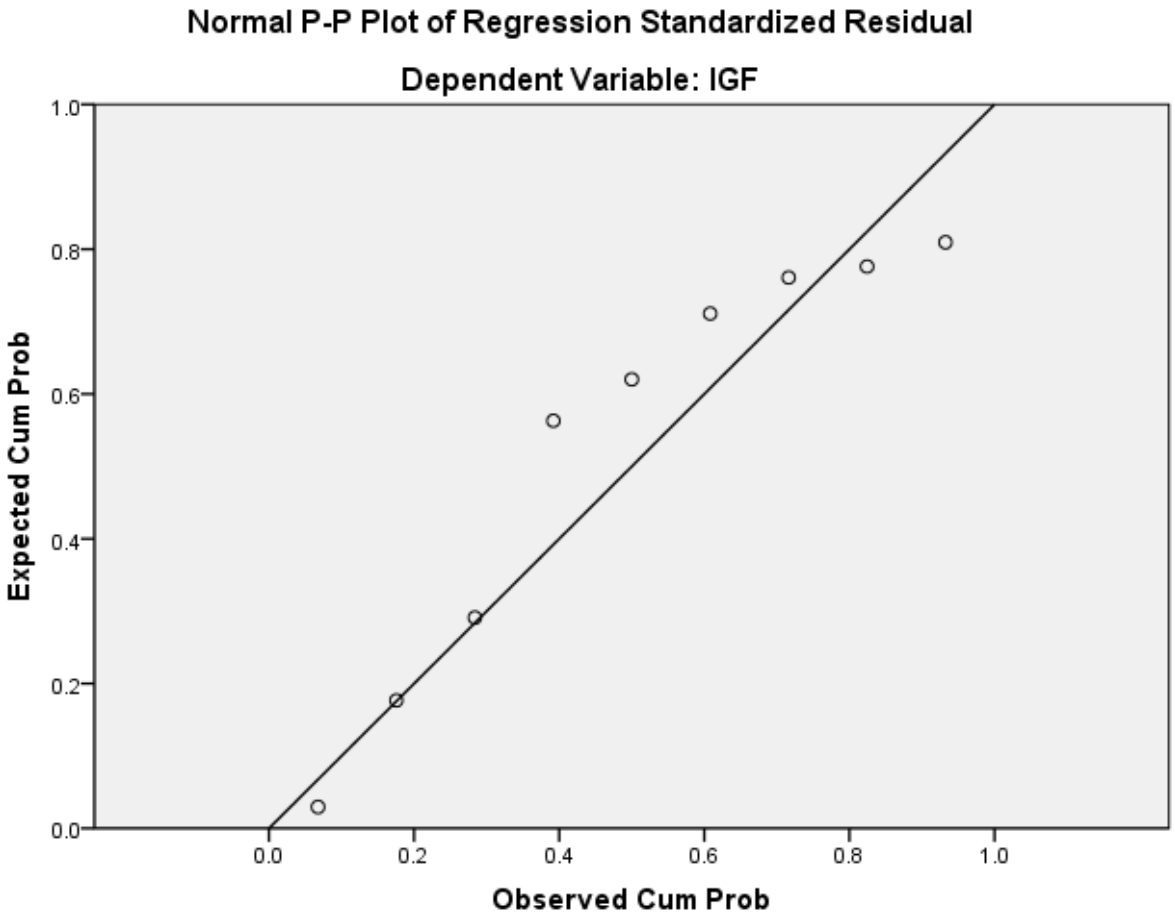
Normal P-P Plot of Regression Standardized Residual
Dependent Variable: IGF
Expected Cum Prob
Observed Cum Prob
0.0
0.2
0.4
0.6
0.8
1.0

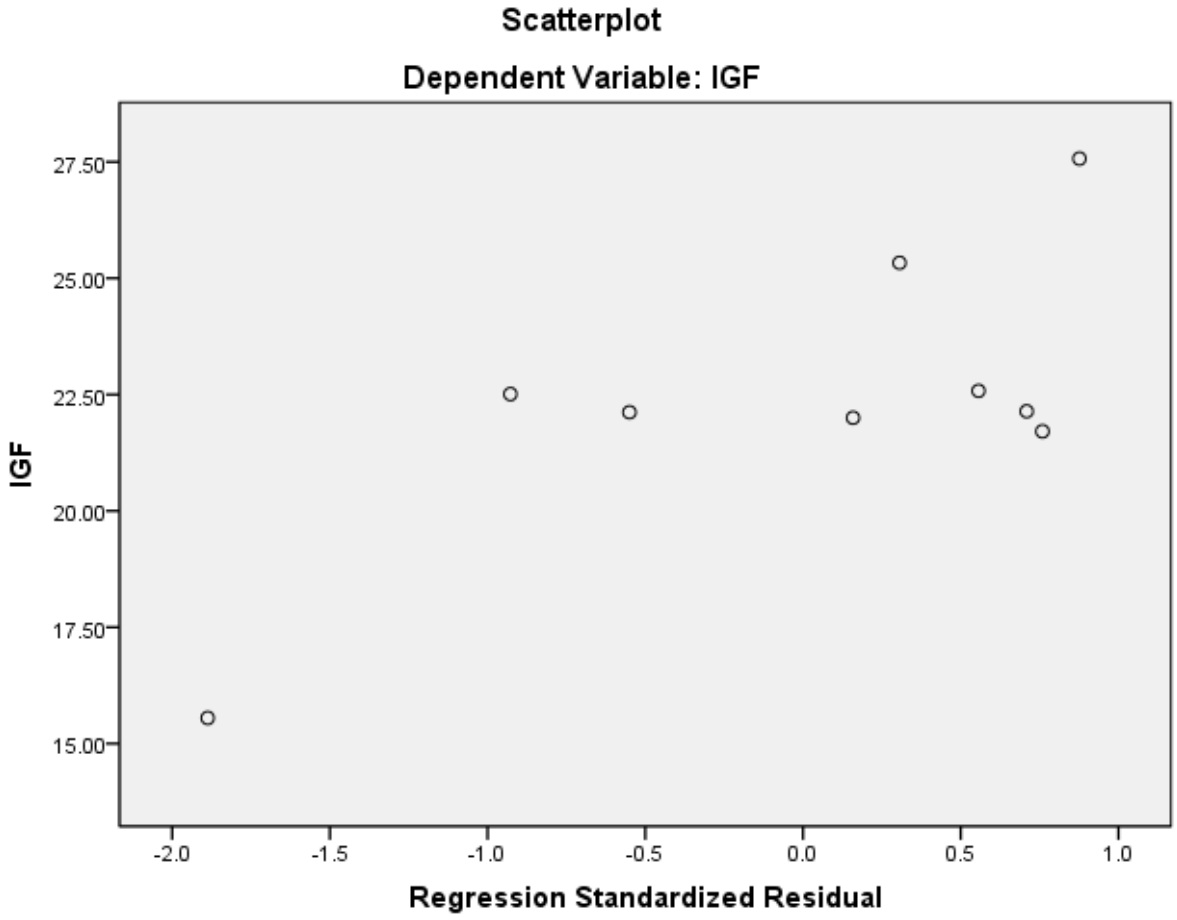
Scatterplot
Dependent Variable: IGF
IGF
27.50
25.00
22.50
20.00
17.50
15.00
-2.0
-1.5
-1.0
-0.5
0.0
0.5
1.0
Regression Standardized Residual

8.2.1.1.6.5 Regression- PGC-1 CT

Variables Entered/Removed[b]

Model	Variables Entered	Variables Removed	Method
1	Gel_Width[a]	.	Enter

a. All requested variables entered.

b. Dependent Variable: PGC

Model Summary[b]

Model	R	R Square	Adjusted R Square	Std. Error of the Estimate
1	.833[a]	.694	.651	1.23082

a. Predictors: (Constant), Gel_Width

b. Dependent Variable: PGC

ANOVA[b]

Model		Sum of Squares	df	Mean Square	F	Sig.
1	Regression	24.103	1	24.103	15.911	.005[a]
	Residual	10.604	7	1.515		
	Total	34.708	8			

ANOVA[b]

Model		Sum of Squares	df	Mean Square	F	Sig.
1	Regression	24.103	1	24.103	15.911	.005[a]
	Residual	10.604	7	1.515		
	Total	34.708	8			

a. Predictors: (Constant), Gel_Width

b. Dependent Variable: PGC

Coefficients[a]

Model		Unstandardized Coefficients		Standardized Coefficients	t	Sig.	Collinearity Statistics	
		B	Std. Error	Beta			Tolerance	VIF
1	(Constant)	16.732	1.575		10.625	.000		
	Gel_Width	4.866	1.220	.833	3.989	.005	1.000	1.000

a. Dependent Variable: PGC

Collinearity Diagnostics[a]

Model	Dimension	Eigenvalue	Condition Index	Variance Proportions	
				(Constant)	Gel_Width
1	1	1.965	1.000	.02	.02
	2	.035	7.544	.98	.98

ANOVA[b]

Model		Sum of Squares	df	Mean Square	F	Sig.
1	Regression	24.103	1	24.103	15.911	.005[a]
	Residual	10.604	7	1.515		
	Total	34.708	8			

a. Dependent Variable: PGC

Residuals Statistics[a]

	Minimum	Maximum	Mean	Std. Deviation	N
Predicted Value	20.7270	25.1502	22.7967	1.73577	9
Residual	-1.72091	1.88981	.00000	1.15132	9
Std. Predicted Value	-1.192	1.356	.000	1.000	9
Std. Residual	-1.398	1.535	.000	.935	9

a. Dependent Variable: PGC

8.2.1.1.6.5.1 Charts

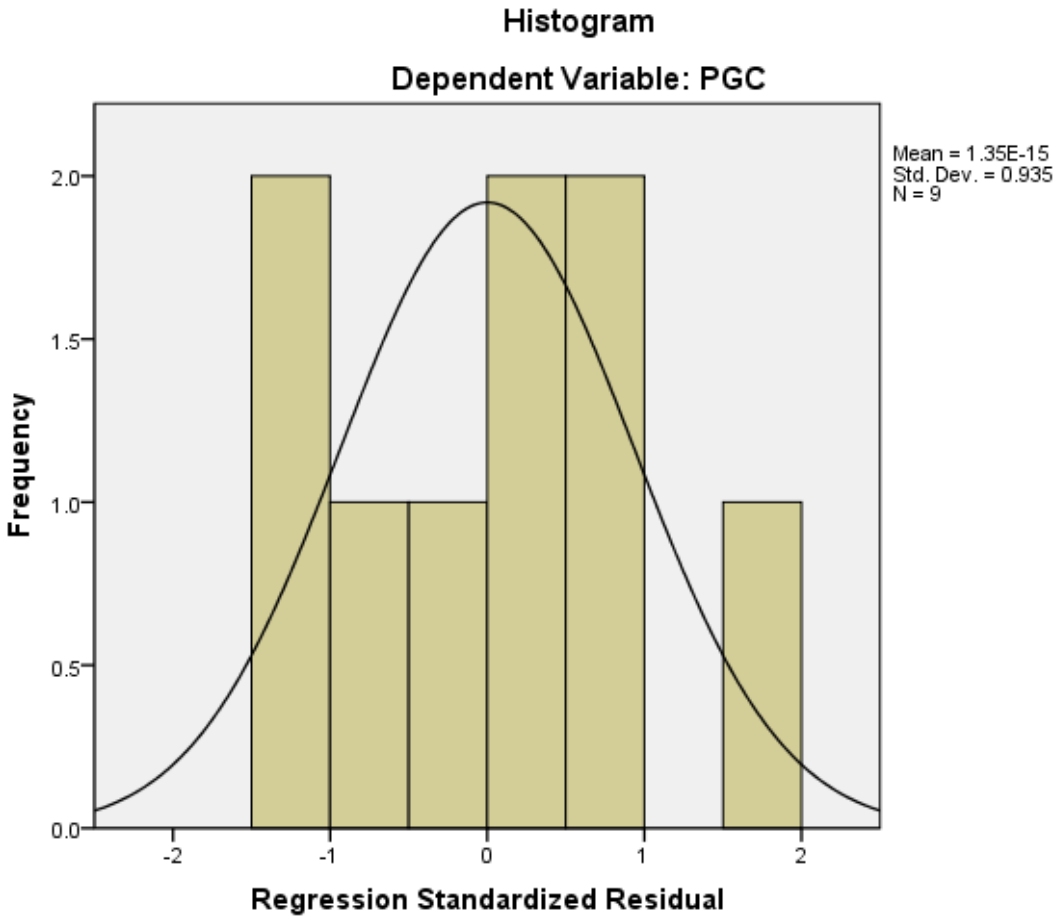

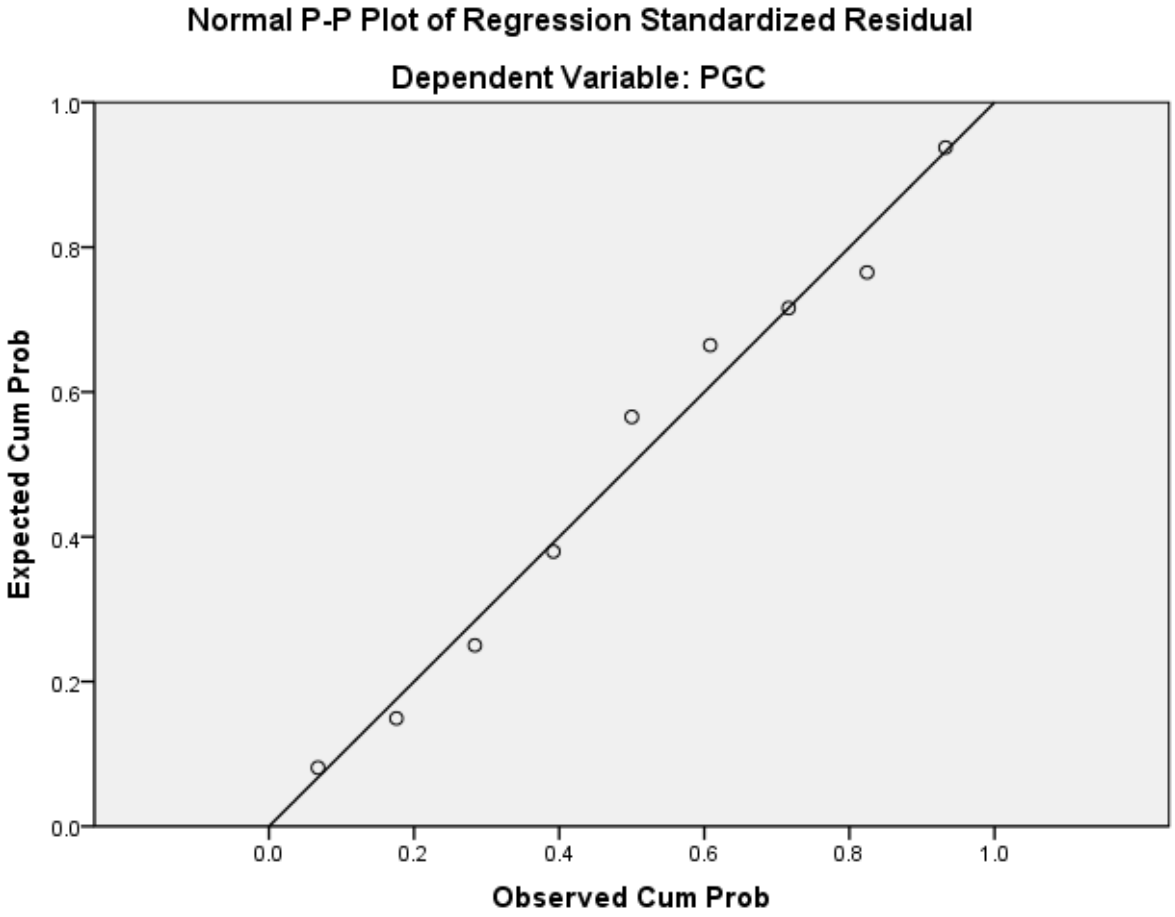
Normal P-P Plot of Regression Standardized Residual
Dependent Variable: PGC
Expected Cum Prob
Observed Cum Prob
0.0
0.2
0.4
0.6
0.8
1.0

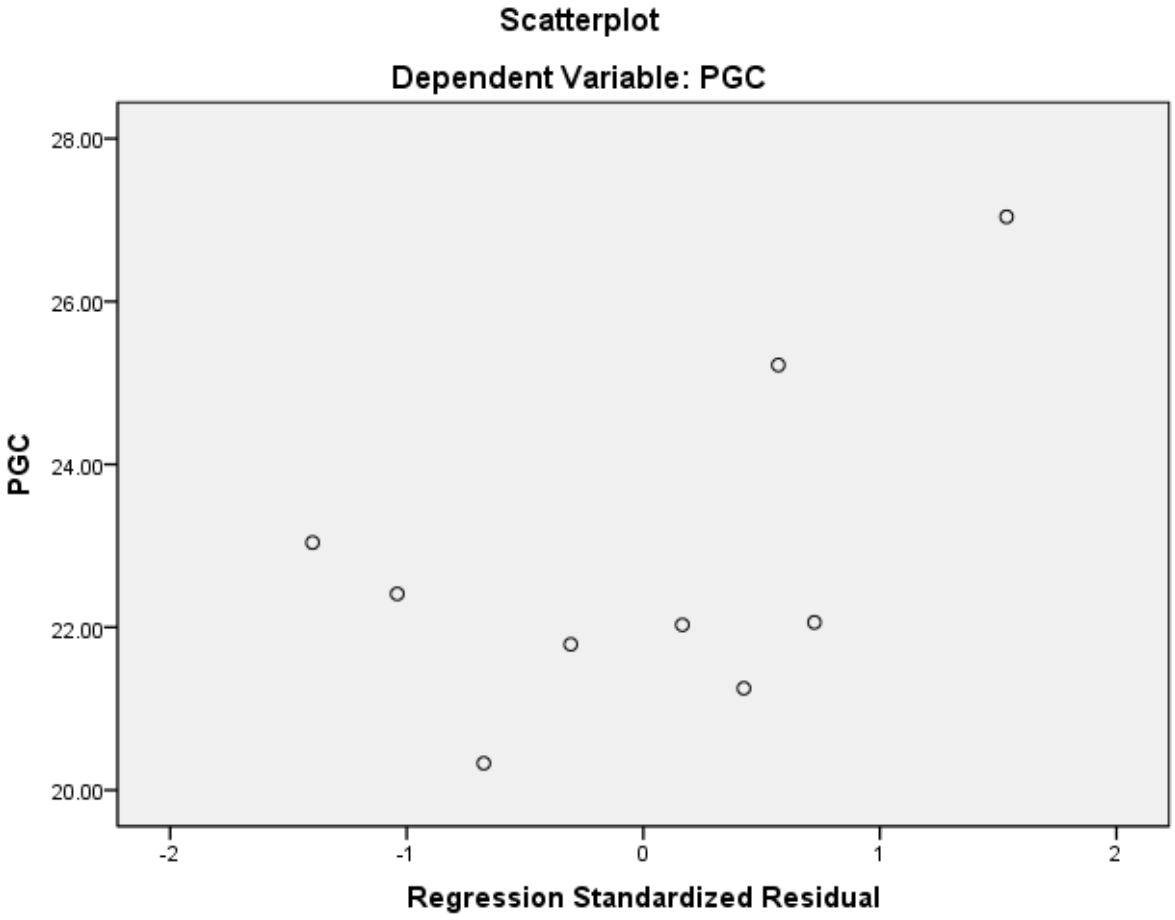
Scatterplot
Dependent Variable: PGC
28.00
26.00
24.00
22.00
20.00
PGC
-2
-1
0
1
2
Regression Standardized Residual

8.2.1.1.7 Cyclic Stretch Gene Expression Analysis

		t-test for Equality of Means						
		t	df	Sig. (2-tailed)	Mean Difference	Std. Error Difference	95% Confidence Interval of the Difference	
							Lower	Upper
PGC	Equal variances assumed	.439	4	.683	.13522	.30783	-.71947	.98990
	Equal variances not assumed	.439	2.000	.703	.13522	.30783	-1.18929	1.45972
MMP9	Equal variances assumed	-.656	4	.548	-.57177	.87178	-2.99222	1.84867
	Equal variances not assumed	-.656	2.000	.579	-.57177	.87178	-4.32273	3.17919
TFAM	Equal variances assumed	130.154	4	.000	.98637	.00758	.96533	1.00741
	Equal variances not assumed	130.154	2.000	.000	.98637	.00758	.95376	1.01897
CYTOC	Equal variances assumed	-1.081	4	.341	-3.71198	3.43378	-13.24568	5.82171
	Equal variances not assumed	-1.081	2.000	.393	-3.71198	3.43378	-18.48633	11.06236
COX	Equal variances assumed	-.871	4	.433	-.40281	.46263	-1.68728	.88166
	Equal variances not assumed	-.871	2.000	.476	-.40281	.46263	-2.39335	1.58773

8.2.1.2 Statistical Analysis Chapter 4

8.2.1.2.1 Normal Distribution Analysis

	Lactate	Glucose	mtDNA	PGC-1a	Tfam	CytoC	MMP-9	NRF-1	NRF-2
Number of values	9	9	9	9	9	9	9	9	9
Minimum	1.4	18.7	140.5	0.4475	0.3276	0.08304	0.8981	0.8766	1
25% Percentile	1.9	19.25	395.2	0.5482	0.3898	0.3117	1.061	1.051	1.32
Median	6.4	19.6	626.8	1	1	1	3.399	1.376	2.428
75% Percentile	7.5	23.25	927.2	2.898	4.209	3.695	8.432	1.702	2.953
Maximum	7.8	23.9	1748	11.22	10.05	4.036	10.63	1.972	4.627
Normality Test 1									
K2	3.323	3.364	6.513	18.52	7.341	4.958	2.041	0.8722	1.699
P value	0.1898	0.186	0.0385	< 0.0001	0.0255	0.0838	0.3603	0.6466	0.4275
Passed normality test?	Yes	Yes	No	No	No	Yes	Yes	Yes	Yes
P value summary	ns	ns	*	****	*	ns	ns	ns	ns
Normality Test 2									
W	0.7841	0.835	0.8987	0.6255	0.7732	0.8218	0.8452	0.9497	0.9378
P value	0.0134	0.0508	0.2443	0.0002	0.0101	0.0361	0.0659	0.6872	0.5593
Passed normality test?	No	Yes	Yes	No	No	No	Yes	Yes	Yes
P value summary	*	ns	ns	***	*	*	ns	ns	ns
Normality Test 3									
KS distance	0.255	0.2877	0.1945	0.3641	0.2644	0.2409	0.214	0.1851	0.1483
P value	0.0943	0.0305	0.2	0.1	0.0695	0.1457	0.2	0.2	0.2
Passed normality test?	Yes	No	Yes	Yes	Yes	Yes	Yes	Yes	Yes
P value summary	ns	*	ns	**	ns	ns	ns	ns	ns

8.2.1.2.2 Peak Glucose and Lactate

Dependent Variable	(I) Condition	(J) Condition	Mean Difference (I-J)	Sig.	95% Confidence Interval	
					Lower Bound	Upper Bound
Lactate	1.00	2.00	-4.900	0.000	-6.392	-3.408
		3.00	-5.767	0.000	-7.258	-4.275
	2.00	1.00	4.900	0.000	-6.392	-3.408
		3.00	-0.8667	0.175	-2.358	0.6251
	3.00	1.00	5.767	0.000	-7.258	-4.275
		2.00	0.8667	0.175	-2.358	0.6251
Glucose	1.00	2.00	3.333	0.008	1.423	5.244
		3.00	4.400	0.000	2.489	6.311
	2.00	1.00	-3.333	0.008	1.423	5.244
		3.00	1.067	0.183	-0.8440	2.977
	3.00	1.00	-4.400	0.000	2.489	6.311
		2.00	-1.067	0.183	-0.8440	2.977

8.2.1.2.3 Nucleic Acid Ratios

Dependent Variable	(I) Condition	(J) Condition	Mean Difference (I-J)	Sig.	95% Confidence Interval	
					Lower Bound	Upper Bound
RNA_DNA	.00	1.00	-.26112	.868	-.9999	.4776
		2.00	-.23154	1.000	-.9703	.5072
	1.00	.00	.26112	.868	-.4776	.9999
		2.00	.02958	1.000	-.7092	.7683
	2.00	.00	.23154	1.000	-.5072	.9703
		1.00	-.02958	1.000	-.7683	.7092

8.2.1.2.4 mtDNA Analysis

(I) Condition	(J) Condition	Mean Difference (I-J)	Sig.	95% Confidence Interval	
				Lower Bound	Upper Bound
1.00	2.00	-201.73926	.563	-1007.7739	604.2954
	3.00	-691.43438	.041	-1497.4690	114.6002
2.00	1.00	201.73926	.563	-604.2954	1007.7739
	3.00	-489.69512	.188	-1295.7297	316.3395
3.00	1.00	691.43438	.041	-114.6002	1497.4690
	2.00	489.69512	.188	-316.3395	1295.7297

8.2.1.2.5 Gene Expression

Dependent Variable	(I) Condition	(J) Condition	Mean Difference (I-J)	Sig.	95% Confidence Interval	
					Lower Bound	Upper Bound
NRF_1	.00	1.00	-.53833*	.021	-.9620	-.1147
		2.00	.40167	.059	-.0220	.8253
	1.00	.00	.53833*	.021	.1147	.9620
		2.00	.94000*	.002	.5164	1.3636
	2.00	.00	-.40167	.059	-.8253	.0220
		1.00	-.94000*	.002	-1.3636	-.5164
NRF_2	.00	1.00	-1.22067	.220	-3.4046	.9633
		2.00	-1.20733	.225	-3.3913	.9766
	1.00	.00	1.22067	.220	-.9633	3.4046
		2.00	.01333	.989	-2.1706	2.1973
	2.00	.00	1.20733	.225	-.9766	3.3913
		1.00	-.01333	.989	-2.1973	2.1706
MMP_9	.00	1.00	2.63667	.878	-37.5359	42.8093
		2.00	-36.76667	.066	-76.9393	3.4059
	1.00	.00	-2.63667	.878	-42.8093	37.5359
		2.00	-39.40333	.053	-79.5759	.7693
	2.00	.00	36.76667	.066	-3.4059	76.9393
		1.00	39.40333	.053	-.7693	79.5759
PGC	.00	1.00	-.17133	.945	-6.0050	5.6623

		2.00	-4.87767	.043	-10.7113	.9560
	1.00	.00	.17133	.945	-5.6623	6.0050
		2.00	-4.70633	.045	-10.5400	1.1273
	2.00	.00	4.87767	.087	-.9560	10.7113
		1.00	4.70633	.045	-1.1273	10.5400
Tfam	.00	1.00	3.49567	.216	-2.6965	9.6878
		2.00	-.25233	.924	-6.4445	5.9398
	1.00	.00	-3.49567	.216	-9.6878	2.6965
		2.00	-3.74800	.189	-9.9402	2.4442
	2.00	.00	.25233	.924	-5.9398	6.4445
		1.00	3.74800	.189	-2.4442	9.9402
CytoC	.00	1.00	1.15267	.077	-.1693	2.4746
		2.00	-2.42033*	.004	-3.7423	-1.0984
	1.00	.00	-1.15267	.077	-2.4746	.1693
		2.00	-3.57300*	.001	-4.8949	-2.2511
	2.00	.00	2.42033*	.004	1.0984	3.7423
		1.00	3.57300*	.001	2.2511	4.8949

8.2.1.3 Statistical Analysis Chapter 5

8.2.1.3.1 Normal Distribution Analysis

	Peak Lactate	IGF-I	MMP-9	Myostatin	MuRF-1	MAFBx
Number of values	9	11	11	12	12	12
Minimum	1.4	0.5434	1	0.007264	0.2207	0.676
25% Percentile	1.9	10.27	4.07	0.02799	0.6704	0.8448
Median	4.9	29.14	10.78	0.1455	1.219	1.003
75% Percentile	6.4	52.89	23.59	0.2857	1.526	1.697
Maximum	6.5	93.05	29.96	7.674	3.306	1.925
Normality Test 1						
K2	2.658	1.871	1.364	32.53	5.138	3.676
P value	0.2647	0.3923	0.5056	< 0.0001	0.0766	0.1591
Passed normality test?	Yes	Yes	Yes	No	Yes	Yes
P value summary	ns	ns	ns	****	ns	ns
Normality Test 2						
W	0.858	0.8639	0.9414	0.4123	0.8916	0.871
P value	0.0912	0.0647	0.5368	< 0.0001	0.1234	0.0672
Passed normality test?	Yes	Yes	Yes	No	Yes	Yes
P value summary	ns	ns	ns	****	ns	ns

Normality Test 3							
KS distance		0.2006	0.2071	0.1588	0.3294	0.2219	0.2528
P value		0.2	0.2	0.2	0.1	0.1056	0.0329
Passed normality test?	Yes		Yes	Yes	Yes	Yes	No
P value summary	ns		ns	ns	ns	ns	*

8.2.1.3.2 Conditioned Media Lactate Analysis

(I) Condition	(J) Condition	Mean Difference (I-J)	Sig.	95% Confidence Interval	
				Lower Bound	Upper Bound
.00	1.00	4.70000*	.000	3.8279	5.5721
	2.00	1.63333*	.003	.7613	2.5054
1.00	.00	-4.70000*	.000	-5.5721	-3.8279
	2.00	-3.06667*	.000	-3.9387	-2.1946
2.00	.00	-1.63333*	.003	-2.5054	-.7613
	1.00	3.06667*	.000	2.1946	3.9387

8.2.1.3.3 Gene Expression Analysis

Dependent Variable	(I) Condition	(J) Condition	Mean Difference (I-J)	Sig.	95% Confidence Interval	
					Lower Bound	Upper Bound
IGF	1.00	2.00	-7.15800	.603	-37.6321	23.3161
		3.00	-61.18646*	.001	-89.4000	-32.9730

	2.00	1.00	7.15800	.603	-23.3161	37.6321
		3.00	-54.02846*	.003	-84.5025	-23.5544
	3.00	1.00	61.18646*	.001	32.9730	89.4000
		2.00	54.02846*	.003	23.5544	84.5025
MMP9	1.00	RL	-18.63386*	.005	-29.9644	-7.3033
		SL	-12.31072*	.027	-22.8007	-1.8207
	2.00	1.00	18.63386*	.005	7.3033	29.9644
		3.00	6.32314	.234	-5.0074	17.6537
	3.00	1.00	12.31072*	.027	1.8207	22.8007
		2.00	-6.32314	.234	-17.6537	5.0074
Myostatin	1.00	2.00	.26107	.883	-3.6429	4.1650
		3.00	-1.31829	.407	-4.7472	2.1106
	2.00	1.00	-.26107	.883	-4.1650	3.6429
		3.00	-1.57936	.364	-5.3123	2.1535
	3.00	1.00	1.31829	.407	-2.1106	4.7472
		2.00	1.57936	.364	-2.1535	5.3123
MuRF1	1.00	2.00	-.61637	.391	-2.1635	.9307
		3.00	.21517	.728	-1.1437	1.5740
	2.00	1.00	.61637	.391	-.9307	2.1635
		3.00	.83154	.235	-.6478	2.3108
	3.00	1.00	-.21517	.728	-1.5740	1.1437
		2.00	-.83154	.235	-2.3108	.6478
MAFBx	1.00	2.00	-.06754	.860	-.9117	.7767

		3.00	-.30525	.376	-1.0467	.4362
	2.00	1.00	.06754	.860	-.7767	.9117
		3.00	-.23772	.522	-1.0449	.5695
	3.00	1.00	.30525	.376	-.4362	1.0467
		2.00	.23772	.522	-.5695	1.0449
IGF_BP5	1.00	2.00	.68000*	.008	.2513	1.1087
		3.00	.55400*	.020	.1253	.9827
	2.00	1.00	-.68000*	.008	-1.1087	-.2513
		3.00	-.12600	.499	-.5547	.3027
	3.00	1.00	-.55400*	.020	-.9827	-.1253
		2.00	.12600	.499	-.3027	.5547
IGF_BP2	1.00	2.00	.58333	.144	-.2653	1.4320
		3.00	-.48900	.208	-1.3376	.3596
	2.00	1.00	-.58333	.144	-1.4320	.2653
		3.00	-1.07233*	.021	-1.9210	-.2237
	3.00	1.00	.48900	.208	-.3596	1.3376
		2.00	1.07233*	.021	.2237	1.9210

8.3 Appendix 3

8.3.1 Ethical Clearance Confirmation

09/12/2009

Ethical scrutiny confirmation

Proposer:	Darren Player
Proposal short title:	In Vitro Model for Assessment of Skeletal Muscle Adaptation Following Exercise Related Physiological Cue

Dear Proposer

Your proposal has now received ethical scrutiny from the Institute for Sport and Physical Activity Research Ethics panel.

I can confirm that this has now been approved, please find below your approval number:

Approval number: **2009MCP001**

You are now clear to proceed with data collection for this project.

Thank you very much for your patience in this matter

Regards

Michelle Miskelly
On behalf of Dr Paul Castle (IREG Chair)